REFERENCE USE ONLY

FAA-7714

REPORT NO. FAA-RD-77-117

VERIFICATION OF WIND MEASUREMENT WITH MOBILE LASER DOPPLER SYSTEM

M.R. Brashears
W.R. Eberle

LOCKHEED MISSILES & SPACE COMPANY, INC.
HUNTSVILLE RESEARCH & ENGINEERING CENTER
4800 Bradford Drive
Huntsville AL 35807

SEPTEMBER 1977

FINAL REPORT

DOCUMENT IS AVAILABLE TO THE U.S. PUBLIC THROUGH THE NATIONAL TECHNICAL INFORMATION SERVICE, SPRINGFIELD, VIRGINIA 22161

Prepared for

U.S. DEPARTMENT OF TRANSPORTATION
FEDERAL AVIATION ADMINISTRATION
Systems Research and Development Service
Washington DC 20591

NOTICE

This document is disseminated under the sponsorship of the Department of Transportation in the interest of information exchange. The United States Government assumes no liability for its contents or use thereof.

Use of trade names of manufacturers in this report does not constitute an official endorsement of such products or manufacturers, either expressed or implied by Lockheed Missiles & Space Company, Inc., or any agency of the United States Government.

Technical Report Documentation Page

1. Report No.	2. Government Accession No.	3. Recipient's Catalog No.
FAA-RD-77-117		

4. Title and Subtitle	5. Report Date
VERIFICATION OF WIND MEASUREMENT WITH MOBILE LASER DOPPLER SYSTEM	September 1977
	6. Performing Organization Code

7. Author(s)	8. Performing Organization Report No.
M.R. Brashears, W.R. Eberle	DOT-TSC-FAA-77-14 LMSC-HREC TR D497071

9. Performing Organization Name and Address	10. Work Unit No. (TRAIS)
Lockheed Missiles & Space Company, Inc.* Huntsville Research & Engineering Center 4800 Bradford Drive Huntsville AL 35807	FA742/R8105
	11. Contract or Grant No. DOT-TSC-1098

12. Sponsoring Agency Name and Address	13. Type of Report and Period Covered
U.S. Department of Transportation Federal Aviation Administration Systems Research and Development Service Washington DC 20591	Final Report July 1975-November 1976
	14. Sponsoring Agency Code

15. Supplementary Notes

*Under Contract to: U.S. Department of Transportation
Transportation Systems Center
Kendall Square
Cambridge MA 02142

16. Abstract

The Lockheed Mobile Atmospheric Unit is a laser Doppler velocimeter system designed for the remote measurement of the three components of atmospheric wind. The unit was tested at the National Oceanic and Atmospheric Administration Table Mountain Test Site to verify the capability of the system to measure wind remotely and to evaluate alternative data-processing algorithms. Remotely measured wind data are compared with concurrent data measured by anemometers on the NOAA 150-meter meteorological tower. The test program showed that the laser Doppler velocimeter system is an accurate instrument for the remote measurement of winds.

17. Key Words	18. Distribution Statement
Wind Atmospheric Effects Laser Doppler Velocimetry Remote Sensing	DOCUMENT IS AVAILABLE TO THE U.S. PUBLIC THROUGH THE NATIONAL TECHNICAL INFORMATION SERVICE, SPRINGFIELD, VIRGINIA 22161

19. Security Classif. (of this report)	20. Security Classif. (of this page)	21. No. of Pages	22. Price
Unclassified	Unclassified	170	

Form DOT F 1700.7 (8-72) Reproduction of completed page authorized

PREFACE

In the past several years, the National Transportation Safety Board has identified wind shear as a factor or probable cause in several aircraft accidents. The most significant of the wind shear-related accidents have been Iberia Flight 933 at Boston (a DC-10), Eastern Airlines Flight 66 at New York (B-727), and Continental Airlines Flight 426 at Denver (B-727). Wind shear is a gradient of wind velocity with respect to altitude above the surface. The accidents have prompted a search for techniques and/or instrumentation for the remote measurement of wind as a function of altitude for the purpose of identifying regions of wind shear and determining the magnitudes and direction of the shear. A primary candidate for the remote measurement of wind is the laser Doppler velocimeter. The test described herein was designed to validate the laser Doppler velocimeter as an instrument for the remote measurement of wind and to evaluate alternative data processing algorithms. This report describes the principles of wind measurement by laser Doppler velocimetry and presents the results of the validation tests.

METRIC CONVERSION FACTORS

Approximate Conversions to Metric Measures

Symbol	When You Know	Multiply by	To Find	Symbol
		LENGTH		
in	inches	2.5	centimeters	cm
ft	feet	30	centimeters	cm
yd	yards	0.9	meters	m
mi	miles	1.6	kilometers	km
		AREA		
in^2	square inches	6.5	square centimeters	cm^2
ft^2	square feet	0.09	square meters	m^2
yd^2	square yards	0.8	square meters	m^2
mi^2	square miles	2.6	square kilometers	km^2
	acres	0.4	hectares	ha
		MASS (weight)		
oz	ounces	28	grams	g
lb	pounds	0.45	kilograms	kg
	short tons (2000 lb)	0.9	tonnes	t
		VOLUME		
tsp	teaspoons	5	milliliters	ml
Tbsp	tablespoons	15	milliliters	ml
fl oz	fluid ounces	30	milliliters	ml
c	cups	0.24	liters	l
pt	pints	0.47	liters	l
qt	quarts	0.95	liters	l
gal	gallons	3.8	liters	l
ft^3	cubic feet	0.03	cubic meters	m^3
yd^3	cubic yards	0.76	cubic meters	m^3
		TEMPERATURE (exact)		
°F	Fahrenheit temperature	5/9 (after subtracting 32)	Celsius temperature	°C

Approximate Conversions from Metric Measures

Symbol	When You Know	Multiply by	To Find	Symbol
		LENGTH		
mm	millimeters	0.04	inches	in
cm	centimeters	0.4	inches	in
m	meters	3.3	feet	ft
m	meters	1.1	yards	yd
km	kilometers	0.6	miles	mi
		AREA		
cm^2	square centimeters	0.16	square inches	in^2
m^2	square meters	1.2	square yards	yd^2
km^2	square kilometers	0.4	square miles	mi^2
ha	hectares (10,000 m^2)	2.5	acres	
		MASS (weight)		
g	grams	0.035	ounces	oz
kg	kilograms	2.2	pounds	lb
t	tonnes (1000 kg)	1.1	short tons	
		VOLUME		
ml	milliliters	0.03	fluid ounces	fl oz
l	liters	2.1	pints	pt
l	liters	1.06	quarts	qt
l	liters	0.26	gallons	gal
m^3	cubic meters	35	cubic feet	ft^3
m^3	cubic meters	1.3	cubic yards	yd^3
		TEMPERATURE (exact)		
°C	Celsius temperature	9/5 (then add 32)	Fahrenheit temperature	°F

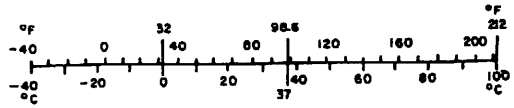

TABLE OF CONTENTS

Section		Page
1.	INTRODUCTION	1
	1.1 Background	1
	1.2 Program Objectives	2
	1.3 Report Format	2
2.	LASER DOPPLER SYSTEM DEVELOPMENT	3
	2.1 System Description	3
	2.2 Winds Aloft Sensing	17
3.	COMPUTER-SOFTWARE SYSTEM DEVELOPMENT	23
	3.1 Description of Laser Doppler Velocimeter Software System	23
	3.2 Operation of Laser Doppler Velocimeter Software System	27
4.	DATA COLLECTION AT TABLE MOUNTAIN	43
	4.1 Test Description	43
	4.2 Test Objectives and Operating Procedure	46
	4.3 Data Analysis of Initial Runs	46
	4.4 Initial Data Comparison	53
	4.5 Fixed Altitude Velocity Azimuth Display Data Comparison	56
	4.6 Effect of Averaging Time	60
	4.7 Effect of Snow	74
5.	CONCLUSIONS AND RECOMMENDATIONS	79
6.	REFERENCES	81
Appendix		
A	Laser Doppler Velocimeter Velocity Azimuth Display Signatures (Runs 21-28)	A-1

TABLE OF CONTENTS (Continued)

Appendix		Page
B	Laser Doppler Velocimeter and Anemometer Wind Comparisons (Runs 21-28)	B-1
C	Report of Inventions	C-1

LIST OF ILLUSTRATIONS

Figure		
2-1	System Configuration	5
2-2	Typical Optical Component Configuration of Lockheed Laser Doppler Velocimeter	6
2-3	Schematic of Scan Equipment on Laser Doppler Velocimeter	8
2-4	Multimode Scanner	9
2-5	Scan Capabilities of Laser Doppler Velocimeter	11
2-6	Lockheed-Huntsville Mobile Atmospheric Unit	12
2-7	Interior View of Mobile Atmospheric Unit Looking Forward	13
2-8	Interior View of Mobile Atmospheric Unit	14
2-9	Typical Laser Doppler Velocimeter Wind Signature as Displayed by Spectrum Analyzer	15
2-10	Output of Signal Processor for Frequency-Modulated Input	16
2-11	Computer Mainframe Teletype and Laser Doppler Velocimeter Electronics	18
2-12	Principle of Velocity Azimuth Display Operation	19
2-13	Azimuth Angle Dependence of Measured Velocity Component	20
3-1	General Elements of Mobile Atmospheric Unit Data Acquisition-and-Processing System	24
3-2	Data Logger Macro Flowchart	25
3-3	Typical Spectrum Analyzer Output in Velocity Azimuth Display Scan	26
3-4	Macro Flowchart of Off-Line Velocity Azimuth Display Program	28

LIST OF ILLUSTRATIONS (Continued)

Figure		Page
3-5	Dump of Sample Output Tape from Data Logger	31
3-6	Sample Output Plot from Velocity Azimuth Display Program (Unedited)	34
3-7	Filtered Line-of-Sight Velocity for Velocity Azimuth Display Mode	36
3-8	Derectified Line-of-Sight Velocity for Velocity Azimuth Display Mode (Edited, but Unfiltered Data)	37
3-9	Line-of-Sight Velocity Signature of Velocity Azimuth Display	38
4-1	National Oceanic and Atmospheric Administration Table Mountain Test Site Layout	44
4-2	Table Mountain Data Collection Site	45
4-3	Comparison of Laser and Tower 16-min Mean Wind Speed at 30-m Altitude	48
4-4	Comparison of Laser and Tower 16-min Mean Wind Speed at 60-m Altitude	49
4-5	Comparison of Laser and Tower 16-min Mean Wind Speed at 90-m Altitude	50
4-6	Comparison of Laser and Tower 16-min Mean Wind Speed at 120-m Altitude	51
4-7	Comparison of Laser and Tower 16-min Mean Wind Speed at 150-m Altitude	52
4-8	Comparison of Data Processing Algorithms at 60-m Altitude (16-min Means of Runs 6, 7, and 9)	54
4-9	Comparison of Data Processing Algorithms at 150-m Altitude (16-min Means of Runs 6, 7, and 9)	55
4-10	Comparison of Lockheed Laser Doppler Anemometer Wind Data vs National Oceanic and Atmospheric Administration's 150-m Tower Data (Run 24; Altitude, 30 m)	58
4-11	Comparison of Laser vs Tower Standard Deviations in Wind Speed and Direction (Run 24; Altitude, 30 m)	59
4-12	Comparison of Laser vs Tower Wind Data (Run 26; Altitude, 30 m)	61
4-13	Comparison of Laser and Tower 15-min Mean Wind Speed Using Peak Algorithm	62

LIST OF ILLUSTRATIONS (Concluded)

Figure		Page
4-14	Comparison of Laser and Tower 15-min Mean Wind Speed Using Spectral Algorithm	63
4-15	Comparison of Laser and Tower 15-min Mean Wind Speed Using Least-Squares Sine Algorithm	64
4-16	Comparison of Laser and Tower 15-min Mean Wind Direction Using Peak Algorithm	65
4-17	Comparison of Laser and Tower 15-min Mean Wind Direction Using Spectral Algorithm	66
4-18	Comparison of Laser and Tower 15-min Mean Wind Direction Using Least-Squares Sine Algorithm	67
4-19	Laser Wind Speed with 1-min Averaging Time	68
4-20	Laser Wind Direction with 1-min Averaging Time	69
4-21	Laser Wind Speed with 6-min Averaging Time	70
4-22	Laser Wind Direction with 6-min Averaging Time	71
4-23	Laser Wind Speed with 15-min Averaging Time	72
4-24	Laser Wind Direction with 15-min Averaging Time	73
4-25	Velocity Azimuth Display in Light Snow	75
4-26	Velocity Azimuth Display in Heavy Snow	77
A-1	Sample Laser Doppler Velocimeter Signatures	A-1
B-1	Comparison of Winds Measured by Laser Doppler Velocimeter and Tower Anemometer	B-1

1. INTRODUCTION

1.1 BACKGROUND

Significant effort is currently being devoted to the development of instrumentation to sense atmospheric flow phenomena remotely. Some of the avenues being pursued are active and passive acoustic sensors, optical sensors, and radio methods. A useful survey of such methods is presented in Ref. 1. Two advantages of remote sensors are that flow conditions can be ascertained in regions of space where it would not be convenient to locate instrumentation hardware, and no interference with the flow at the point of interest is introduced by their use. The Laser Doppler Velocimeter (LDV) is a particularly attractive device for remote sensing of atmospheric phenomena. In the LDV system, the laser radiation backscattered by moving particulates in the atmosphere is used to determine the velocity of the flow. Since it is possible to direct the laser focal volume at a selected sequence of points in space, data from a scanning LDV system can be used to determine the velocity field rapidly and over a range of altitudes. A CO_2 laser Doppler velocimeter system has the following advantages over other remote sensing techniques: (1) the sensing volume can be varied with ease as only optic pointing and focusing operations are involved; (2) the ambient aerosol provides a sufficient scattering target; and (3) the sensing mechanism is non-mechanical which results in the potential for a high-frequency turbulence sensor.

The feasibility of utilizing an LDV system for the remote sensing of low altitude winds and for the detection and tracking of aircraft wake vortices has been demonstrated (Refs. 2 through 5). However, the development of an effective LDV system for monitoring wind and wind shear required a further refinement and application of the technology.

1.2 PROGRAM OBJECTIVES

The primary objectives of the Table Mountain test were to establish the validity of the Velocity Azimuth Display (VAD) for three-dimensional wind measurements for a range of wind speeds and to assess the validity of selected VAD data-processing techniques. Another objective was to investigate the effect of averaging time on the accuracy of VAD measurements.

1.3 REPORT FORMAT

A brief description of the mobile laser Doppler system is presented in the following sections. A more complete description is presented in Ref. 5. A description of the LDV is presented in Section 2 followed by a description of the computer software algorithms in Section 3. The field tests at the Table Mountain site are described in Section 4 along with analysis of the VAD data and comparisons with the meteorological tower data. Section 5 presents the conclusions and recommendations.

2. LASER DOPPLER SYSTEM DEVELOPMENT

2.1 SYSTEM DESCRIPTION

An LDV remote wind sensor senses air movement by measurement of the Doppler frequency shift of laser radiation backscattered by the atmospheric aerosol. An instrument must incorporate means to transmit the laser radiation to the region of interest, collect the radiation scattered from the atmospheric aerosol, and to photomix on a photodetector the scattered radiation and a portion of the transmitted beam. The difference between the transmitted frequency and the returned frequency is the Doppler shift frequency. The Doppler frequency shift signal is generated at the photodetector and is directly proportional to the magnitude* of the wind-velocity component in the direction of the line-of-sight of the laser beam. This velocity component is hereafter called the line-of-sight velocity. The magnitude of the Doppler shift, Δf, is given by

$$\Delta f = \frac{2}{\lambda} |\overline{V}| \cos\theta,$$

where

$\overline{V}$ = the velocity vector in the region being sensed,

θ = the angle subtended by the velocity vector and the optic system line-of-sight, and

λ = the laser radiation wavelength (10.6 microns for CO_2 laser).

A Doppler shift of 188 kHz results per m/sec of line-of-sight velocity component. Measurement of the Doppler shift frequency, Δf, yields directly the line-of-sight velocity component, $|\overline{V}| \cos\theta$. Some typical advantages of the laser Doppler method are: (1) the Doppler shift is a direct absolute measure of the line-of-sight velocity (for example, a hot wire yields wind speed via a cooling effect on the wire); (2) the ease with which the sensing volume can be varied (only optics pointing and focusing operations being involved); (3) the ambient

*Techniques for resolving the sign of the line-of-sight velocity component are available. They are not discussed here because they were not available for the subject test.

aerosol provides sufficient scattering, thus enabling operation in "clear air" conditions; and (4) the ambient aerosol tracer has a small inertia and responds quickly to variations in airspeed and, thus, can be a good turbulence indicator.

A useful instrument must also incorporate means for scanning the focal volume through a selected sequence of points in space and to effect the required signal processing, on-line readout, and permanent recording requirements. The hardware implementation of the mobile laser Doppler unit used during this investigation is discussed in the following subsections. The overall configuration is summarized in Fig. 2-1.

2.1.1 Basic Laser Doppler Velocimeter Optical System

The optical system is of monostatic design and utilizes a continuous-wave laser. The arrangement depends on focusing the transmitter telescope at the location of interest for its spatial resolution property. Details of the optical arrangement are shown in Fig. 2-2.

A horizontally polarized, 20-watt, continuous-wave CO_2 laser beam (10.6-micron wavelength) emerges from the laser (1) and is deflected 90 degrees by a mirror (2) and by a 90% reflecting beamsplitter (3). The approximately 6-mm diameter beam then passes through a Brewster window (4) and a CdS quarter waveplate (5) which converts the beam to circular polarization. The beam impinges on the secondary mirror (6) and is expanded and reflected into the primary mirror (30-cm diameter) (7) and then focused out into the atmosphere. A small portion of the original laser beam is transmitted through the beamsplitter (3) and is used as a local oscillator after being rotated to vertical polarization by a half waveplate (9). Energy scattered by aerosols at the focal volume (13) is collected by the primary mirror (7), collimated by the secondary (6), and passed through the quarter waveplate (5). A wire stop (16) eliminates most of the secondary mirror reflection of the outgoing beam. The quarter waveplate changes the polarization of the aerosol backscattered radiation from circular to vertical linear polarization. The vertically

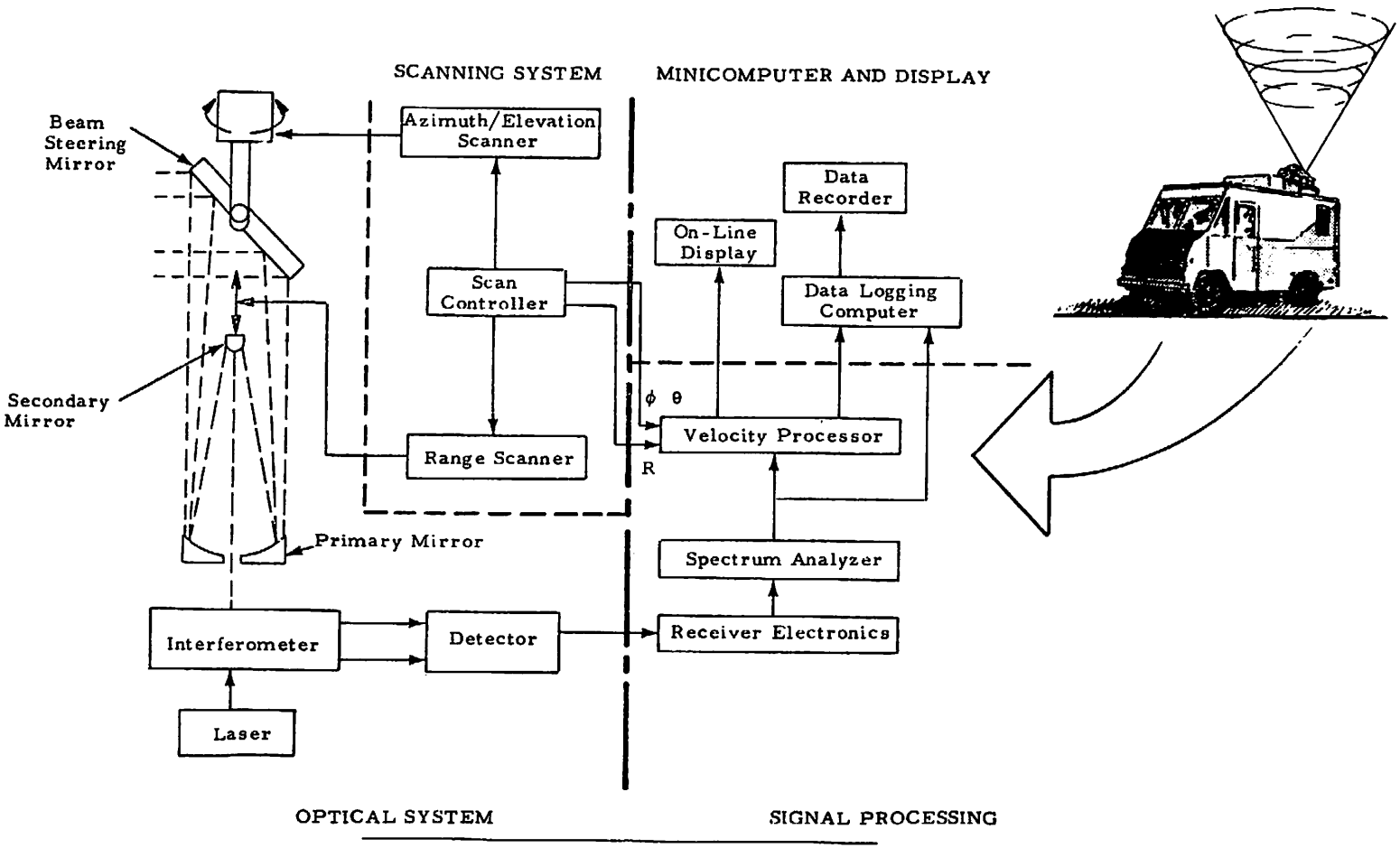

FIGURE 2-1. SYSTEM CONFIGURATION.

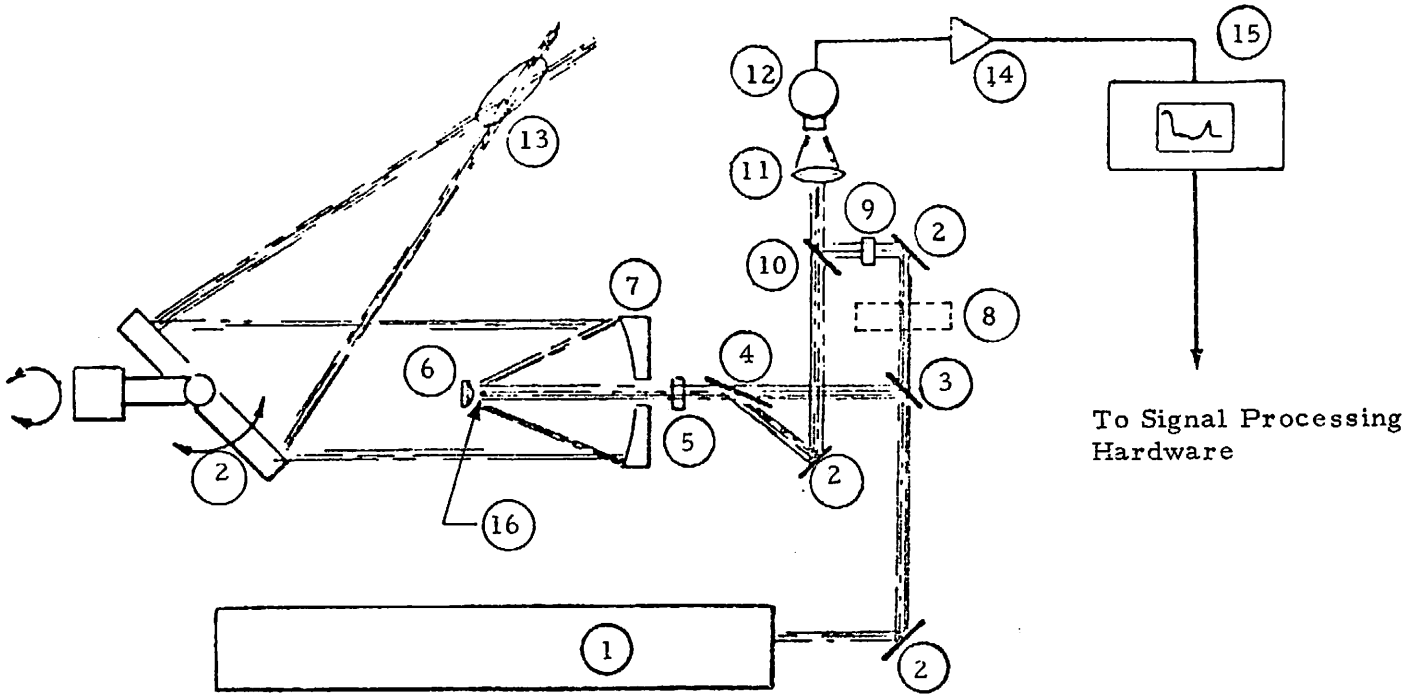

1. CO_2 Laser
2. Mirror
3. Beamsplitter (90% R)
4. Brewster Window
5. Quarter Wave Plate
6. Secondary Mirror
7. Primary Mirror
8. Optional Beam Stop
9. Half Wave Plate
10. Beamsplitter (90% T)
11. Lens
12. Photodetector
13. Focal Volume
14. Preamplifier
15. Spectrum Analyzer
16. Wire Beam Stop

FIGURE 2-2. TYPICAL OPTICAL COMPONENT CONFIGURATION OF LOCKHEED LASER DOPPLER VELOCIMETER.

polarized beam is approximately 78% reflected off the Brewster window (4) and directed through the beamsplitter (10) where it is combined with the local oscillator radiation. After passing through the collecting lens (11), the two beams are photomixed on the detector (12) in a heterodyne configuration. The electrical output of the detector (12) is amplified (14) with a 5-MHz bandwidth, 20-dB gain low-noise-type preamplifier and fed into a spectrum analyzer (15).

An alternative operating configuration consisted of utilizing the portion of the outgoing beam backscattered into the interferometer by the secondary mirror (6) as the local oscillator beam. This mode of operation is less susceptible to optical misalignment difficulties and was the technique used during this investigation. When incorporated, the optical leg (3)(2)(9) was deactivated by the beam stop (8) and the wire stop (16) was removed.

2.1.2 Optical Scanning System

In order to provide the flexibility to operate in various modes for which the system was designed, a scanning arrangement as shown in Fig. 2-3 is used. Modes of operation include vortex tracking (not required for the measurements described in this document) and Velocity Azimuth Display (VAD) for the measurement of atmospheric wind. The mirror assembly, AB, can be rotated about the vertical axis for the scanning in azimuth necessary for the VAD (also called the conical scan mode of operation). Mirror A is adjusted to control the elevation angle of the beam, thus controlling the cone angle of the conical scan. The scanning hardware as deployed on the mobile van is shown in Fig. 2-4.

Range scanning of the system's focal volume is accomplished by varying the distance between the telescope secondary mirror, E, and the primary mirror, D. This is effected by varying the position of the mirror, E, in a controlled manner by an electric-motor/optical-encoder combination.

The operator inputs for the scanning system are made through a control panel incorporating thumbswitch controls and light-emitting-diode

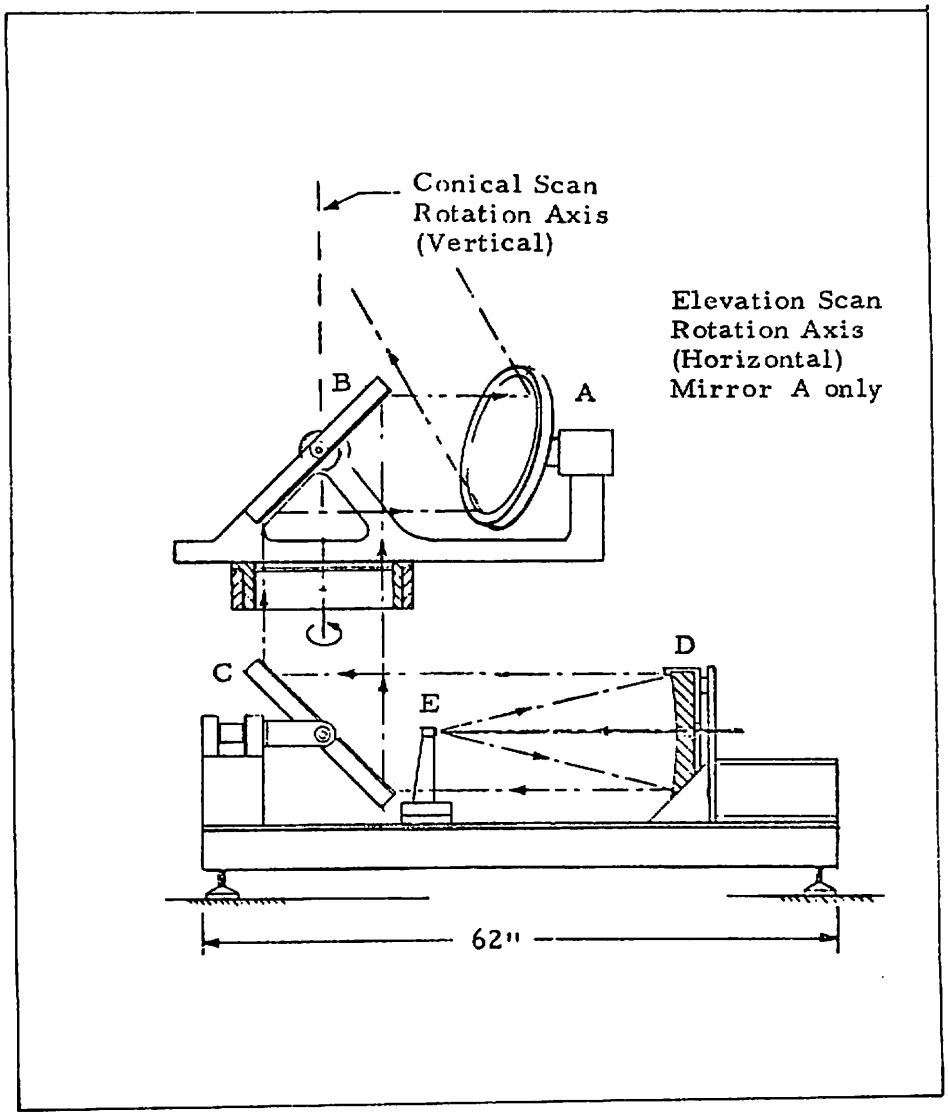

FIGURE 2-3. SCHEMATIC OF SCAN EQUIPMENT ON LASER DOPPLER VELOCIMETER.

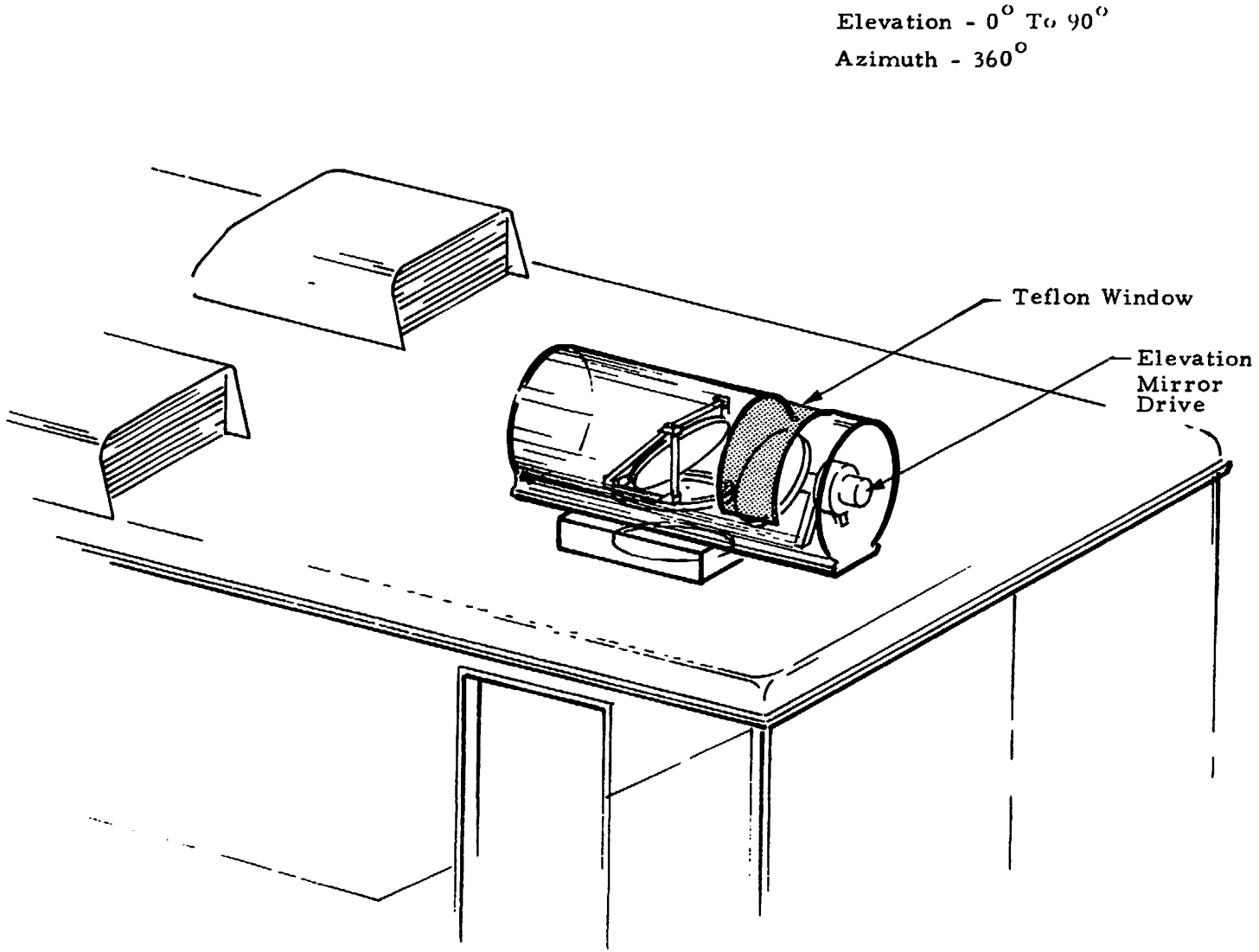

FIGURE 2-4. MULTIMODE SCANNER.

monitors. The system's scan capabilities are summarized in Fig. 2-5. A view of the mobile unit is presented in Fig. 2-6. Interior views of the mobile unit are shown in Figs. 2-7 and 2-8.

2.1.3 Signal Processing System

The Doppler frequency shift of the photodetector output is determined through the use of a sampled spectrum analyzer which provides frequency spectra (intensity of returned signal as a function of Doppler shift) at a rate of 70 signatures per second. A typical Doppler wind signature is shown in Fig. 2-9. To yield a line-of-sight velocity estimate, a voltage which has the same time behavior as the Doppler shift, f_d, given by the peak of the spectrum is generated.

The implementation of this technique is, in essence, a recursive comparison method. The spectrum analyzer scan is driven by a sawtooth voltage derived from a D/A converter, the input to which is counterclocked at a constant rate, hence the digital output of the counter represents frequency on a linear scale. At each new count, the spectrum analyzer output is converted to a digital representation by an A/D converter, and the binary number representing the current sample is compared with that obtained on the previous count. If the current sample is the larger of the two, it is saved by storing in a latch, along with the binary number representing its frequency; if it is smaller, the previous one is retained until the next comparison. This process is continued for the entire sweep. It is evident that the number remaining in the frequency-store latch, when the sweep is completed, corresponds to the highest signal power observed; i.e., the peak of the spectrum. At the end of each sweep, the new peak frequency replaces that obtained on the previous sweep. An example of the output is shown in Fig. 2-10 for the case of an FM signal of center frequency 2.0 MHz (f_o) modulated sinusoidally to $\pm$200 kHz about f_o at a 5-Hz rate. The raw spectral information (output of the spectrum analyzer) is also made available to the Systems Engineering Laboratories (SEL) 810A data-logging minicomputer which is programmed to generate its own estimate of the spectral peak.

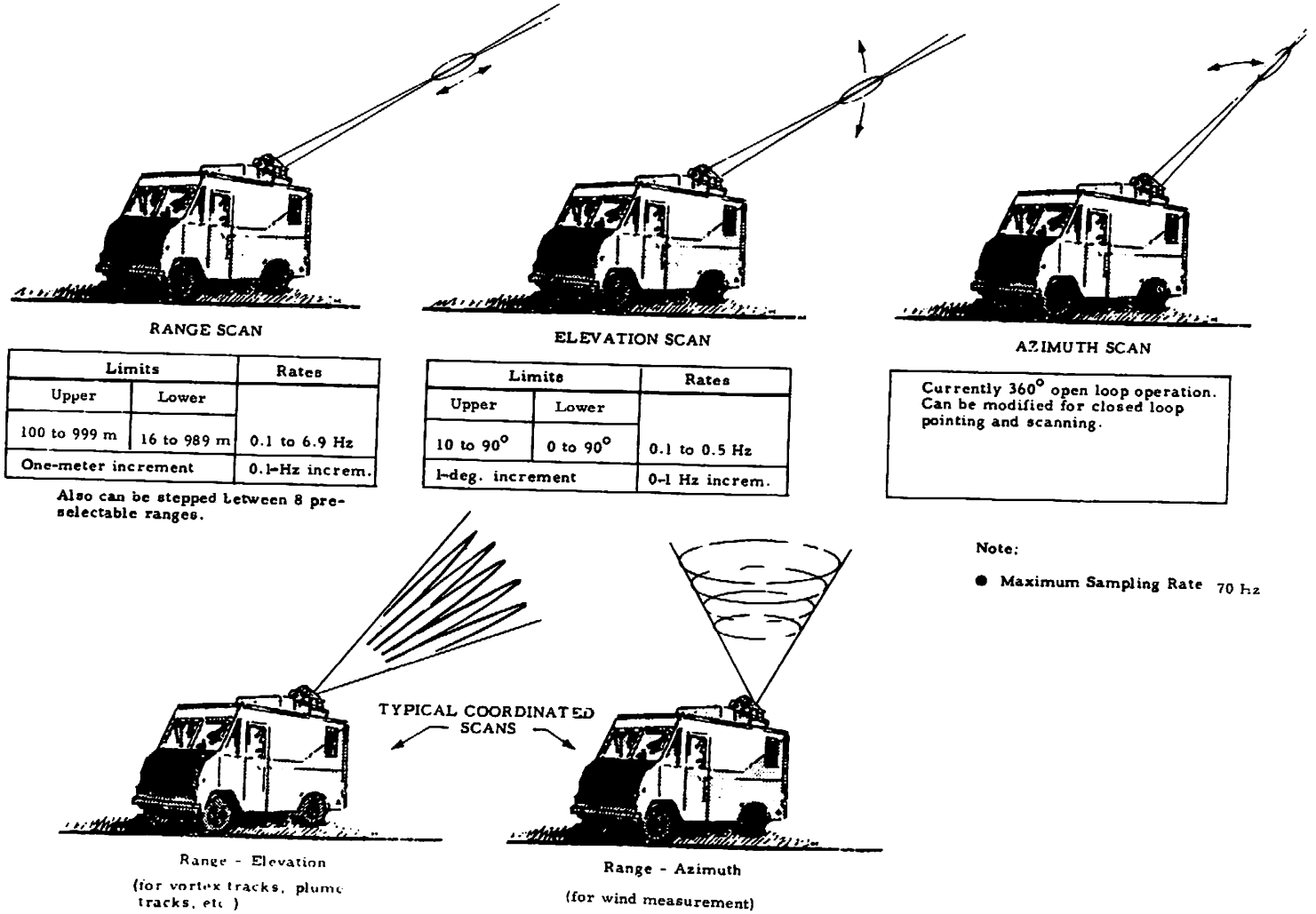

FIGURE 2-5. SCAN CAPABILITIES OF LASER DOPPLER VELOCIMETER.

FIGURE 2-6. LOCKHEED-HUNTSVILLE MOBILE ATMOSPHERIC UNIT.

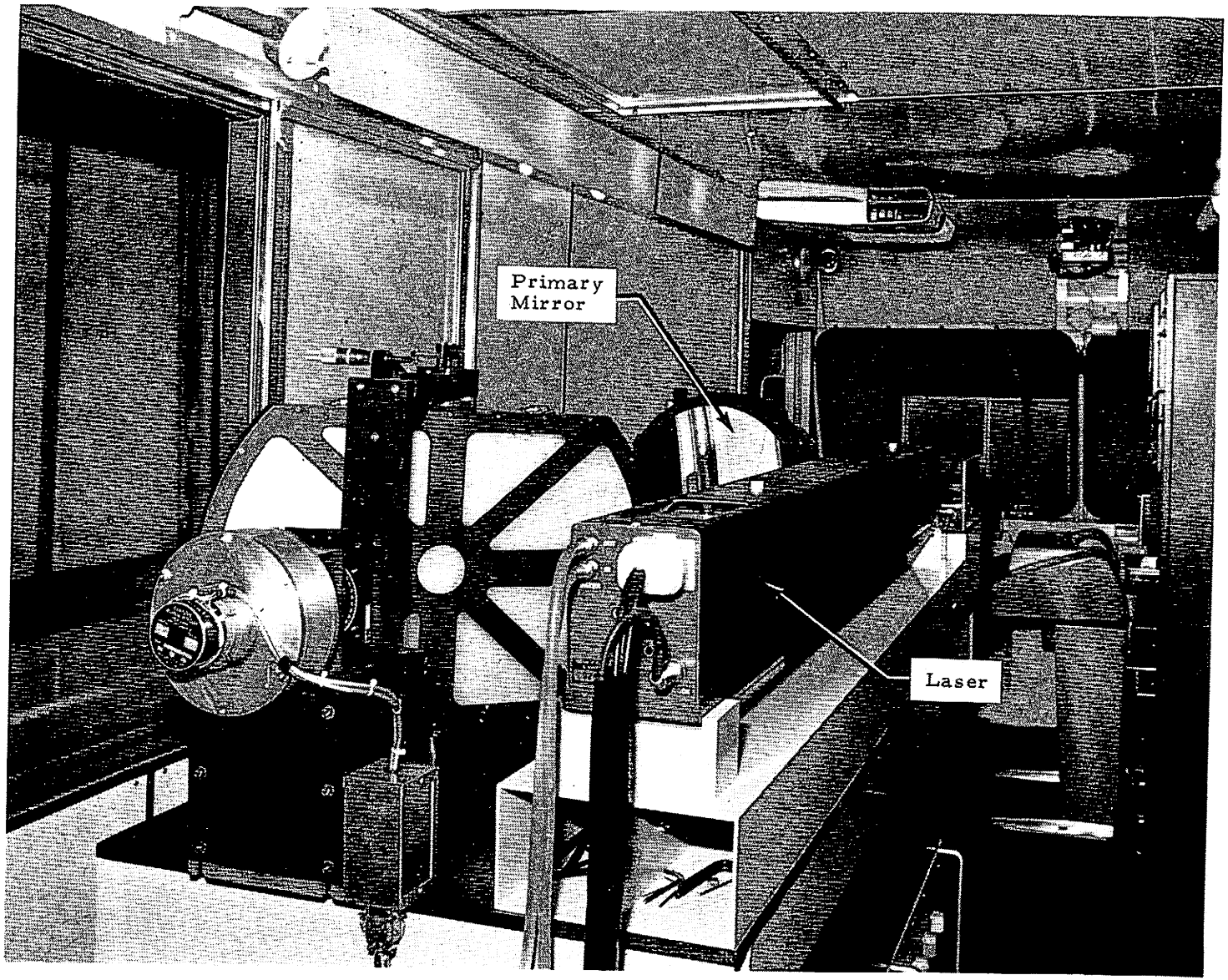

FIGURE 2-7. INTERIOR VIEW OF MOBILE ATMOSPHERIC UNIT LOOKING FORWARD.

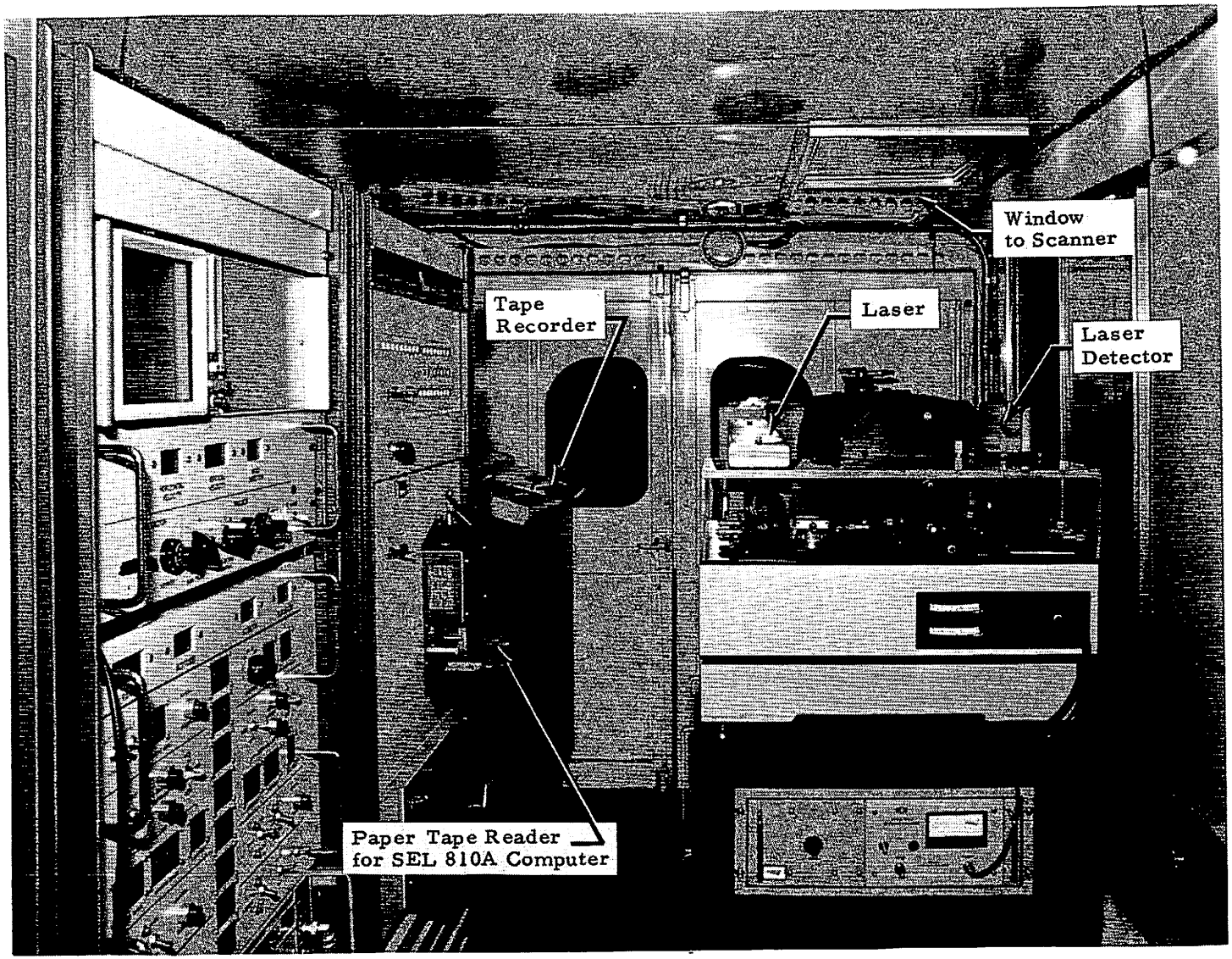

FIGURE 2-8. INTERIOR VIEW OF MOBILE ATMOSPHERIC UNIT.

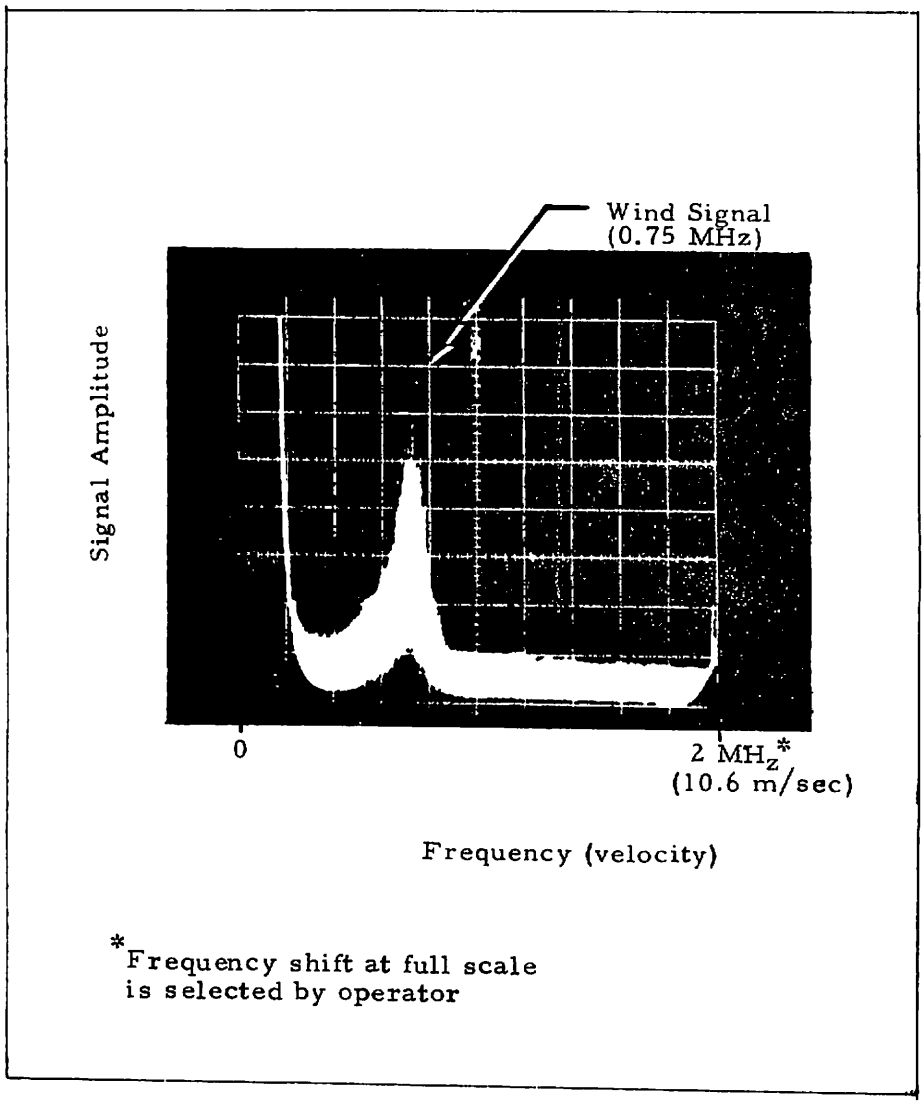

FIGURE 2-9. TYPICAL LASER DOPPLER VELOCIMETER WIND SIGNATURE AS DISPLAYED BY SPECTRUM ANALYZER.

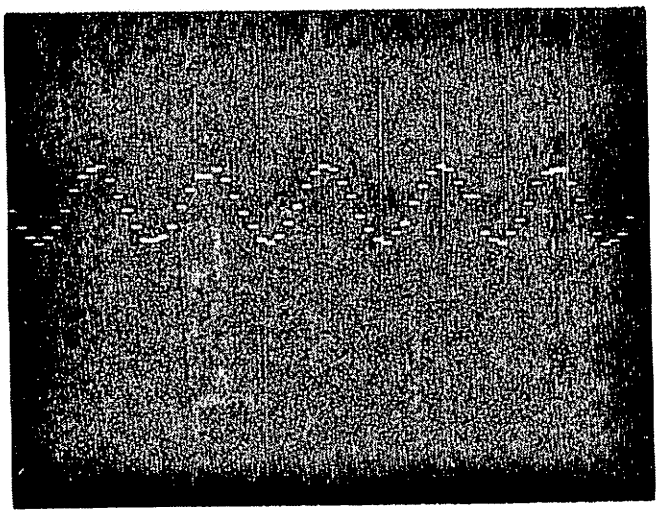

f_m = 5 Hz Sine Wave

Oscilloscope Data
Horiz. = .1 sec/div
Vert. = 1 V/div

FIGURE 2-10. OUTPUT OF SIGNAL PROCESSOR FOR FREQUENCY MODULATED INPUT.

A provision is included for tracking single-sideband suppressed-carrier signals, with an identification of upper or lower sideband such that when used in conjunction with an acousto-optic modulator the unit can discriminate the sign of the Doppler shift. The signal feedthrough at the translated frequency can also be discriminated against digitally, thus eliminating the need for a notch filter. Such a translating device was not used in the data collection described herein.

2.1.4 Data Recording and Display

The primary data-gathering function is performed by the SEL 810A general-purpose minicomputer. Data acquired by the Mobile Atmospheric Unit is formatted by the computer software and stored on magnetic tape for subsequent off-line processing. The SEL 7-track tape control and magnetic tape units allow digital recording of data at 800 bpi at 45 ips. The data logged by the computer include:

All scan volume location parameters
"Mode of operation" identifier
The instantaneous line-of-sight velocity information
The Doppler spectrum peak strength
Full spectrum intensity and frequency information
A data-quality identifier.

Properties of the Doppler spectrum; namely, the amplitude and frequency corresponding to the spectral peak, are obtained as a result of on-line computer processing except for the frequency, which is also obtained by the spectral peak locator (velocity processor) discussed previously. The latter allows some flexibility for on-line operator displays (see below). The velocity processor estimate of the instantaneous line-of-sight velocity, updated at a 70-Hz rate, is available in analog format which can be recorded directly on a stripchart recorder, an option which is extremely useful during the VAD mode of operation for monitoring the characteristic profile.

A view of the computer and associated LDV electronics is shown in Fig. 2-11.

2.2 WINDS ALOFT SENSING

Using the basic system outlined previously it is possible, by scanning operations, to determine the three-component wind field at any altitude between 16 and 865 meters. The scanning method employed is commonly referred to as the Velocity Azimuth Display (VAD) technique and was first used by Lhermitte and Atlas in conjunction with a microwave radar (Ref. 6).

The telescope is focused at the altitude of interest, the beam being directed at a zenith angle, α. The beam is then scanned in azimuth, thus tracing out a circle at the selected altitude (Fig. 2-12).

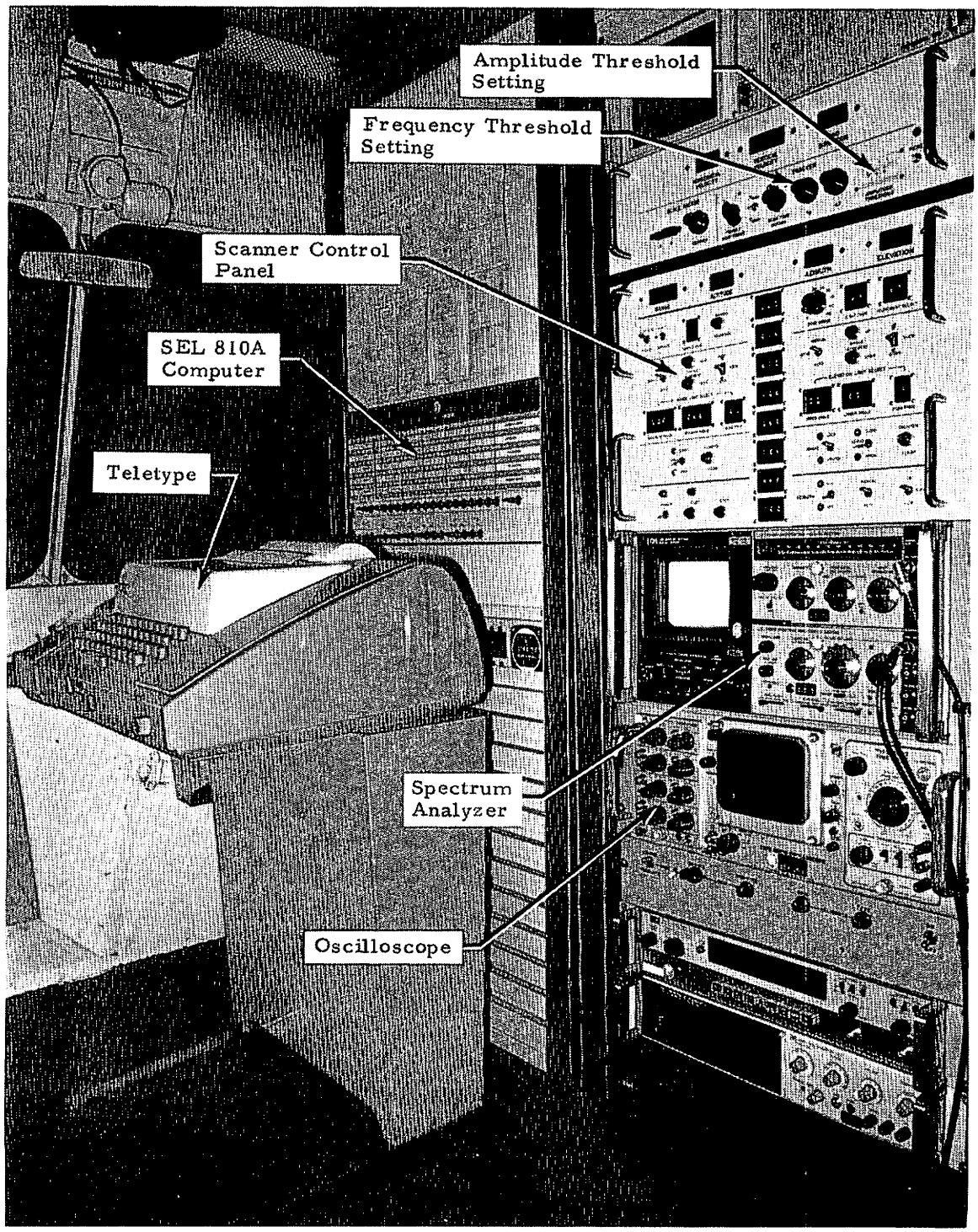

FIGURE 2-11. COMPUTER MAINFRAME TELETYPE AND LASER DOPPLER VELOCIMETER ELECTRONICS.

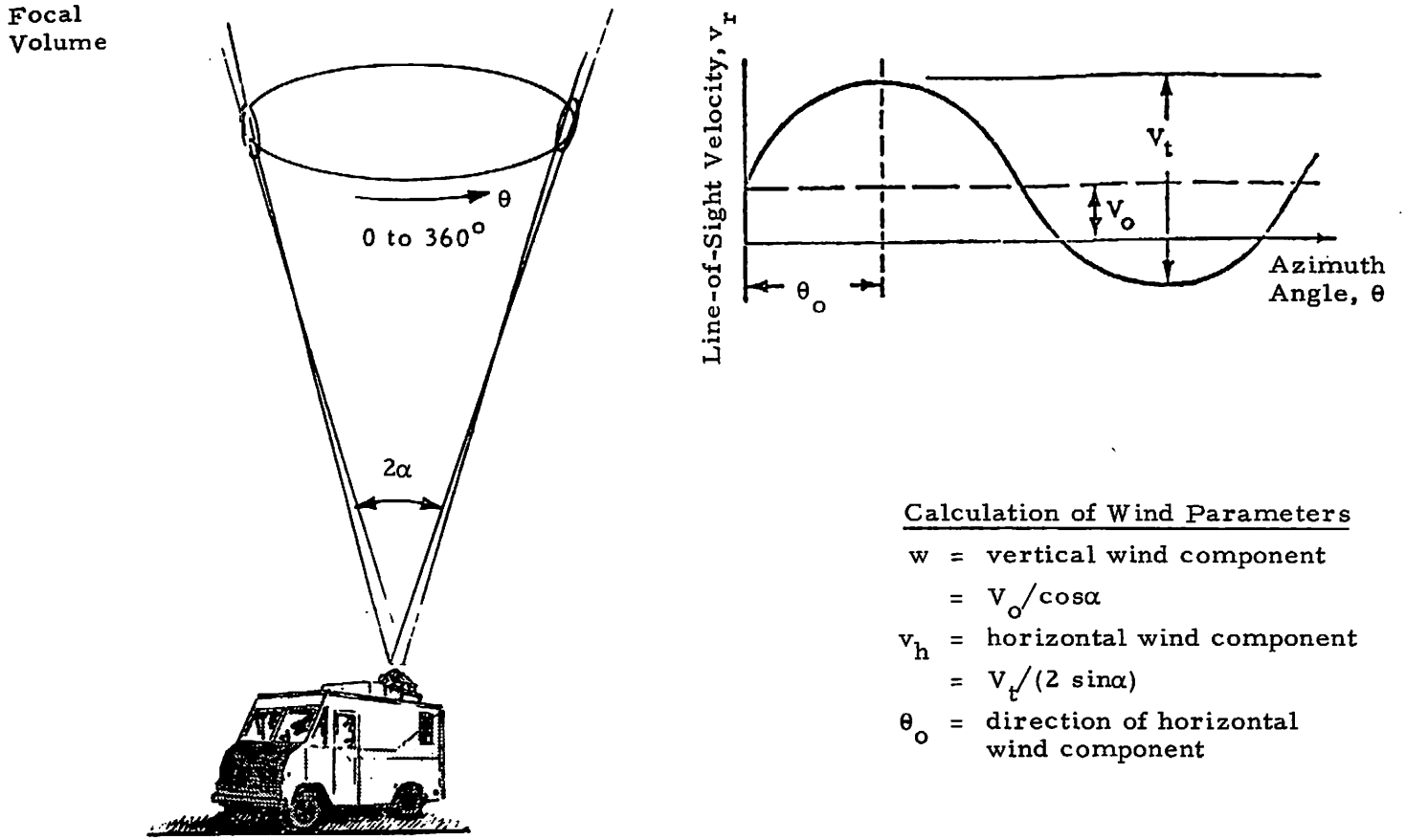

Calculation of Wind Parameters

w = vertical wind component
  = $V_o/\cos\alpha$

v_h = horizontal wind component
  = $V_t/(2\sin\alpha)$

θ_o = direction of horizontal wind component

FIGURE 2-12. PRINCIPLE OF VELOCITY AZIMUTH DISPLAY OPERATION.

The instantaneous line-of-sight component of velocity within the sensing volume as measured by the LDV, v_r, is given by

$$v_r = v_h \sin\alpha \cos(\theta - \theta_o) + w \cos\alpha ,$$

v_h and θ_o, respectively, being the speed and direction of the horizontal wind component, and w the vertical component at the height being sampled. The azimuthal dependence of v_r is sufficient to yield the horizontal speed and direction and the vertical component of velocity.

In the present mode of operation, the system is unable to distinguish between positive and negative values of v_r. Therefore, it is the absolute value of v_r ($|v_r|$) that is sensed. This results in a signal as shown in Fig. 2-13 instead of the sinusoidal signal as shown in Fig. 2-12. Thus, there is an ambiguity of 180 deg in the wind direction since it is uncertain which peak in Fig. 2-13 represents looking into the wind. In practice, the ambiguity is removed by the operator recording approximate wind direction. The data processing technique can then calculate exact wind direction. This resolves all wind direction ambiguities if the operator's input estimate is within ± 89 deg of the true wind direction.

$$v_h = (V_1 + V_2)/(2 \sin\alpha)$$
$$w = (V_1 - V_2)/(2 \cos\alpha)$$

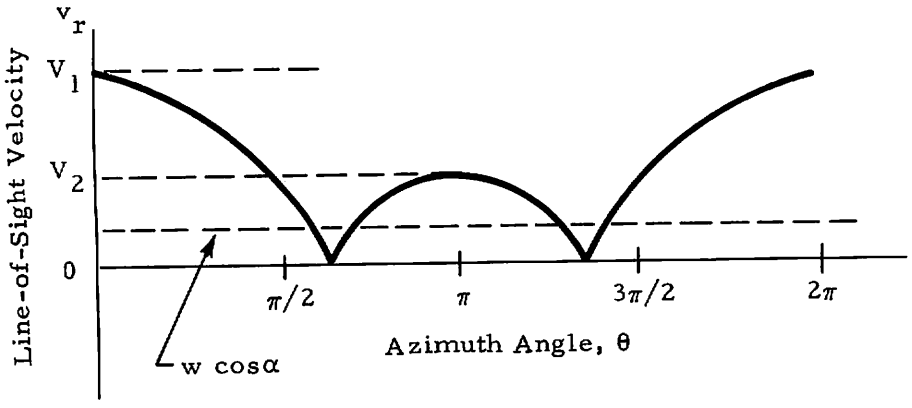

FIGURE 2-13. AZIMUTH ANGLE DEPENDENCE OF MEASURED VELOCITY COMPONENT

While operating in the VAD mode, the system is capable of measuring winds at n (n = 1 through 8) altitudes (that can be dialed in by using thumb-switches) in sequence over a total time period of 5np seconds, where

5 sec = time for conical sweep at one altitude for this test,
n = number of altitudes to be interrogated, and
p = number of VAD scans at each altitude (can be chosen to be 1 through 7).

During this investigation, n = 8, p = 1 were utilized, thus allowing the measurement of wind at eight altitudes every 40 seconds. Sequencing through the eight altitudes was performed for the test duration required. Data were also taken with continuous scanning at one altitude (n=1, p=1).

3. COMPUTER-SOFTWARE SYSTEM DEVELOPMENT

Acquisition and processing of the LDV signature is accomplished by means of a compact data-handling system developed specifically for the Lockheed-Huntsville MAU. The general elements of the MAU data acquisiton-and-processing system are shown in Fig. 3-1. The digitized LDV intensity versus frequency signal along with its coordinates in space is fed into the SEL 810 minicomputer. Preprocessing of the LDV signal is carried out on the minicomputer utilizing on-line computer programs written in SEL machine language. Information from the SEL 810 is stored on magnetic tape and is used as an input to the off-line processing algorithms. Off-line processing of the LDV signal is carried out on a Univac 1108 computer with programs written in FORTRAN language and using card inputs with information from the data logs to supplement the data. The final output consists of printouts and plots. A description of the data logger program and the VAD program and the operational characteristics of these programs is given in the following sections.

3.1 DESCRIPTION OF LASER DOPPLER VELOCIMETER SOFTWARE SYSTEM

Data acquisition in the MAU is carried out by the SEL Data Logger program. The Data Logger program preprocesses and records the LDV signal. A flowchart of the Data Logger program is given in Fig. 3-2. A sweeping spectrum analyzer is used to detect the Doppler shift frequency. A diagram of the output of the spectrum analyzer is shown in Fig. 3-3. For each sweep of 10-, 20-, or 50-millisecond duration, the Data Logger saves the maximum amplitude LDV signal, I_{ms}, and its corresponding frequency, V_{ms}, which are above both the amplitude and frequency thresholds. The definition of I_{ms} and V_{ms} and the shape of the characteristic LDV spectrum are shown in Fig. 3-3. The velocity at maximum signal intensity is V_{ms} and is taken

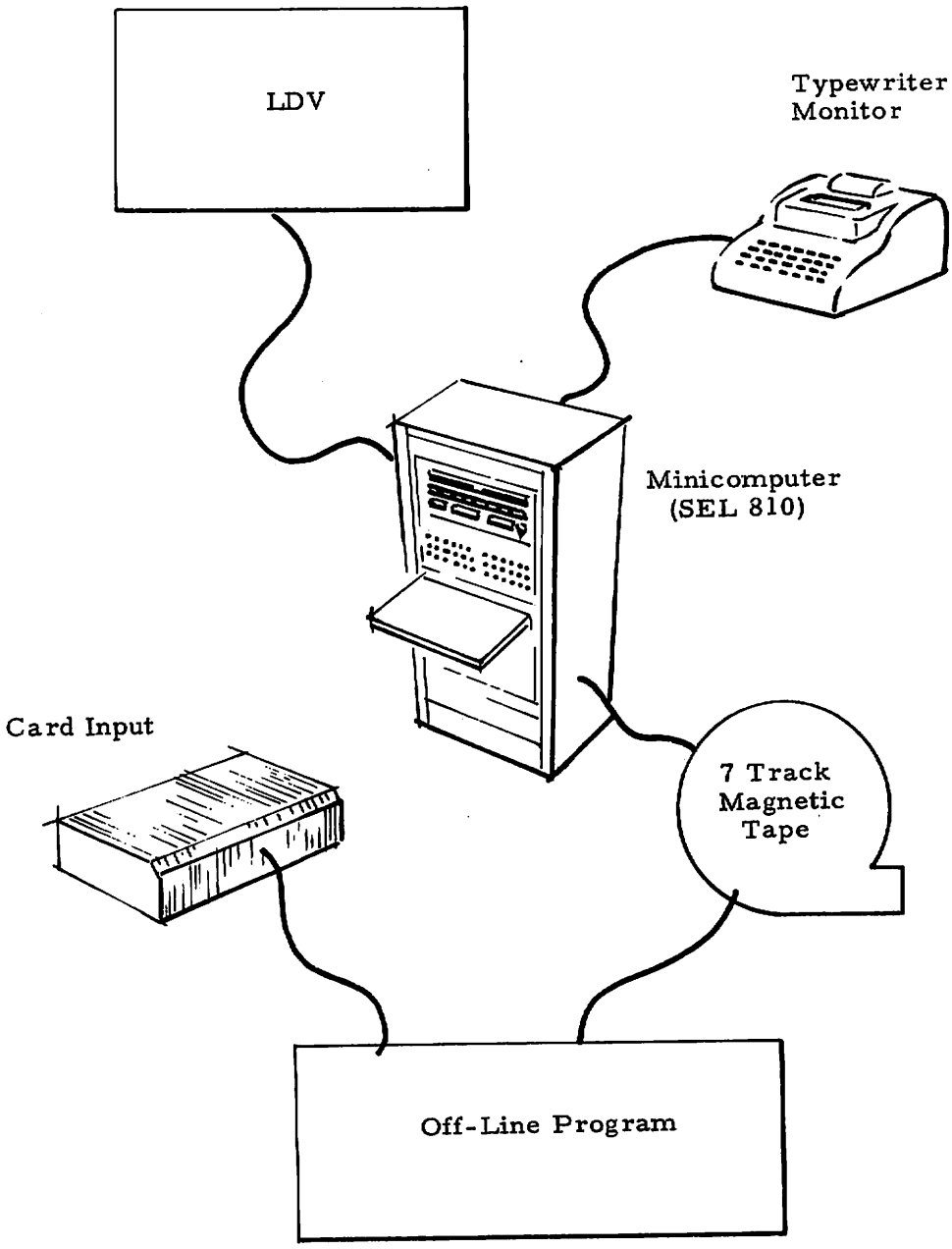

FIGURE 3-1. GENERAL ELEMENTS OF MOBILE ATMOSPHERIC UNIT DATA ACQUISITION-AND-PROCESSING SYSTEM.

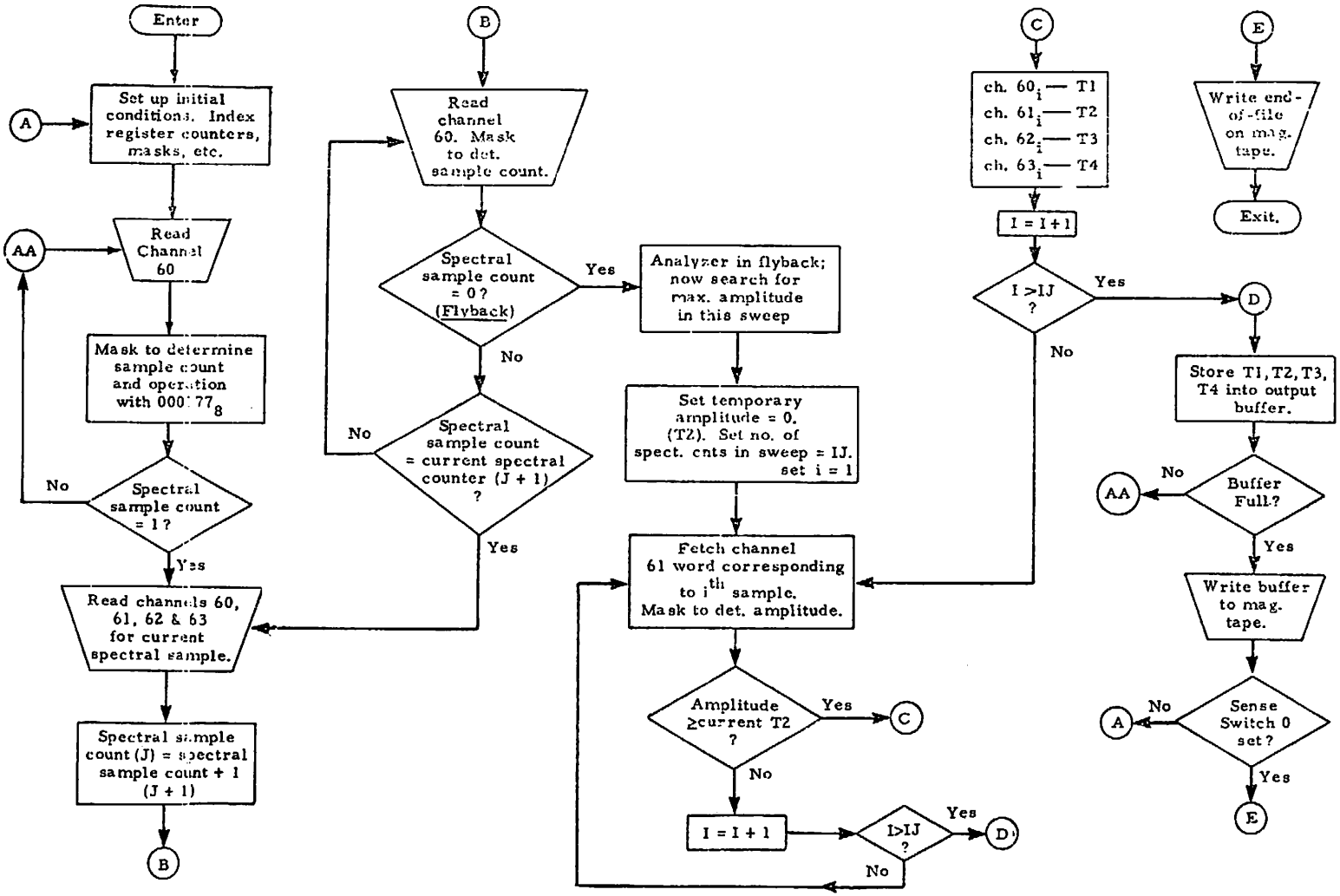

FIGURE 3-2. DATA LOGGER MACRO FLOWCHART.

V_{pk} = Line-of-sight velocity corresponding to highest Doppler frequency shift detectable above amplitude threshold

V_{ms} = Line-of-sight velocity corresponding to Doppler frequency shift at maximum signal intensity

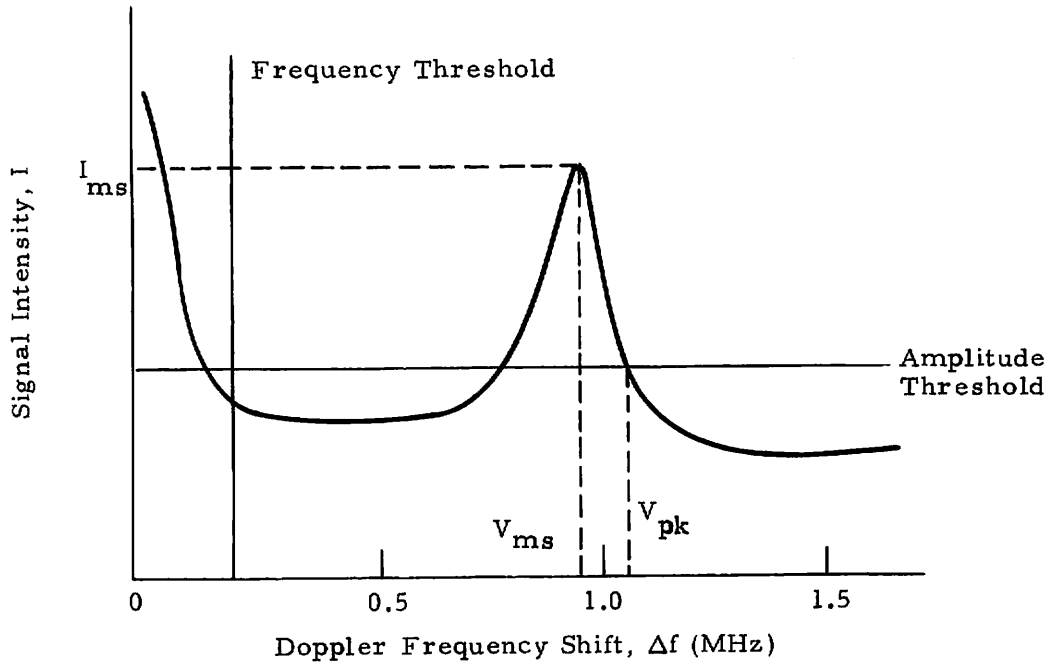

FIGURE 3-3. TYPICAL SPECTRUM ANALYZER OUTPUT IN VELOCITY AZIMUTH DISPLAY SCAN.

to be the characteristic line-of-sight velocity associated with the flow phenomenon. This choice is made because the maximum signal intensity is obtained from the center of the focal volume.

The output from the Data Logger program consists of V_{ms} as a function of time and space. From the output of the Data Logger, the wind field can be reconstructed using off-line processing routines.

Final processing of the LDV measurements is carried out by the VAD program. A macro flowchart of the VAD program is shown in Fig. 3-4. In this off-line program the array of V_{ms} values which is a function of time and space is processed to yield the three-dimensional wind field in the VAD mode. The program is formulated to calculate winds for both the translated and non-translated LDV signal. A translated signal is provided when the LDV system includes a frequency translator which distinguishes between positive and negative values of line-of-sight velocity. A non-translated signal provides only the absolute value of line-of-sight velocity as shown in Fig. 2-13. However, during the course of this research effort, all of the data acquisition-and-processing were done in the non-translate mode.

Three techniques have been implemented to compute the three-dimensional wind components: (1) a peak algorithm where the magnitude and location of the peak signal in the sinusoidal LDV VAD signature are used to compute the velocity components; (2) a spectral processing for the winds using the derectified signal; and (3) a sine curve fit. The final output is a printout (and selected plots) of the wind velocity components as a function of altitude and time. Wind velocity components are given for both rectilinear orthogonal components and cylindrical components.

3.2 OPERATION OF LASER DOPPLER VELOCIMETER SOFTWARE SYSTEM

Operation of the Lockheed-Huntsville MAU involves initialization of the SEL Data Logger program and the recording of the LDV signatures. After

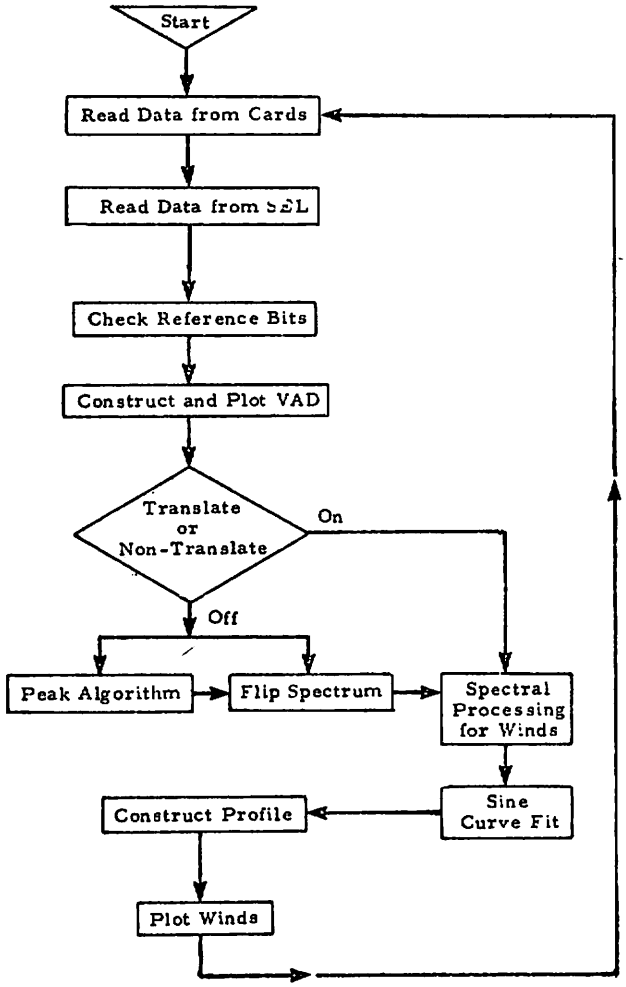

FIGURE 3-4. MACRO FLOWCHART OF OFF-LINE VELOCITY AZIMUTH DISPLAY PROGRAM.

the measurements have been recorded at the proper threshold settings, the VAD program is used to process the data into VAD plots. It is useful to examine the data-processing operations involved in determining the three-dimensional wind velocity field from the LDV measurements in terms of on-line preprocessing and off-line processing.

3.2.1 On-Line Data Processing

The conical scan VAD measurements are preprocessed on the SEL computer and recorded on magnetic tape. The output from the SEL computer consists of the basic V_{ms} signal as well as additional test parameters which are listed in Table 3-1. It is useful to consider the type of data recorded by the SEL during normal operations in the VAD mode.

A dump of a sample output tape from the Data Logger operating in the VAD mode is shown in Fig. 3-5, each row of data corresponding to information recorded for each spectrum-analyzer sweep. The information, packed into four computer words on tape, is separated into 13 columns in the printout with interpretation of the various columns being as follows:

Column	Interpretation
1 (PEAK/MAX)	An indication as to whether the peak Doppler frequency (f_{pk} corresponding to V_{pk} in Fig. 3-4) or maximum signal Doppler frequency (f_{ms} corresponding to V_{ms} in Fig. 3-4) is used. Indication is 0 if maximum signal frequency is used and is 1 if peak velocity signal is used.
2 (θ = 0)	A conical-scan azimuth reference which is nonzero when the reference switch is activated.
3 (NOR/VAD)	An indication as to whether the system is operating in the normal (vortex track) (1) or VAD (0) mode.
4 (SWEEP SPEED)	Sweep speed of the spectrum analyzer trace in msec/cm
5 (DIG TRCK)	The computer-calculated estimate of f_{pk} (percent of full scale).
6 (DATA ACCEPT)	An indication that there is (1) or is not (0) an output above the frequency and amplitude thresholds during a sweep.

TABLE 3-1

INPUT FROM SYSTEMS ENGINEERING LABORATORIES COMPUTER

Each VAD run is in a separate file. The following data are recorded for each spectrum analyzer sweep.

1. Spectral Sample Count Across Spectrum Analyzer S /eep, Corresponding to V_{max}
2. Amplitude at Above Point
3. Data Acceptable Flag
4. Flag for Spectrum Analyzer Sweep Speed
5. Flag for Translator
6. Flag for Positive or Negative Frequency (used only when translator is used)
7. Flag for V_{pk} or V_{ms}
8. Flag for Conical Scan or Normal Scan

For Conical Scan

9. Height above Van
10. Flag for Azimuth Switch
11. Cone Angle

WORD NO 1					WORD NO 2				WORD NO 3		WORD NO 4	
PEAK/ MAX	C=O	NOR/ VAD	SWEEP SPEED	DIG TRCK	DATA ACCEPT	+/-	TRANS/ NRN	SPECTRUM INTNSITY	NAR ROIN	ALT (MI)	LTRNG TRCK	CONE ANGLE
1	C	C	1C	38	1	1	C	232	1	323	37	3C
1	C	C	1C	38	1	1	C	208	1	323	36	3C
1	C	C	1C	39	1	1	C	190	1	323	37	3C
1	C	C	1C	39	1	1	C	254	1	323	38	3C
1	C	C	1C	36	1	1	C	192	1	323	38	3C
1	C	C	1C	38	1	1	C	190	1	323	35	3C
1	C	C	1C	38	1	1	C	144	1	323	36	3C
1	C	C	1C	40	1	1	C	190	1	323	36	3C
1	C	C	1C	41	1	1	C	142	1	323	38	3C
1	C	C	1C	40	1	1	C	144	1	323	40	3C
1	C	C	1C	42	1	1	C	144	1	323	39	3C
1	C	C	1C	2	1	1	C	1023	1	323	41	3C
1	C	C	1C	40	1	1	C	190	1	323	127	3C
1	C	C	1C	39	1	1	C	140	1	323	38	3C
1	C	C	1C	41	1	1	C	190	1	323	38	3C
1	C	C	1C	41	1	1	C	200	1	323	40	3C
1	C	C	1C	39	1	1	C	280	1	323	40	3C
1	C	C	1C	40	1	1	C	254	1	323	37	3C
1	C	C	1C	42	1	1	C	238	1	323	38	3C
1	C	C	1C	41	1	1	C	126	1	323	41	3C
1	C	C	1C	39	1	1	C	222	1	323	37	3C
1	C	C	1C	39	1	1	C	150	1	323	38	3C
1	C	C	1C	40	1	1	C	254	1	323	38	3C
1	C	C	1C	41	1	1	C	192	1	323	38	3C
1	C	C	1C	39	1	1	C	208	1	323	39	3C
1	C	C	1C	40	1	1	C	190	1	323	37	3C
1	C	C	1C	41	1	1	C	256	1	323	39	3C
1	C	C	1C	38	1	1	C	160	1	323	0	3C
1	C	C	1C	42	1	1	C	126	1	323	37	3C
1	C	C	1C	38	1	1	C	178	1	323	41	3C
1	C	C	1C	41	1	1	C	162	1	323	36	3C
1	C	C	1C	39	1	1	C	144	1	323	39	3C
1	C	C	1C	41	1	1	C	126	1	323	35	3C
1	C	C	1C	41	1	1	C	144	1	323	40	3C
1	C	C	1C	41	1	1	C	256	1	323	40	3C
1	C	C	1C	42	1	1	C	126	1	323	127	3C
1	C	C	1C	42	1	1	C	182	1	323	40	3C
1	C	C	1C	38	1	1	C	176	1	323	40	3C
1	C	C	1C	43	1	1	C	200	1	323	37	3C
1	C	C	1C	40	1	1	C	146	1	323	42	3C
1	C	C	1C	37	1	1	C	128	1	323	39	3C
1	C	C	1C	43	1	1	C	128	1	323	36	3C
1	C	C	1C	35	1	1	C	160	1	323	39	3C
1	C	C	1C	41	1	1	C	128	1	323	33	3C
1	C	C	1C	41	1	1	C	126	1	323	127	3C
1	C	C	1C	37	1	1	C	128	1	323	40	3C
1	C	C	1C	39	1	1	C	150	1	323	34	3C
1	C	C	1C	40	1	1	C	126	1	323	38	3C
1	C	C	1C	38	1	1	C	126	1	323	36	3C
1	C	C	1C	35	1	1	C	128	1	323	36	3C

FIGURE 3-5. DUMP OF SAMPLE OUTPUT TAPE FROM DATA LOGGER (With System Operating in Velocity Azimuth Display Mode).

Column	Interpretation
7 (+/-)	An indication as to the sense of the Doppler shift: 1 = moving toward MAU, 0 = moving away from MAU.
8 (TRANS/NON-TRANS)	An indication as to whether or not a frequency translator was incorporated. During this investigation, it was not incorporated. 1 = Yes, 0 = No.
9 (SPECTRUM INTENSITY)	Peak amplitude of the Doppler spectrum in region above a frequency threshold (arbitrary units ranging from 0 to 1024).
10 (NBR ROTN)	Number of successive VAD scans for a particular altitude.
11 (ALT (M))	Altitude of VAD for particular sweep in meters.
12 (LTRNC TRCK)	On-line frequency-tracker estimate of f_{pk} (should be approximately equal to column 5).
13 (CONE ANGLE)	Half-angle of VAD cone in degrees.

3.2.2 Off-Line Data Processing

Three algorithms for calculating the mean wind speed and direction from the VAD signature have been developed. For each of these algorithms, mean wind speed and direction are calculated for each 5-second VAD sweep. Standard deviations of wind speed and direction can be calculated from multiple VAD sweeps. The data output of the LDV system operating in the VAD mode are line-of-sight velocities measured at a selected number (usually 350 in the current Lockheed system) of distinct points around the VAD cone. Recall that the line-of-sight velocity signature is theoretically sinusoidal in the VAD mode (cf., Fig. 2-12).

For all the processing algotithms, preprocessing of the data occurs; the preprocessing includes:

a. Save line-of-sight velocities for one roation of scanner.

b. If two or more rotations occur at the same altitude, average with previous rotation(s).

c. Assign azimuth angle to each point (assuming constant rotation rate).

d. Edit data to eliminate spurious points. Eliminated points are declared unacceptable.

e. Plot line-of-sight velocity versus azimuth angle.

The edit criterion for the elimination of spurious points is that the i^{th} point is eliminated if

$$\left|v_{r,i} - v_{r,i+1}\right| > .2\, v_{r,i+1},$$

and

$$\left|v_{r,i} - v_{r,i-1}\right| > .2\, v_{r,i-1}.$$

A sample plot of unedited line-of-sight velocity versus azimuth angle is shown in Fig. 3-6. Points for unacceptable data are shown as zero velocity.

3.2.2.1 Peak Algorithm

For the calculation of wind velocity by the peak algorithm, the procedure is:

a. Filter data with an n-point moving average.

b. Identify the two peak velocity points, V_{p1} and V_{p2}, that occur at a minimum of 90 degrees apart.

c. Compute the magnitude of the horizontal component of the wind

$$V_h = \frac{V_{p1} + V_{p2}}{2 \sin\alpha}.$$

d. Compute horizontal wind angle with help of estimated wind direction.

e. Compute the vertical component of the wind

$$w_v = \frac{V_{p1} - V_{p2}}{2 \cos\alpha}.$$

f. Derectify VAD signal if no translator is present and plot derectified signal. The signal is derectified, so that the positive peak of the derectified signature is the peak which is closer to the estimated wind direction recorded by the operator at the time the data are measured.

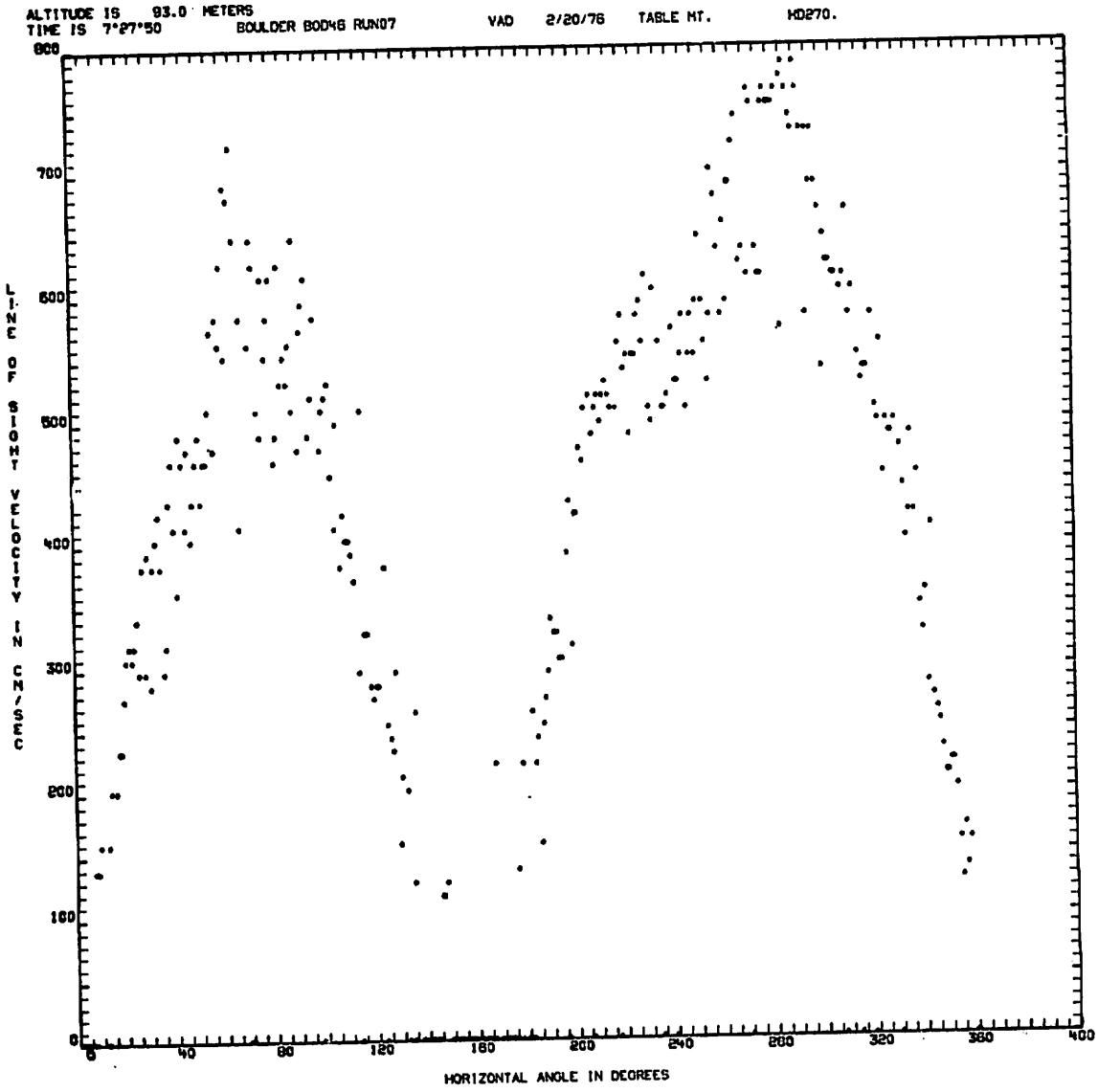

FIGURE 3-6. SAMPLE OUTPUT PLOT FROM THE VELOCITY AZIMUTH DISPLAY PROGRAM (Unedited).

The purpose of the filter is the elimination of nonuniformities in the data. This is especially important for the peak algorithm. The individual data points are filtered with an n-point moving average filter (n is usually 21). Thus, each line-of-sight point is filtered by

$$\overline{V}_{r,i} = \left[V_{r,i-\frac{n-1}{2}} + \cdots + V_{r,i-1} + V_{r,i} + V_{r,i+1} + \cdots + V_{r,i+\frac{n-1}{2}} \right] / n ,$$

where $\overline{V}_{r,i}$ is the filtered value of the line-of-sight velocity to be used in further calculations. A plot of the filtered line-of-sight velocities for a 21-point filter is shown in Fig. 3-7. Additional samples of LDV signatures (including raw data, filtered data, and derectified data) are presented in Appendix A.

When the LDV data are measured, an approximation of the wind angle is recorded. The calculated wind angle is the azimuth angle of the peak which is closer to the estimated wind angle. For small values of vertical component of velocity the wind angle plus 90 deg is the angle at which the line-of-sight velocity is theoretically zero. This angle is used for the derectification of the line-of-sight signal. A plot of the derectified (edited but unfiltered) line-of-sight velocity is presented in Fig. 3-8.

3.2.2.2 Fourier Coefficient Algorithm

The Fourier coefficient (or spectral) algorithm computes the fundamental harmonic of the line-of-sight velocity. The Fourier series for a generalized periodic function is

$$f(x) = \frac{a_o}{2} + \sum_{n=1}^{\infty} (a_n \cos nx + b_n \sin nx),$$

where the Fourier coefficients are given by

$$a_n = \frac{2}{L} \sum_{i=1}^{L} V_i \cos\left(\frac{2\pi i n}{L}\right),$$

$$b_n = \frac{2}{L} \sum_{i=1}^{L} V_i \sin\left(\frac{2\pi i n}{L}\right),$$

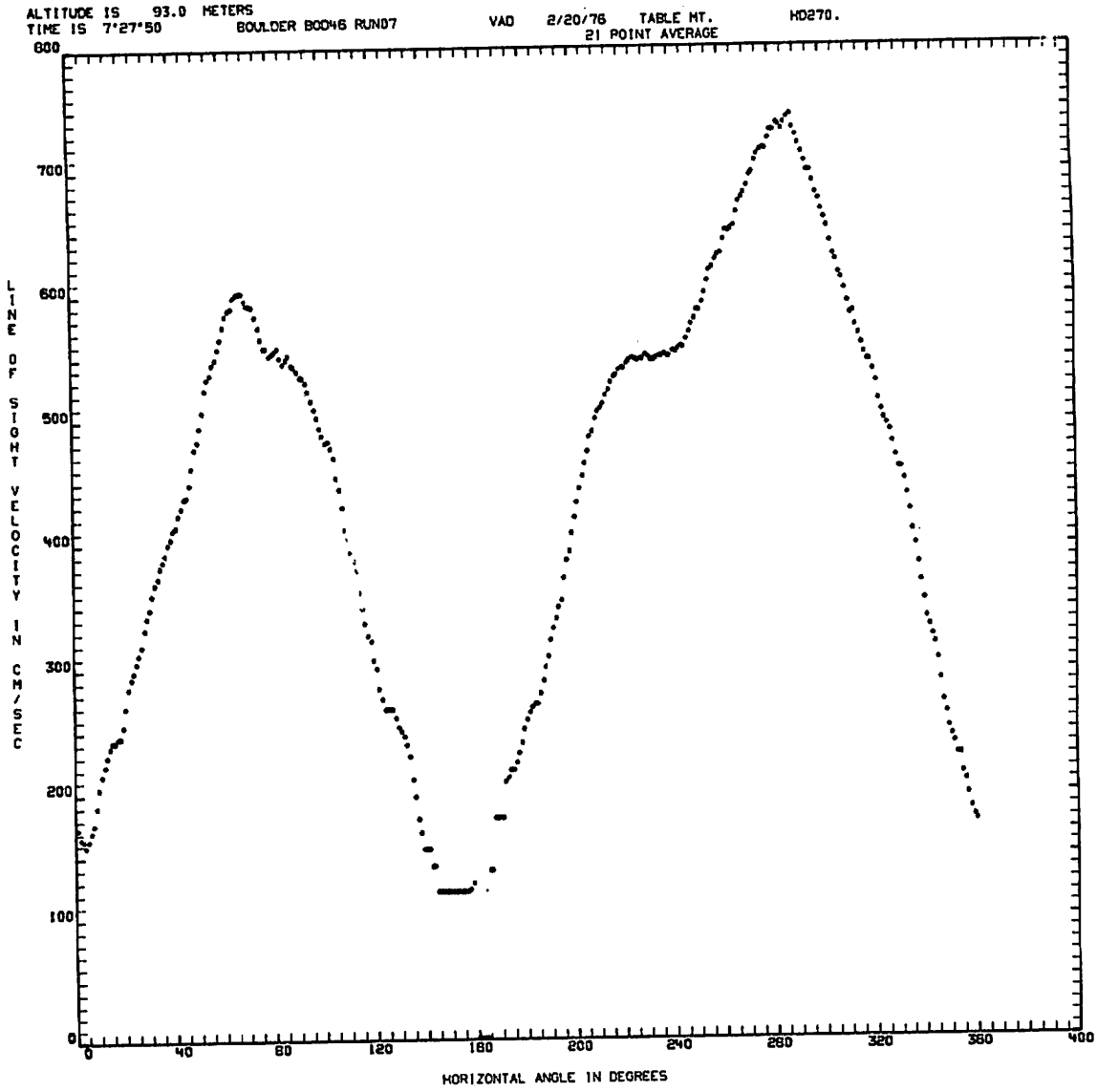

FIGURE 3-7. FILTERED LINE-OF-SIGHT VELOCITY FOR VELOCITY AZIMUTH DISPLAY MODE.

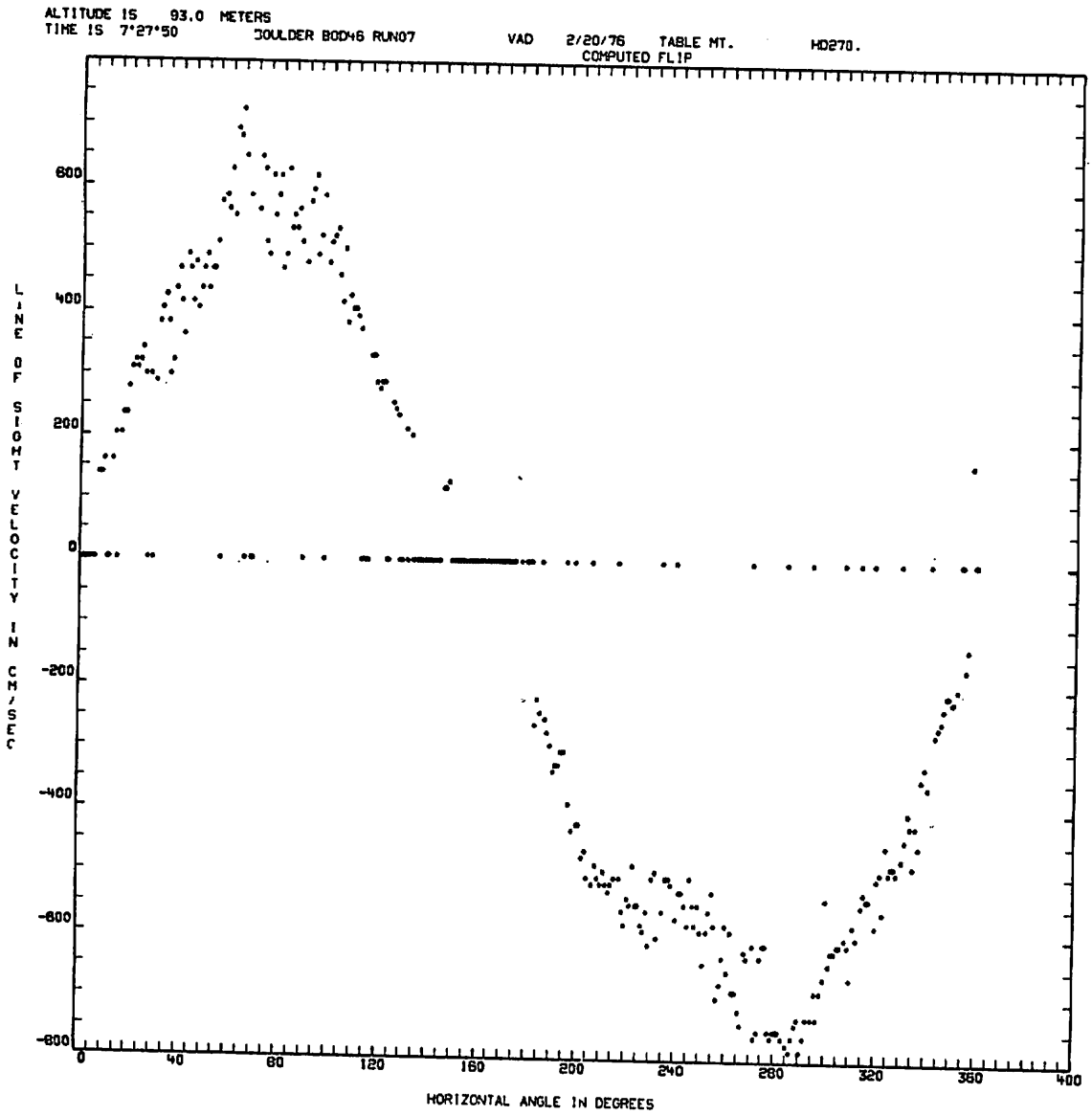

FIGURE 3-8. DERECTIFIED LINE-OF-SIGHT VELOCITY FOR VELOCITY AZIMUTH DISPLAY MODE (Edited, but Unfiltered Data).

where the L discrete points are uniformly spaced between 0 and 2π, and V_i is the line-of-sight velocity for the i^{th} point in the scan. For the calculation of the three wind components, it is necessary to calculate only a_0, a_1, and b_1. However, the second and third harmonics (i.e., n = 2 and n = 3) are also calculated as an indication of the nonuniformity of the wind. A correction factor must be applied to compensate for the absence of data points which lie below the velocity threshold. Although the line-of-sight signature in the VAD mode is theoretically sinusoidal, the existence of the velocity threshold causes the signature to appear as shown in Fig. 3-9. For the purposes of deriving the correction factor, the origin is chosen so that

$$v_r = \frac{a_0}{2} + b_1 \sin\theta.$$

In Fourier analysis, $a_0/2$ is the d-c component. If the vertical component of velocity is small compared with the magnitudeof the velocity threshold, the range of azimuth angles for which the signature is zero is as shown in Fig. 3-9. The parameter, Z, is the ratio of the number of zero points to the total

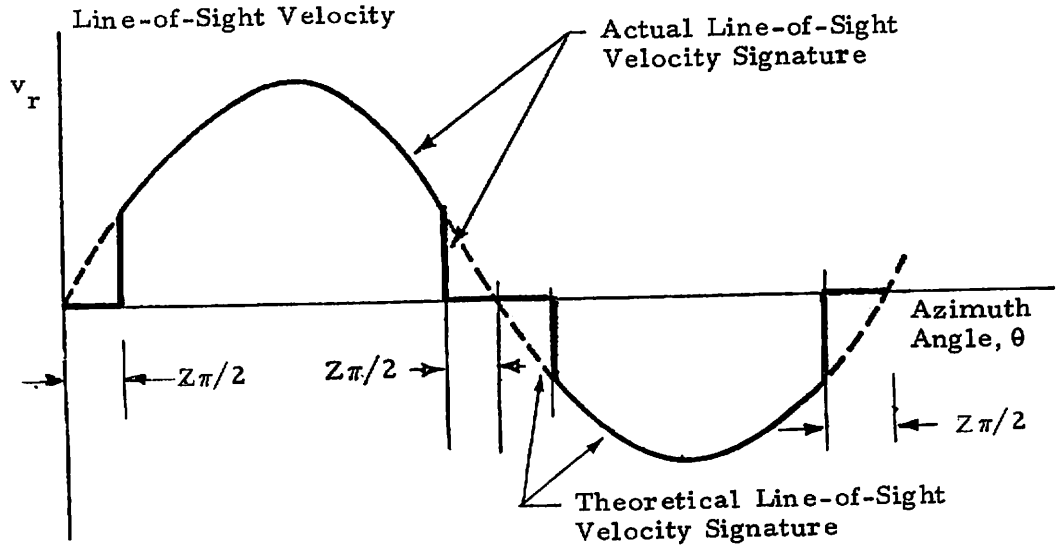

FIGURE 3-9. LINE-OF-SIGHT VELOCITY SIGNATURE OF VELOCITY AZIMUTH DISPLAY.

number of points in the VAD scan. Let a_0^* and b_1^* be the values of the Fourier coefficients calculated from the line-of-sight velocity signature. The integral form of the equations for the Fourier coefficients is used. For the theoretical velocity signature,

$$a_0^* = 1/\pi \int_0^{2\pi} (a_0/2 + b_1 \sin\theta)\, d\theta = a_0.$$

However, for the actual velocity signature,

$$a_0^* = 1/\pi \left[\int_{Z\pi/2}^{\pi - Z\pi/2} (a_0/2 + b_1 \sin\theta)\, d\theta + \int_{\pi + Z\pi/2}^{2\pi - Z\pi/2} (a_0/2 + b_1 \sin\theta)\, d\theta \right] = a_0 (1 - Z).$$

Therefore, a correction factor of $1/(1-Z)$ must be applied to the calculated value of a_0.

For the sine term, the theoretical velocity signature,

$$b_1^* = 1/\pi \int_0^{2\pi} (a_0/2 + b_1 \sin\theta) \sin\theta\, d\theta = b_1.$$

For the actual velocity signature,

$$b_1^* = 1/\pi \left[\int_{Z\pi/2}^{\pi - Z\pi/2} (a_0/2 + b_1 \sin\theta) \sin\theta\, d\theta + \int_{\pi + Z\pi/2}^{2\pi - Z\pi/2} (a_0/2 + b_1 \sin\theta) \sin\theta\, d\theta \right]$$

$$= b_1 \left[1 - Z + \frac{\sin Z\pi}{\pi} \right].$$

Therefore, a correction factor $1/[1 - Z + (\sin Z\pi)/\pi]$ must be applied to the horizontal wind components.

The calculation procedure for the spectral algorithm is:

a. Compute the Fourier coefficients for the d-c level and the first three harmonics (n=1, 2, 3):

$$a_n = 2/L \sum_{i=1}^{L} V_i \cos(2\pi i n/L),$$

$$b_n = 2/L \sum_{i=1}^{L} V_i \sin(2\pi i n/L).$$

b. Compute the corrected fundamental harmonic:

$$\text{Corrected Value} = \frac{1}{1 - Z + (\sin Z\pi)/\pi} * \text{Calculated Fundamental.}$$

c. Compute the vertical wind correction:

$$\text{Corrected Value} = \frac{1}{1 - Z} * \text{Calculated Value.}$$

d. Compute the magnitude of the horizontal component of velocity:

$$V_h = \frac{\sqrt{a_1^2 + b_1^2}}{\sin\alpha}$$

e. Compute the horizontal angle:

$$\text{Angle}_h = \text{Atan}(b_1/a_1).$$

f. Compute the vertical component of wind velocity:

$$w = \frac{-a_0}{2\cos\alpha.}$$

3.2,2.3 Sine-Curve-Fit Technique

The line-of-sight velocity signature is sinusoidal for a uniform wind. Therefore, the best sinusoidal wave which fits the data in a least-

squares sense is determined by finding the values of the coefficients A, B, and C which minimize (summing over all acceptable data points)

$$\sum_i (V_i - C - A\cos\theta_i - B\sin\theta_i)^2,$$

where V_i is the line-of-sight velocity (derectified) at point i, and θ_i is the azimuth at point i. A, B, and C are obtained from

$$\left[\sum_i \cos^2\theta_i\right]A + \left[\sum_i \cos\theta_i \sin\theta_i\right]B + \left[\sum_i \cos\theta_i\right]C = \sum V_i \cos\theta_i,$$

$$\left[\sum_i \cos\theta_i \sin\theta_i\right]A + \left[\sum_i \sin^2\theta_i\right]B + \left[\sum_i \sin\theta_i\right]C = \sum V_i \sin\theta_i,$$

$$\left[\sum_i \cos\theta_i\right]A + \left[\sum_i \sin\theta_i\right]B + nC = \sum_i V_i.$$

The steps for calculating the wind using the least-squares algorithm are:

a. Find the least-squares curve fit for a sine wave to minimize

$$\sum_i (V_i - C - A\cos\theta_i - B\sin\theta_i)^2,$$

where

V_i is line-of-sight velocity at point i,
θ_i is azimuth at point i, and
C, A, and B are coefficients to be calculated.

b. Compute the magnitude of the horizontal component of velocity:

$$V_h = \frac{\sqrt{A^2 + B^2}}{\cos\alpha}$$

c. Compute the horizontal angle:

$$\text{Angle}_h = \text{Atan}(B/A).$$

4. Compute the vertical component of wind velocity:

$$w_v = \frac{-C}{\cos\alpha}$$

4. DATA COLLECTION AT TABLE MOUNTAIN

4.1 TEST DESCRIPTION

During February and March 1976, the mobile LDV was deployed at the National Oceanic and Atmospheric Administration's Table Mountain Test Site, about 16 km north of Boulder, Colorado. During this period, the wind varied from 0 to 15 m/sec at the 30-m altitude Above Ground Level (AGL) to 0 to 18 m/sec at 148-m altitude. Light to moderate snowfall occurred twice, and no rainfall occurred during this period of time. Data were collected under atmospheric conditions from nearly laminar, thermally stable flow to strong, gusty, thermally unstable flow. A diagram of the test site layout is shown in Fig. 4-1, and a photograph of the test site is shown in Fig. 4-2.

By standard meteorological convention, the wind direction is the direction from which the wind comes. Therefore, when wind is given in speed-direction coordinates, the direction is the direction from which the wind comes, measured from north. The coordinates chosen for the test are shown in Fig. 4-1. For wind expressed in rectangular coordinates, the positive u component represents wind coming from the positive x direction (i.e., from east to west). Similarly, a positive v component represents wind coming from the positive y component (i.e., from north to south). For example, a wind coming from 135-deg has a positive u component and a negative v component.

The tower was instrumented with propeller-vane anemometers, Model 8002 manufactured by R.M. Young Co. at approximately 30, 60, 90, 120, and 150 m. The true altitudes AGL of the tower instrumentation were 31, 67, 95, 125, and 148 m and, in this report, are used interchangeably with the approximate values. As reported in Ref. 7, the anemometers were mounted on booms extended 2.5 m north of the tower structure and provided sensor exposure with undisturbed airflow except for a 90-deg sector centered roughly on 175-deg

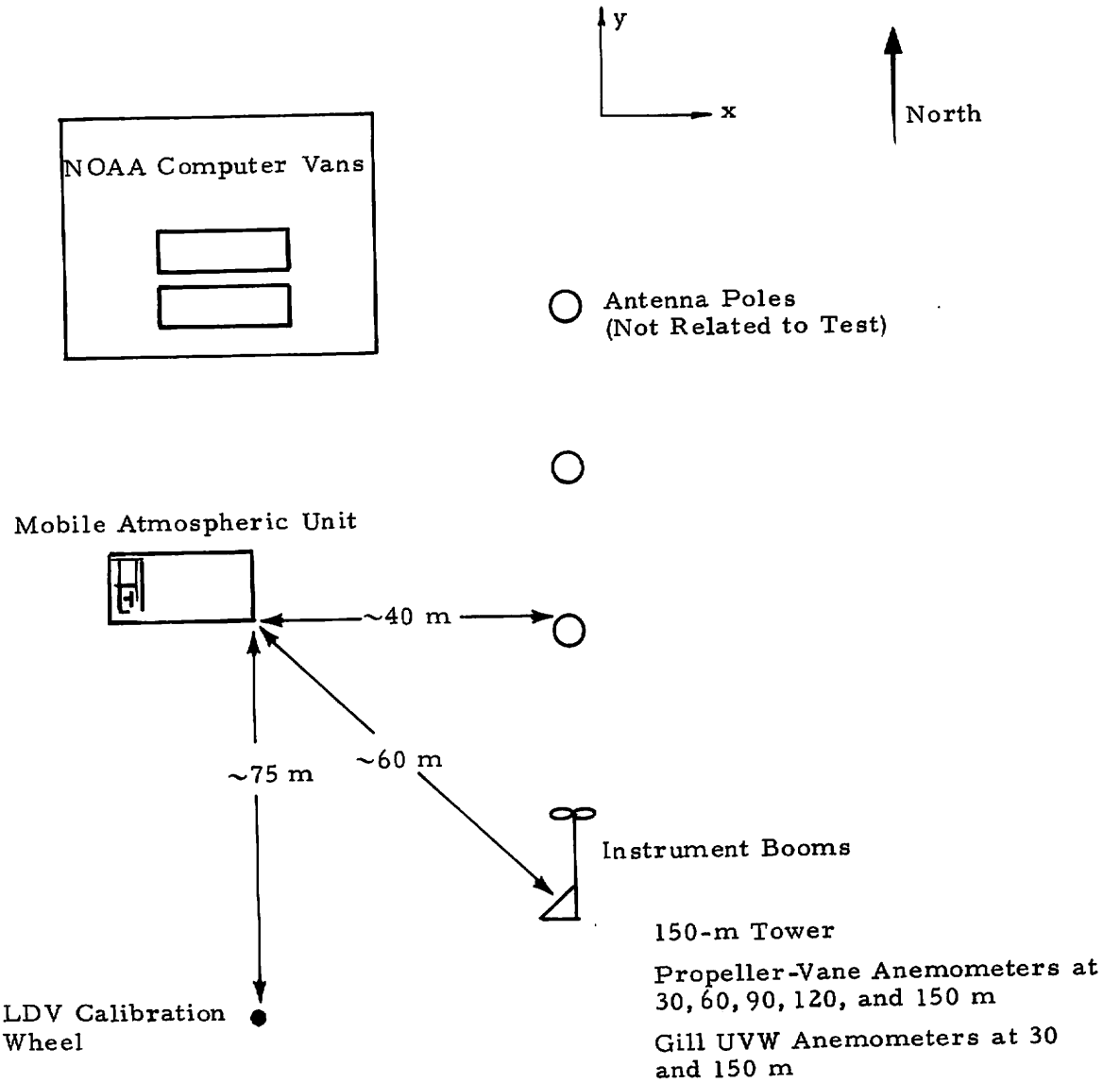

FIGURE 4-1. NATIONAL OCEANIC AND ATMOSPHERIC ADMINISTRATION TABLE MOUNTAIN TEST SITE LAYOUT.

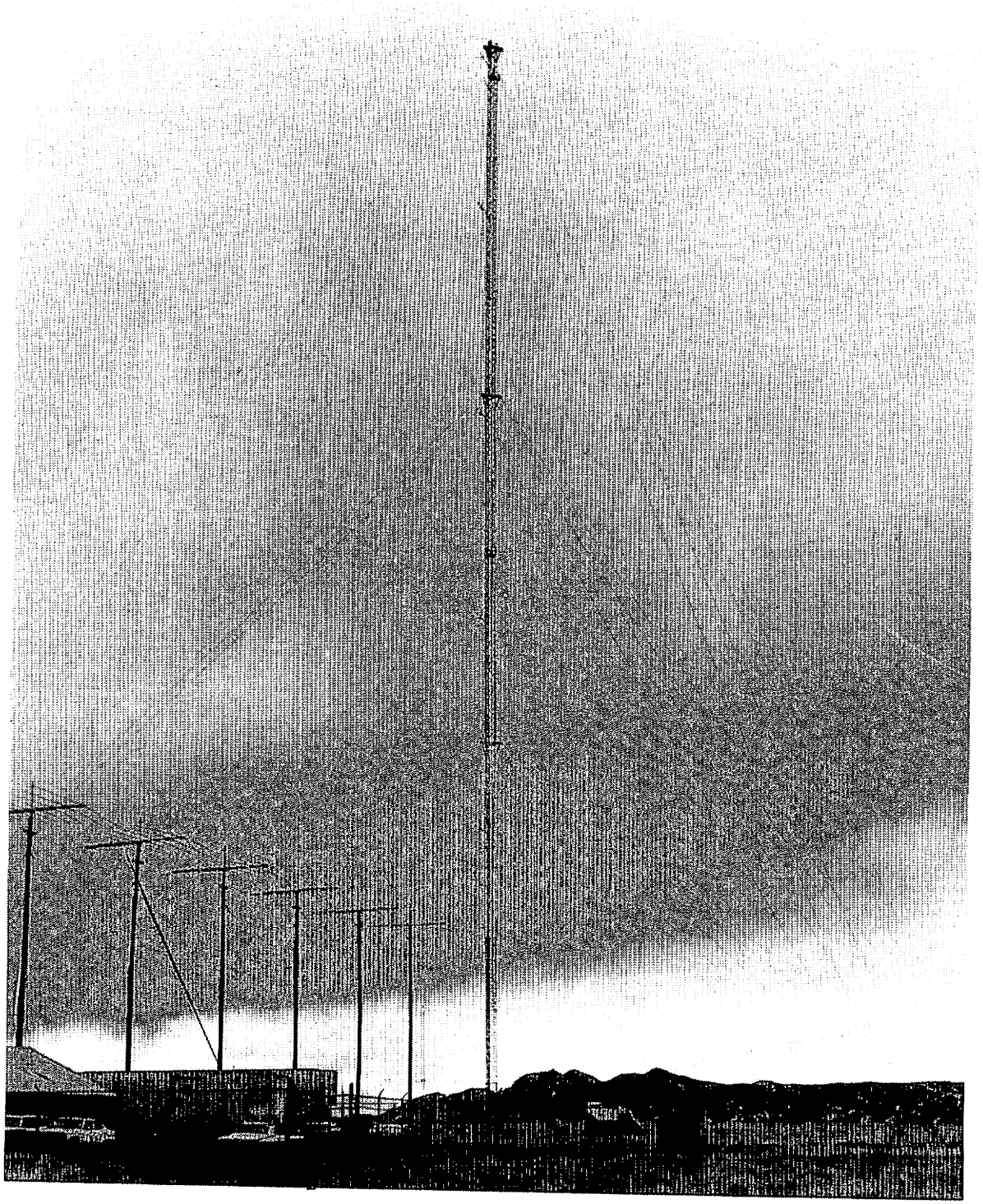

FIGURE 4-2. TABLE MOUNTAIN DATA COLLECTION SITE.

azimuth. A careful calibration was employed to certify the tower instrumentation measurements prior to their mounting on the tower. The calibration showed no observable systematic bias errors and less than $\pm$10 cm/sec difference between anemometers.

The anemometer outputs were transmitted to a computer-controlled data-acquisition system where each output was sampled once per second and the data processed in real time to yield the time-averaged wind data.

A summary of runs for which measurements were made is shown in Table 4-1.

4.2 TEST OBJECTIVES AND OPERATING PROCEDURE

The primary objectives of the test were to establish the validity of the VAD technique for three-dimensional wind measurement and to optimize data-processing algorithms to improve the accuracy of VAD wind measurement. A secondary objective was to investigate the effect of averaging time on the accuracy of VAD wind measurement relative to the tower measurements.

As discussed in Section 2, the MAU VAD scan capability allows wind measurement to be made at eight altitudes, each requiring 5 seconds for a 360-degree azimuth rotation. This requires 40 seconds for a complete scanning of the eight altitudes. The test was initiated with the laser scanning at 30, 45, 60, 75, 90, 120, 150, and 300-m altitudes.

4.3 DATA ANALYSIS OF INITIAL RUNS

The winds calculated with the three algorithms described in Section 3 are shown in Figs. 4-3 through 4-7 for one 16-minute sample. The sole difference between the three parts of each figure is the data-processing algorithm used. Some general observations are that the peak algorithm tends to give mean wind values that are biased slightly high compared with the tower-measured mean winds. This is primarily due to temporal variations in the

TABLE 4-1

SUMMARY OF RUNS AT TABLE MOUNTAIN, COLORADO

Run	Date (1976)	Start Time (MST)	End Time (MST)	Altitudes (m)	Comments
1	2-17	1540	1630	30, 45, 60, 75, 90, 150, 300	
2	2-18	1054	1216	30, 45, 60, 75, 90, 150, 300	
3	2-18	1319	1422	30, 45, 60, 75, 90, 150, 300	
4	2-18	1440	1549	30, 45, 60, 75, 90, 150, 300	
5	2-19	2206	0207	30, 45, 60, 75, 90, 150, 300	Heavy Snow
6	2-20	0245	0700	30, 45, 60, 75, 90, 150, 300	Heavy Snow
7	2-20	0725	1130	30, 45, 60, 75, 90, 150, 300	Overcast with Light Snow
8	2-20	1212	1331	30, 45, 60, 75, 90, 150, 300	
9	2-20	1235	1330	30, 45, 60, 75, 90, 150, 300	
10	2-20	1341	1455	30, 45, 60, 75, 90, 150, 300	Very Clear Air
11	2-20	1515	1637	30, 45, 60, 75, 90, 150, 300	
12	2-25	1410	1427	30, 60, 90, 120, 150, 300	
13	2-25	1451	1555	30, 60, 90, 120, 150, 300	
14	2-26	1023	1112	30	No Tower Data
21	3-7	1127	1227	150	
22	3-7	1335	1406	90	
23	3-9	1610	1710	90	
24	3-10	1550	1750	30	
25	3-10	1934	2049	150	
26	3-11	1955	2045	30	
27	3-11	2357	0358	90	Snowing ~ 1 cm/hr
28	3-12	0430	0745	150	
29	3-12	1308	1424	300, 270	

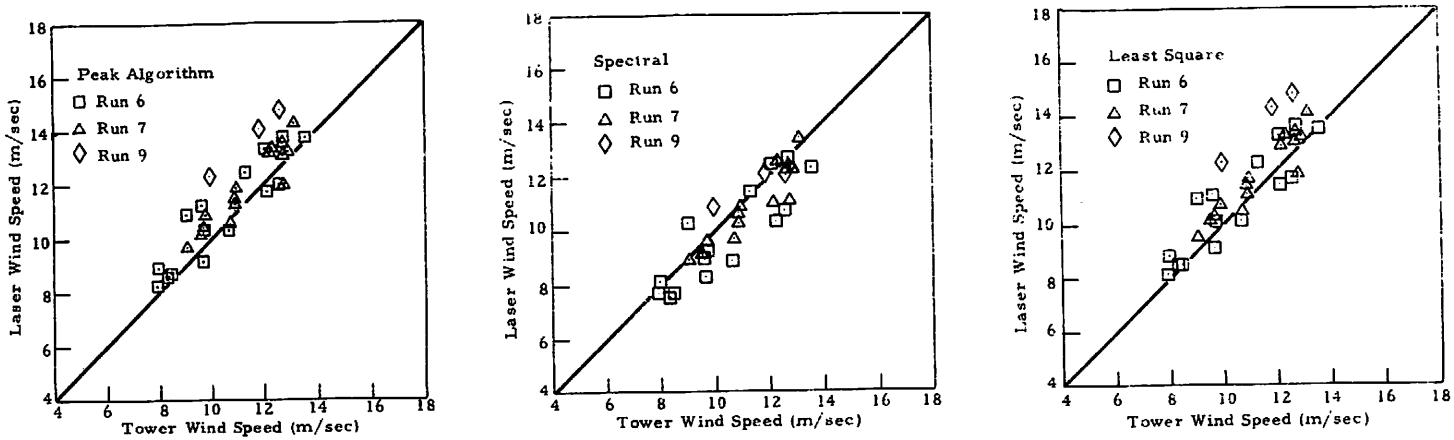

FIGURE 4-3. COMPARISON OF LASER AND TOWER 16-MIN WIND SPEED AT 30-M ALTITUDE.

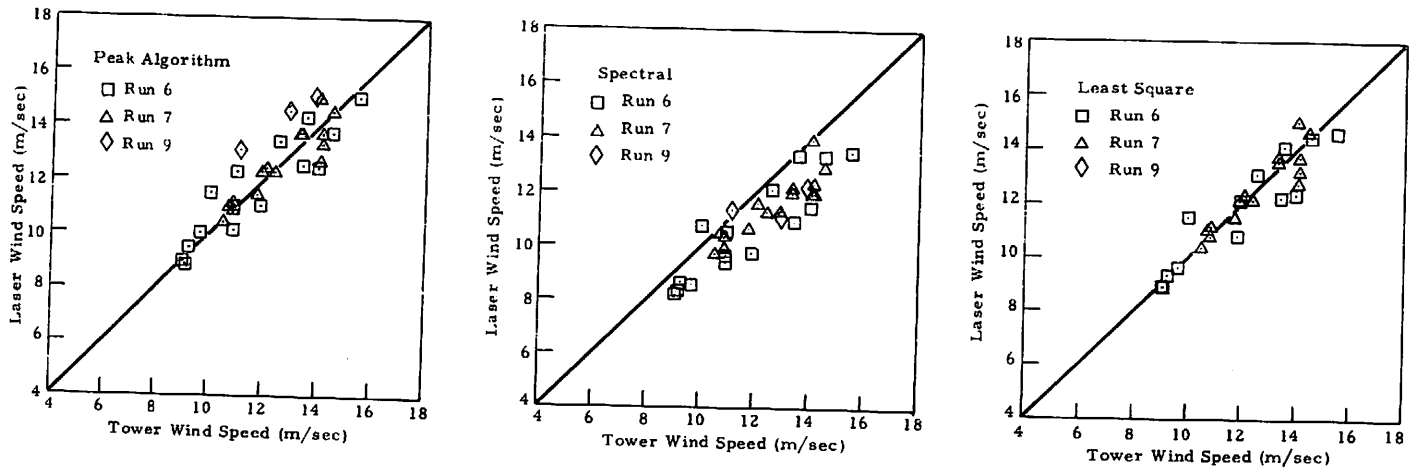

FIGURE 4-4. COMPARISON OF LASER AND TOWER 16-MIN MEAN WIND SPEED AT 60-M ALTITUDE.

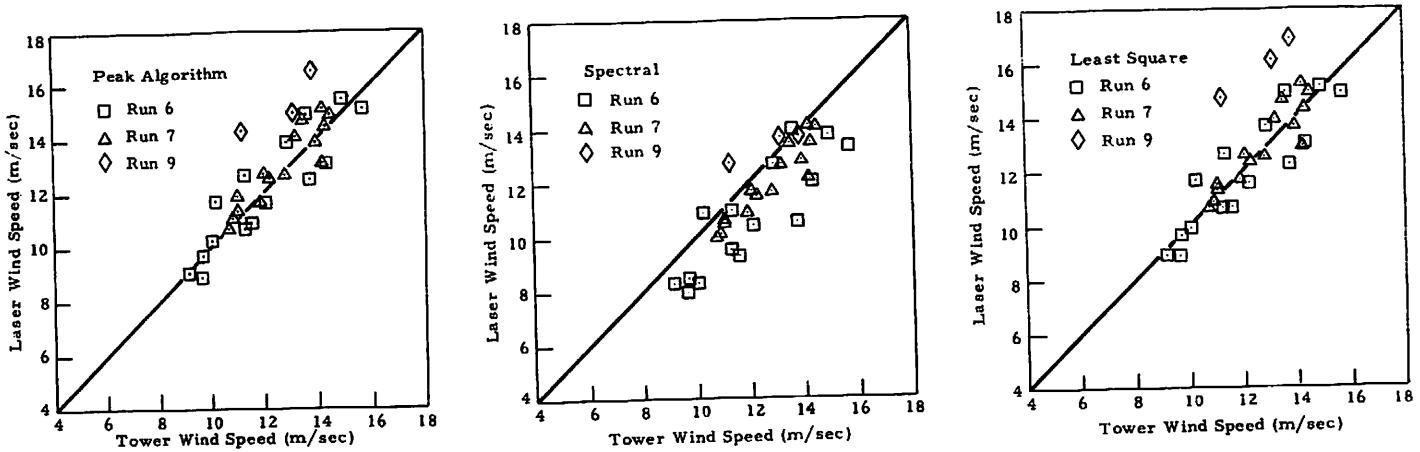

FIGURE 4-5. COMPARISON OF LASER AND TOWER 16-MIN MEAN WIND SPEED AT 90-M ALTITUDE.

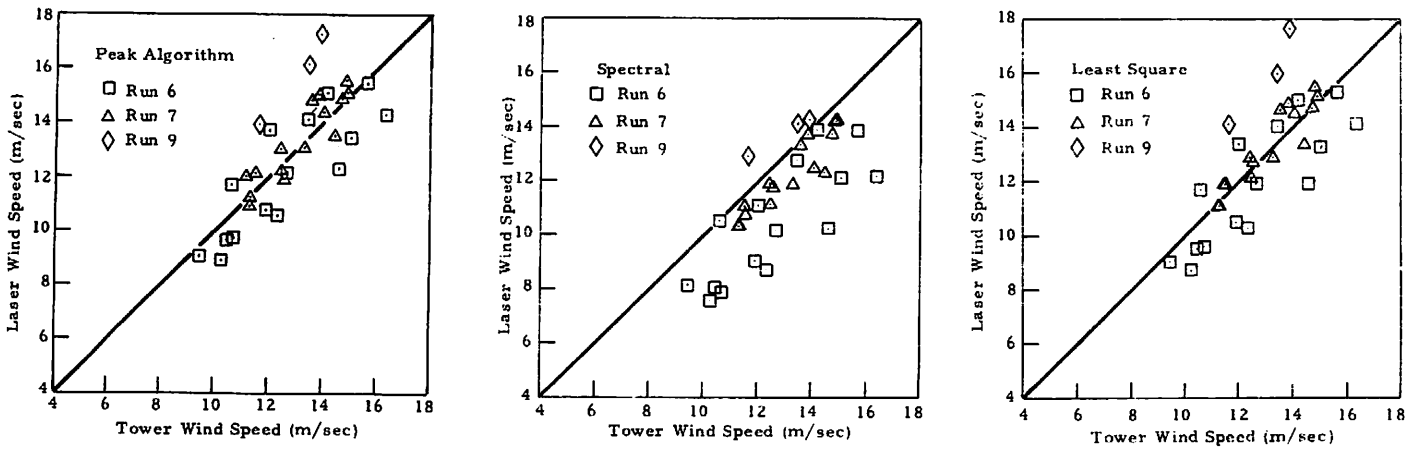

FIGURE 4-6. COMPARISON OF LASER AND TOWER 16-MIN MEAN WIND SPEED AT 120-M ALTITUDE.

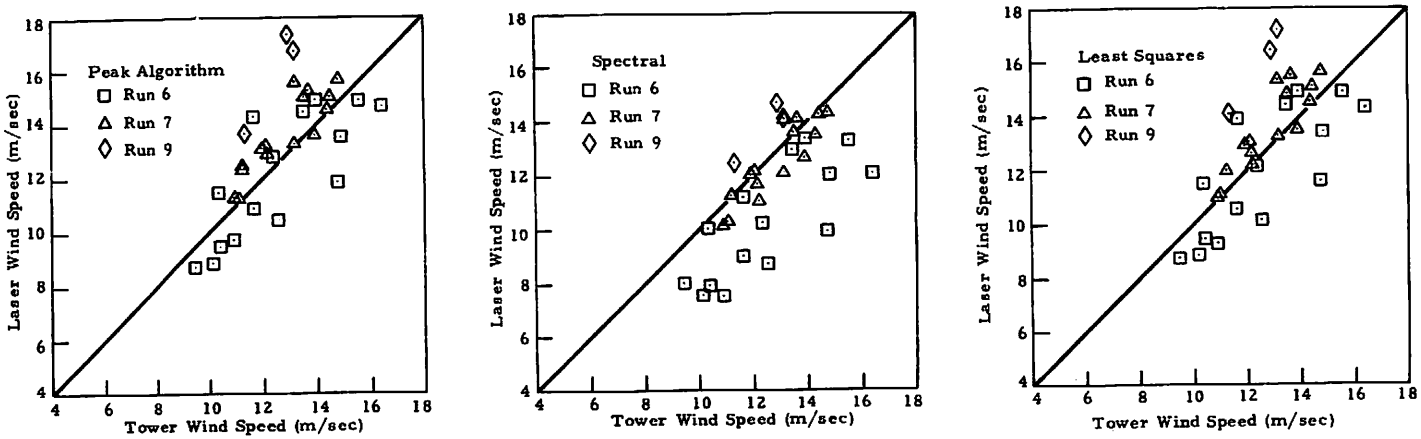

FIGURE 4-7. COMPARISON OF LASER AND TOWER 16-MIN MEAN WIND SPEED AT 150-M ALTITUDE.

wind at higher frequencies than the fundamental frequency in the VAD signature; thus, the peak of the signature (i.e., the fundamental frequency with superimposed higher-frequency variations) has a value that is higher than the averaged values. The interpretation is confirmed by the fact that the runs for which the greatest deviation above the diagonal line occurred are the runs for which the greatest value of wind standard deviation (measured by the tower) occurred. In particular, for the points of Run 9 farthest off the 45-degree line in Figs. 4-5 and 4-6, the standard deviation of the wind speed was 1.82 m/sec and 1.75 m/sec, respectively, whereas the standard deviation of the wind speed was usually between 0.9 m/sec and 1.4 m/sec.

It is also observed that the spectral algorithm tends to give mean wind values that are biased slightly low compared with the tower-measured mean winds. It was observed during the data processing that the magnitude of the bias is a function of the number of valid line-of-sight velocities obtained during the VAD scan. The bias was insignificant for data when more than 50 valid data points were obtained during each VAD scan. It is noted that a number of data points below this value was obtained only rarely at Table Mountain and that the low number of data points should never occur in air with a larger quantity of natural aerosol than the very clean air above Table Mountain. The least-squares sine algorithm seems to present no systematic bias, and the scatter of the data about the 45-degree line is less for the sine algorithm than for the other two processing techniques. A comparison of the peak algorithm and the spectral algorithm with the sine algorithm is shown in Figs. 4-8 and 4-9. For the peak algorithm, the deviation from the 45-degree line increases as turbulence increases, and, for the spectral algorithm, the deviation from the 45-degree line increases as the number of valid points in VAD scan decreases below 50.

4.4 INITIAL DATA COMPARISON

Laser and tower data shown in Figs. 4-3 through 4-7 consist of a direct comparison of 16-minute mean wind speed. The proximity of individual data

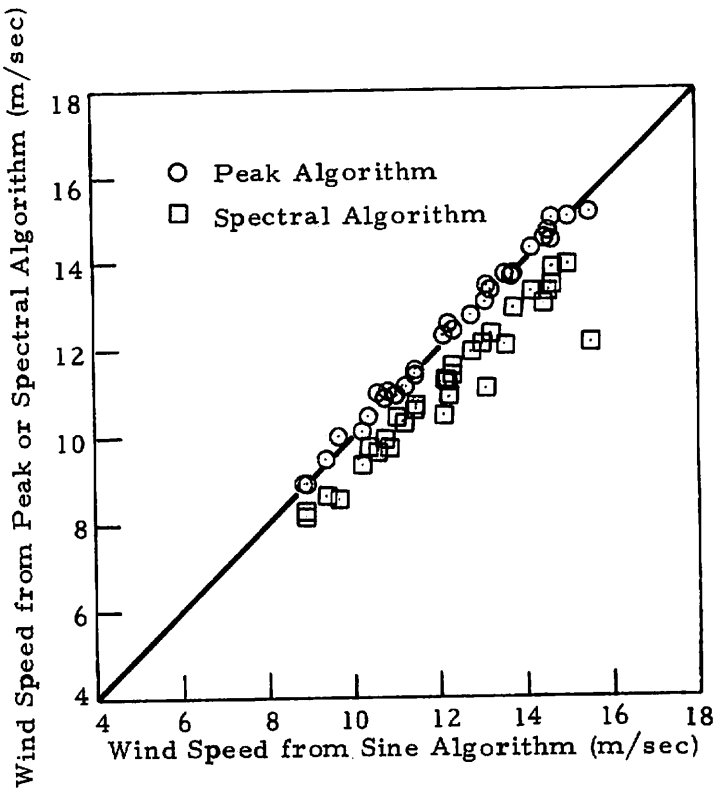

FIGURE 4-8. COMPARISON OF DATA PROCESSING ALGORITHMS AT 60-M ALTITUDE (16-Min Means of Runs 6,7, and 9).

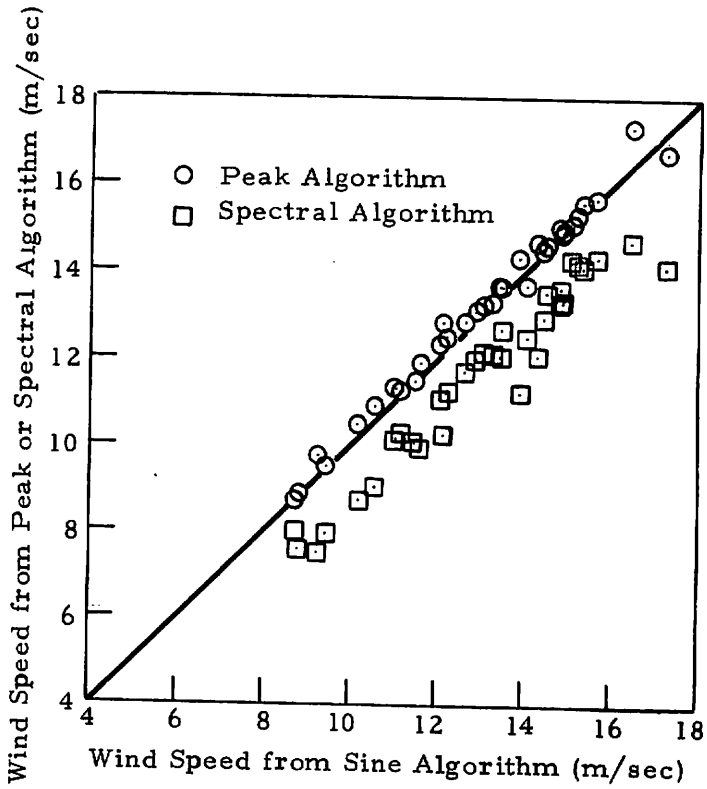

FIGURE 4-9. COMPARISON OF DATA PROCESSING ALGORITHMS AT 150-M ALTITUDE (16-min Means of Runs 6, 7, and 9).

points to the 45-degree line is a direct measure of the difference between the independent measurements.

An important observation is that the scatter in the data is somewhat greater than expected for all altitudes and all data-processing algorithms. This was determined to be a statistical problem rather than inherent problems associated with the VAD assumptions. The rotation rate of the azimuth scan has a period of 5 seconds, and the discrete range scan is hardwired for performing scans at a maximum of eight preselected altitudes, resulting in 40 seconds for a profile to be mapped out with one wind calculation performed per altitude during each 40-second period. In a 16-minute time frame, 24 points per altitude are used in the average wind calculations. In contrast, the propeller vanes are digitized at one point per second, which yields 960 points per 16-minute time frame. It was believed that the relatively small number of values contributing to the mean wind speed when all eight altitudes were utilized is the major factor in the scatter of the laser data. Accordingly, in later runs, fixed altitude VAD measurements were implemented to allow inclusion of a greater number of individual VAD wind measurements in the 16-minute average. It was believed that this would reduce the scatter of the comparative data and, thus, would allow a more meaningful evaluation of the VAD concept.

4.5 FIXED-ALTITUDE VAD DATA COMPARISON

Ideally, the solution to the scatter caused by a low number of data points in a 16-minute average would be an increased rotation rate. For the test, this solution was not possible because the rotation rate of the Lockheed LDV is fixed. However, in order to quantify the degree to which accuracy could be enhanced by an increased number of scans in a 16-minute average, fixed-altitude VAD measurements were made. By making all scans at one altitude, the number of scans in each 16-minute average was increased from 24 (as for the data discussed in the previous section) to 192. This increase was deemed necessary in order to make meaningful conclusions about the validity of the VAD assumptions.

The MAU did not have a real-time wind-processing capability. To alleviate the problems of the inability to assess the quality of data in the field, a simplified wind-speed processing algorithm was implemented on the computer in the tower data-processing van (Ref. 8). This allowed post-test comparisons between the LDV and tower data to be made on a daily basis, and proved to be a valuable asset.

Analysis of the fixed-altitude data showed that the peak algorithm exhibits a slightly high bias of the wind speed. This characteristic was also noted in the multiple-altitude data. The bias is clearly seen in Fig. 4-10. It is noted that the wind-speed scale has been expanded to display the difference. As noted in Section 4.3, the reason for the bias is believed to be turbulent fluctuations superimposed on the sinusoidal VAD signature which would result from a uniform wind. The fact that the bias is present in both single- and multiple-altitude data indicates that the bias is not due to averaging over multiple scans, but is related to the process by which the wind from each scan is calculated. This fact supports the hypothesis that the bias is due to turbulent fluctuations.

The spectral algorithm was incorporated into the off-line processing program to alleviate this problem. The concept of the spectral algorithm was that the mean wind would be indicated by the first harmonic (in a Fourier sense), and turbulent fluctuations would be indicated by higher harmonics. Turbulent fluctuations would not influence the magnitude of the fundamental harmonic. The results are also shown in Fig. 4-10, where excellent agreement between the LDV and tower measurements is observed.

The average wind speed and direction as calculated by the least-squares sine fit is also shown in Fig. 4-10. Maximum deviations between LDV and tower measurements are less than 20 cm/sec in wind speed and 2 degrees in wind direction. The corresponding standard deviation in wind speed and direction are depicted in Fig. 4-11, where maximum deviations are seen to be 15 cm/sec in speed and 7 degrees in direction.

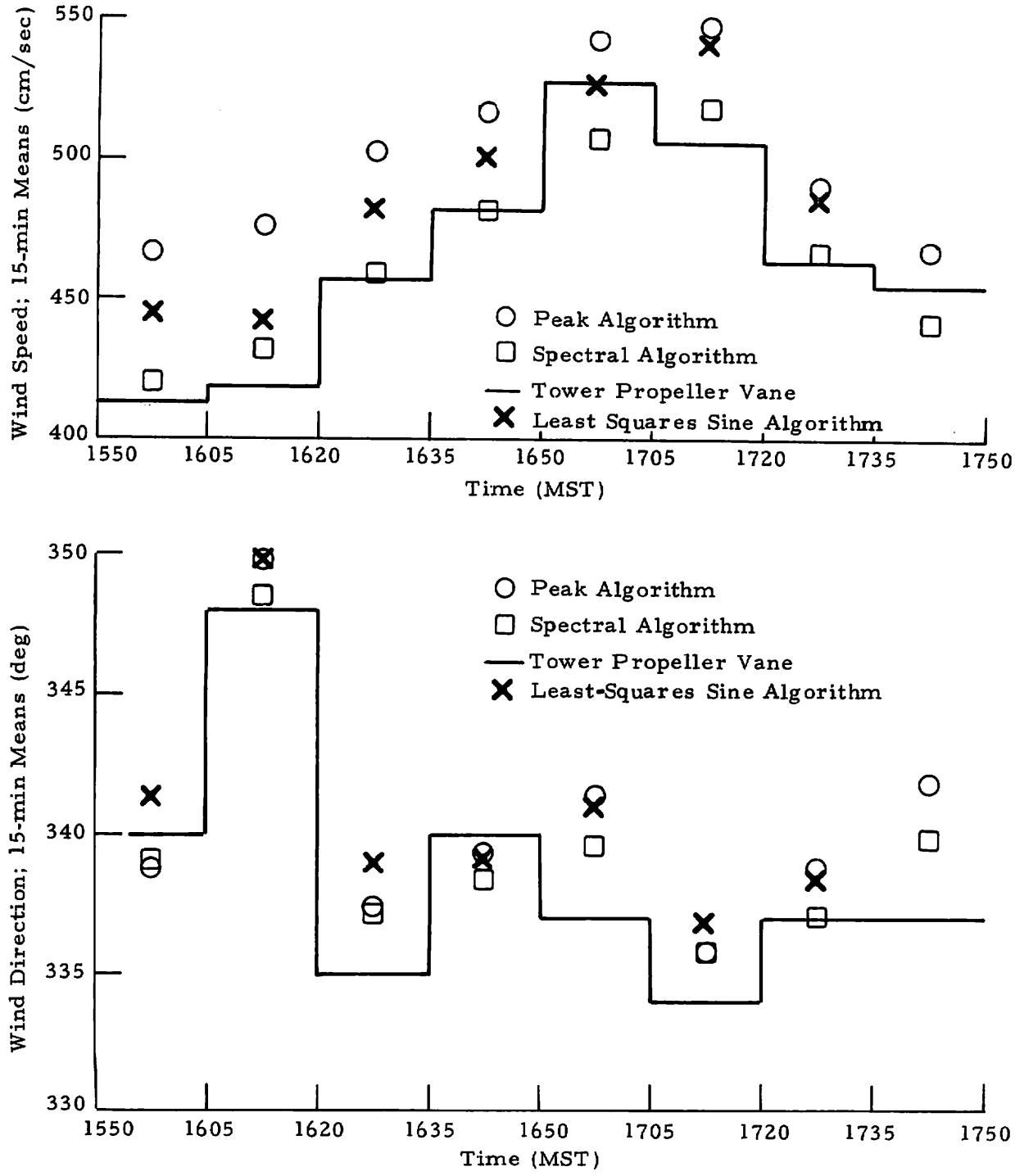

FIGURE 4-10. COMPARISON OF LOCKHEED LASER DOPPLER ANEMOMETER WIND DATA VS NATIONAL OCEANIC AND ATMOSPHERIC ADMINISTRATION'S 150-M TOWER DATA (Run 24; Altitude, 30 m).

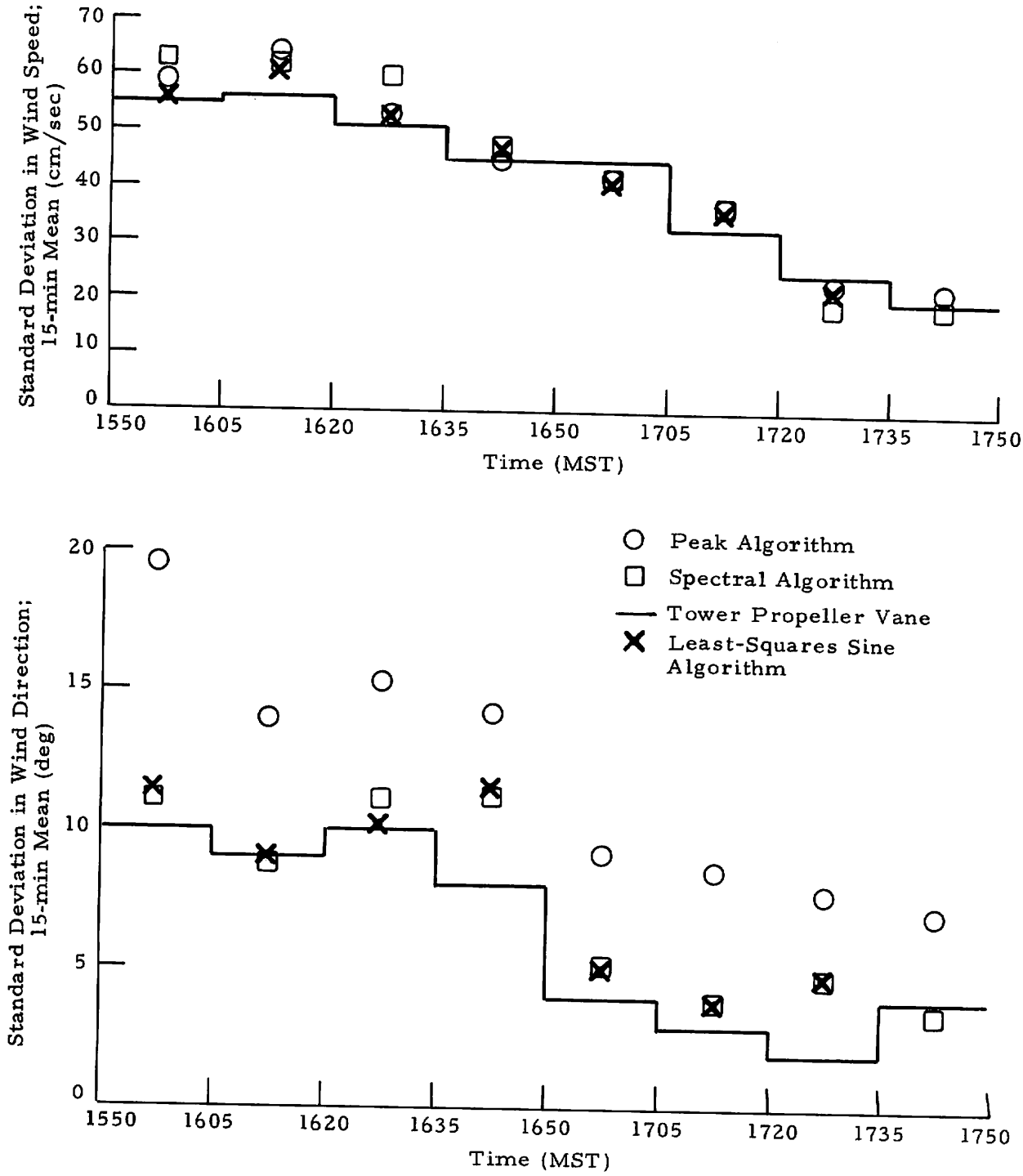

FIGURE 4-11. COMPARISON OF LASER VS TOWER STANDARD DEVIATIONS IN WIND SPEED AND DIRECTION (Run 24; Altitude, 30 m).

An interesting record of data is shown in Fig.4-12. During a one and one-half hour period the wind direction changed approximately 70 degrees; the comparisons in both mean speed and direction are excellent with a maximum deviation of less than 15 cm/sec in wind speed and 4 degrees in wind direction for the sine algorithm.

Comparative plots are shown in Figs.4-13 through 4-15 for laser versus tower wind speed and in Figs.4-16 through 4-18 for wind direction comparisons. In general, excellent agreement is observed. However, there is still a slightly high bias for the peak algorithm, a slightly low bias for the spectral algorithm and no systematic bias for the least-squares sine algorithm. It is noted that the 150-m altitude generally exhibits greater data scatter than the lower altitudes. Therefore, the scatter at lower altitudes would be less than that shown in Figs.4-13 through 4-18.

4.6 EFFECT OF AVERAGING TIME

As expected, the effect of increasing averaging time is to decrease the scatter of the data about the 45-degree comparison line. This is illustrated for both wind speed and direction for the sine algorithm in Figs.4-19 through 4-24. The one-minute averages (i.e., twelve data points in the average) exhibit a fair amount of scatter. However, the six-minute average (i.e., 72 data points in each average) shows significantly less scatter. The 15-minute averages exhibit almost no scatter.

Similar trends were also observed for the peak and spectral algorithms. The data are presented in Appendix B in a manner similar to that of Figs.4-19 through 4-24.

Much of the data scatter is attributable to the distance between the meteorological tower and the Mobile Atmospheric Unit, rather than to inaccuracies in the measurements made by the Mobile Atmospheric Unit. It is expected that over a long period of time, the average winds at the two locations will be approximately equal. However, for short-time periods, the

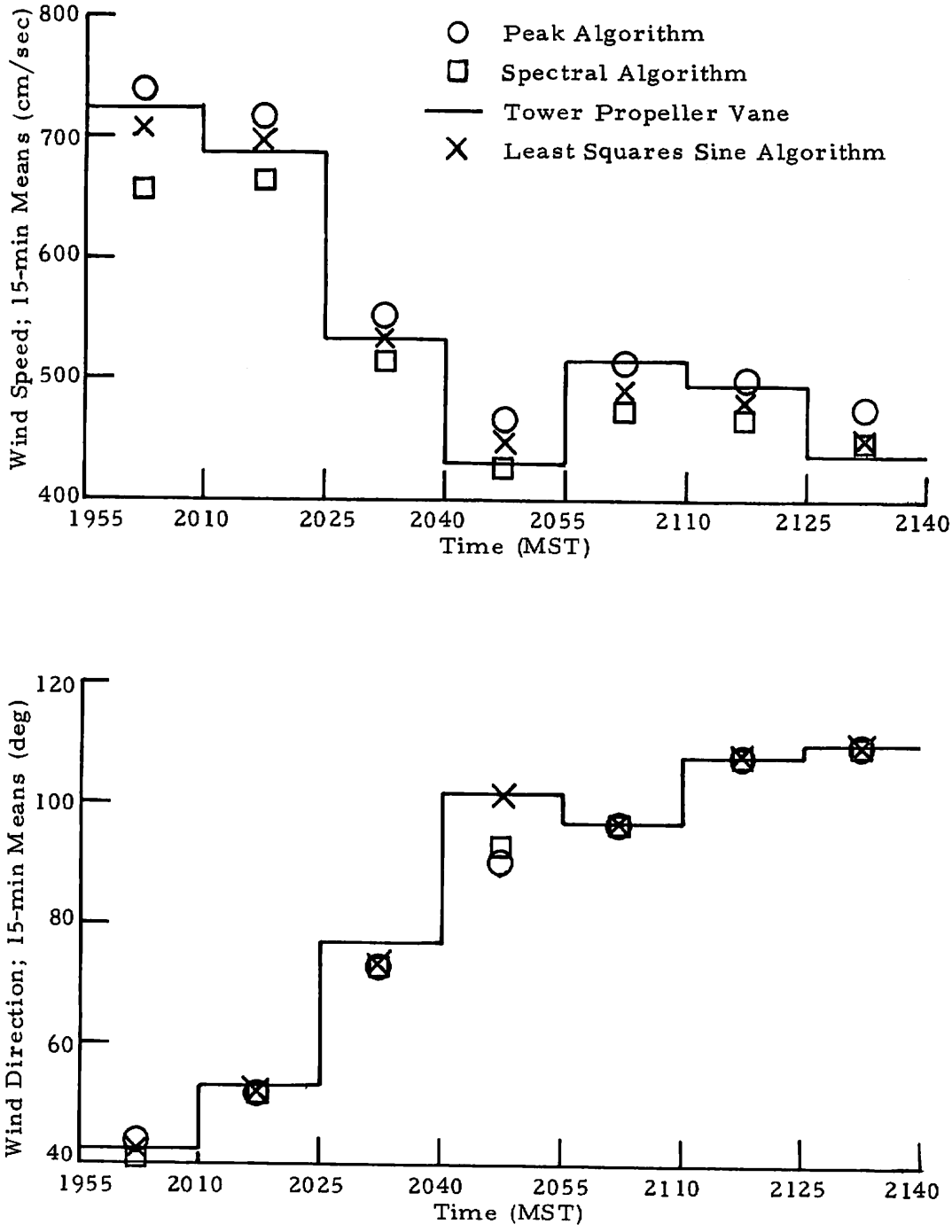

FIGURE 4-12. COMPARISON OF LASER VS TOWER WIND DATA (Run 26; Altitude, 30 m).

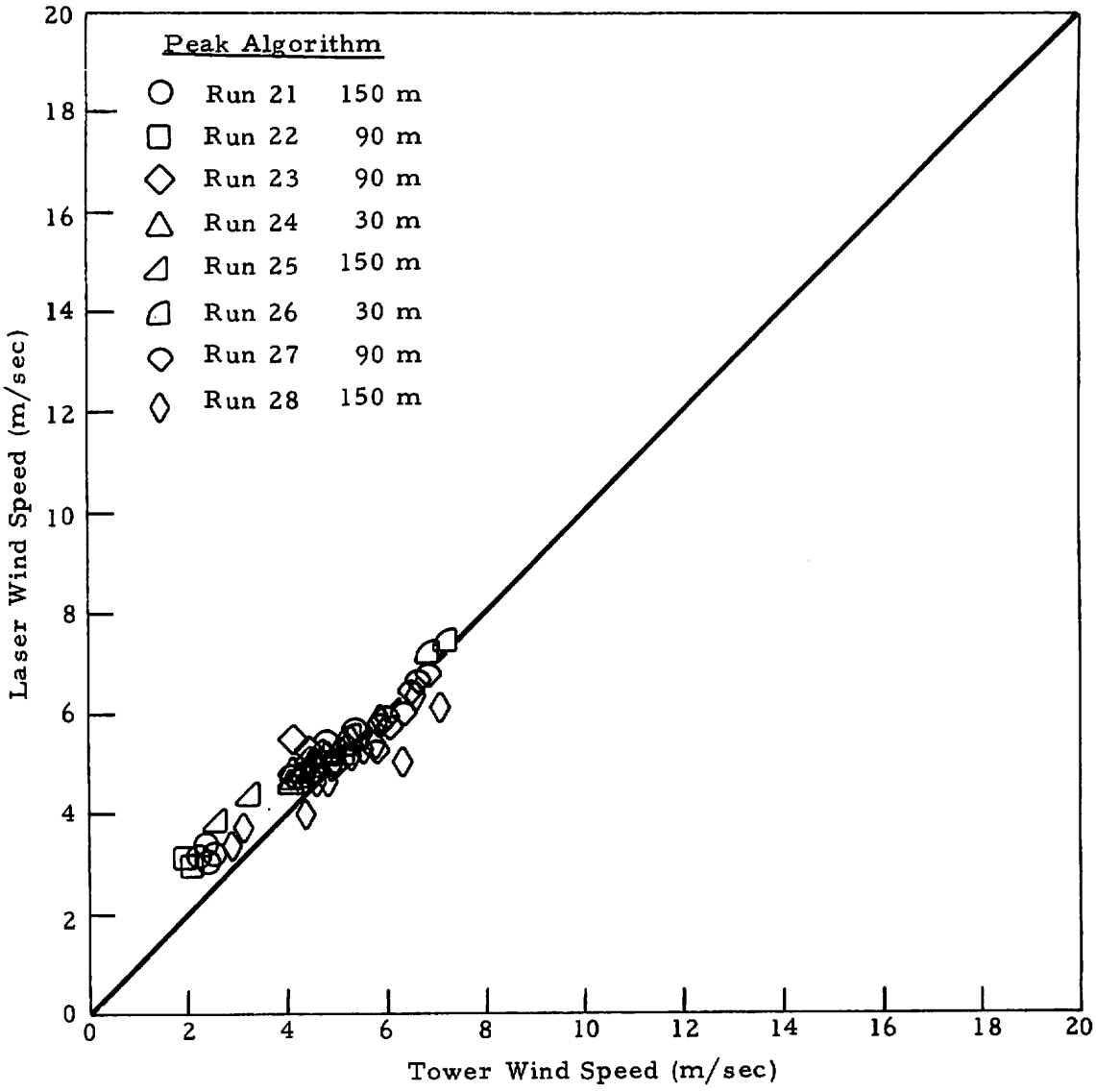

FIGURE 4-13. COMPARISON OF LASER AND TOWER 15-MIN MEAN WIND SPEED USING PEAK ALGORITHM.

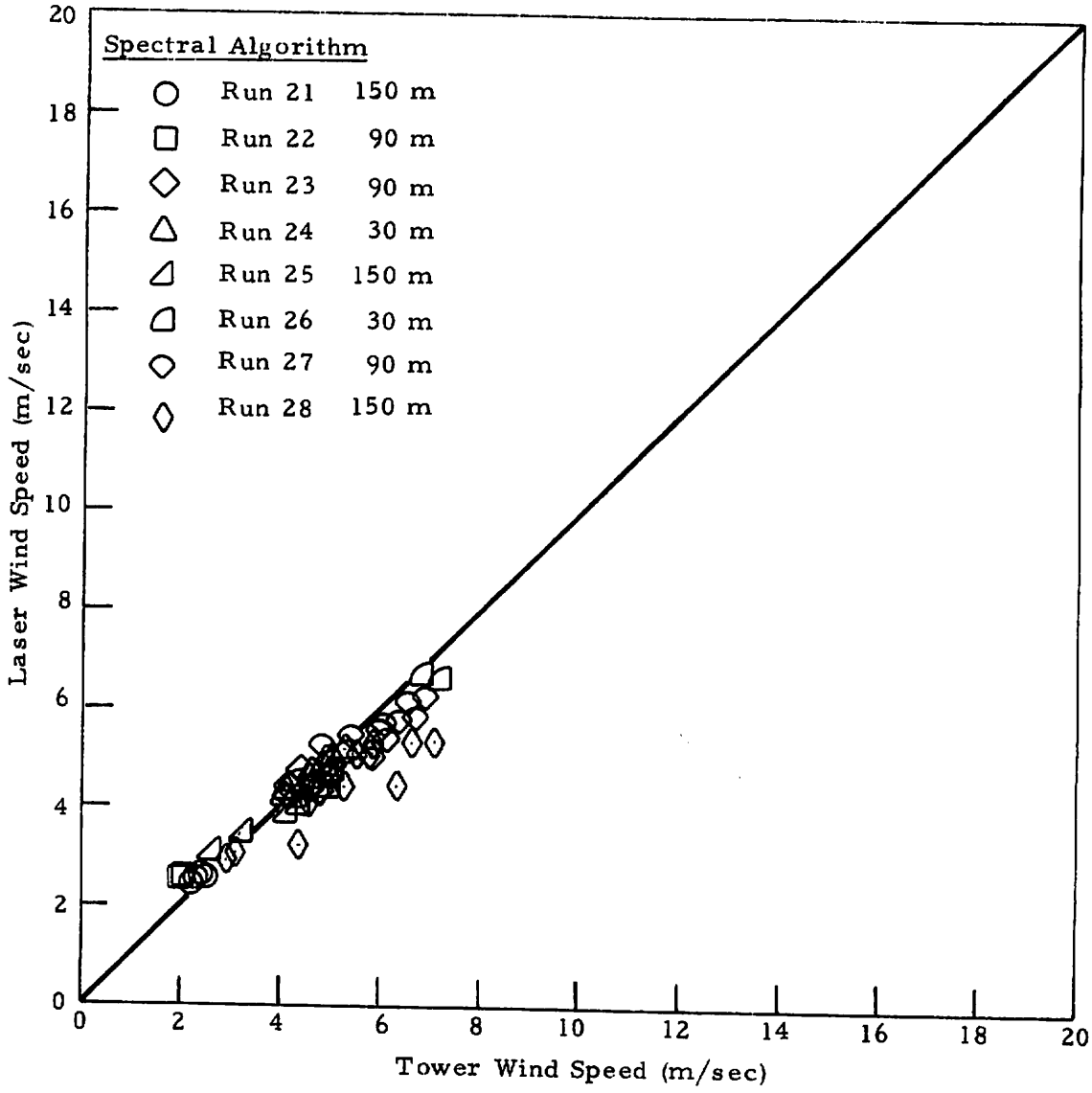

FIGURE 4-14. COMPARISON OF LASER AND TOWER 15-MIN MEAN WIND SPEED USING SPECTRAL ALGORITHM.

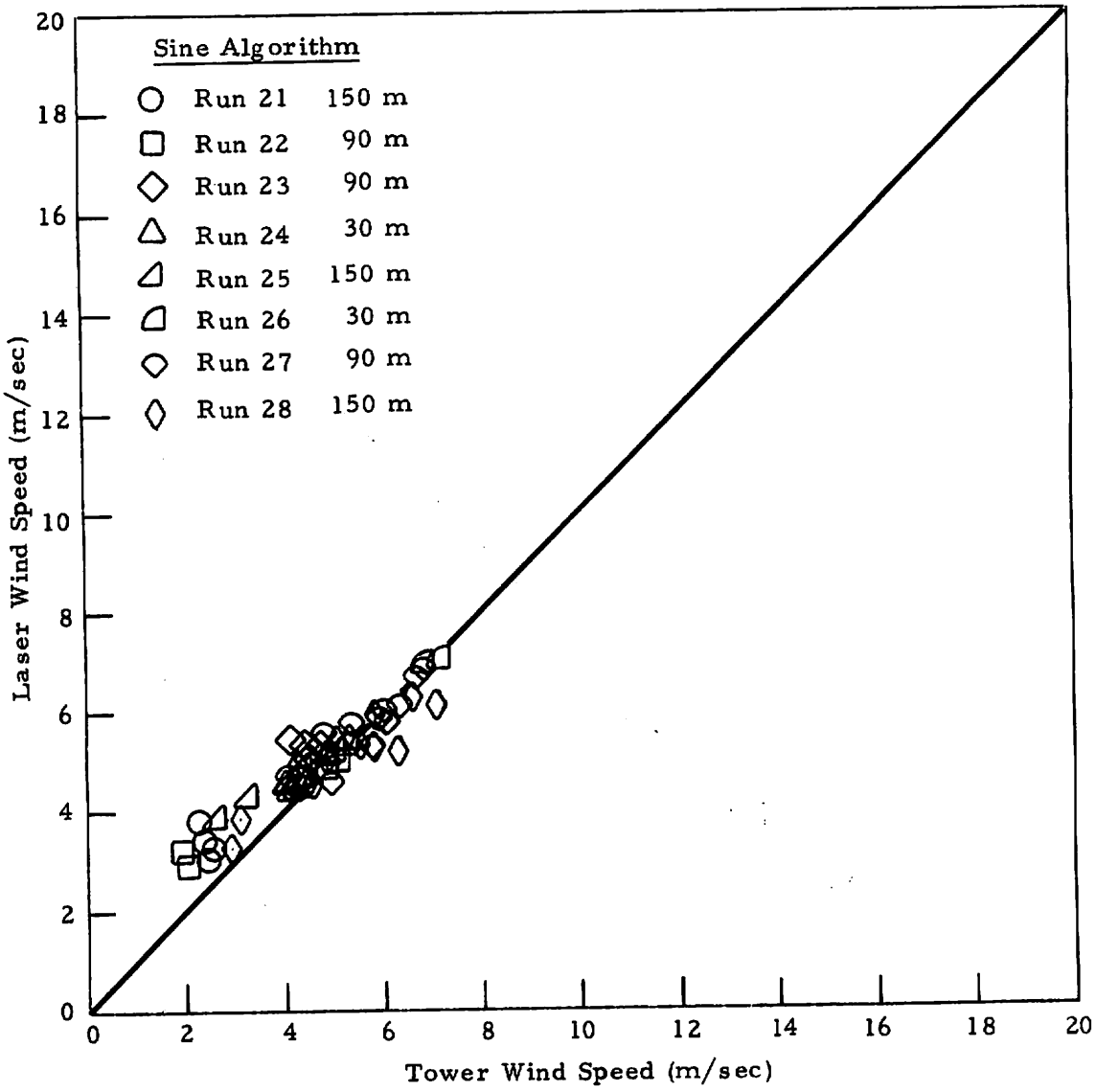

FIGURE 4-15. COMPARISON OF LASER AND TOWER 15-MIN MEAN WIND SPEED USING LEAST-SQUARES SINE ALGORITHM.

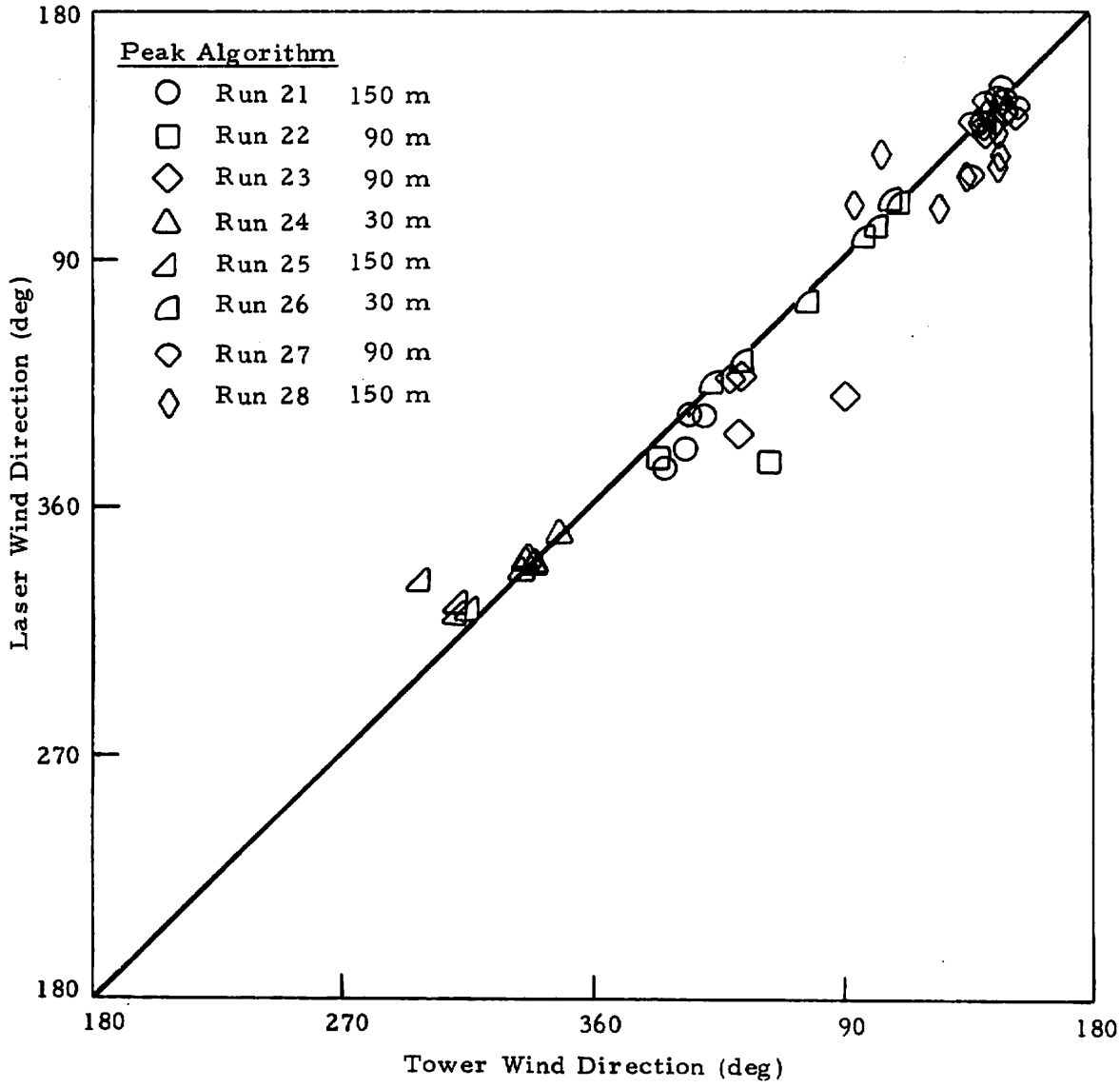

FIGURE 4-16. COMPARISON OF LASER AND TOWER 15-MIN MEAN WIND DIRECTION USING PEAK ALGORITHM.

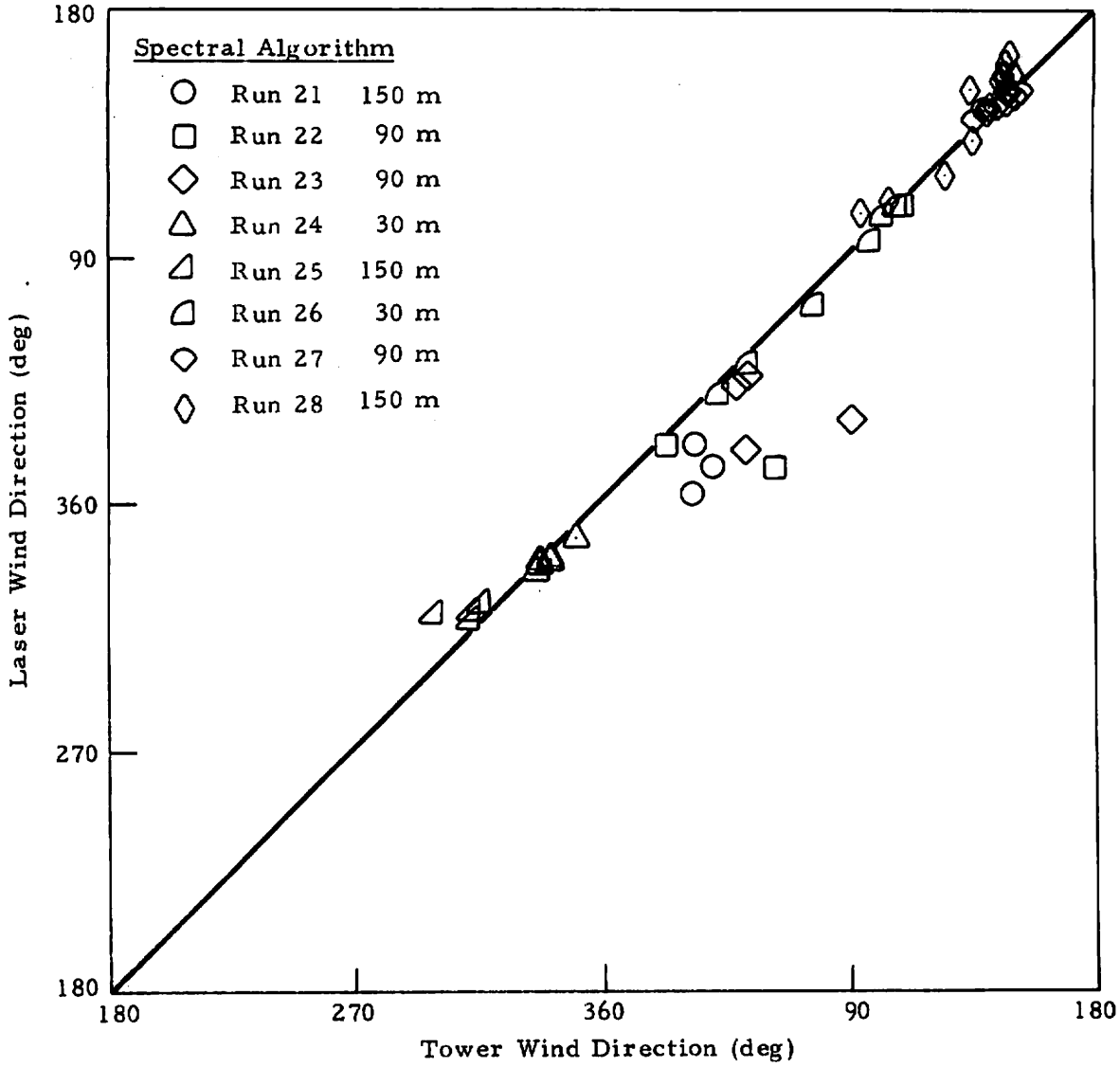

FIGURE 4-17. COMPARISON OF LASER AND TOWER 15-MIN MEAN WIND DIRECTION USING SPECTRAL ALGORITHM.

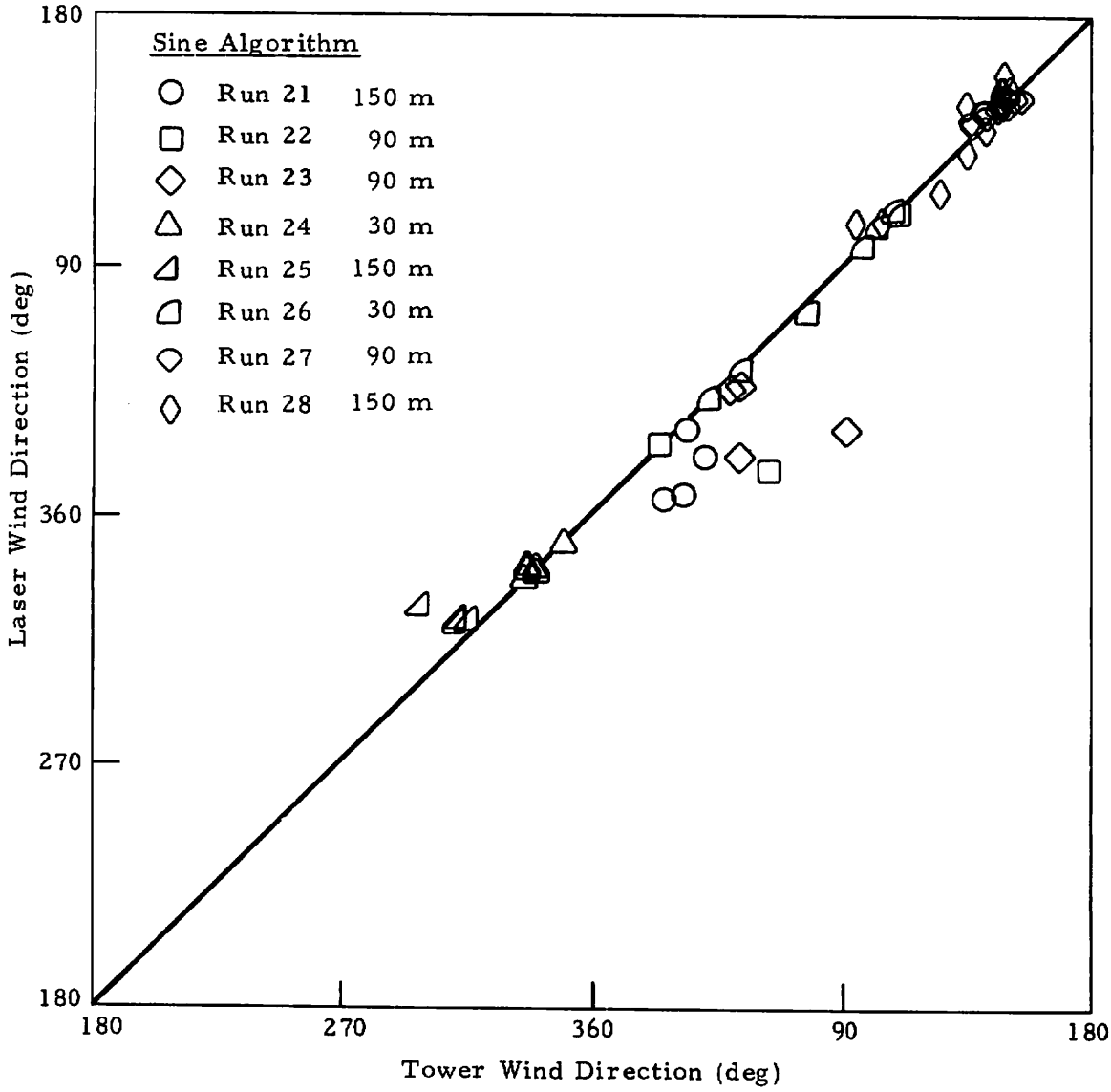

FIGURE 4-18. COMPARISON OF LASER AND TOWER 15-MIN MEAN WIND DIRECTION USING LEAST-SQUARES SINE ALGORITHM.

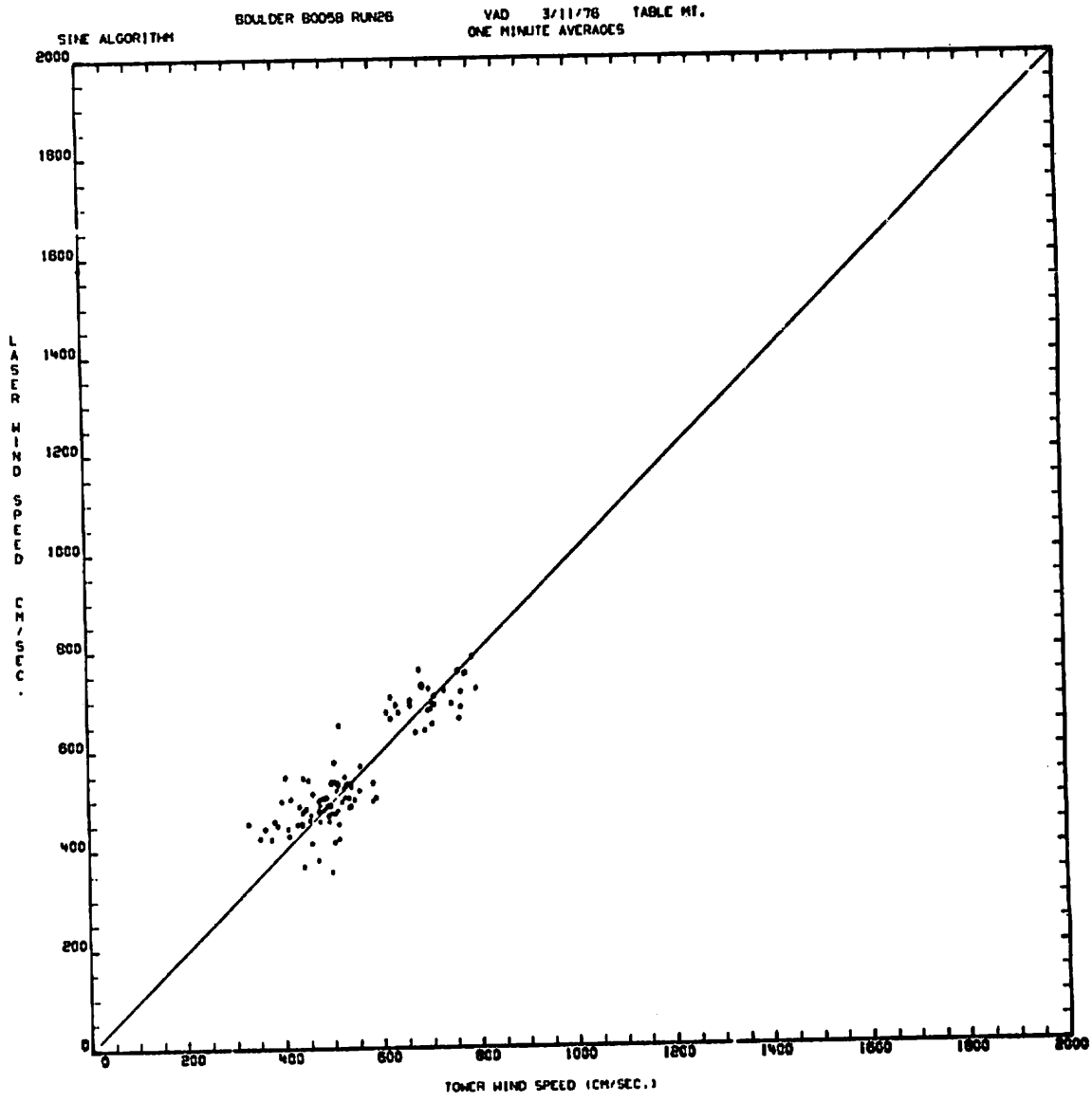

FIGURE 4-19. LASER WIND SPEED WITH 1-MIN AVERAGING TIME.

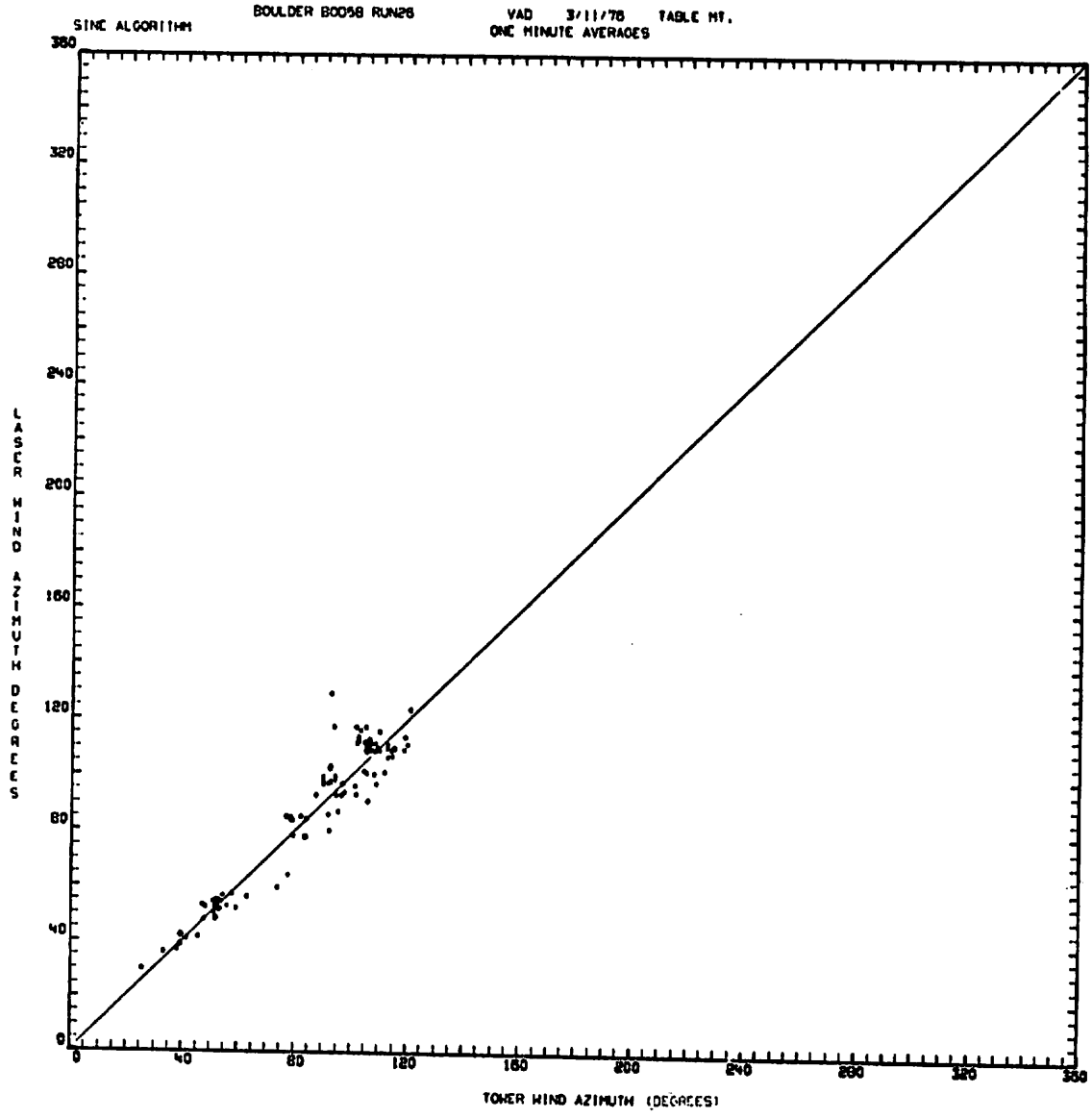

FIGURE 4-20. LASER WIND DIRECTION WITH 1-MIN AVERAGING TIME.

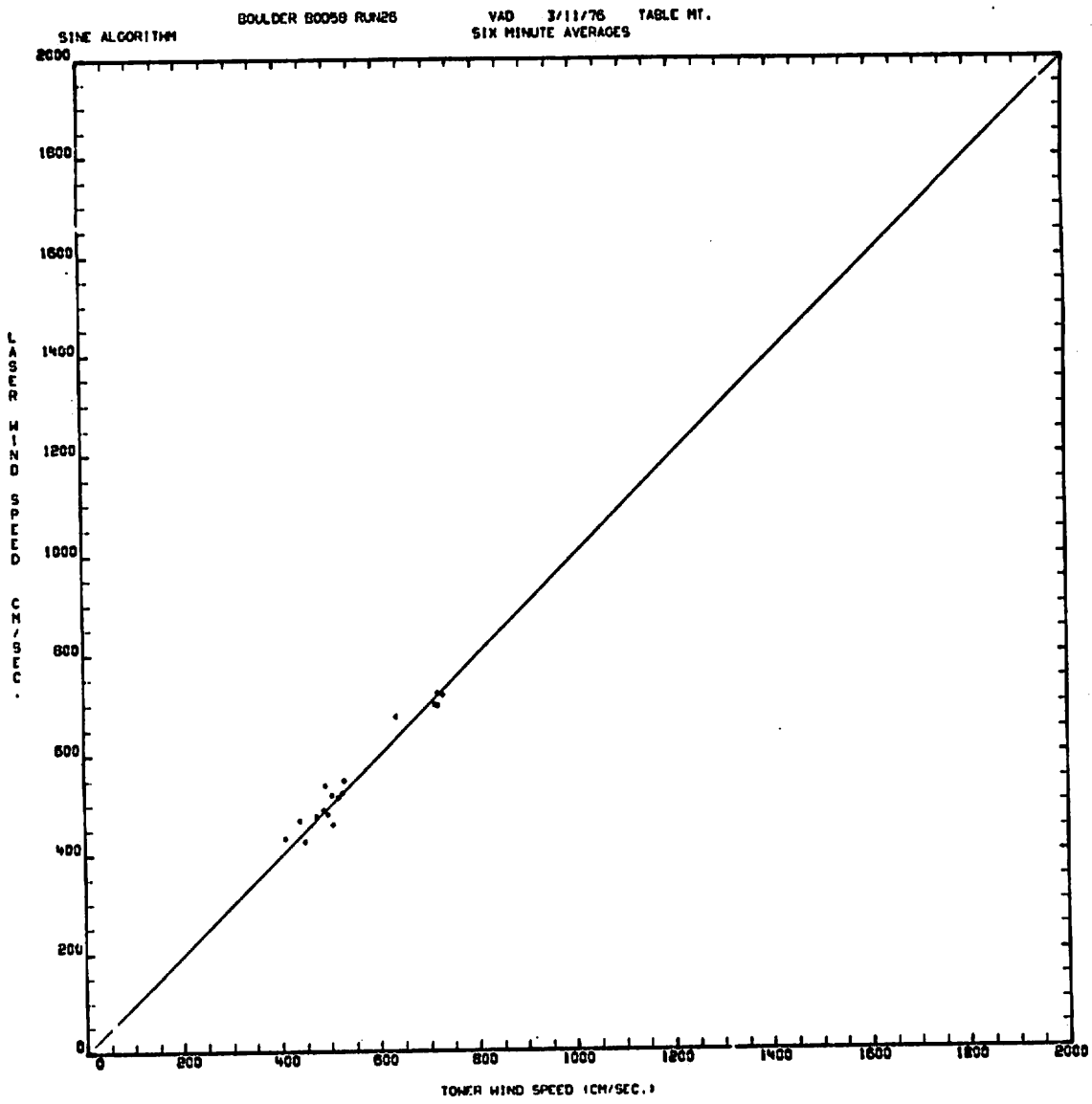

FIGURE 4-21. LASER WIND SPEED WITH 6-MIN AVERAGING TIME.

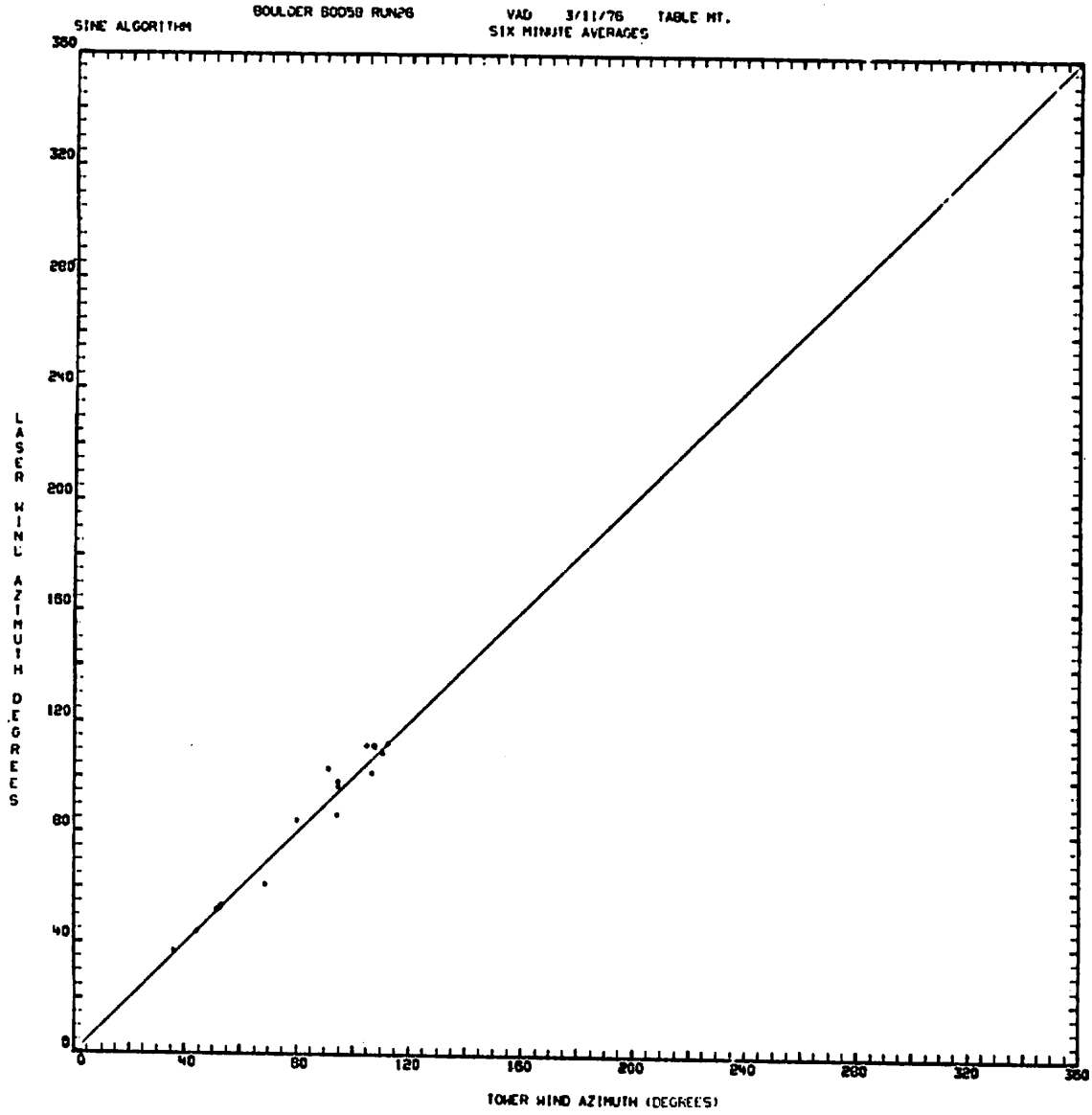

FIGURE 4-22. LASER WIND DIRECTION WITH 6-MIN AVERAGING TIME.

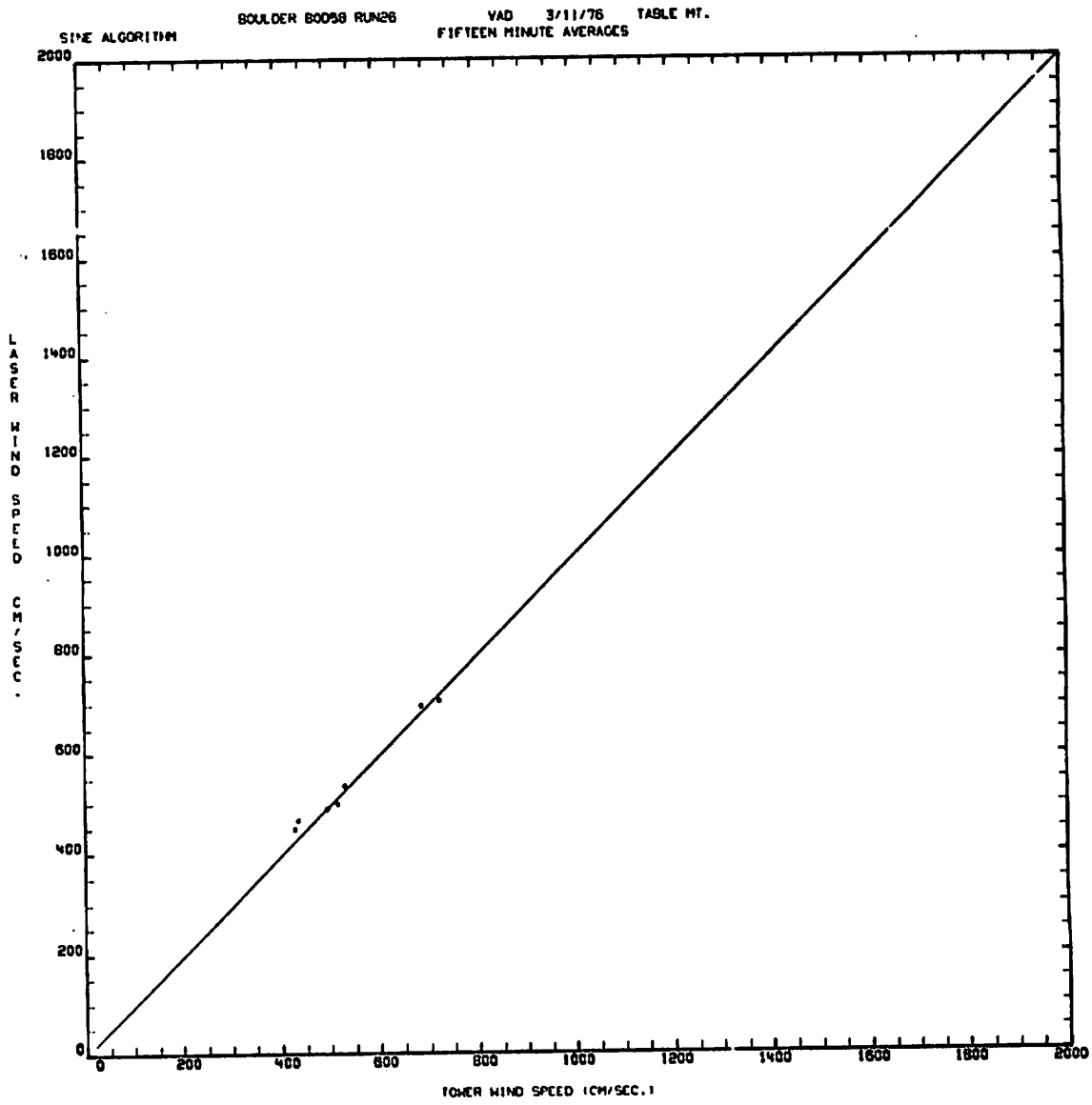

FIGURE 4-23. LASER WIND SPEED WITH 15-MIN AVERAGING TIME.

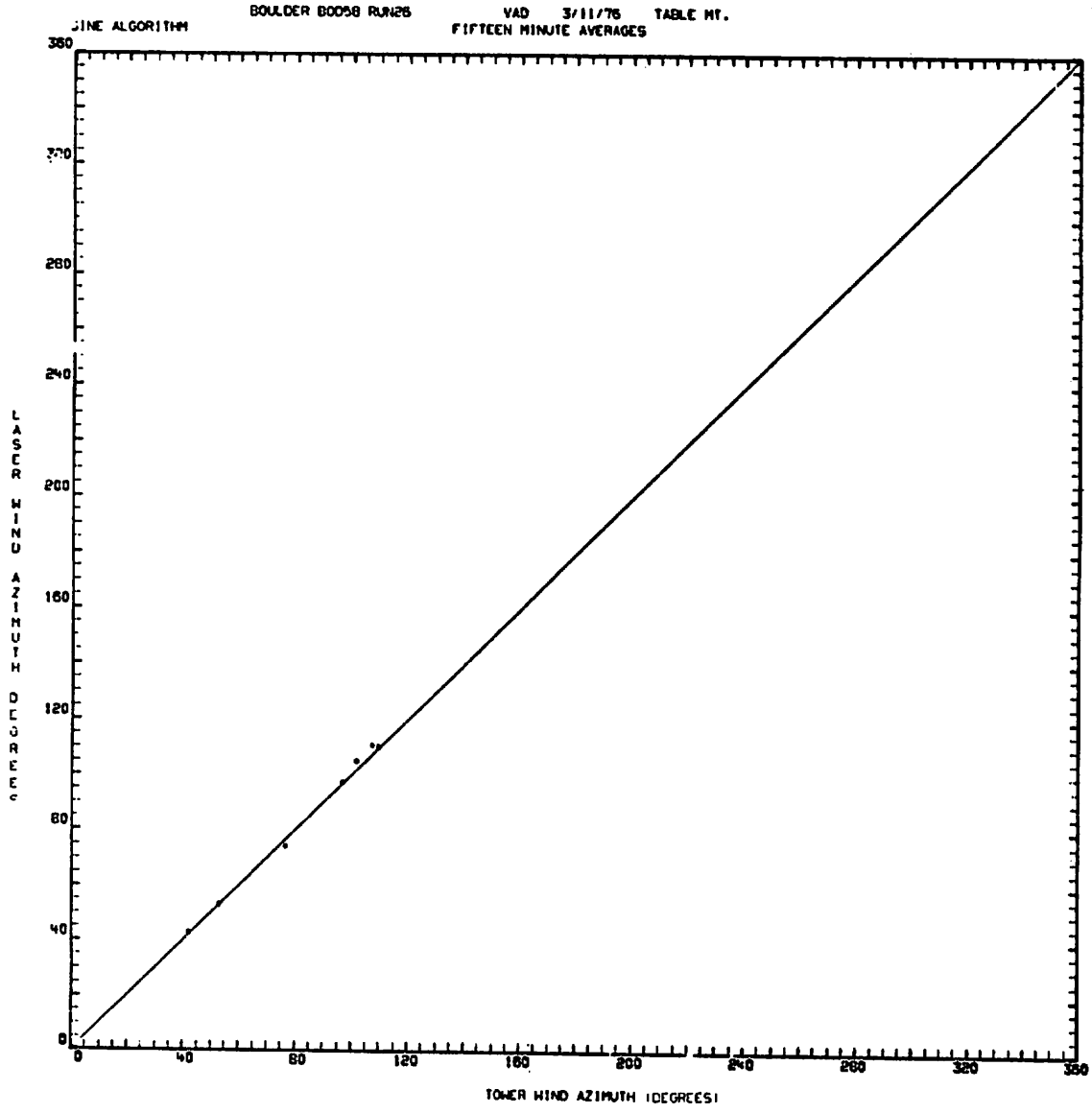

FIGURE 4-24. LASER WIND DIRECTION WITH 15-MIN AVERAGING TIME.

two measurements would not be expected to be equal, especially when the standard deviation of wind speed is 10% of the mean wind speed. This is illustrated by the fact that the data scatter about the 45-degree line is greater for the one-minute means than for longer averaging times.

4.7 EFFECT OF SNOW

The presence of snow during LDV wind measurements creates a negative vertical component of velocity, but does not affect the measurement of horizontal components of velocity. A typical VAD signature for light snow is shown in Fig.4-25. The signature is taken from Run 27 for which the snowfall was approximately 1 cm/hour. There is a distinct double signature. The upper signature is due to laser reflection from atmospheric aerosol. The lower signature is due to laser reflection from snow. For light snow, reflections from both atmospheric aerosol and snow are detected. If a snow particle is in the focal volume, the maximum signal intensity is probably derived from reflection from the snow particle. If there is no snow particle in the focal volume, the maximum signal intensity comes from a particle of the atmospheric aerosol.

All of the data-processing algorithms average the two signatures, weighted by the number of points in each of the signatures. The result is a signature which lies between the "clear air" and snow signatures. Since the amplitude and phase angle of the sine wave are unaffected by this process, the wind speed and direction are unaffected. For example, in Figs. 4-13 through 4-18, the data from Run 27 exhibit no distinguishing characteristics. However, a negative component of vertical velocity is superimposed on the wind velocity. For example, the vertical component of velocity for Run 27 is approximately -1 m/sec, whereas that for Run 23 (at the same altitude and approximately equal wind speed), the vertical component of velocity is approximately -0.1 m/sec.

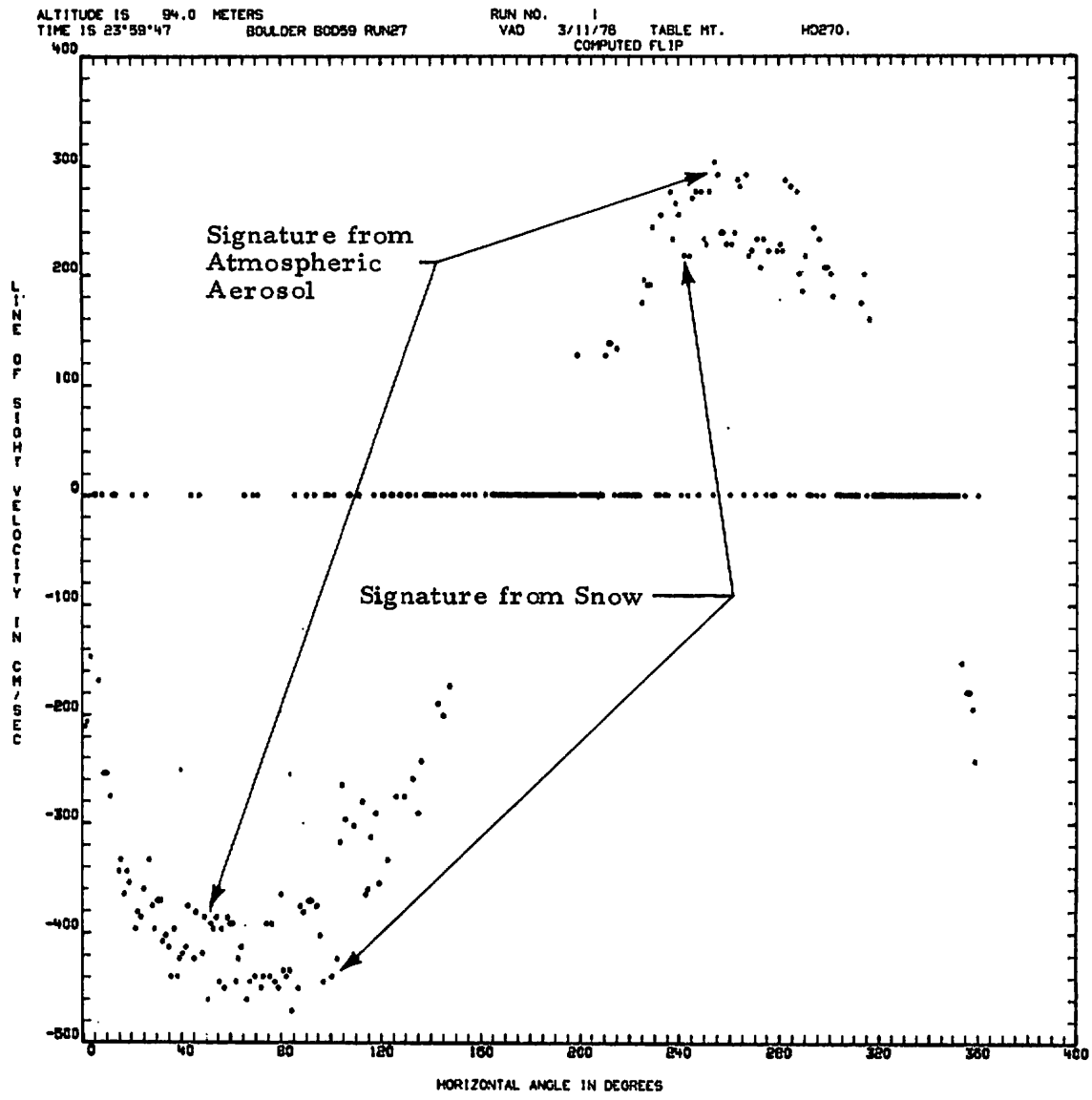

FIGURE 4-25. VELOCITY AZIMUTH DISPLAY SIGNATURE IN LIGHT SNOW.

For heavy snow (Runs 6 and 7), a double signature does not occur, but a definite vertical component of velocity is observed. A typical VAD signature in heavy snow is shown in Fig. 4-26. The vertical component of velocity is approximately -1 m/sec for Run 6.

For run 27, the variation in returned laser intensity is much greater than is normally experienced. For example, a typical example of a sequence of relative signal intensities on a linear scale is:....444, 168, 680, 272, 190, 576, 238, 154, 190, 142, 176, 160, 304, 574, 384, 222, 160, 228, 144, 320, 576, 352, 190, 320, 120, 144, 312, 224, 252... It is hypothesized that the large values of intensity are reflection from snow, and smaller values of intensity are reflection from natural ambient aerosol. The higher intensities usually exhibit a line-of-sight velocity which is discernibly different from its adjacent points with lower intensities, but this characteristic is not universal. There are points for which the line-of-sight velocity is discernibly different from its adjacent points, but the signal intensity is small. It is possible to identify points which may be reflections from snow based upon deviations in line-of-sight velocity or signal intensity. However, it is not possible to identify individual points positively as reflection from snow on the basis of a one-to-one correspondence between deviations in line-of-sight velocity and deviations in signal intensity.

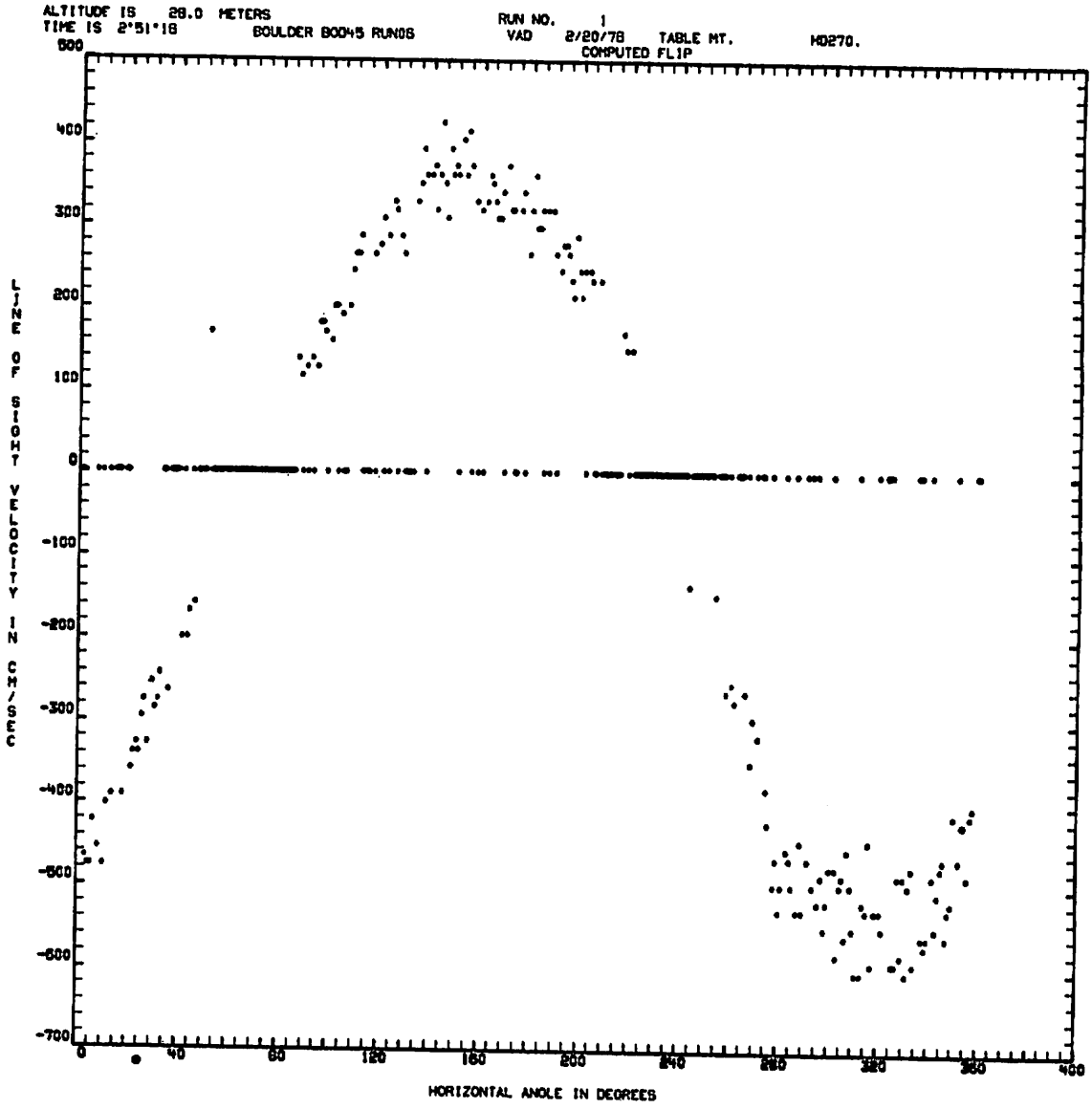

FIGURE 4-26. VELOCITY AZIMUTH DISPLAY SIGNATURE IN HEAVY SNOW.

5. CONCLUSIONS AND RECOMMENDATIONS

The laser Doppler velocimeter using the VAD technique is an accurate and reliable method for the remote measurement of atmospheric wind. Three data-processing algorithms have been investigated in order to determine the optimal algorithm. It appears that the least-squares sine-fit algorithm provides the most consistent data compared with anemometer data from a meteorological tower. The peak algorithm yields wind-speed data which are slightly above those measured by the tower-mounted anemometers and given by the sine algorithm. The Fourier algorithm yields wind-speed data which are 1 to 1.5 m/sec below that given by the tower anemometers and the sine algorithm.

Based on comparisons between the tower anemometers and the laser-measured wind as calculated by the least-squares sine algorithm and shown in Appendix B, the accuracy of the LDV varies from ± 2 m/sec in wind speed and $\pm 20^{\circ}$ in wind azimuth for one-minute averages to ± 1 m/sec in wind speed and $\pm 10^{\circ}$ in wind azimuth for 15-minute averages.

6. REFERENCES

1. Little, C.G., V.E. Derr, R.H. Kleen, and R.S. Lawrence, "Remote Sensing of Wind Profiles in the Boundary Layer," Environmental Sciences Service Administration Technical Report ERL 168-WPL12, Wave Propagation Laboratory, Boulder, CO, June 1970.
2. Lawrence, T.R., M.C. Krause, L.K. Morrison, and C.E. Craven, "A Study on Laser Doppler Velocimeter Atmospheric Wind Interrogation Systems — Final Report," LMSC-HREC TR D306888, Lockheed Missiles & Space Company, Huntsville, AL, October 1973.
3. Huffaker, R.M., H.B. Jeffreys, E.A. Weaver, J.W. Bilbro, G.D. Craig, R.W. George, E.H. Gleason, P.J. Marrero, E.J. Reinbolt, and J.E. Shirley, "Development of a Laser Doppler System for the Detection, Tracking, and Measurement of Aircraft Wake Vortices," FAA-RD-74-213, NASA Marshall Space Flight Center, Huntsville, AL, March 1975.
4. Bilbro, J.W., H.B. Jeffreys, E.A. Weaver, R.M. Huffaker, G.D. Craig, R.W. George, and P.J. Marrero, "Laser Doppler Velocimeter Wake Vortex Tests," NASA TM X-64988, March 1976.
5. Brashears, M.R., T.R. Lawrence, and A.D. Zalay, "Mobile Laser Doppler System Check Out and Calibration," LMSC-HREC TR D497036, Lockheed Missiles & Space Company, Huntsville, AL, September 1976.
6. Lhermitte, R.M. and D. Atlas, "Precipitation Motion by Pulse Doppler Radar," Proceedings of Ninth Radar Conference, Boston, MA, 1961, pp. 343-346.
7. Haugen, D., Performance Test Results Xonics Acoustic Doppler Sounder," National Oceanic and Atmospheric Administration, National Oceanic and Atmospheric Administration Technical Memorandum ERL WPL-16, Wave Propagation Laboratory, Boulder, CO, May 1976.
8. Haugen, D., Personal Communication.

Appendix A

LASER DOPPLER VELOCIMETER VELOCITY AZIMUTH DISPLAY SIGNATURES

(Runs 21-28)

This appendix contains sample velocity azimuth display signatures to define data quality of each data run taken at Table Mountain test site. The signatures are presented in sets of three figures. The first figure in each set is the raw data. The second figure is the edited and filtered data, and the third figure is the derectified signature (edited, but unfiltered).

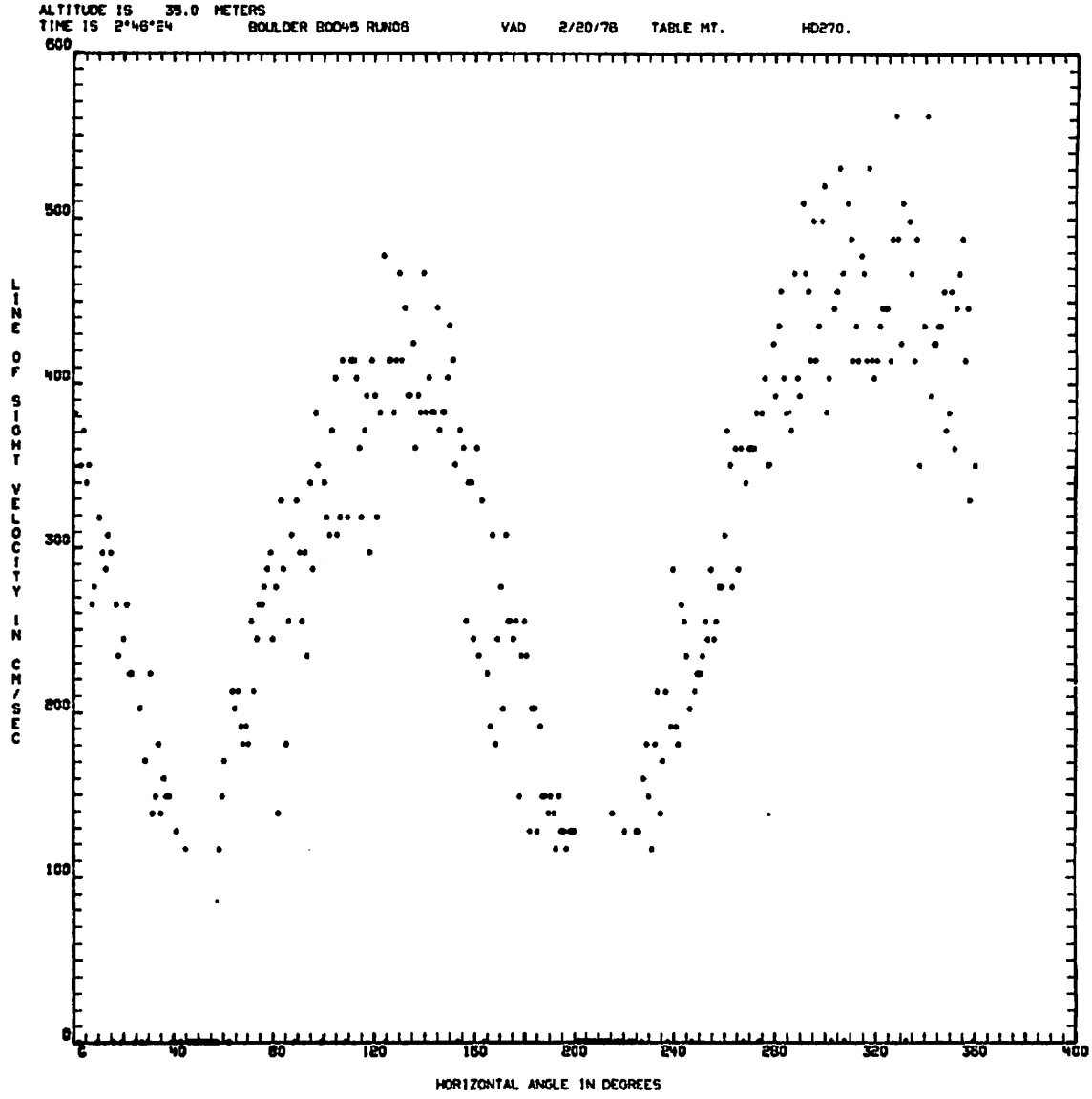

FIGURE A-1. SAMPLE LASER DOPPLER VELOCIMETER SIGNATURES.

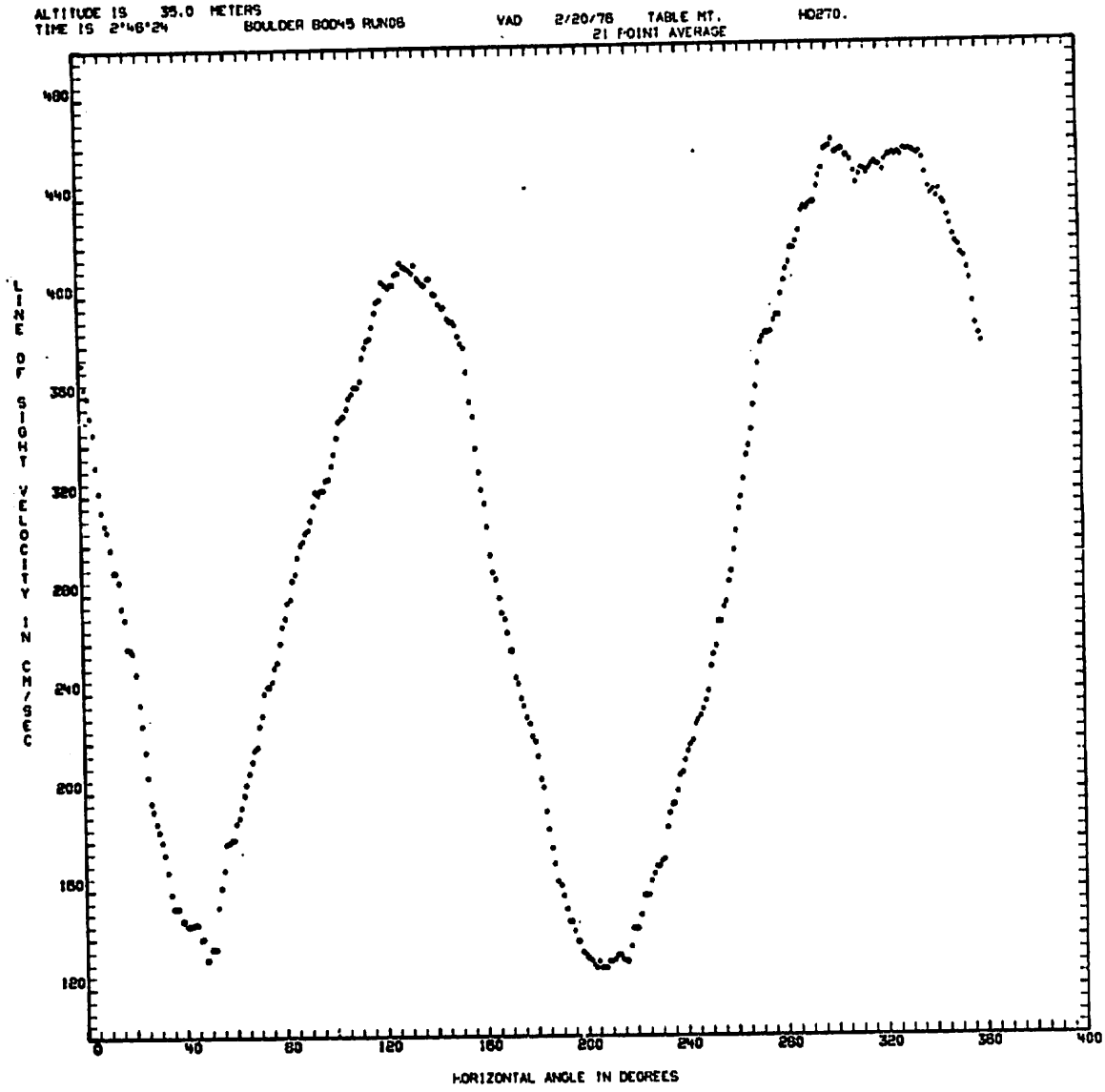

FIGURE A-1 (Continued).

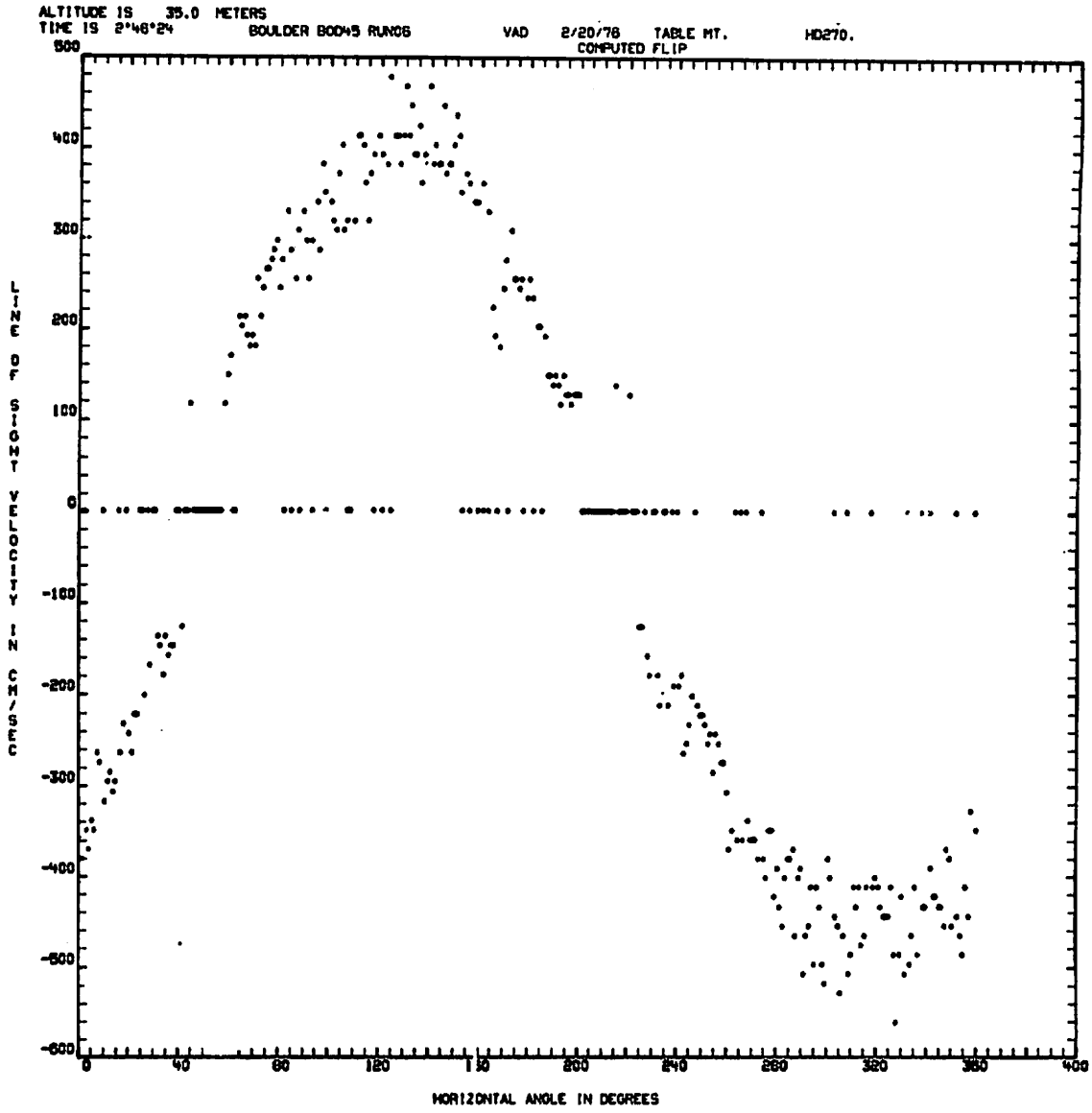

FIGURE A-1 (Continued).

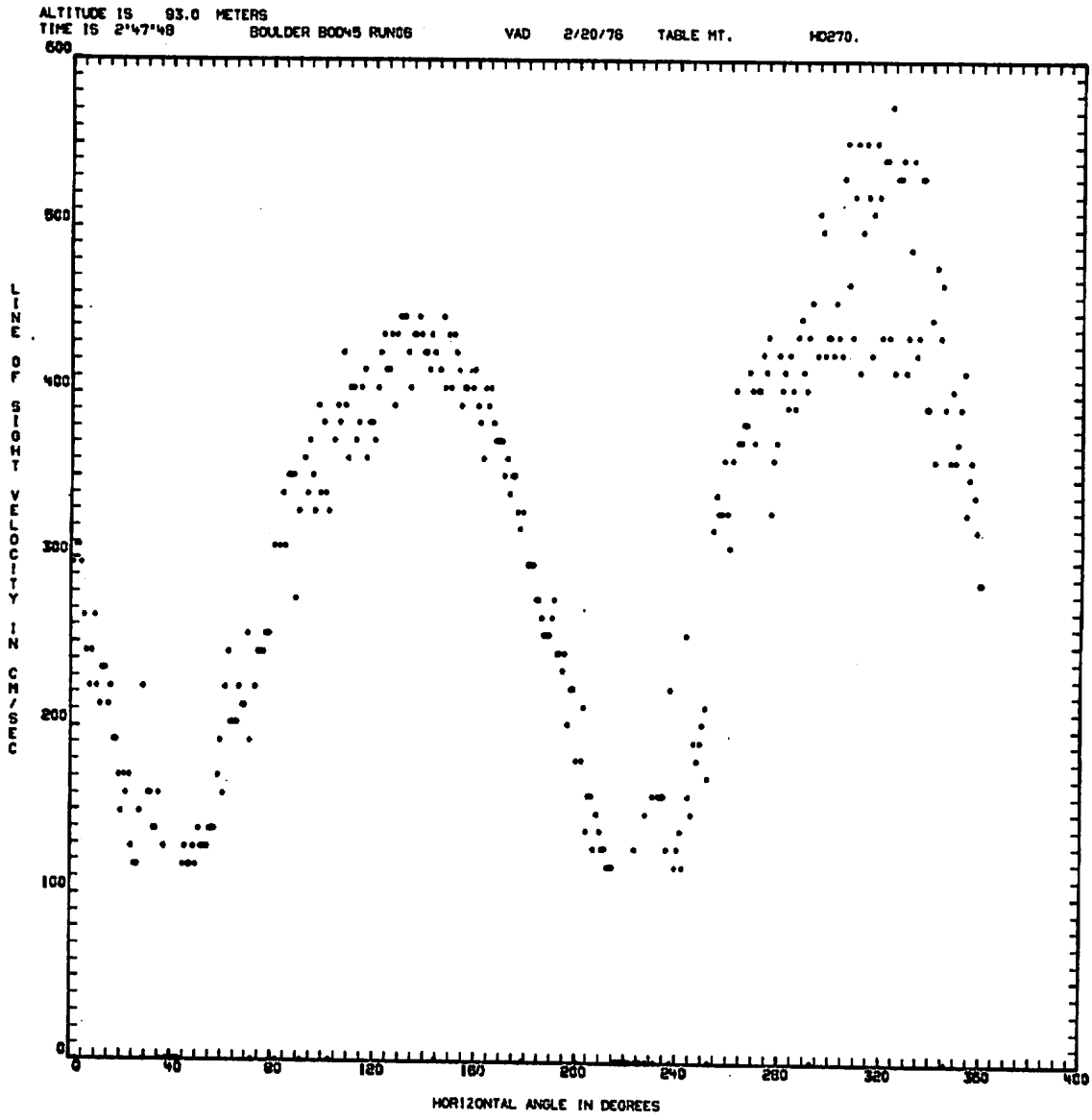

FIGURE A-1 (Continued).

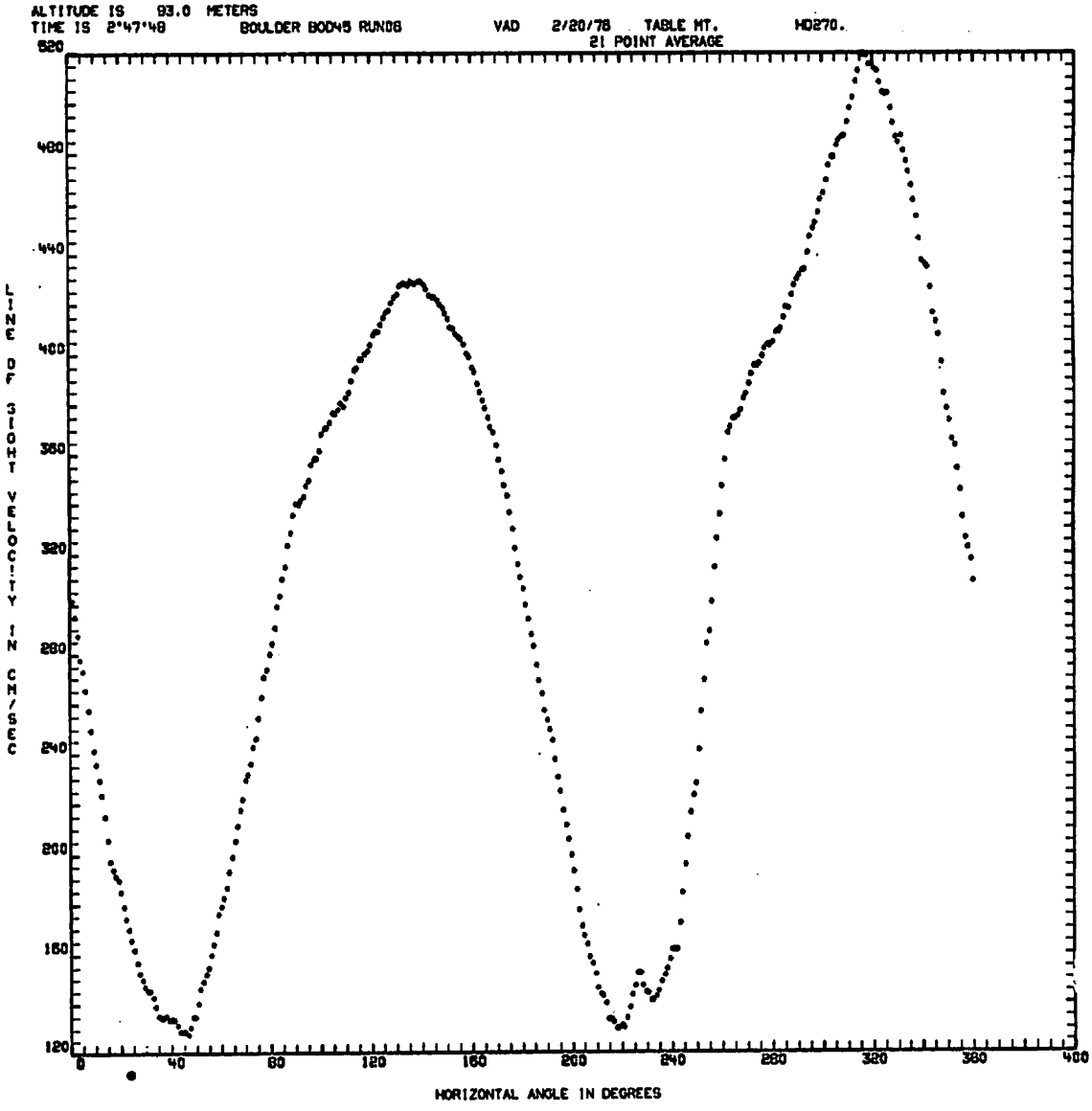

FIGURE A-1 (Continued).

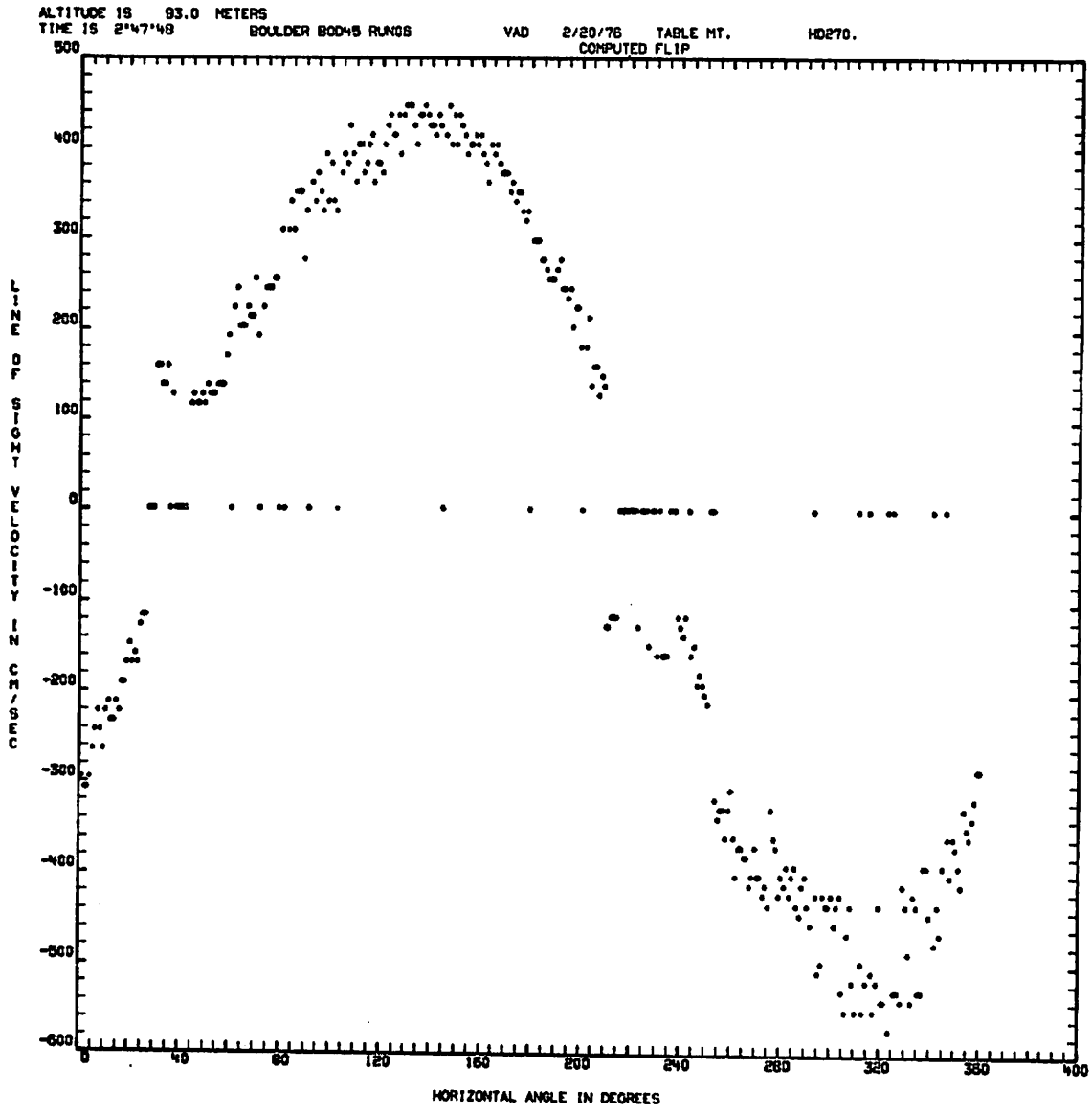

FIGURE A-1 (Continued).

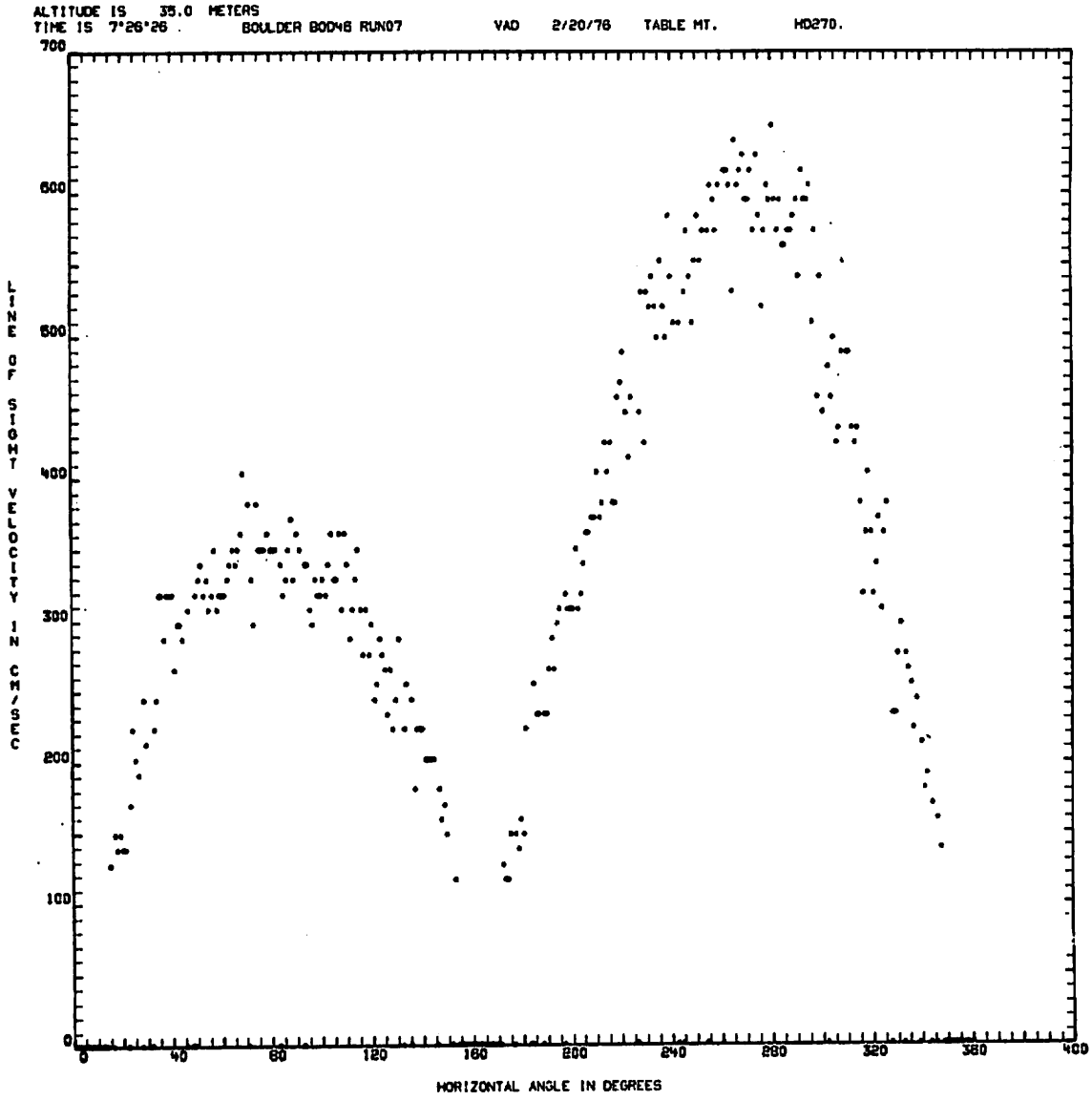

FIGURE A-1 (Continued).

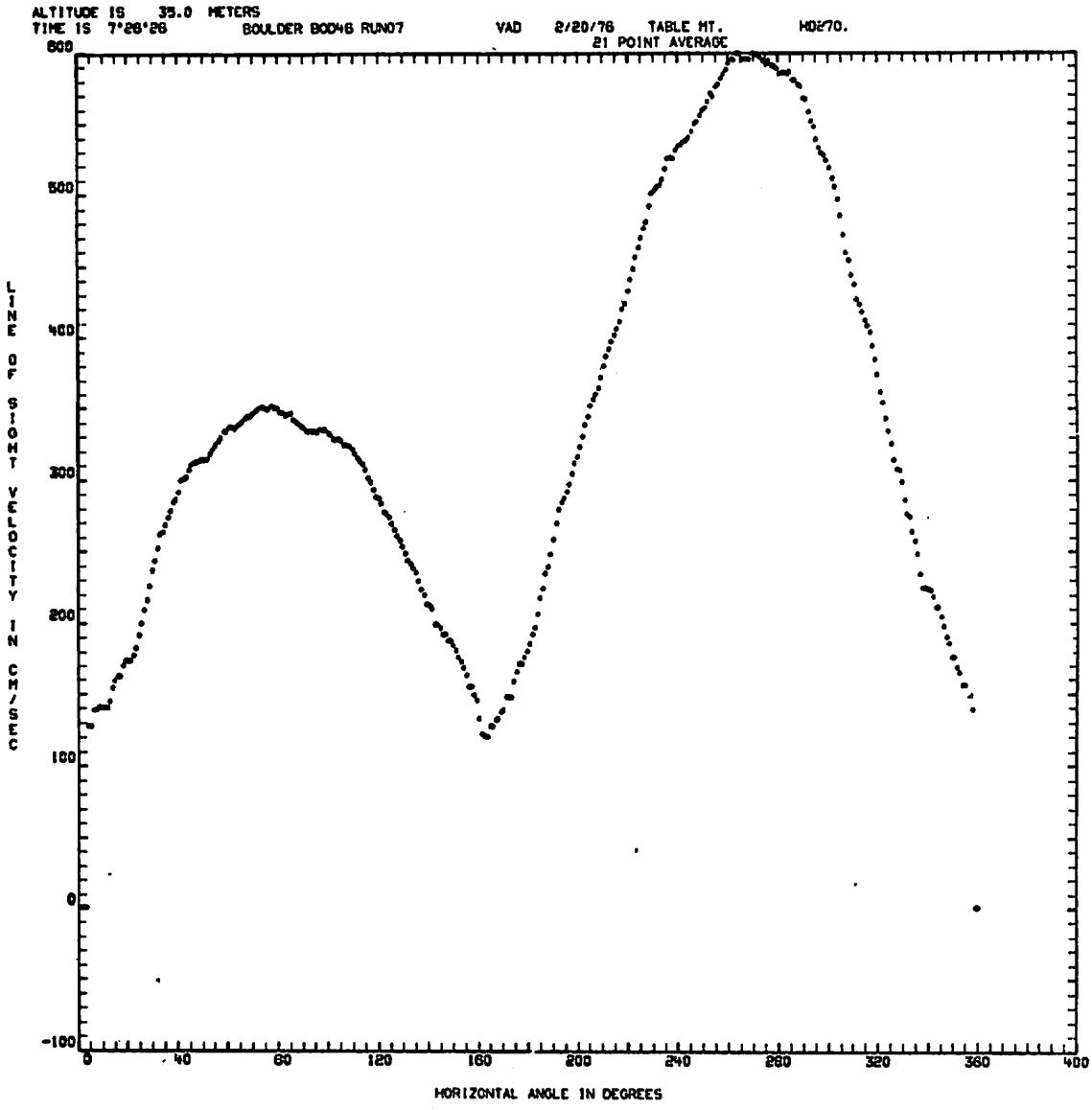

FIGURE A-1 (Continued).

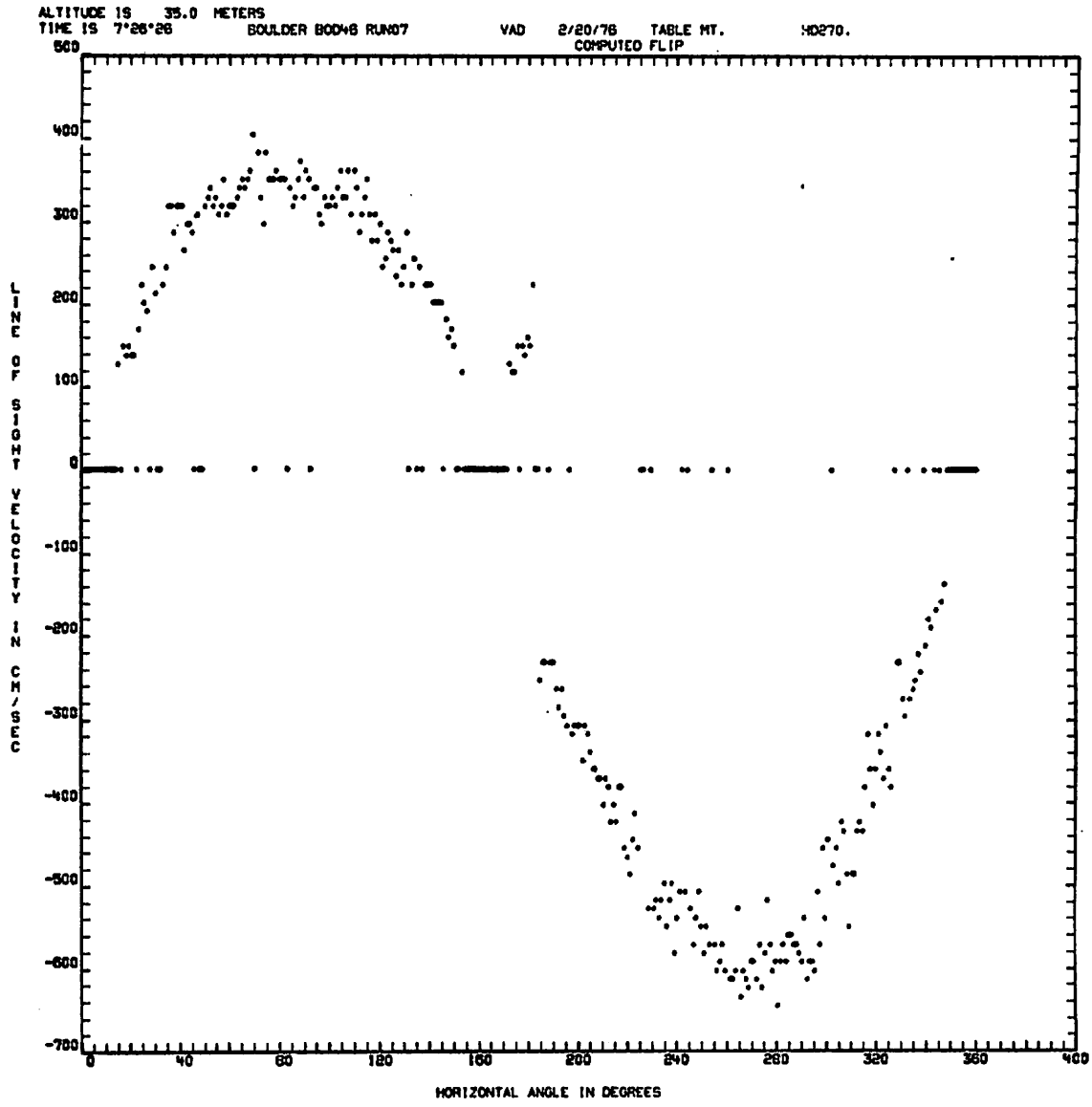

FIGURE A-1 (Continued).

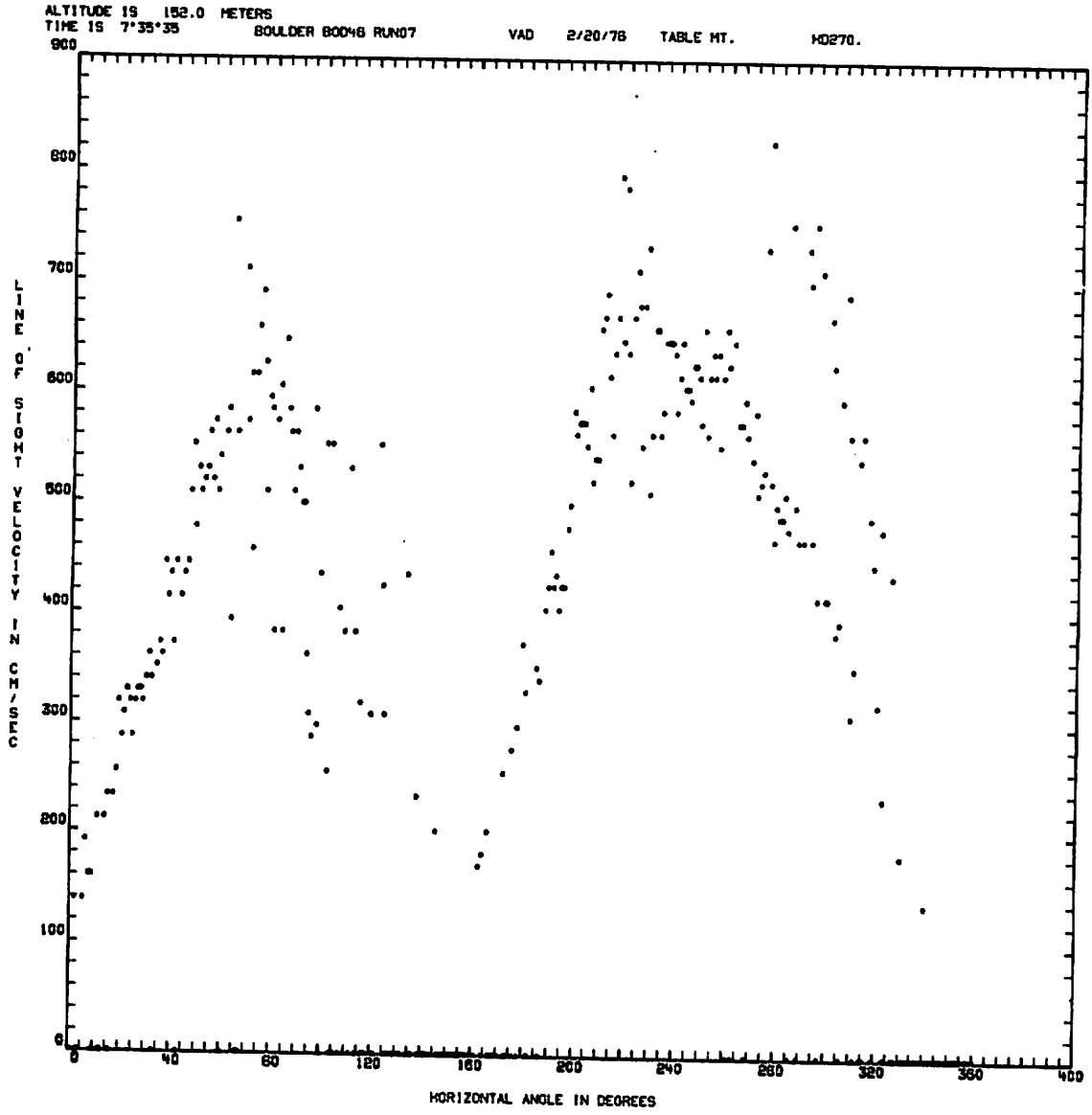

FIGURE A-1 (Continued).

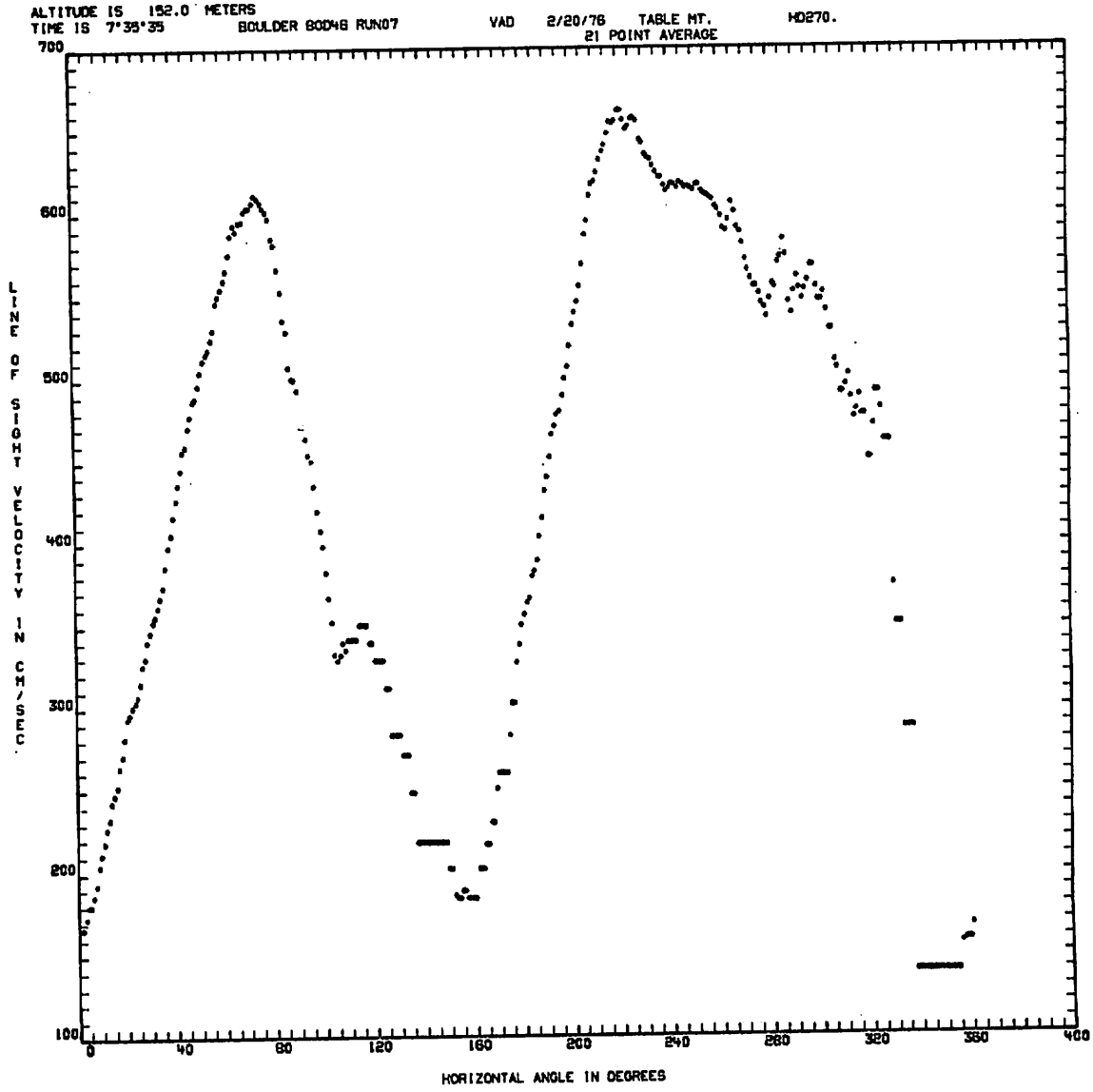

FIGURE A-1 (Continued).

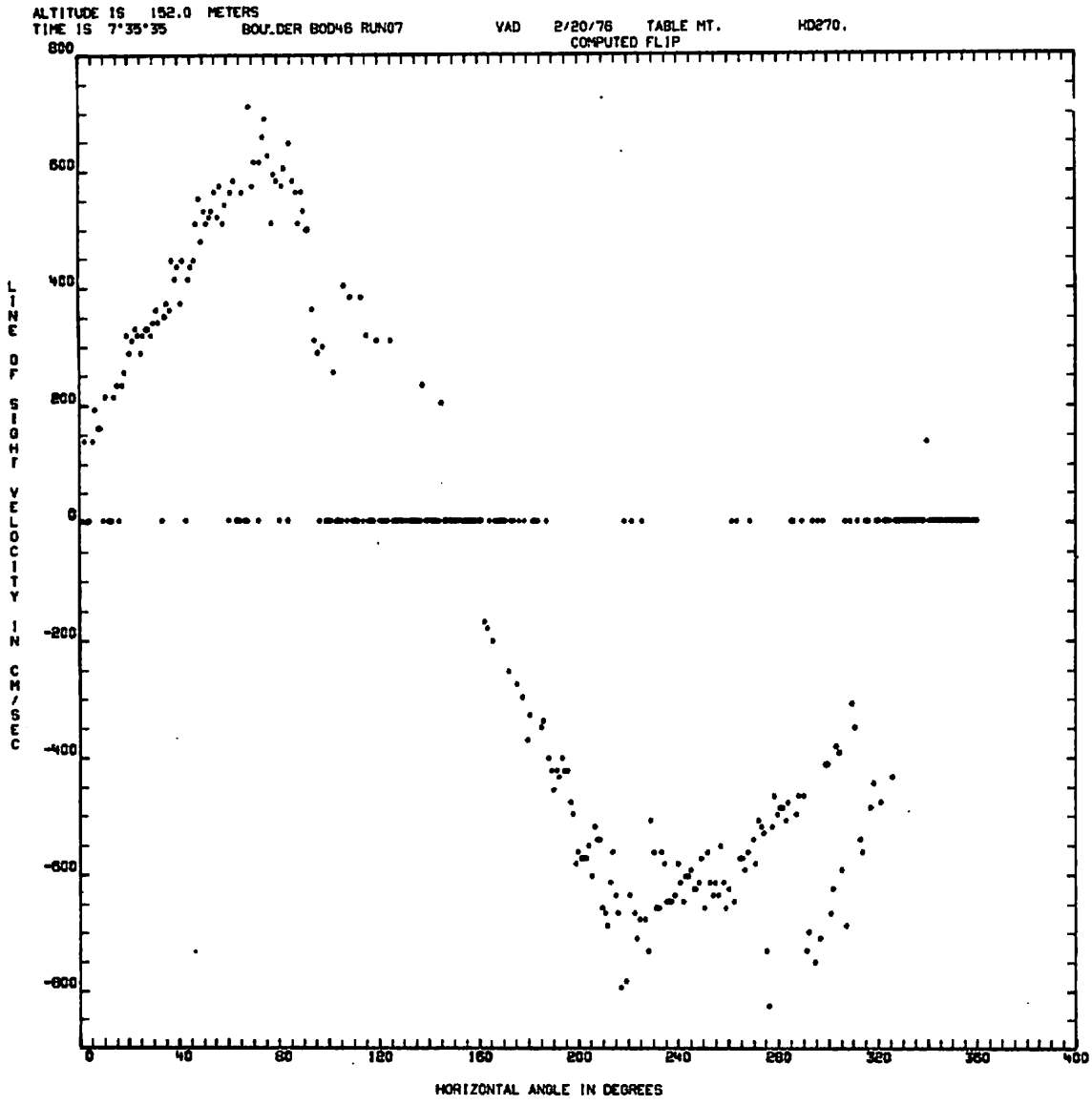

FIGURE A-1 (Continued).

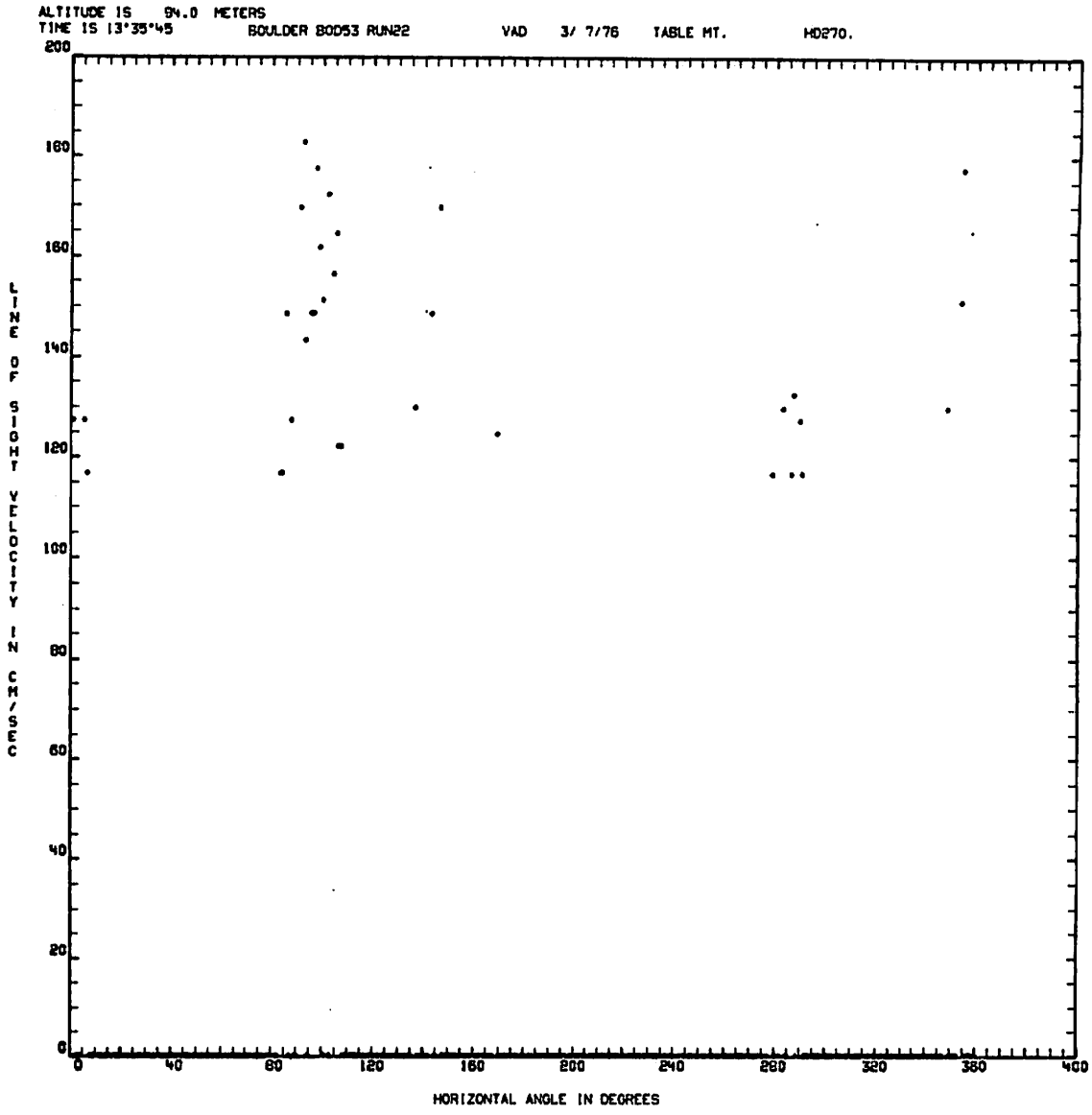

FIGURE A-1 (Continued).

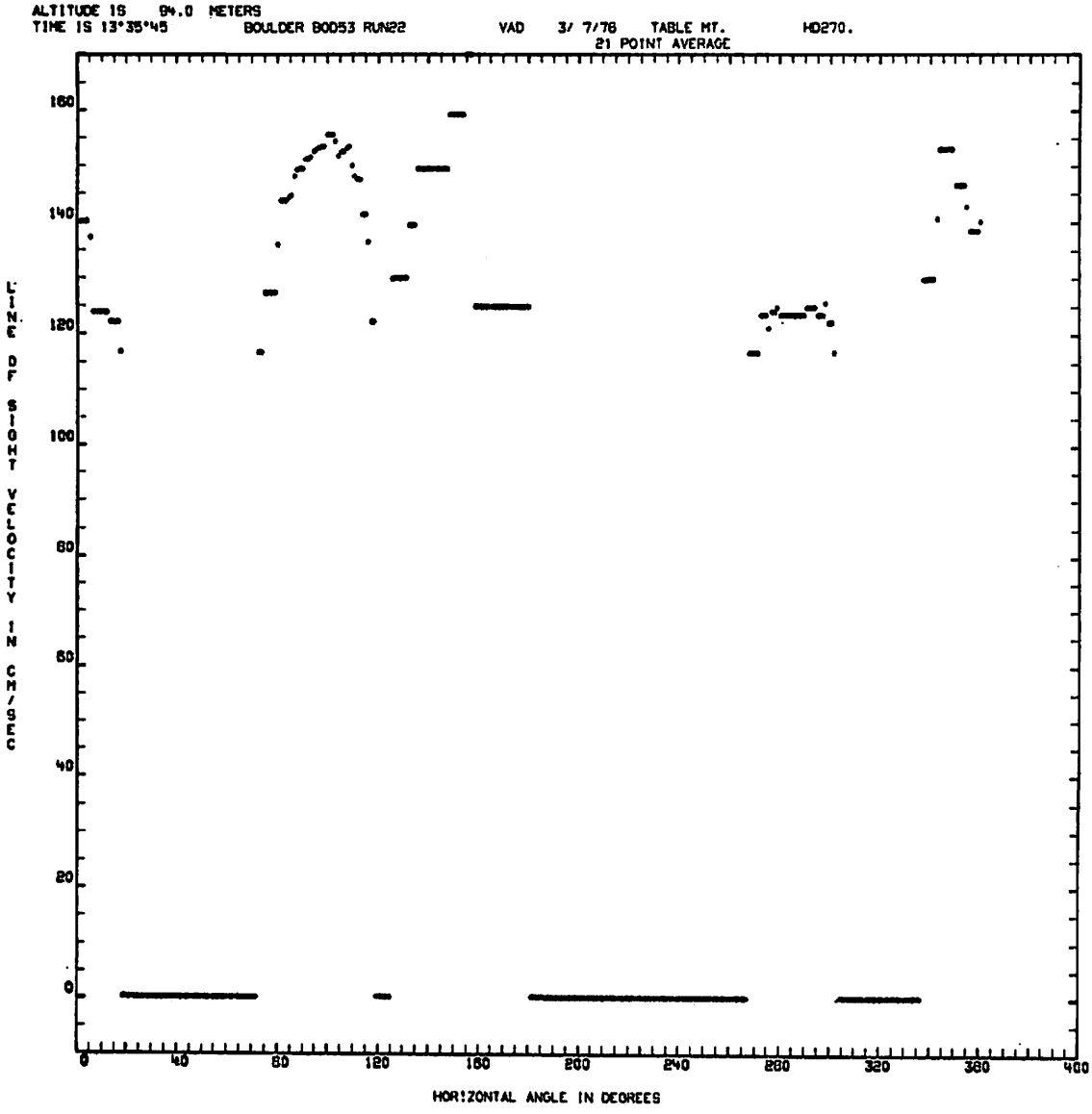

FIGURE A-1 (Continued).

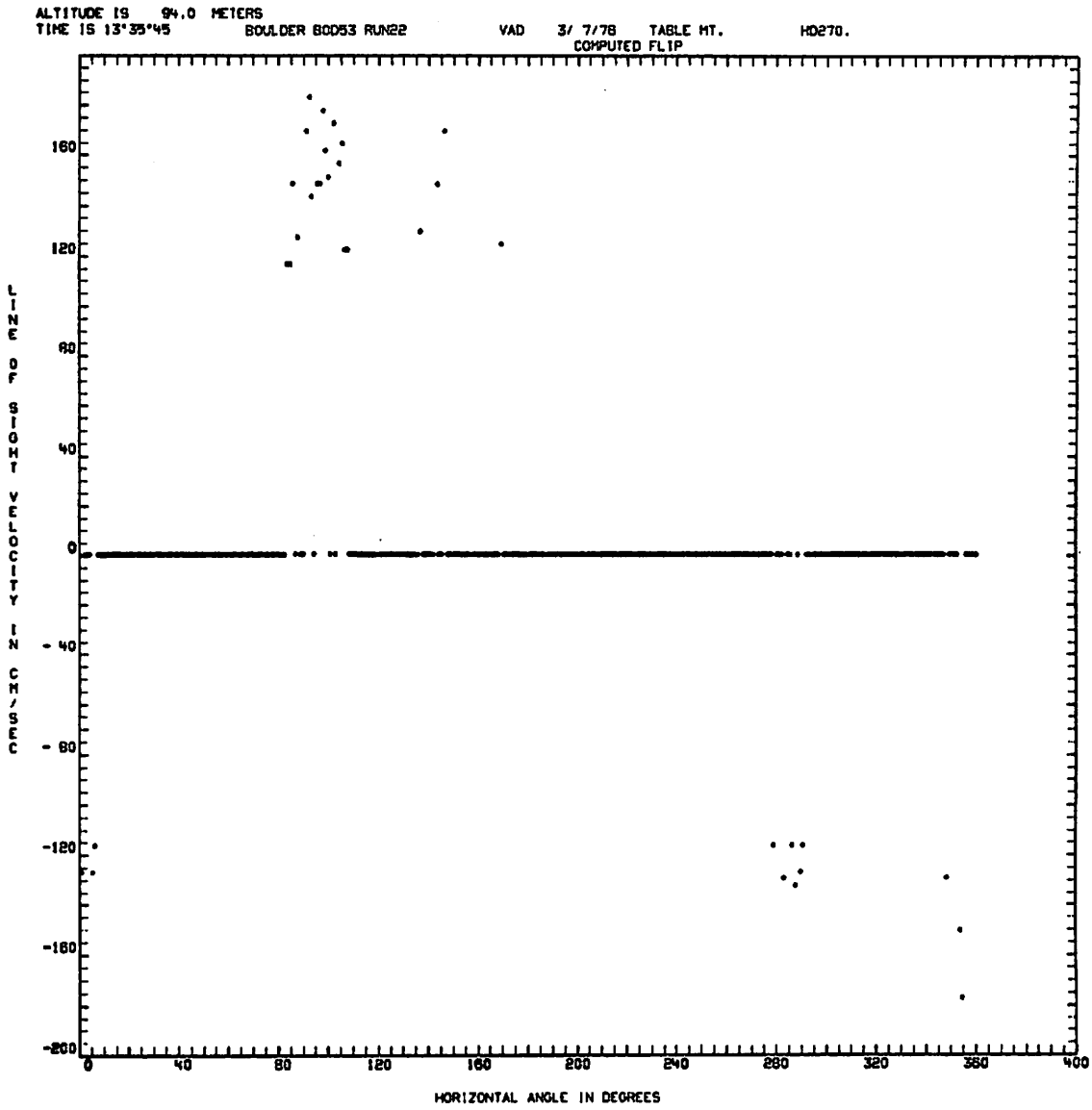

FIGURE A-1 (Continued).

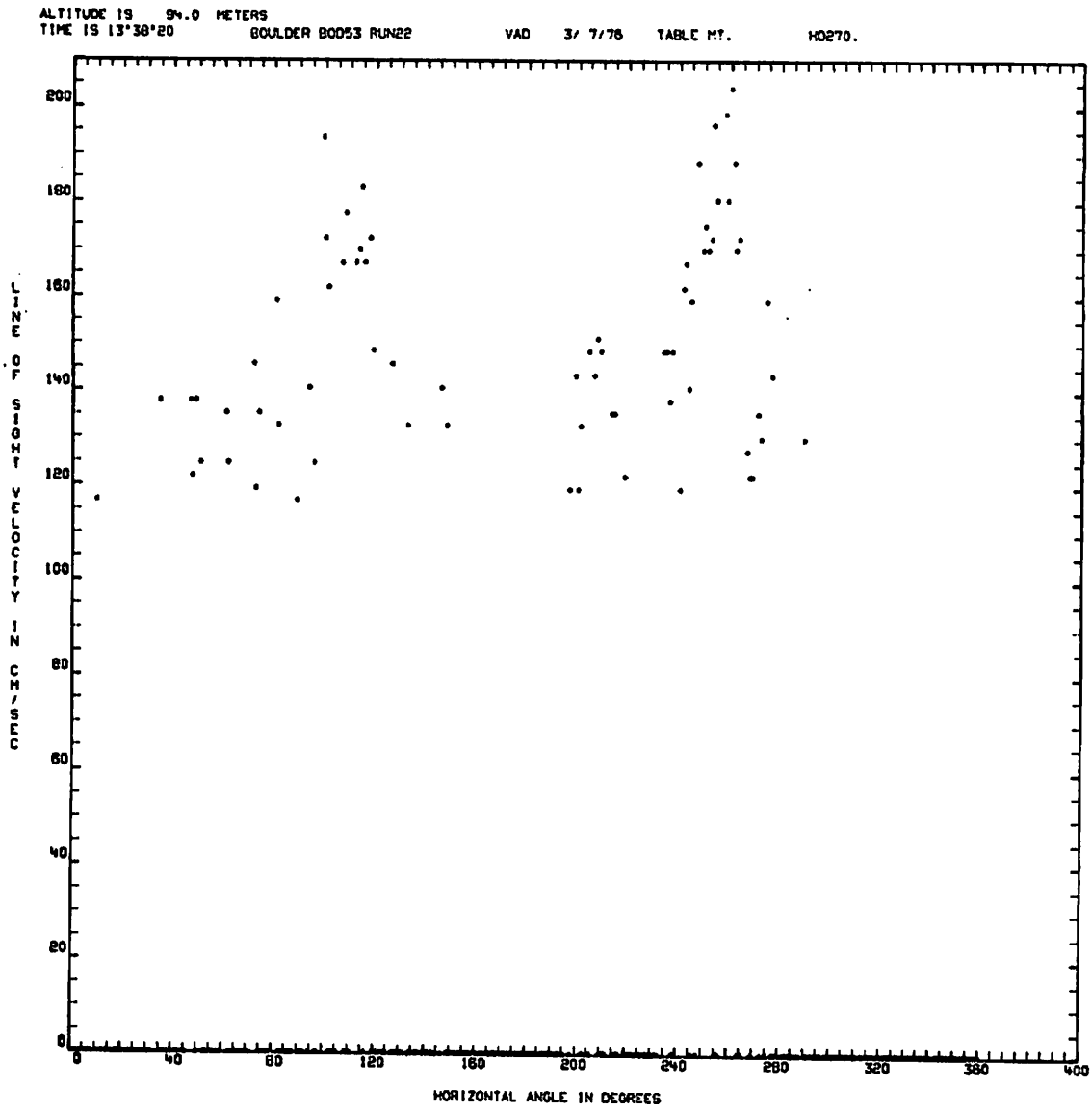

FIGURE A-1 (Continued).

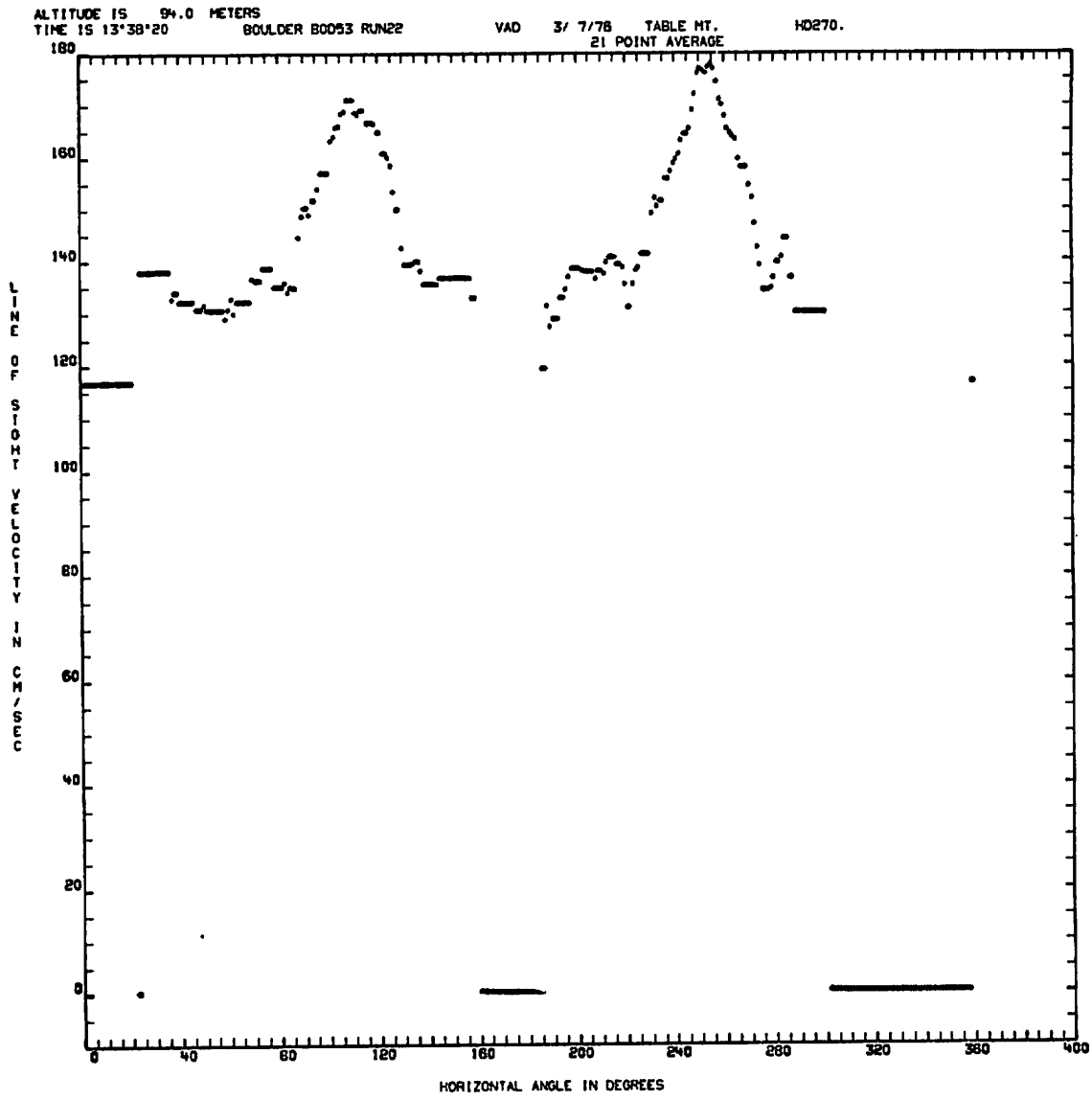

FIGURE A-1 (Continued).

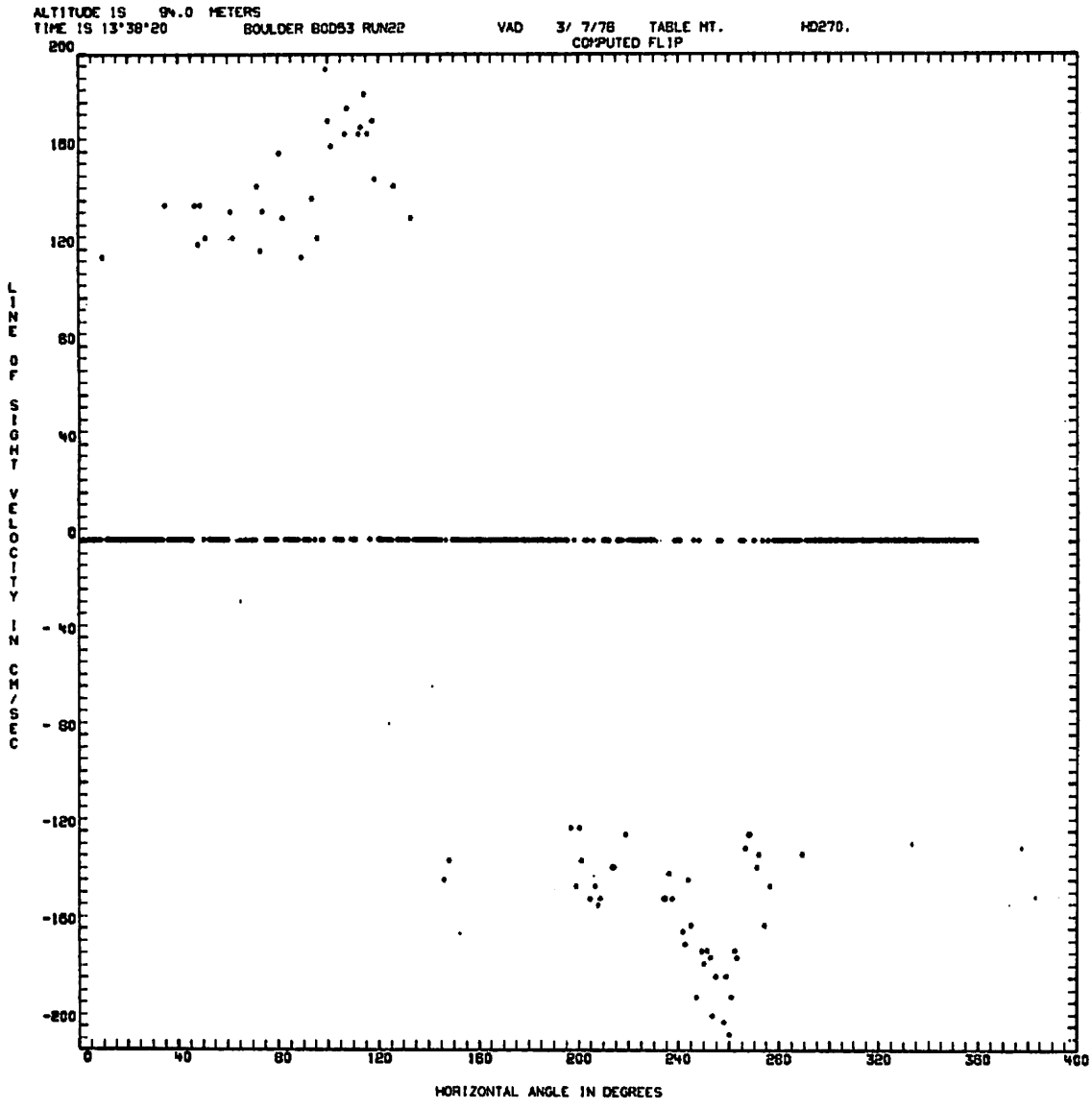

FIGURE A-1 (Continued).

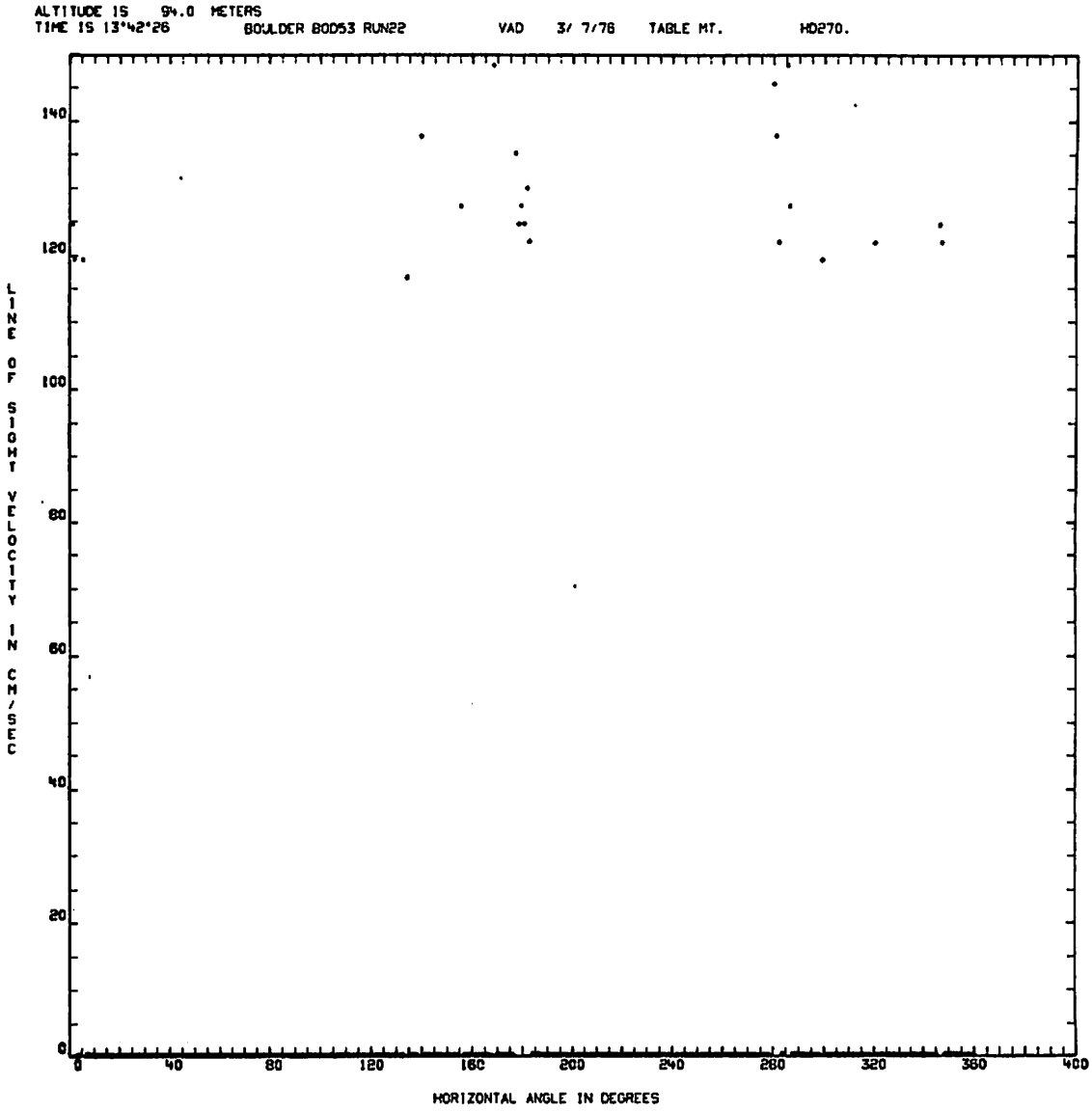

FIGURE A-1 (Continued).

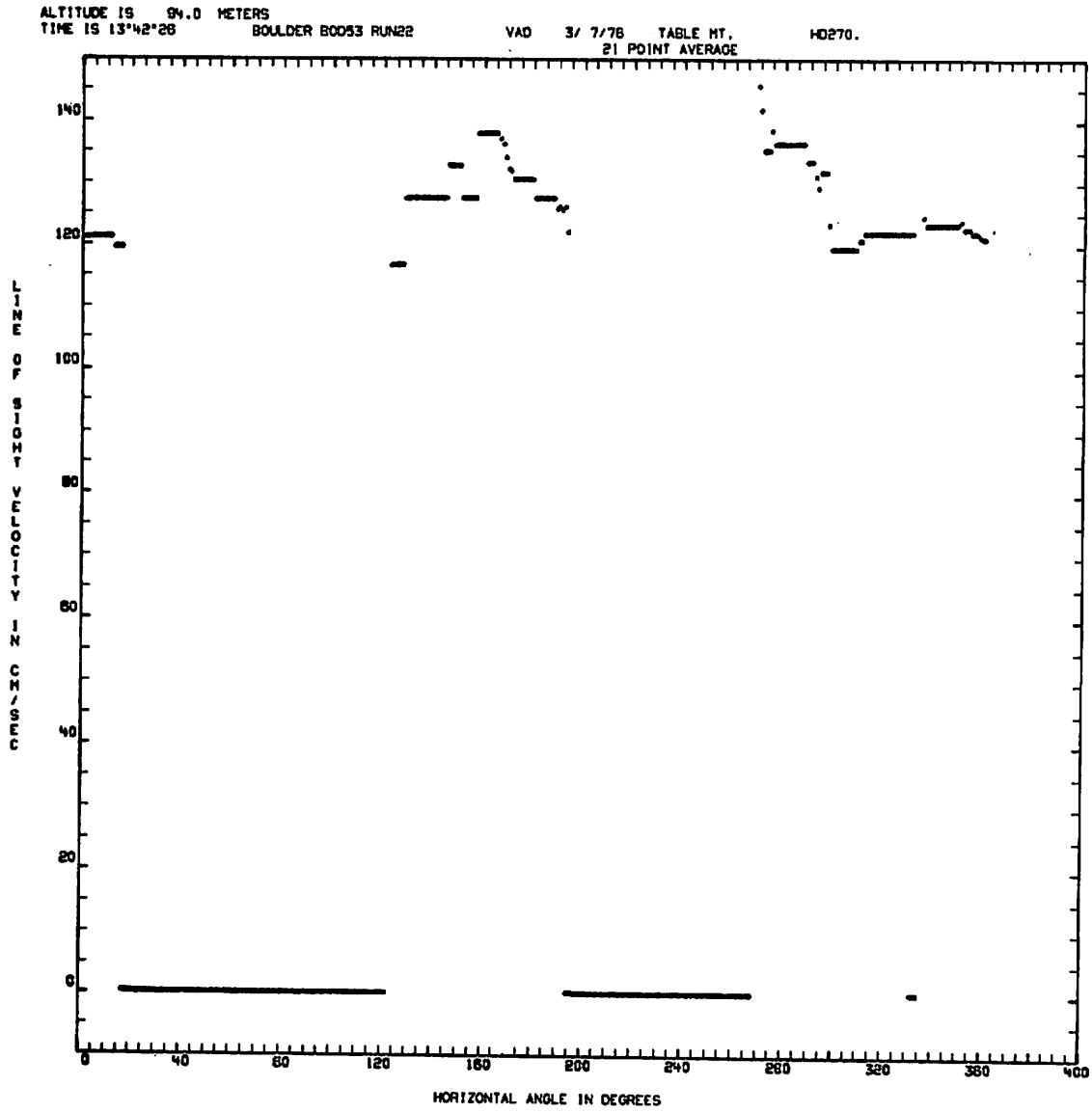

FIGURE A-1 (Continued).

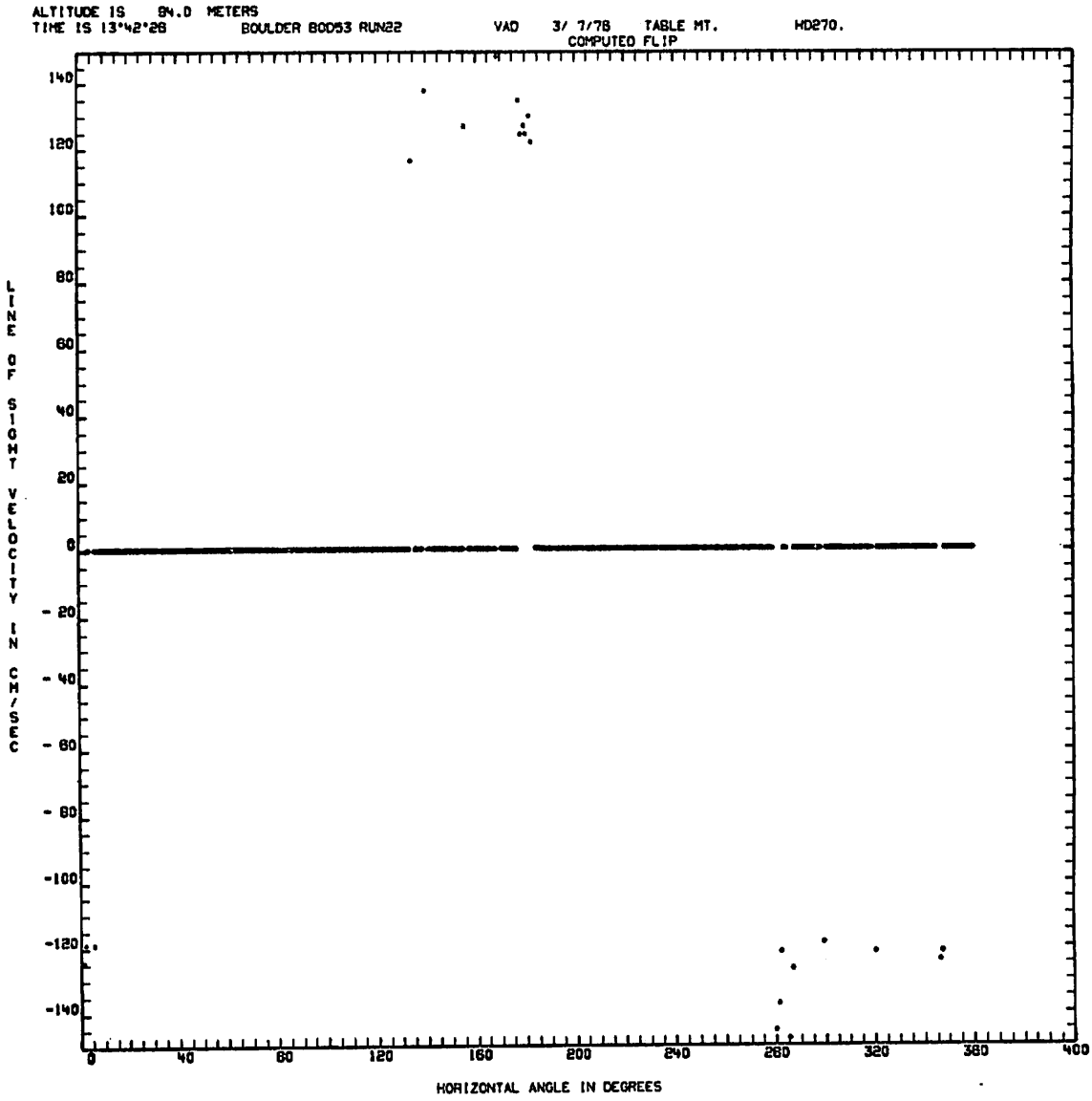

FIGURE A-1 (Continued).

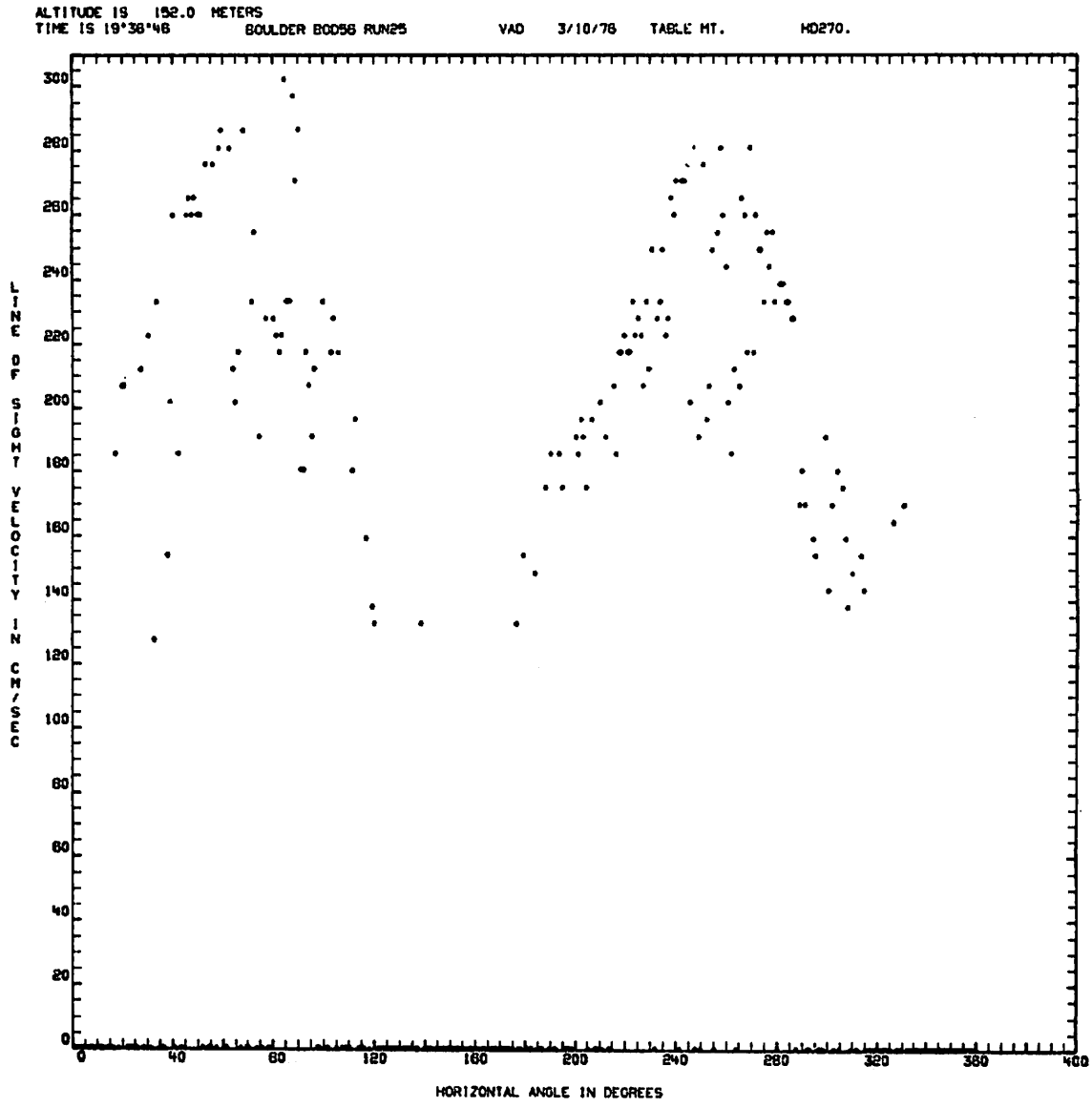

FIGURE A-1 (Continued).

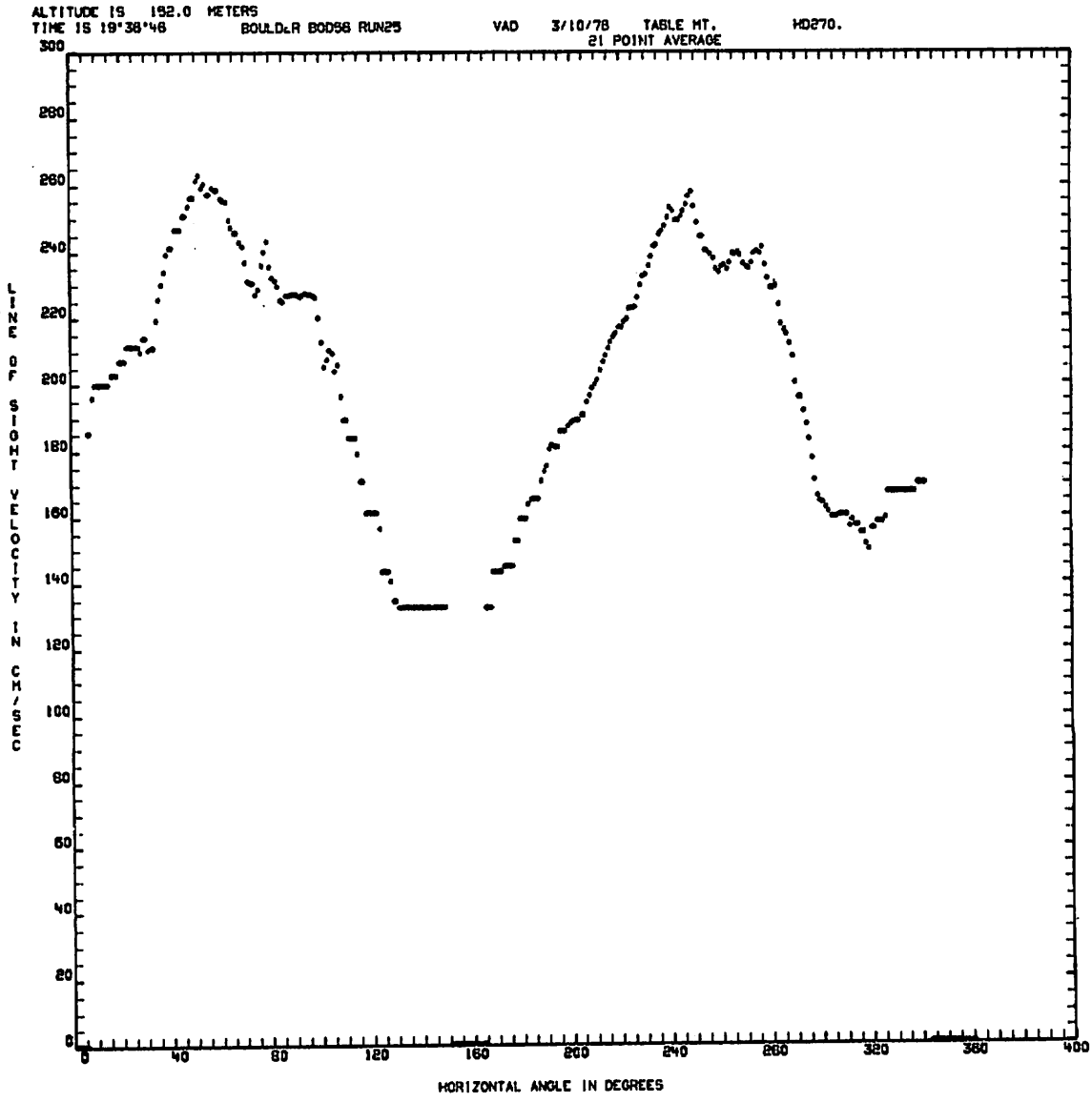

FIGURE A-1 (Continued).

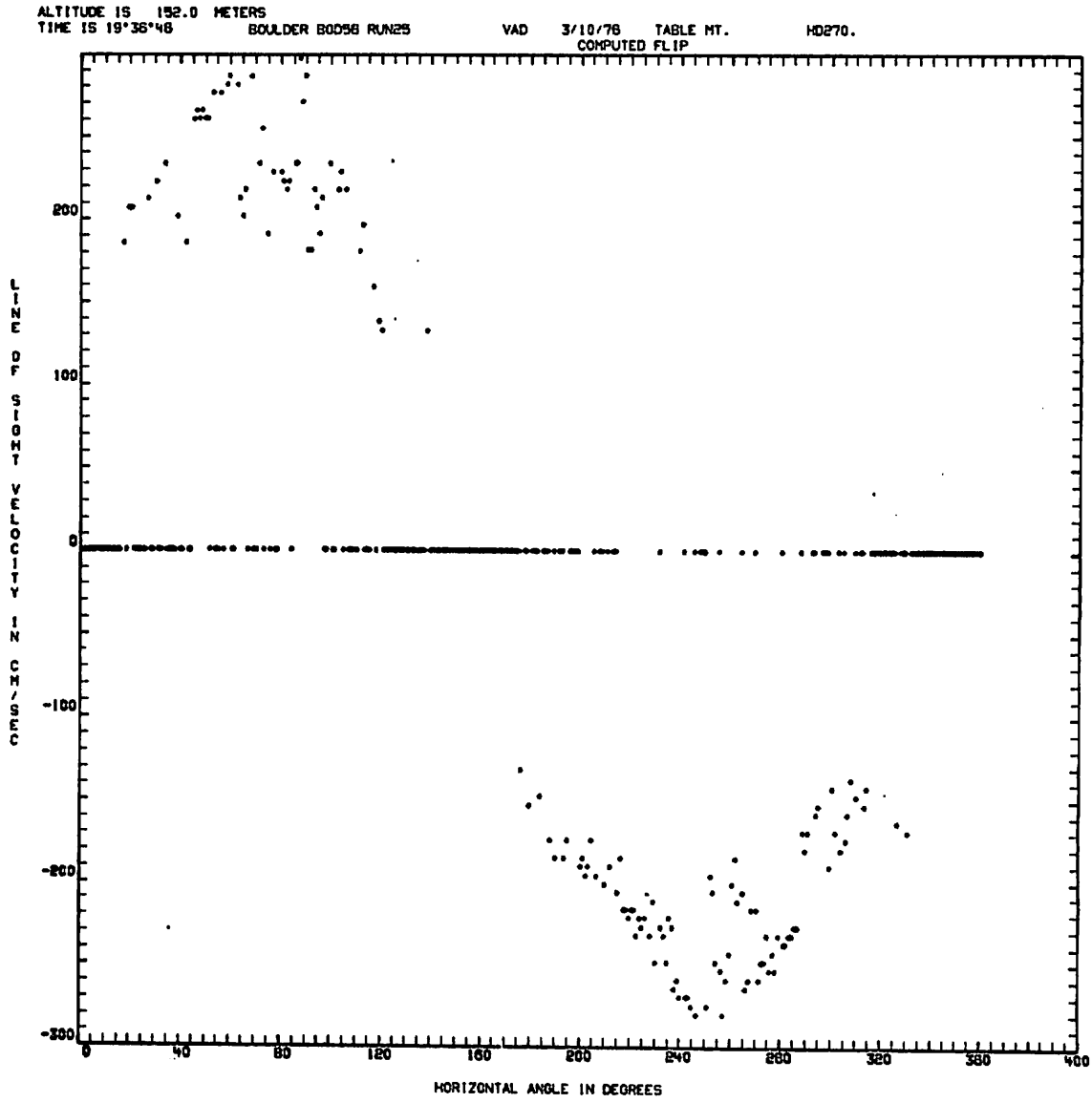

FIGURE A-1 (Continued).

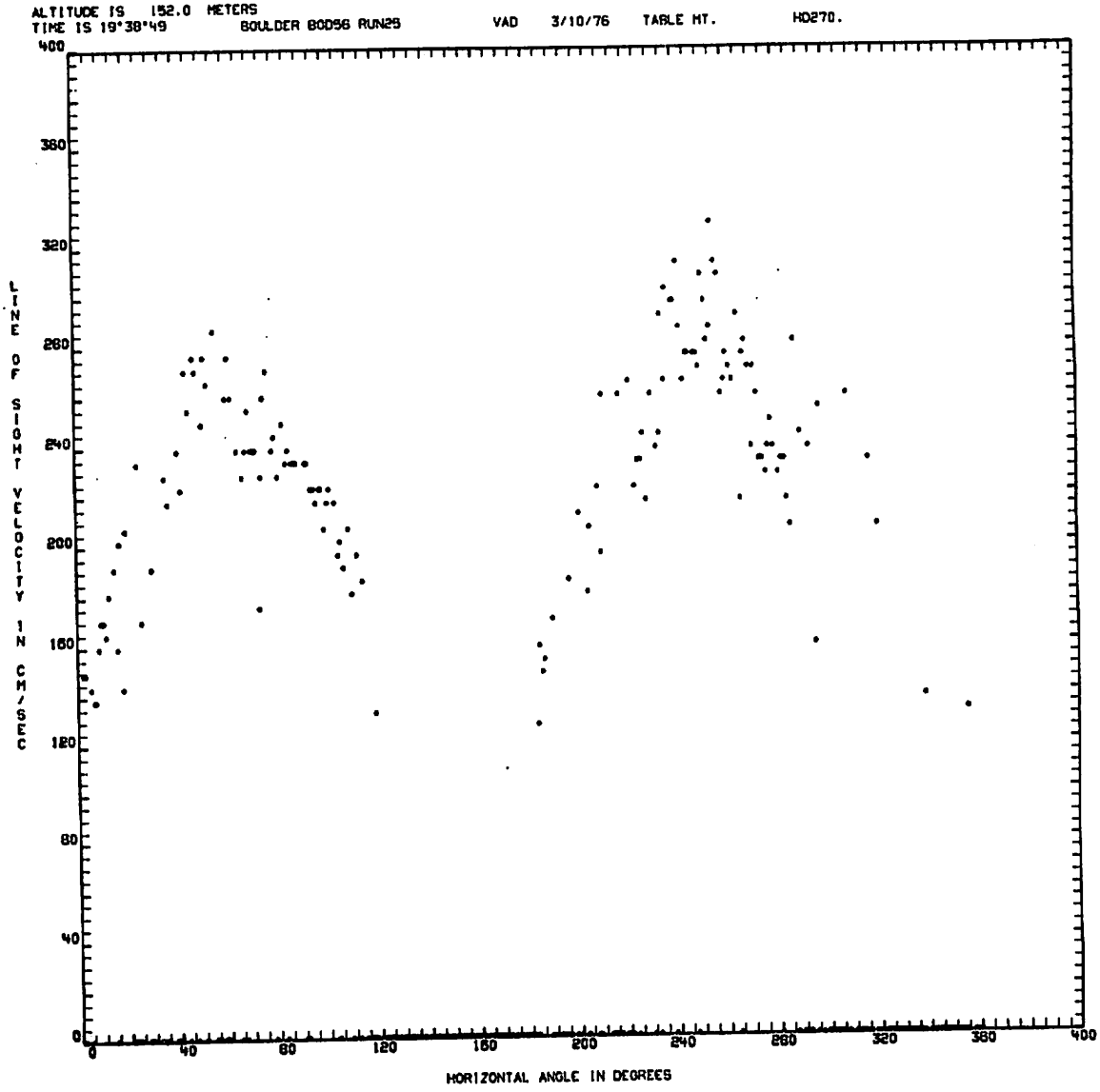

FIGURE A-1 (Continued).

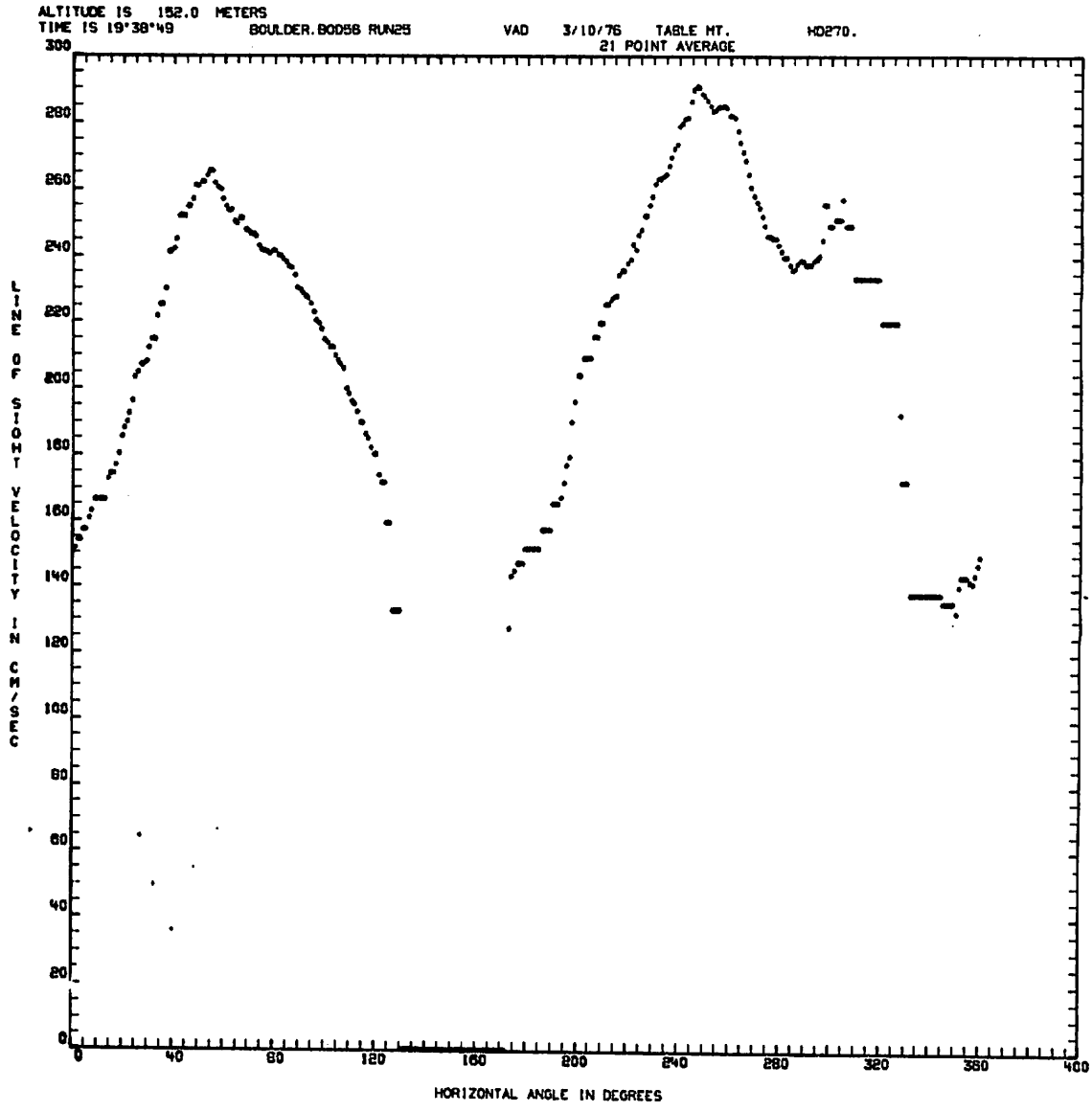

FIGURE A-1 (Continued).

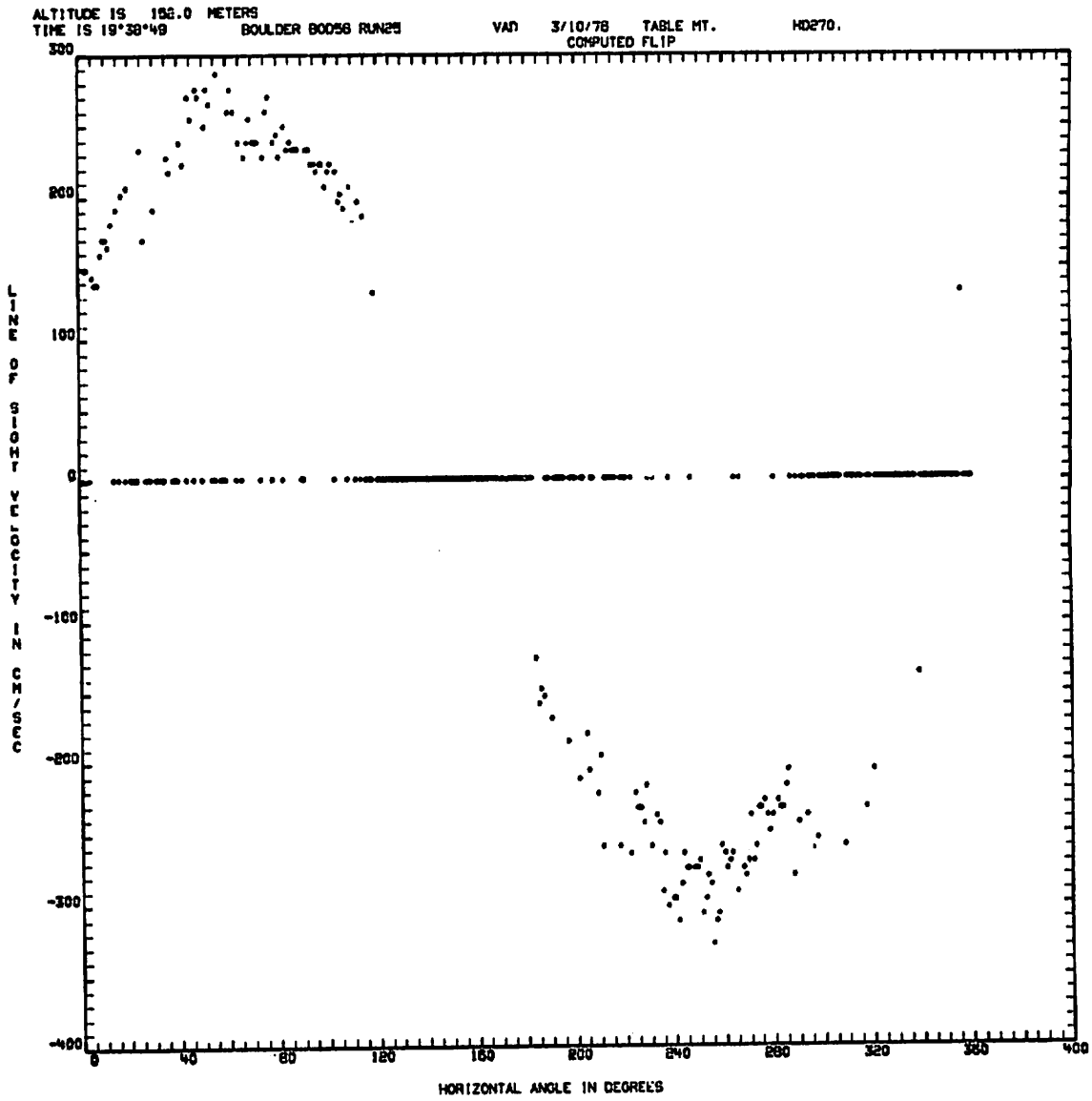

FIGURE A-1 (Continued).

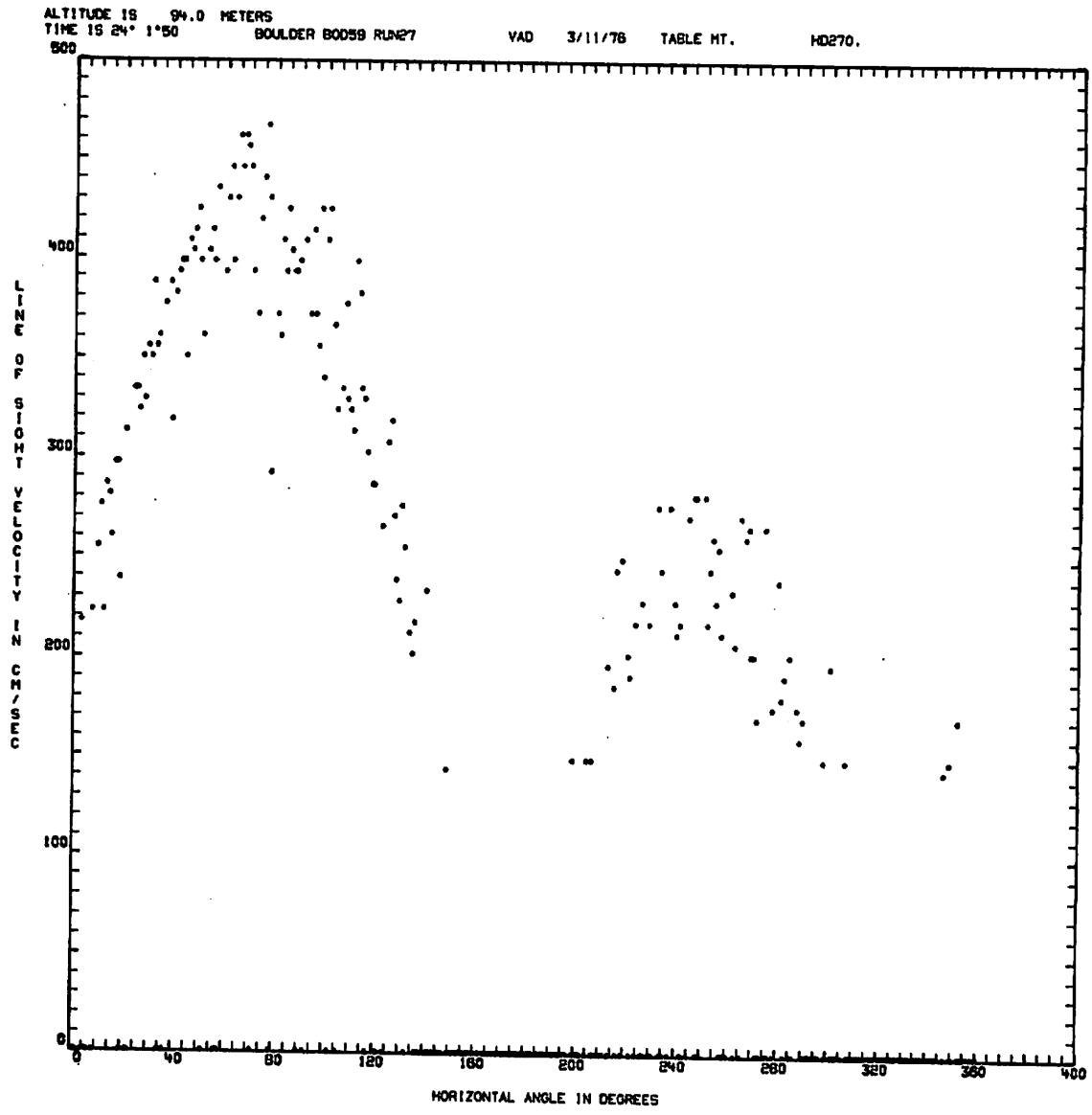

FIGURE A-1 (Continued).

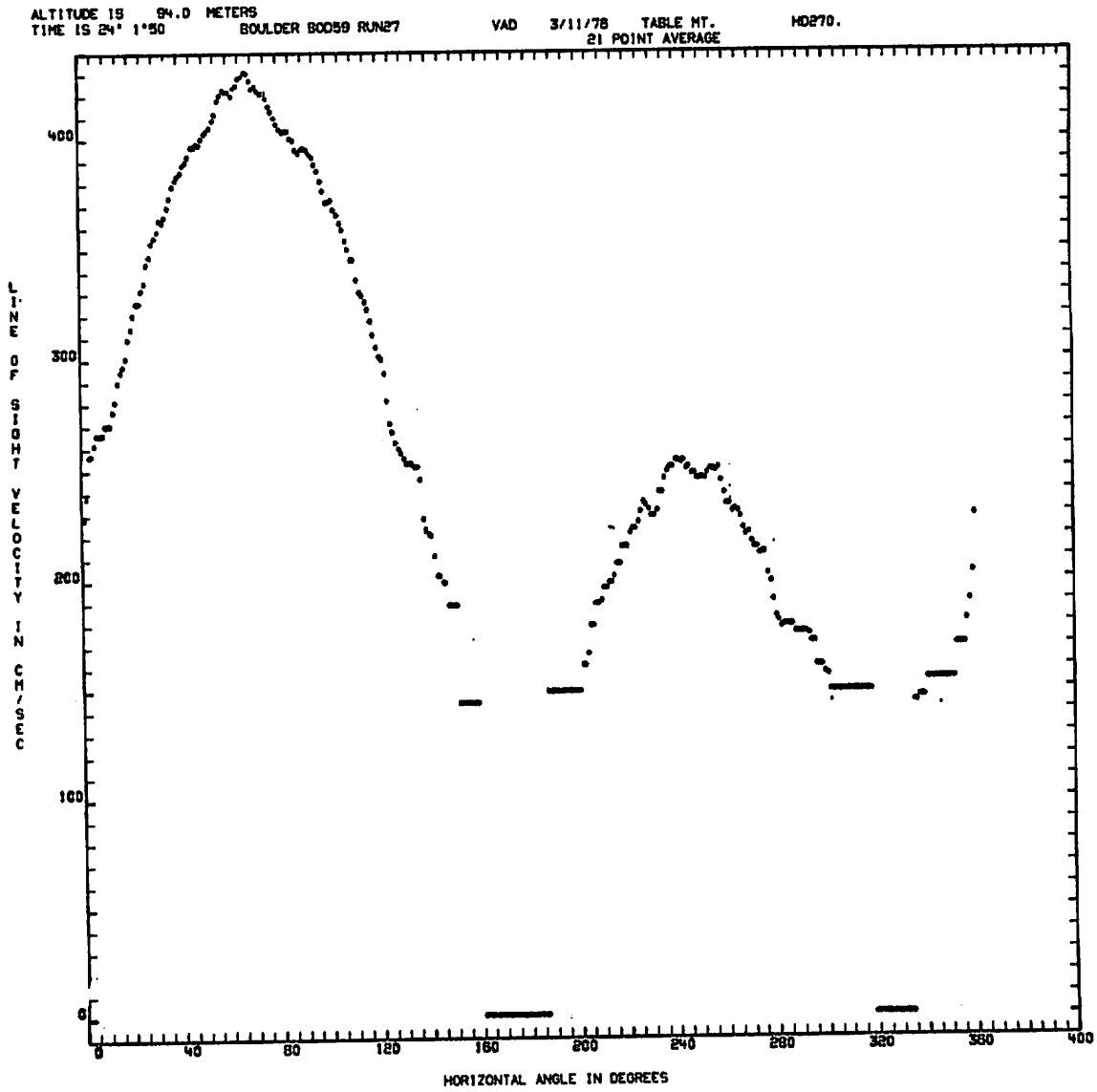

FIGURE A-1 (Continued).

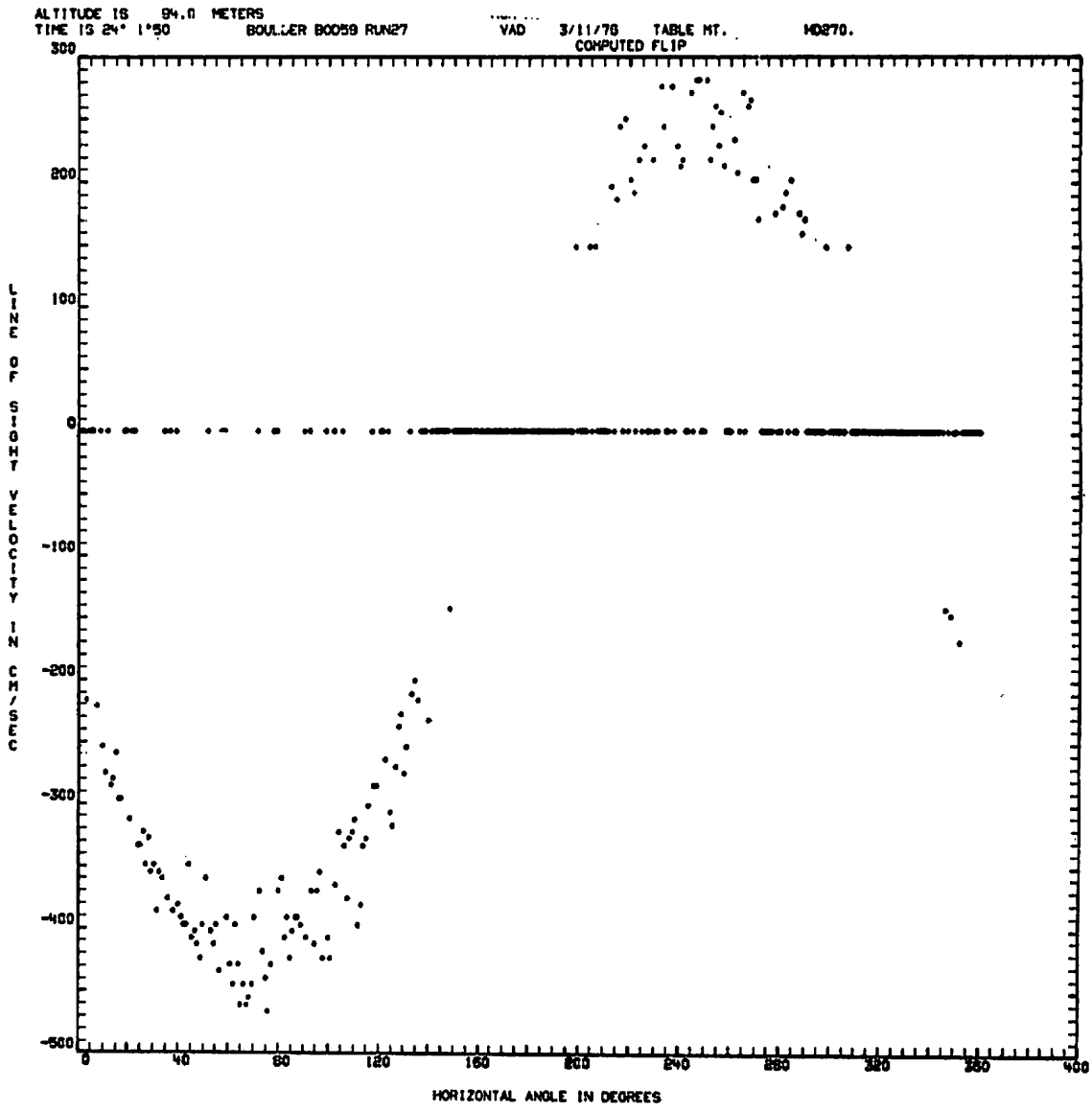

FIGURE A-1 (Concluded).

Appendix B

LASER DOPPLER VELOCIMETER AND ANEMOMETER WIND COMPARISONS

(Runs 21-28)

The least-squares sine algorithm is used as the basis of comparison for winds measured by the LDV and those measured by the tower-mounted anemometers. Wind-speed and direction comparisons are given for 1-, 6-, and 15-minute averages. No anemometer data were available for Run 24.

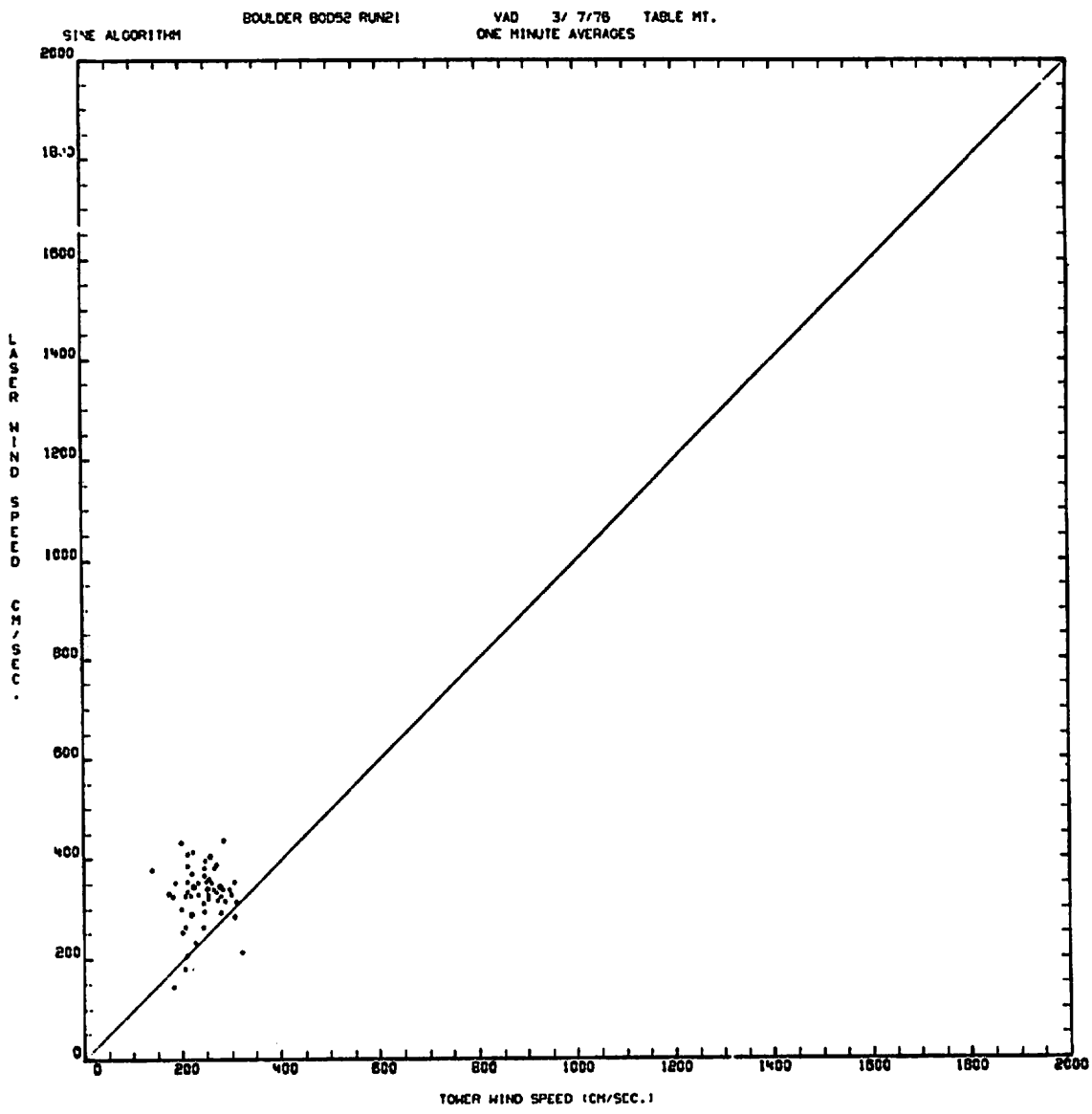

FIGURE B-1. COMPARISON OF WINDS MEASURED BY LASER DOPPLER VELOCIMETER AND TOWER ANEMOMETER.

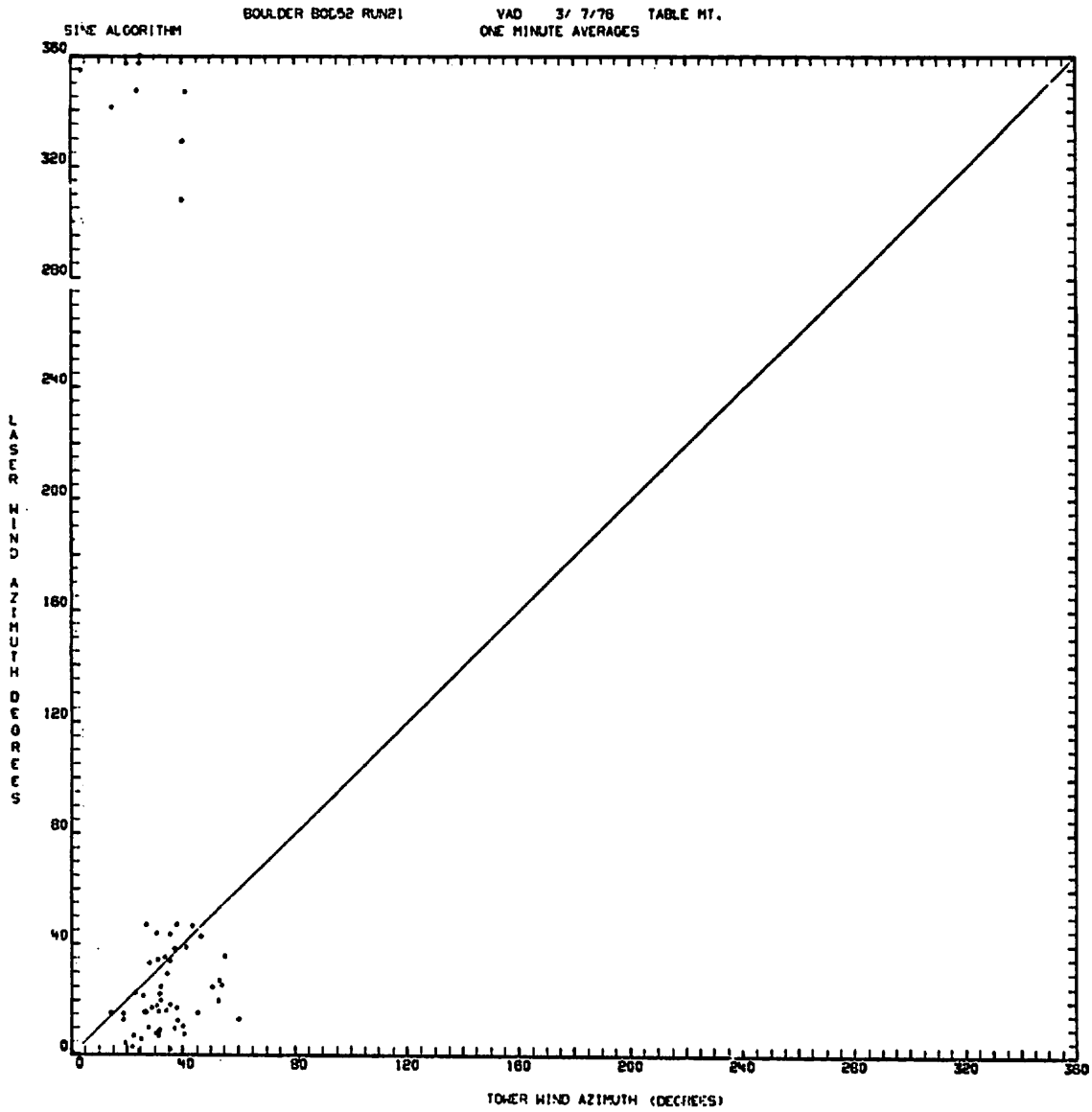

FIGURE B-1 (Continued).

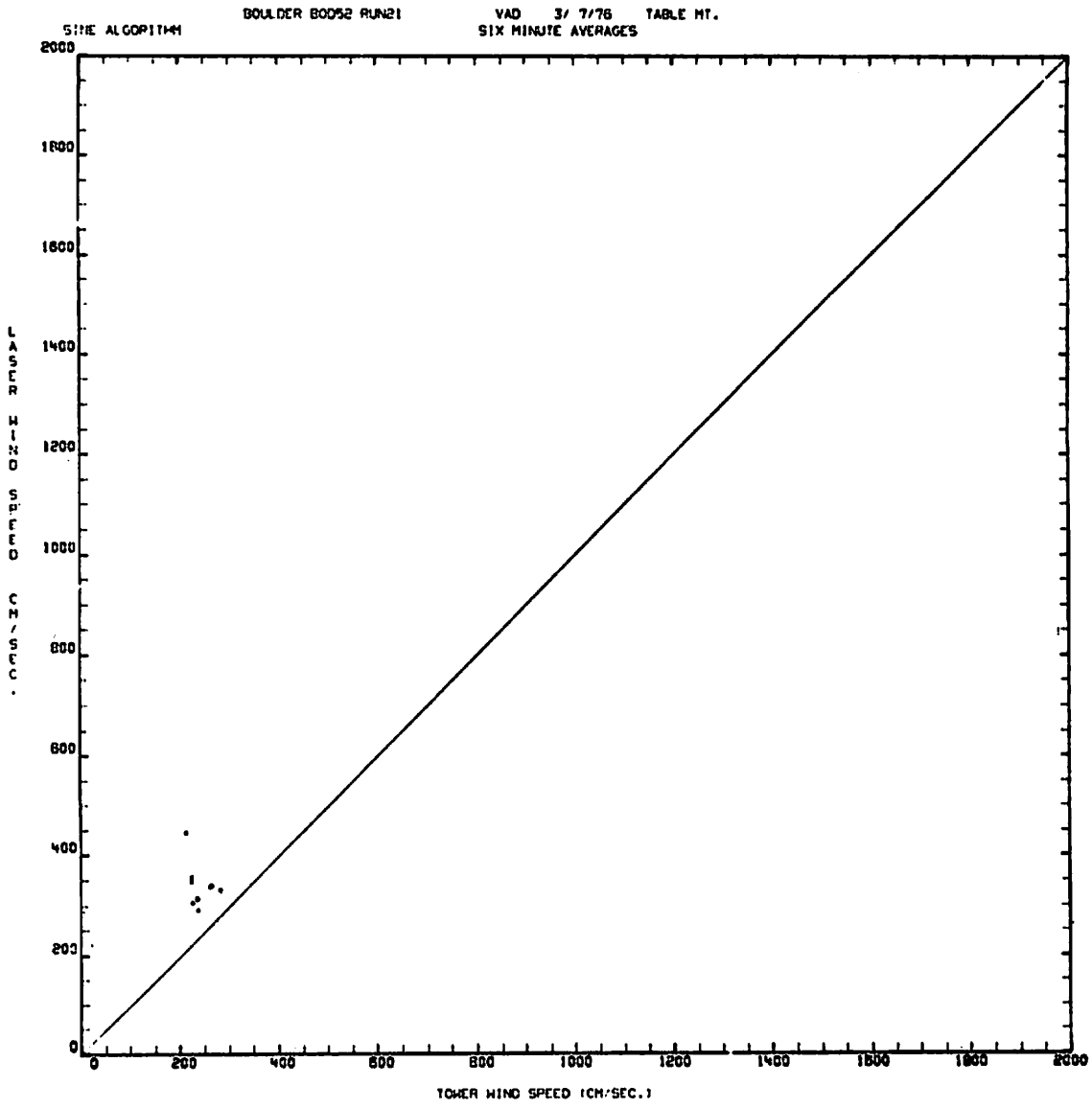

FIGURE B-1 (Continued).

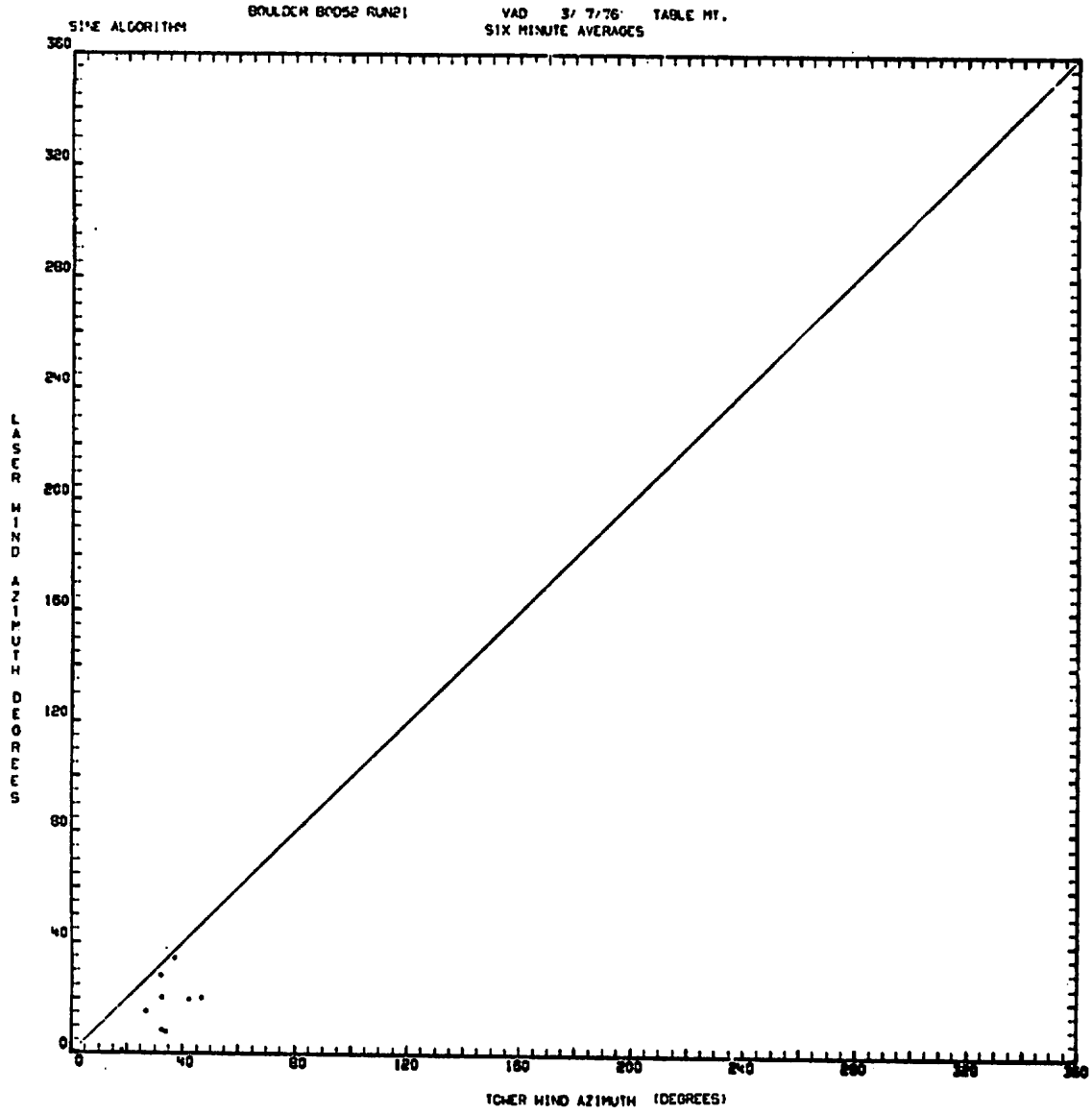

FIGURE B-1 (Continued).

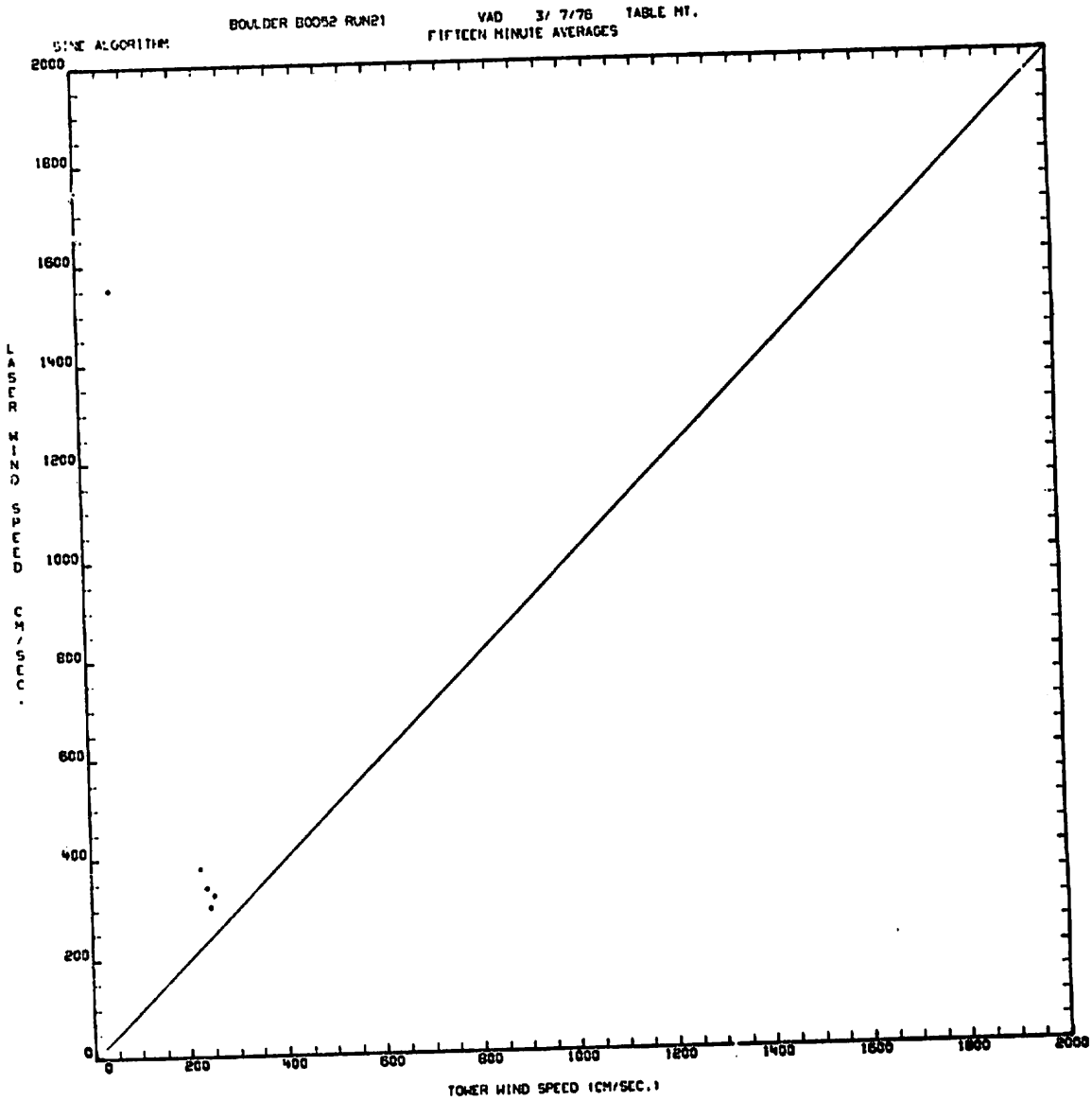

FIGURE B-1 (Continued).

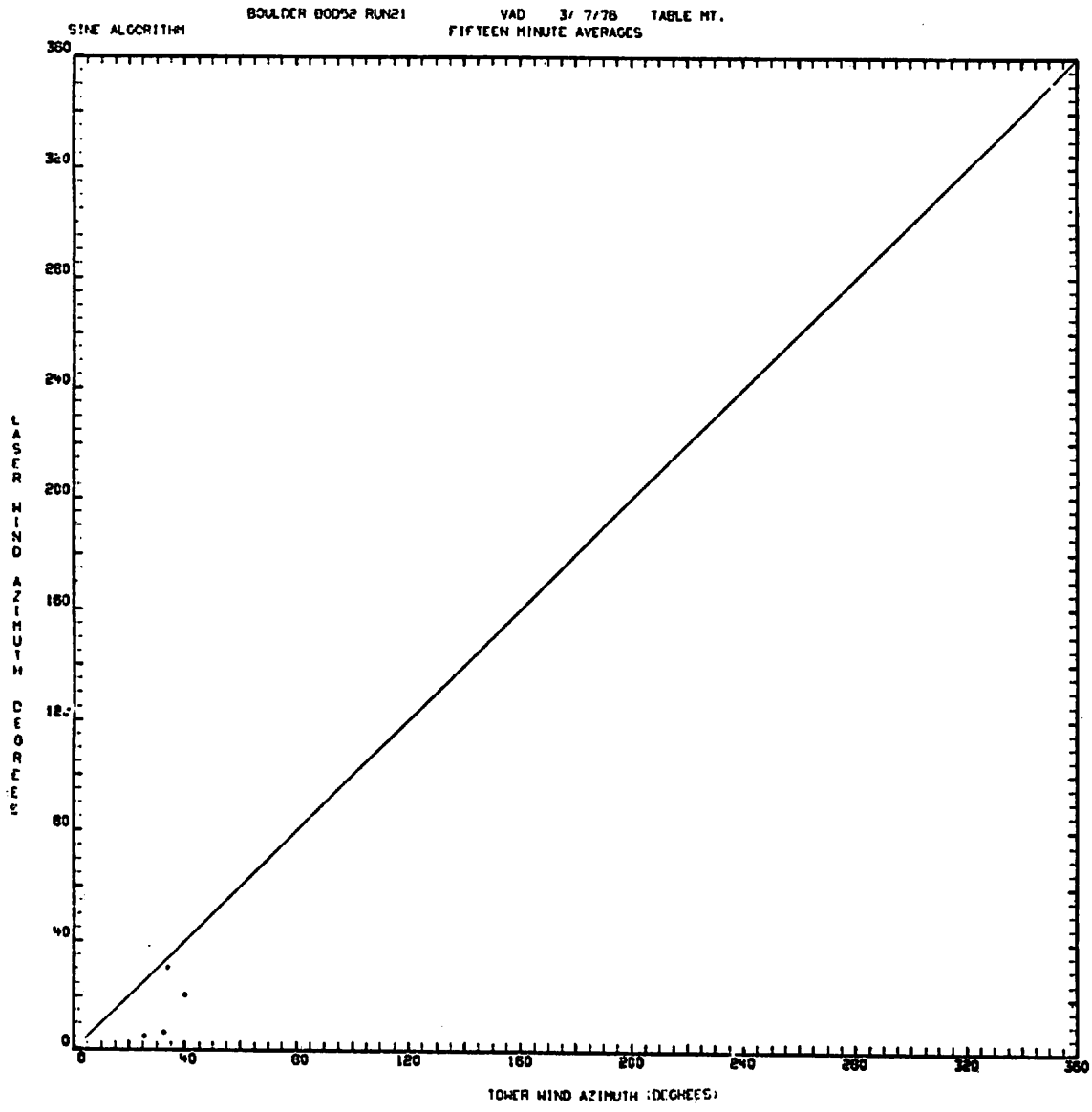

FIGURE B-1 (Continued).

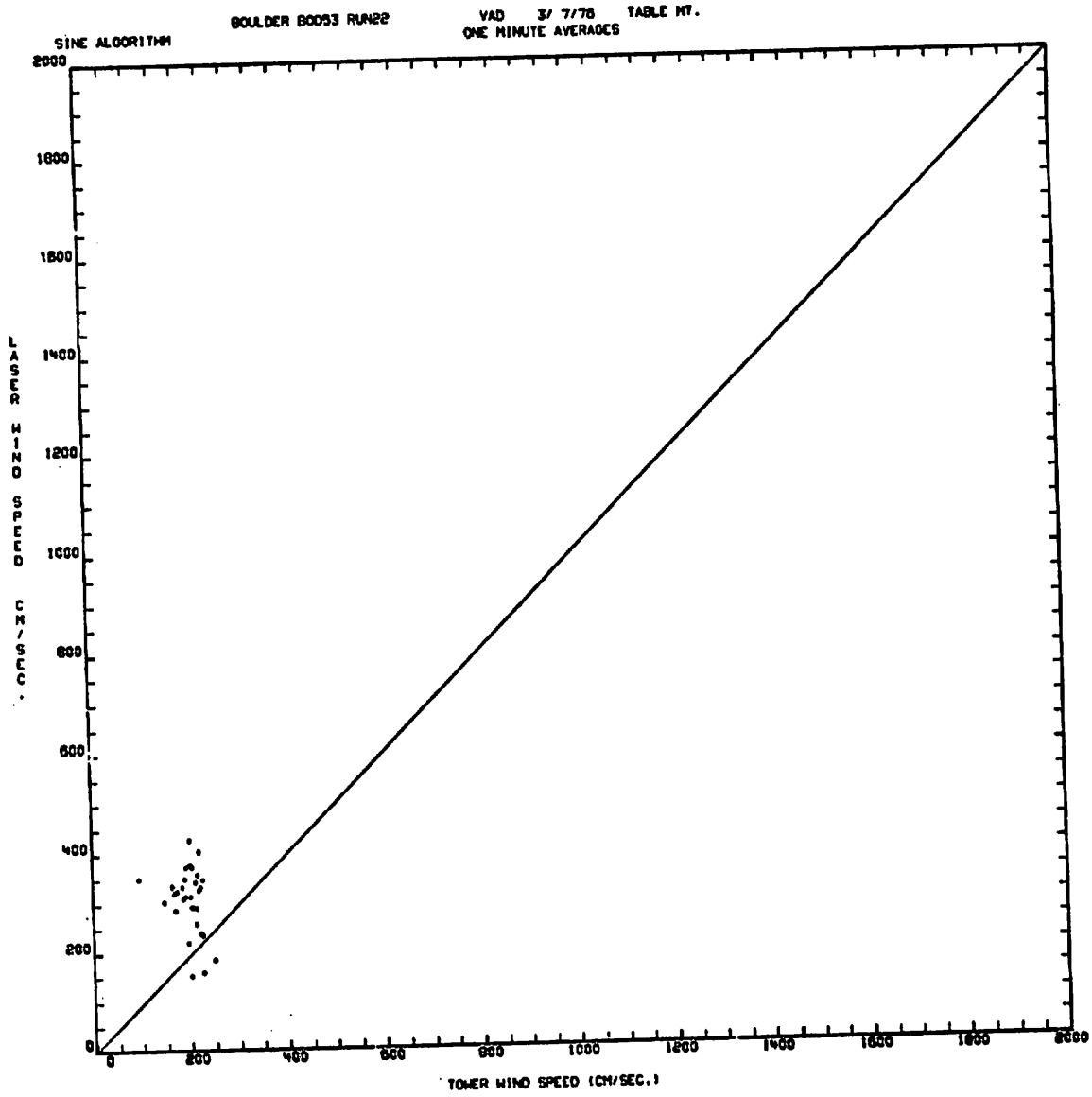

FIGURE B-1 (Continued).

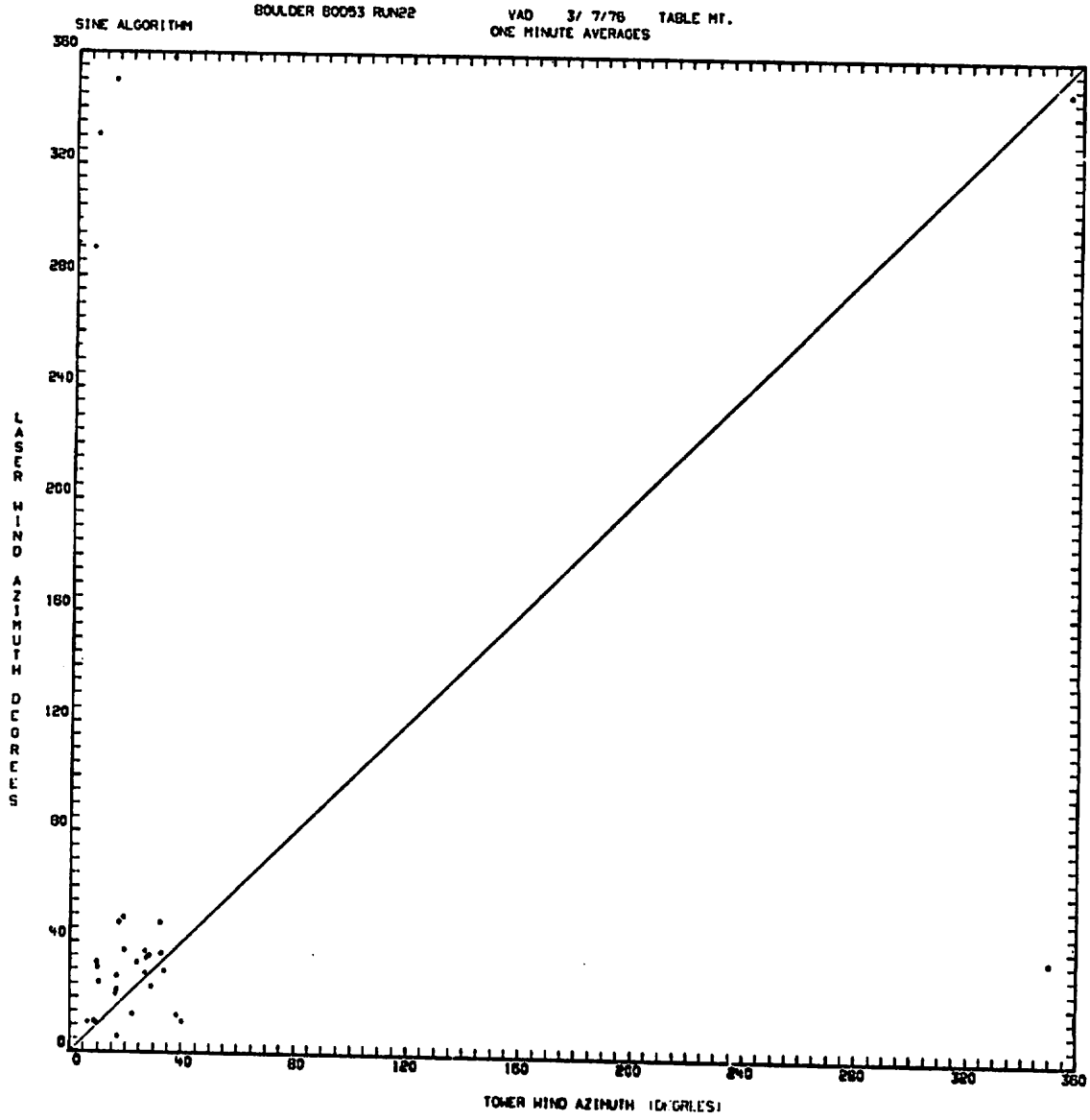

FIGURE B-1 (Continued).

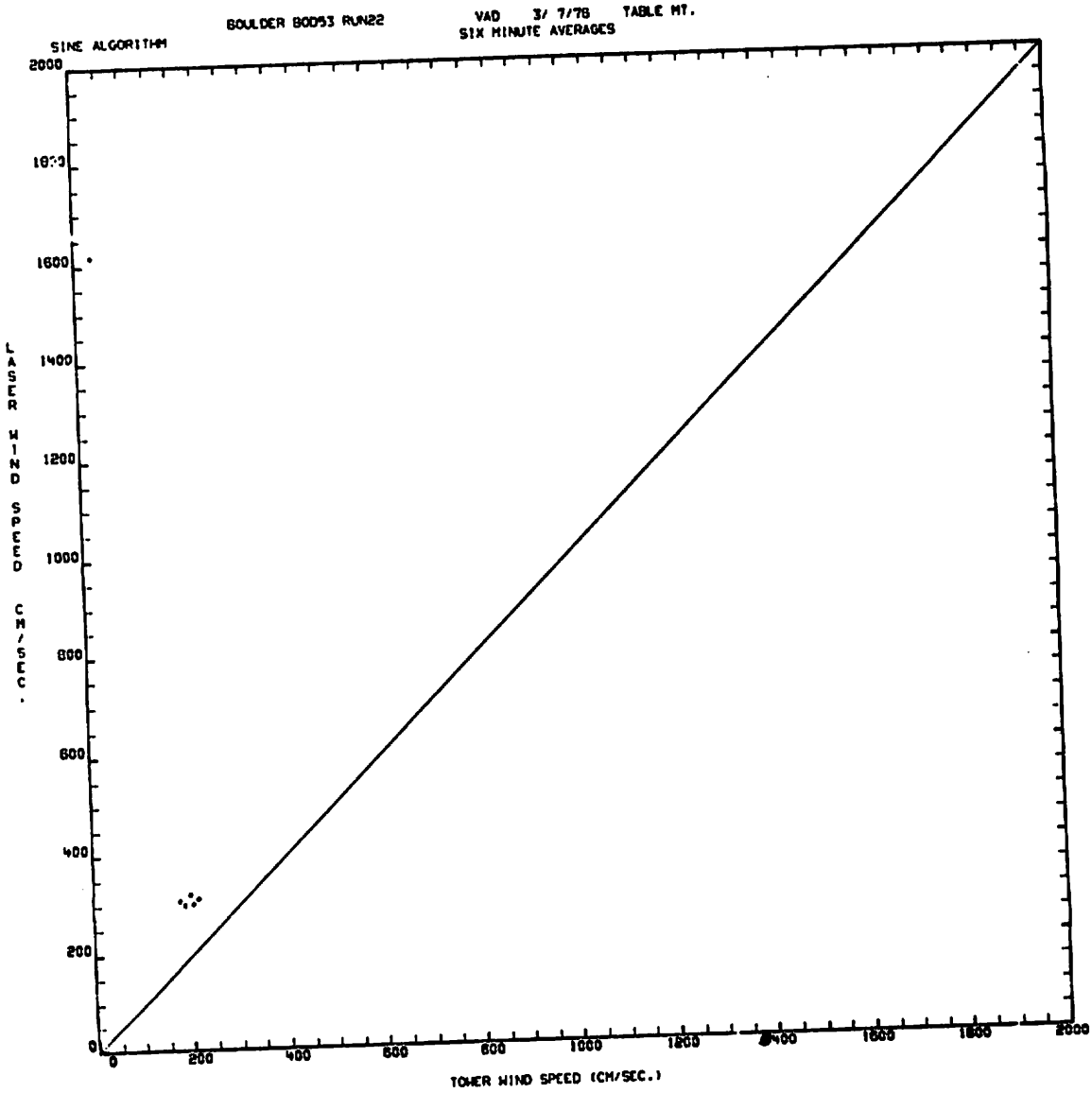

FIGURE B-1 (Continued).

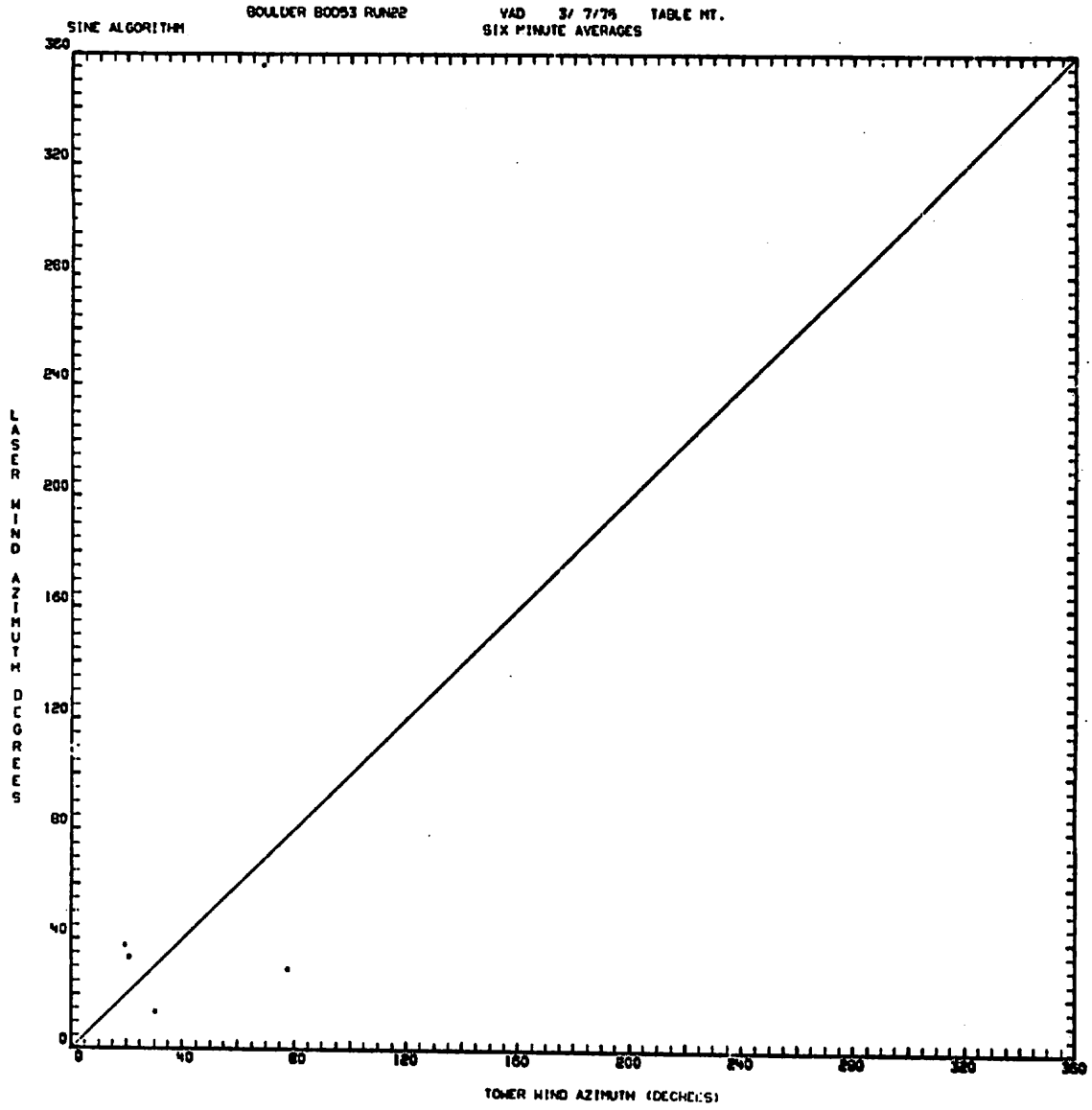

FIGURE B-1 (Continued).

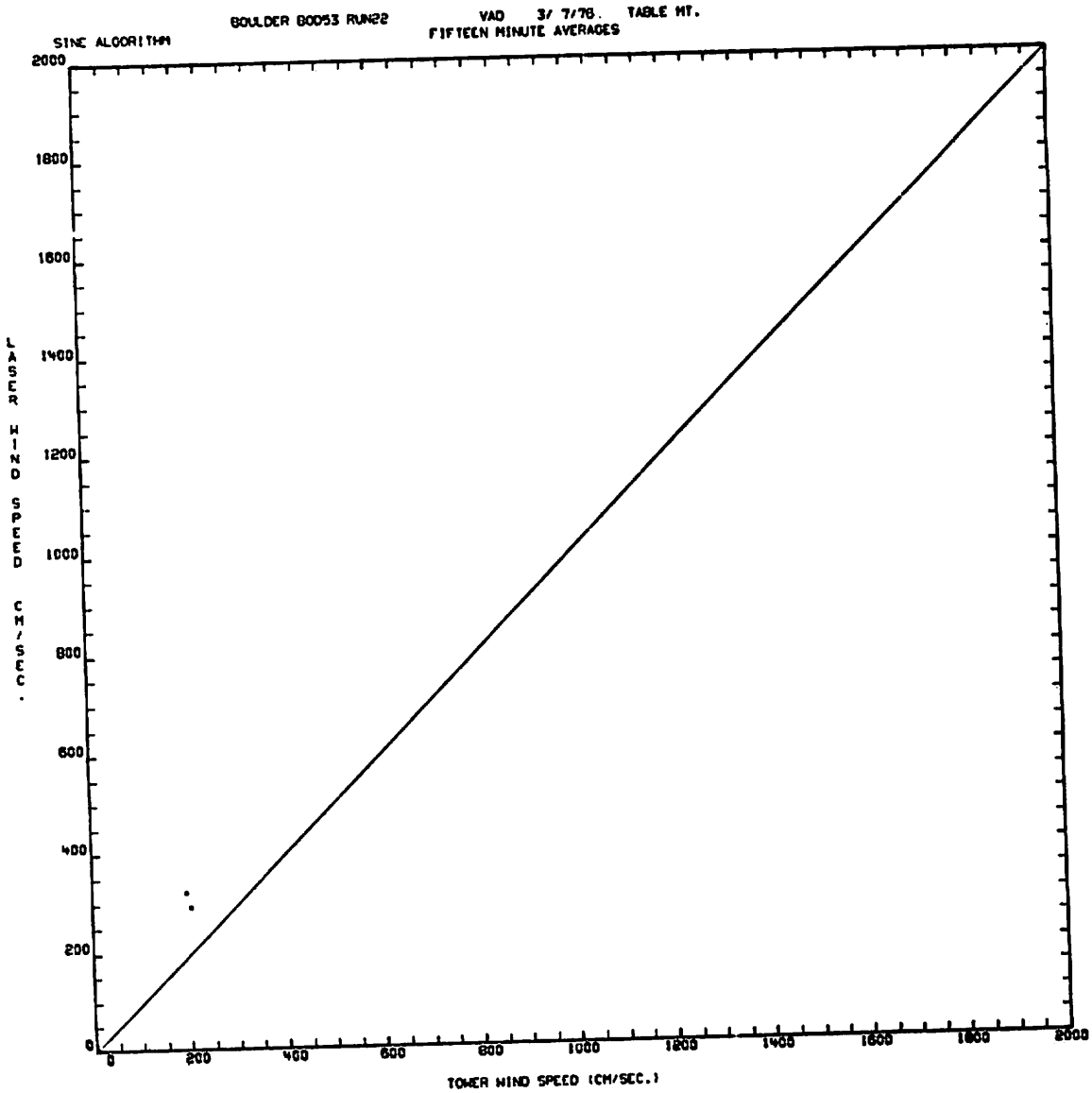

FIGURE B-1 (Continued).

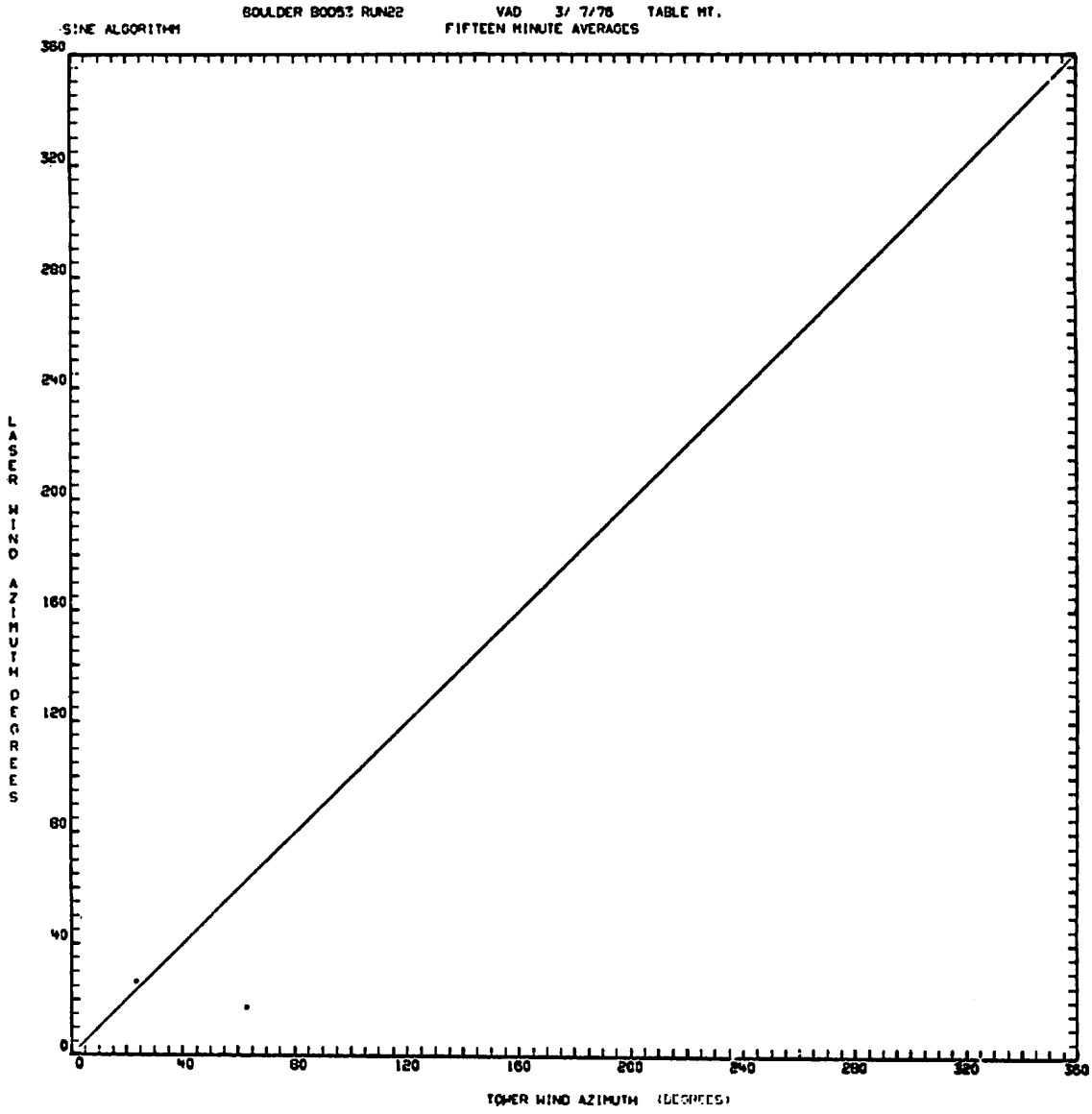

FIGURE B-1 (Continued)

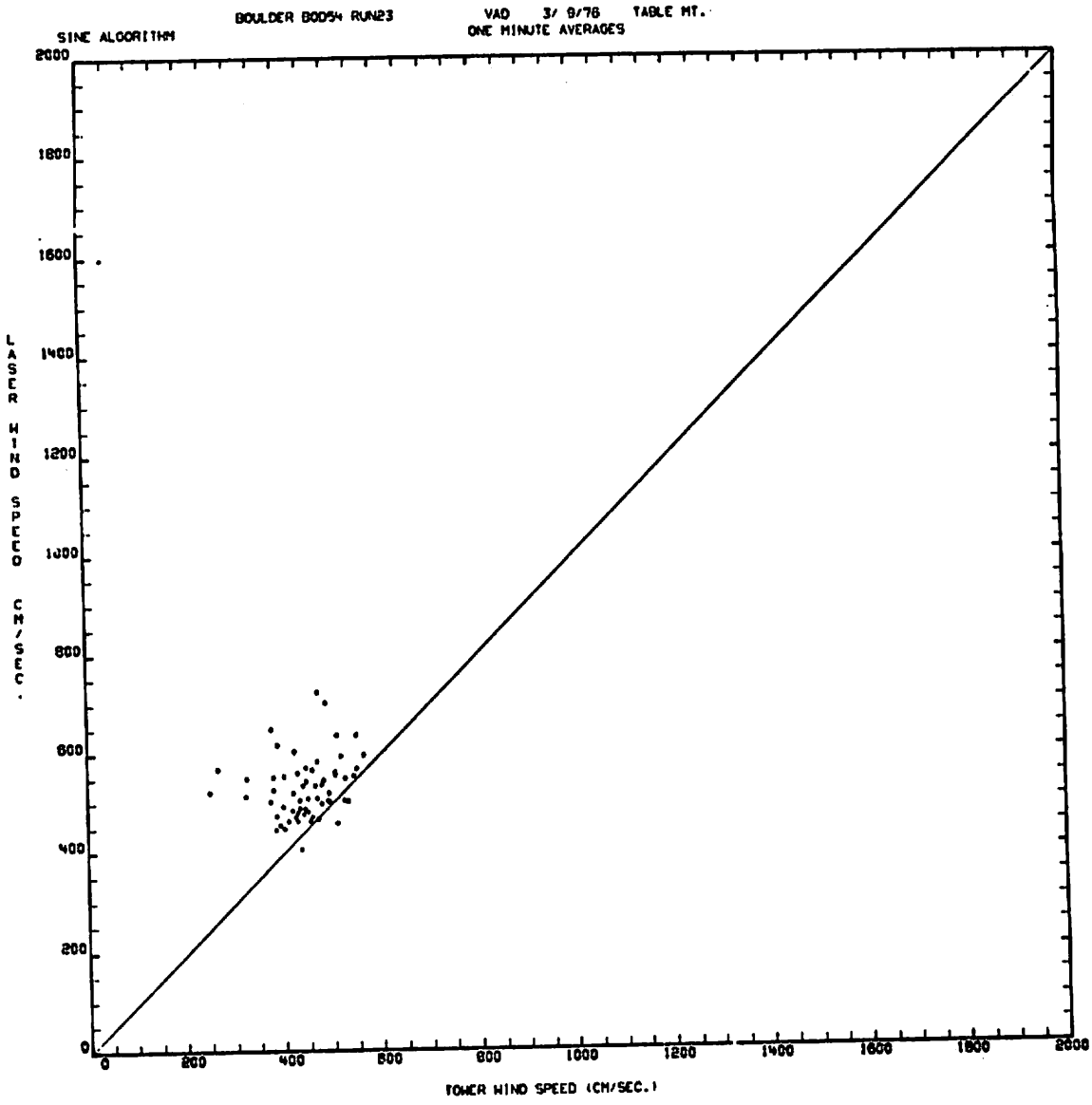

FIGURE B-1 (Continued)

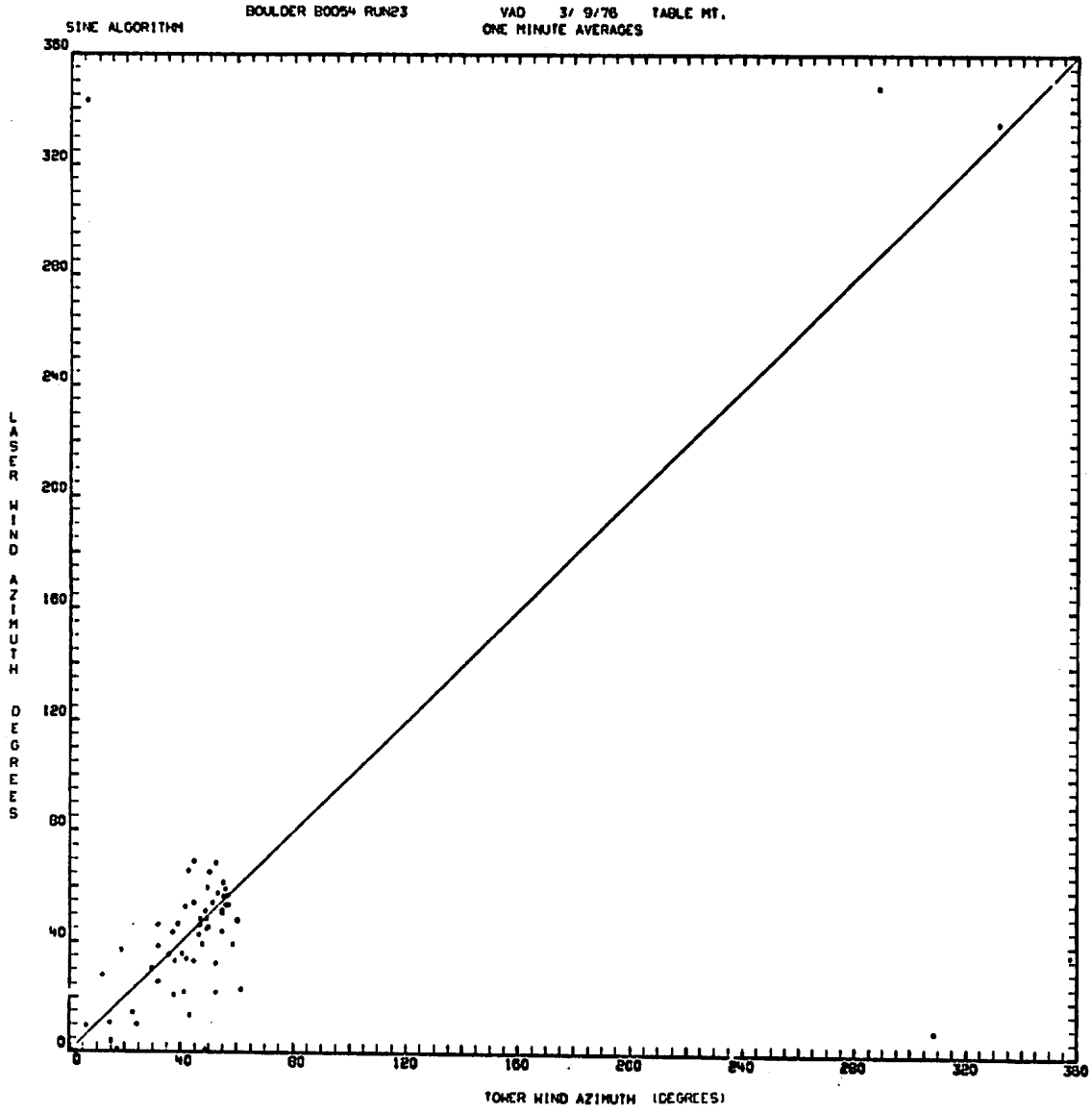

FIGURE B-1 (Continued).

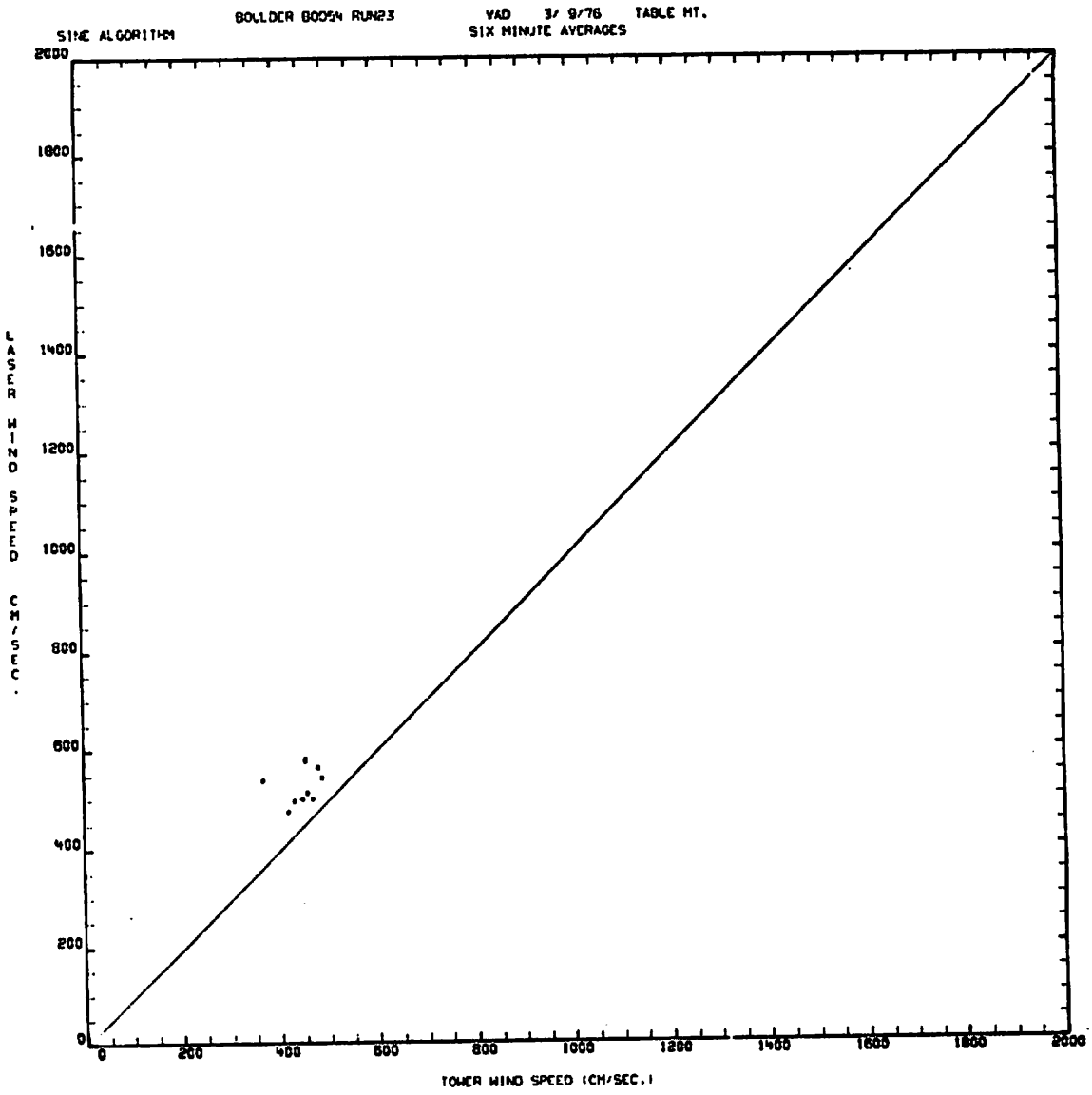

FIGURE B-1 (Continued).

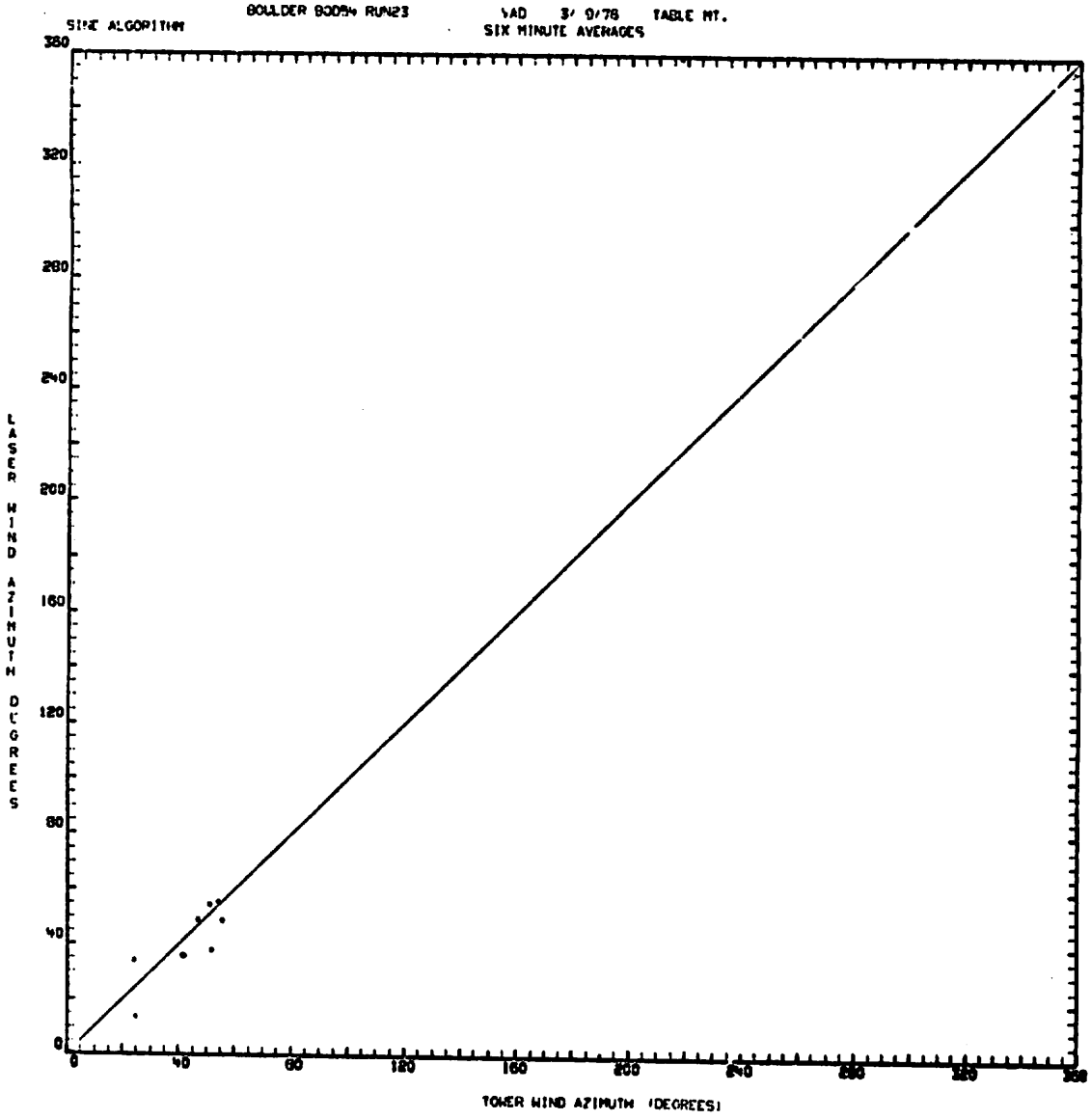

FIGURE B-1 (Continued).

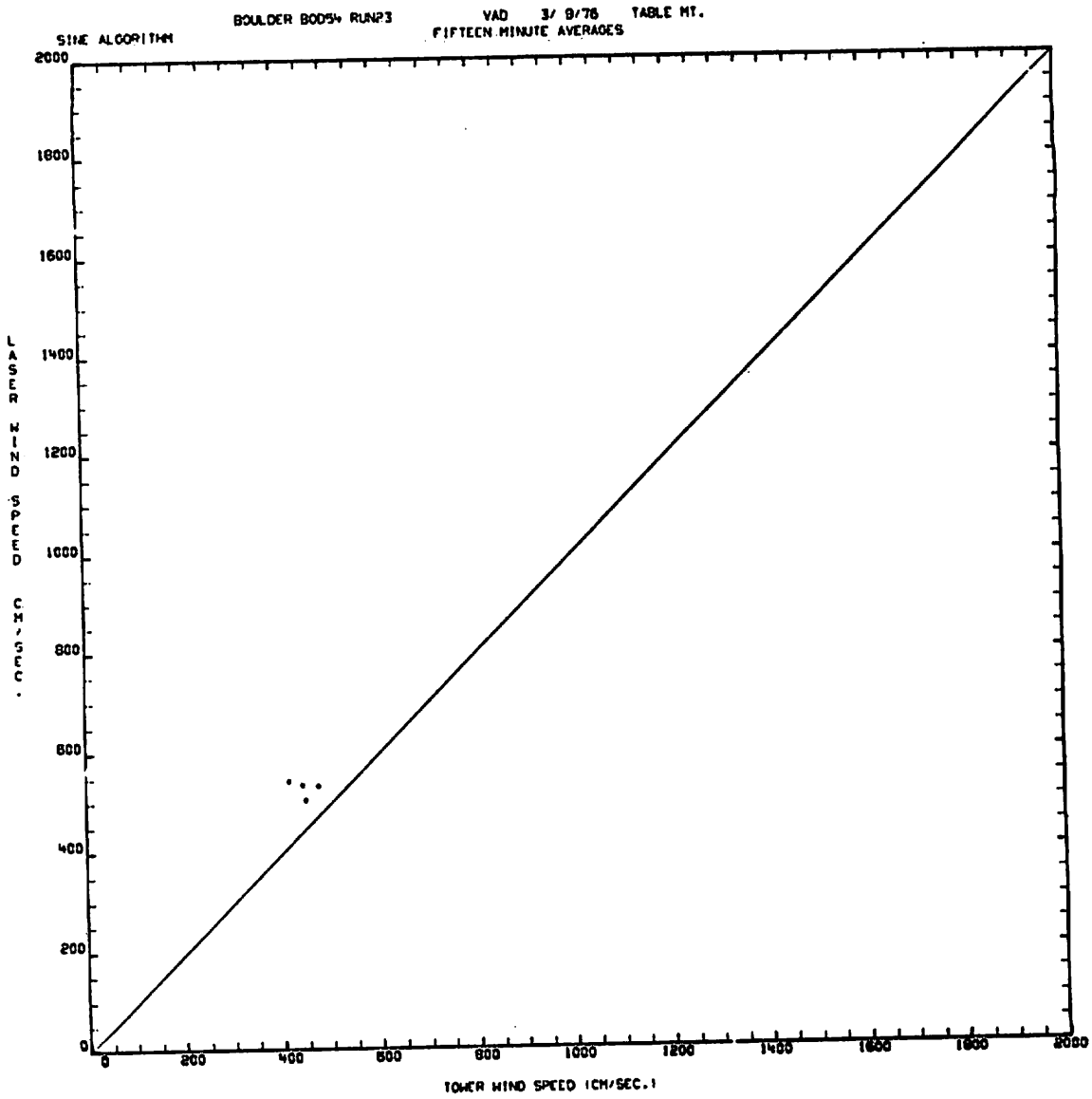

FIGURE B-1 (Continued).

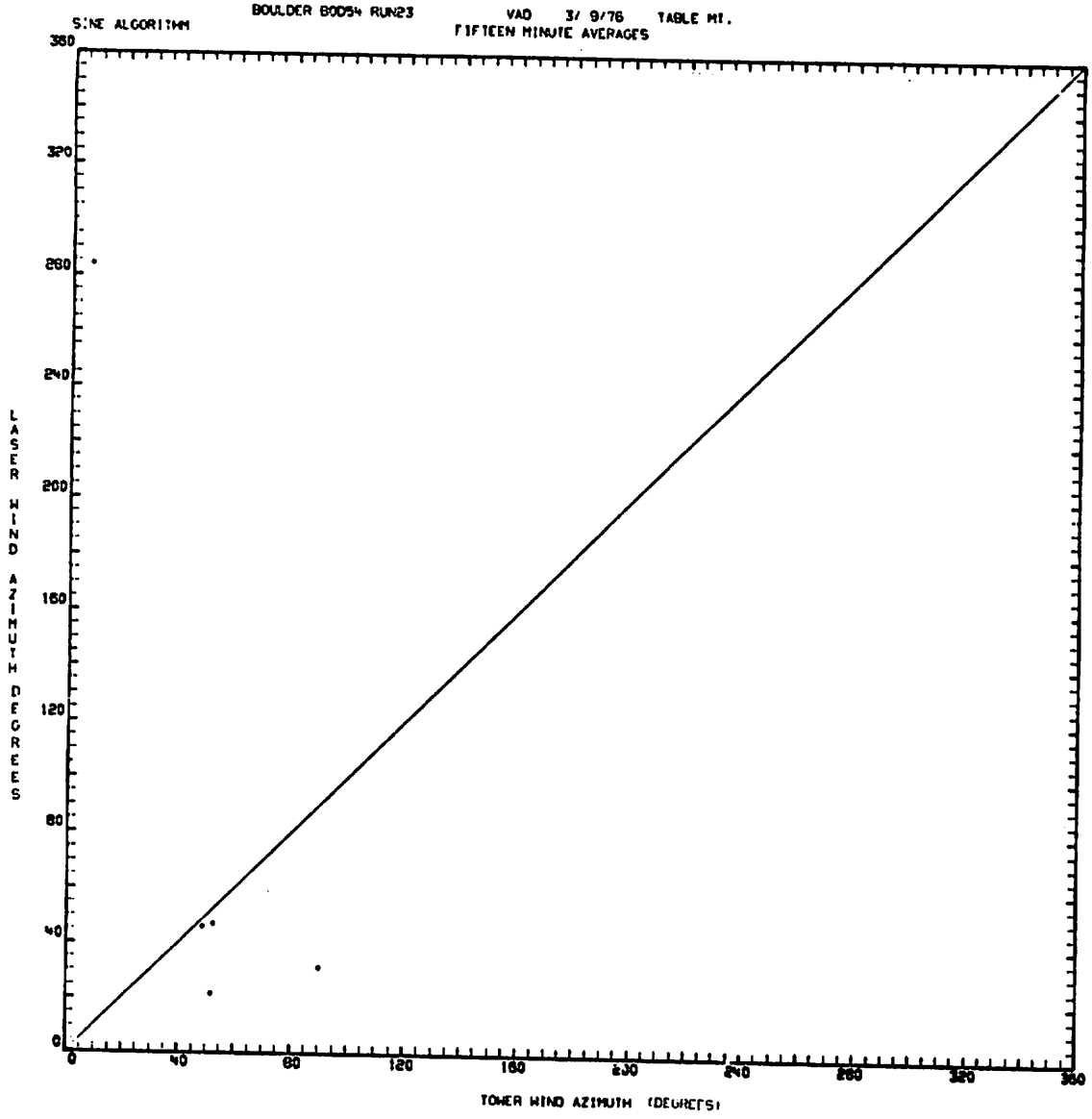

FIGURE B-1 (Continued).

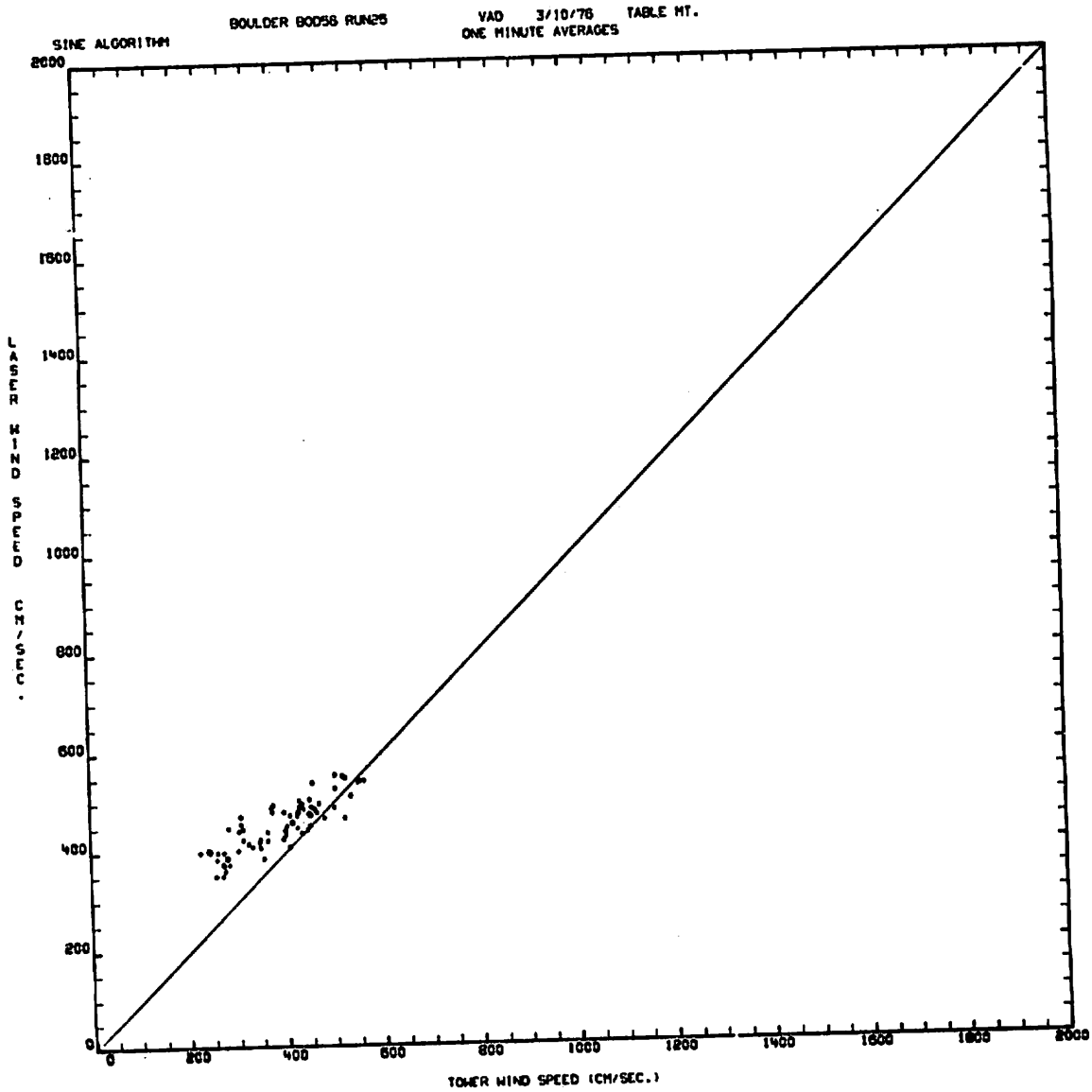

FIGURE B-1 (Continued).

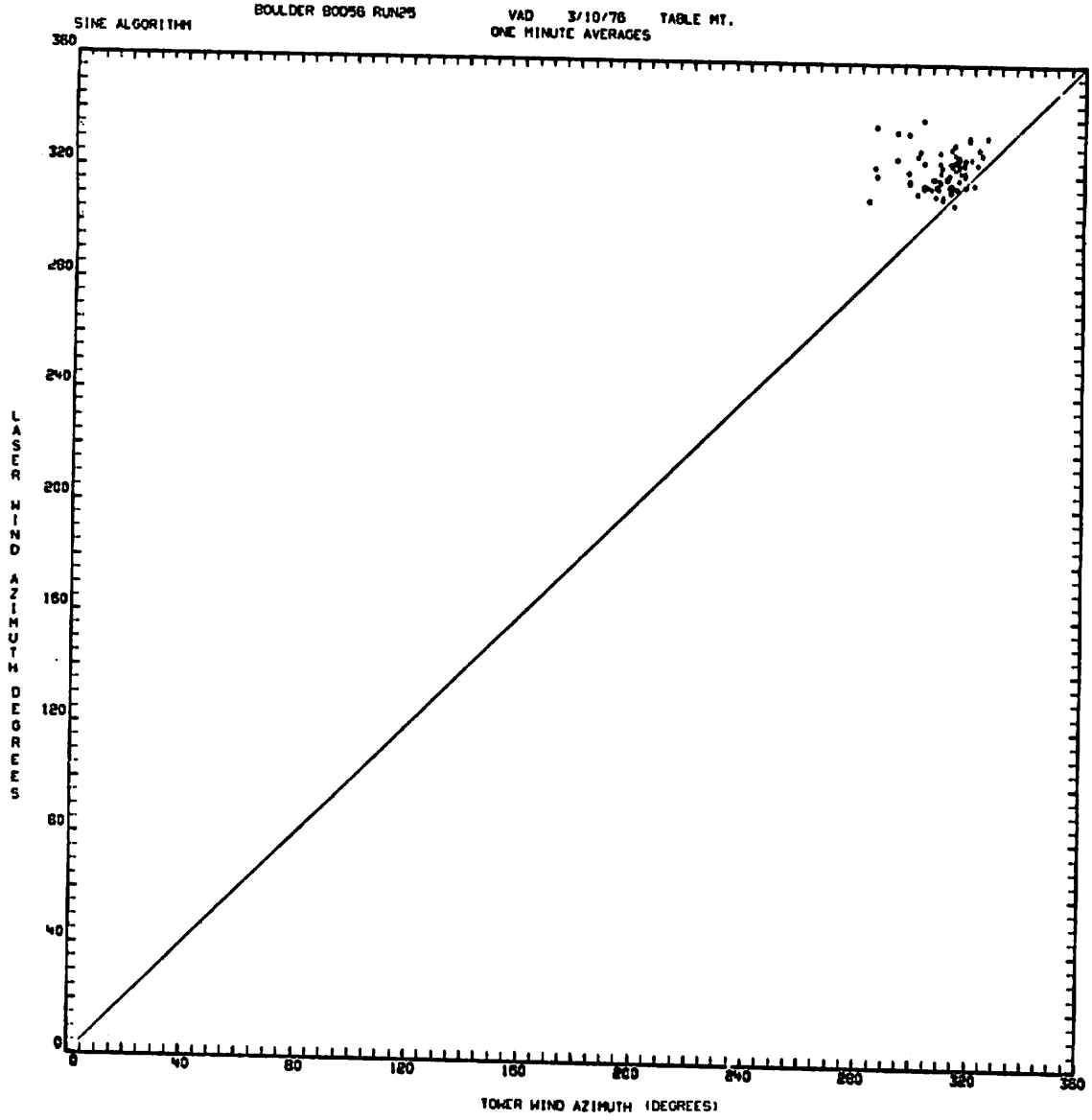

FIGURE B-1 (Continued).

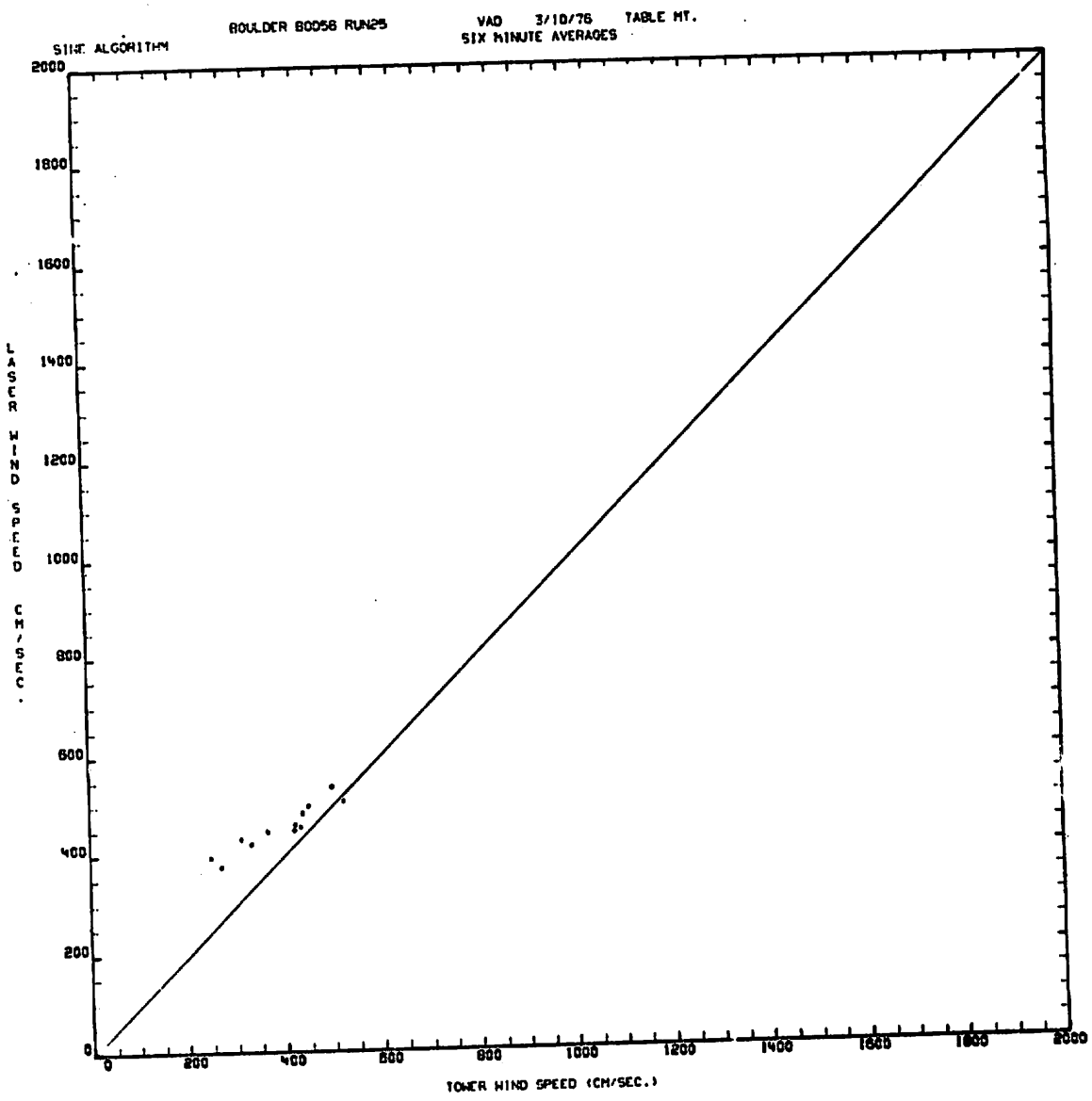

FIGURE B-1 (Continued).

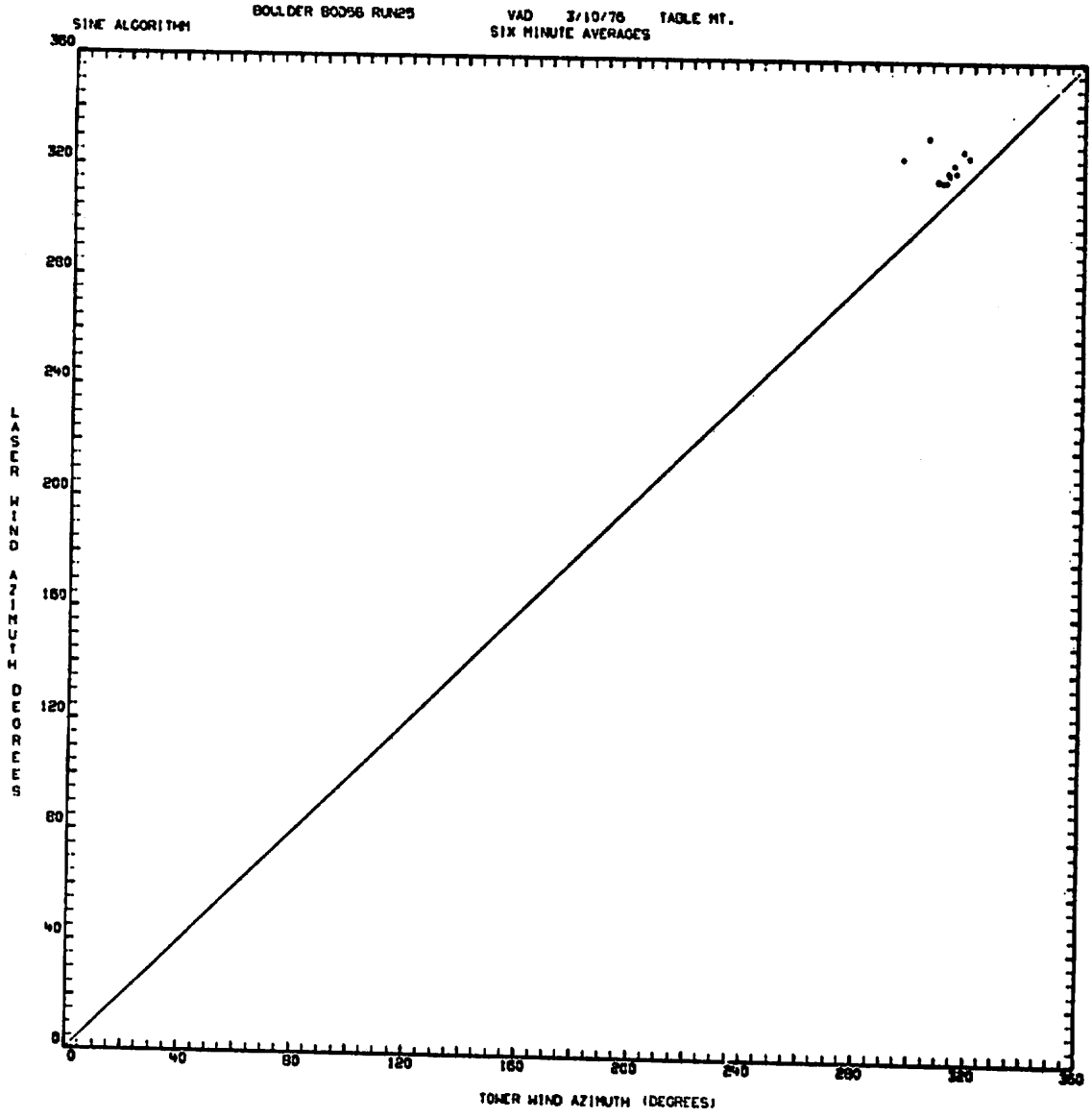

FIGURE B-1 (Continued).

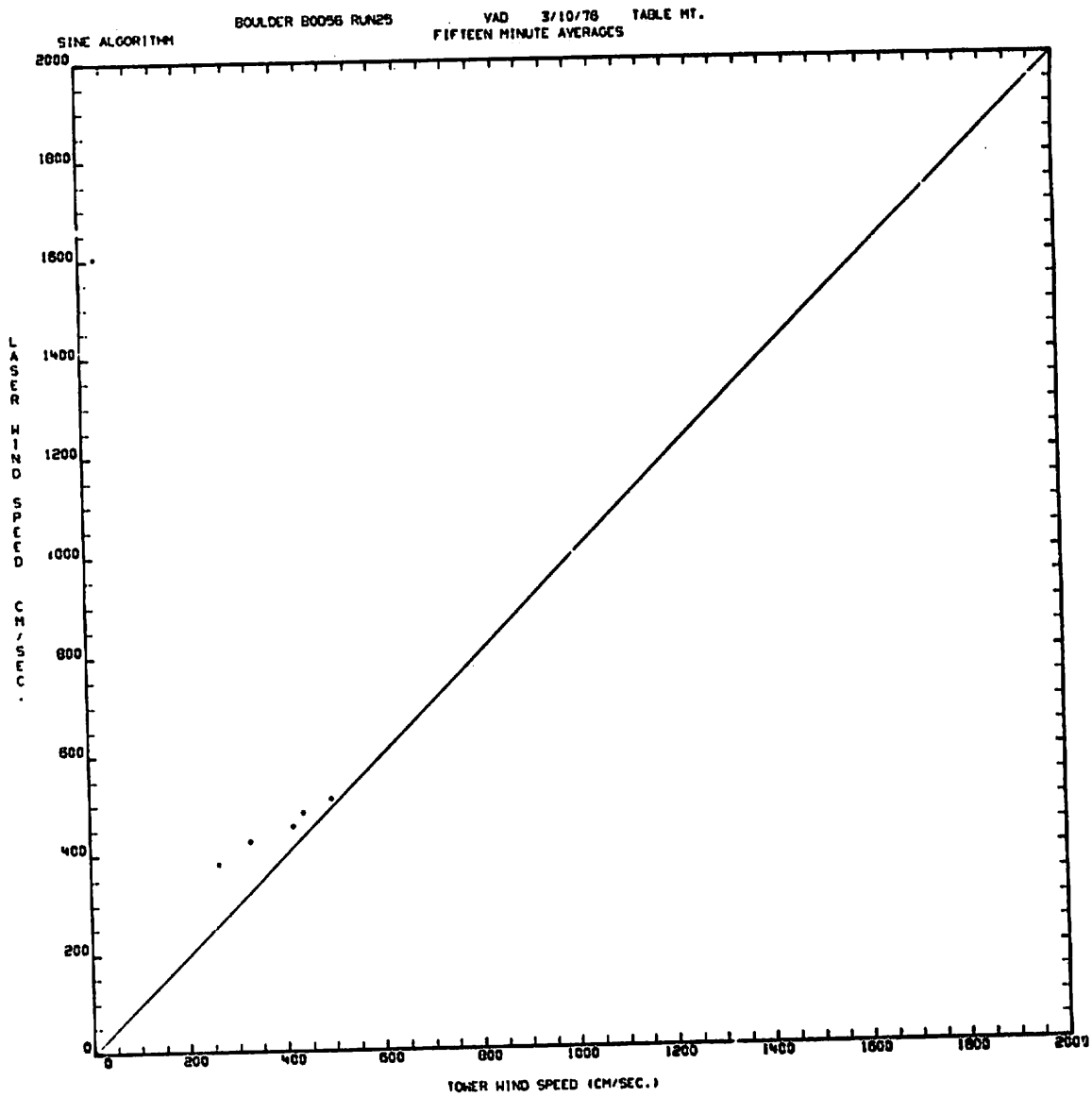

FIGURE B-1 (Continued).

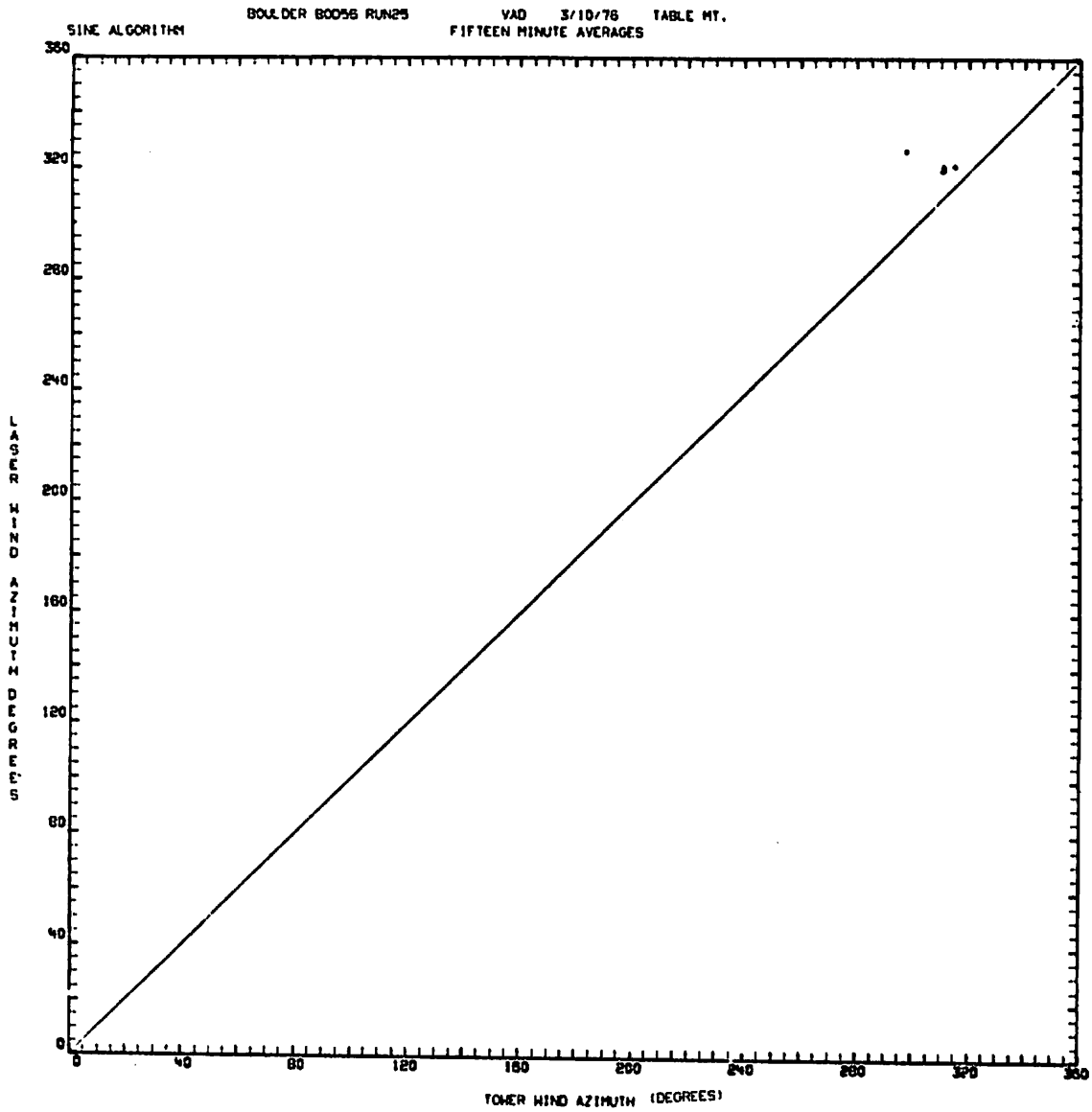

FIGURE B-1 (Continued).

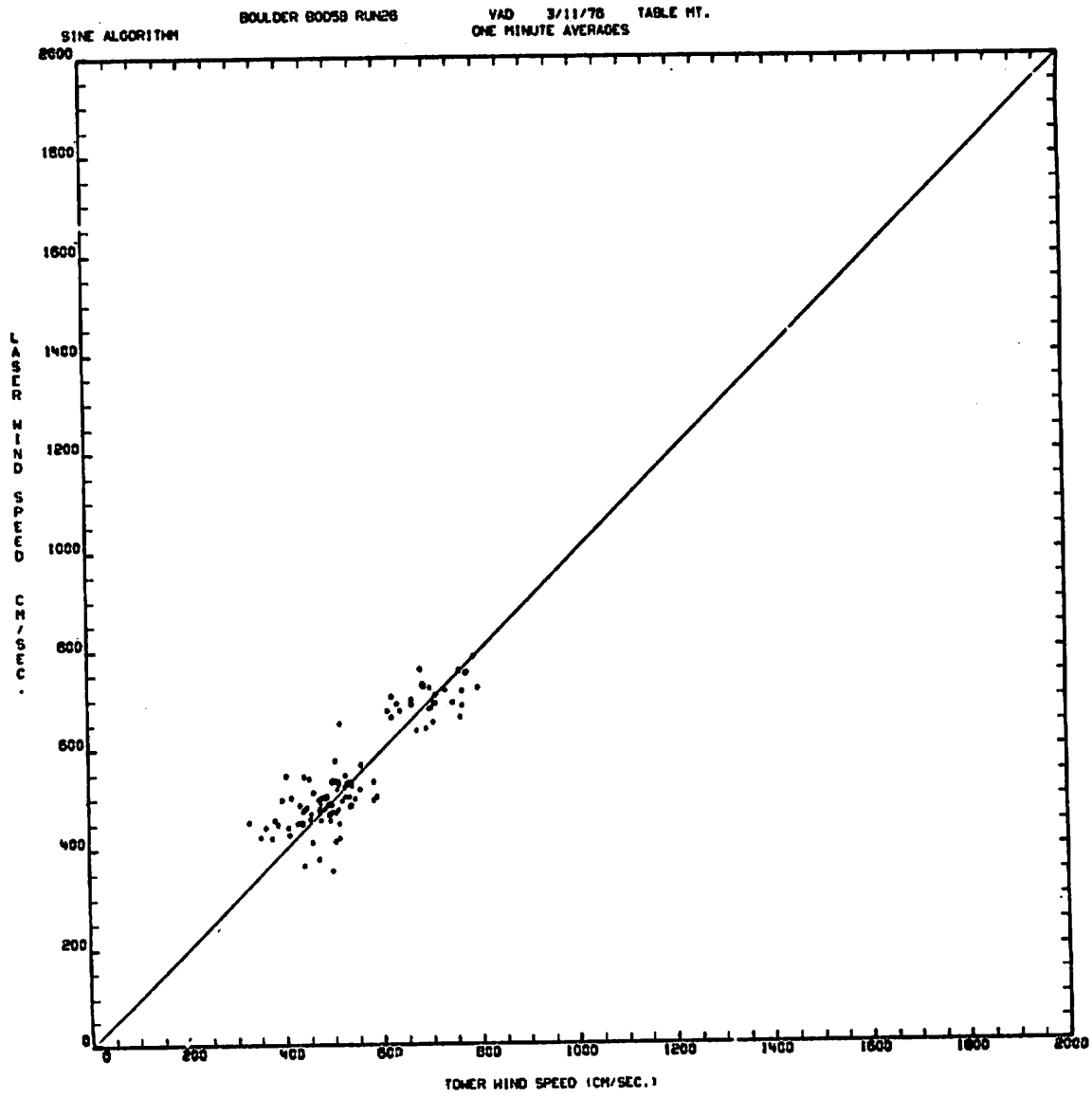

FIGURE B-1 (Continued).

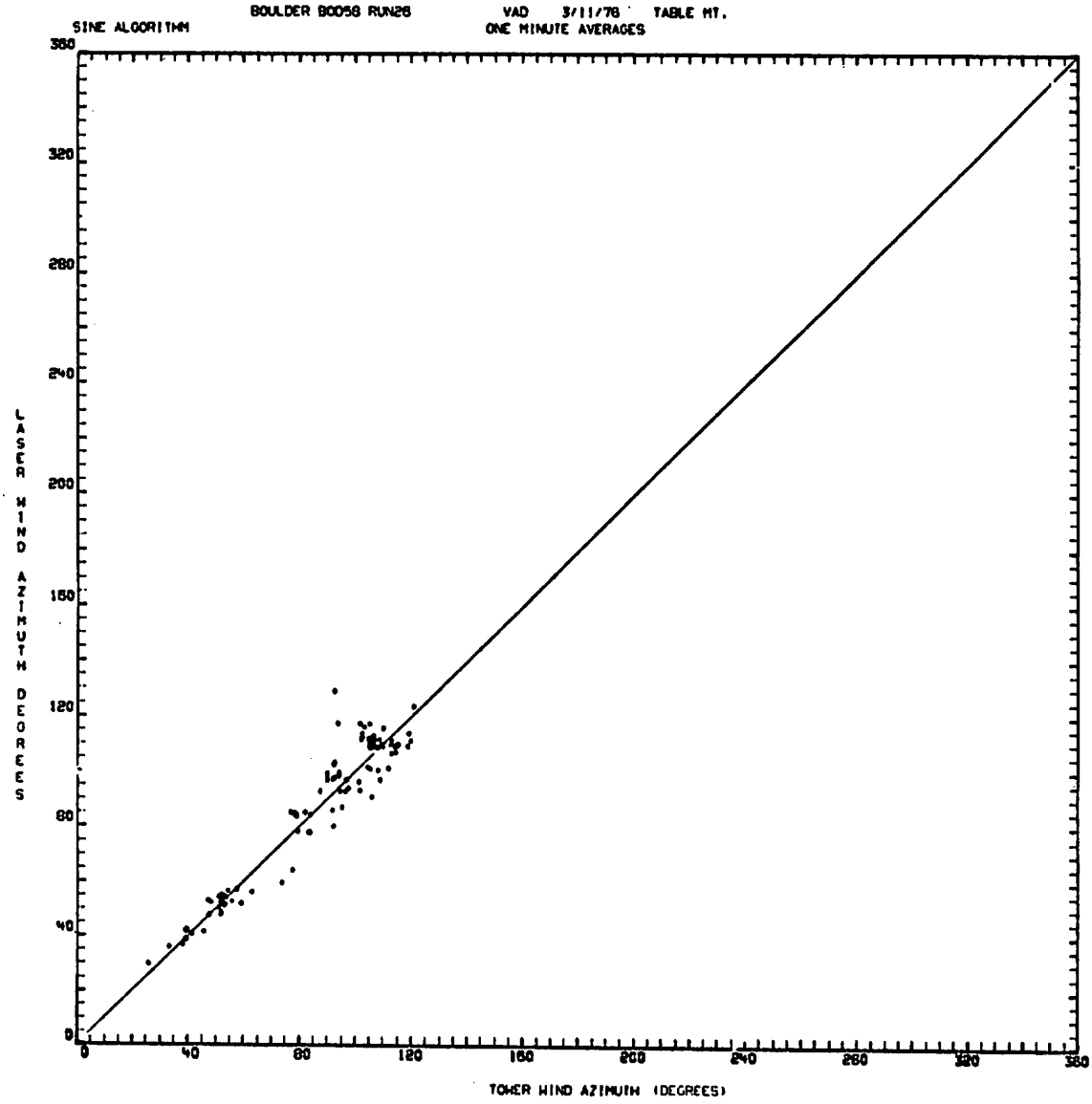

FIGURE B-1 (Continued).

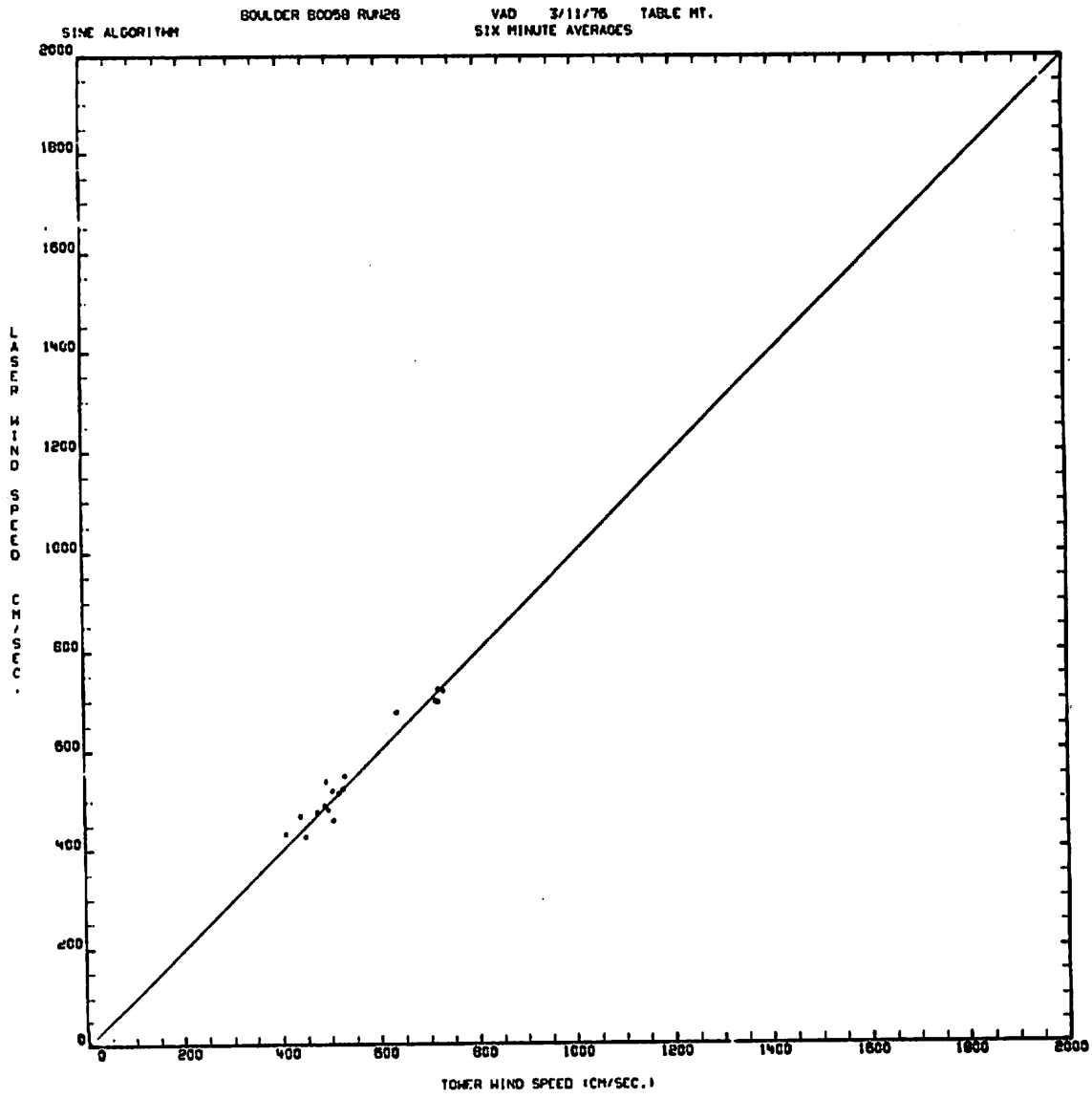

FIGURE B-1 (Continued).

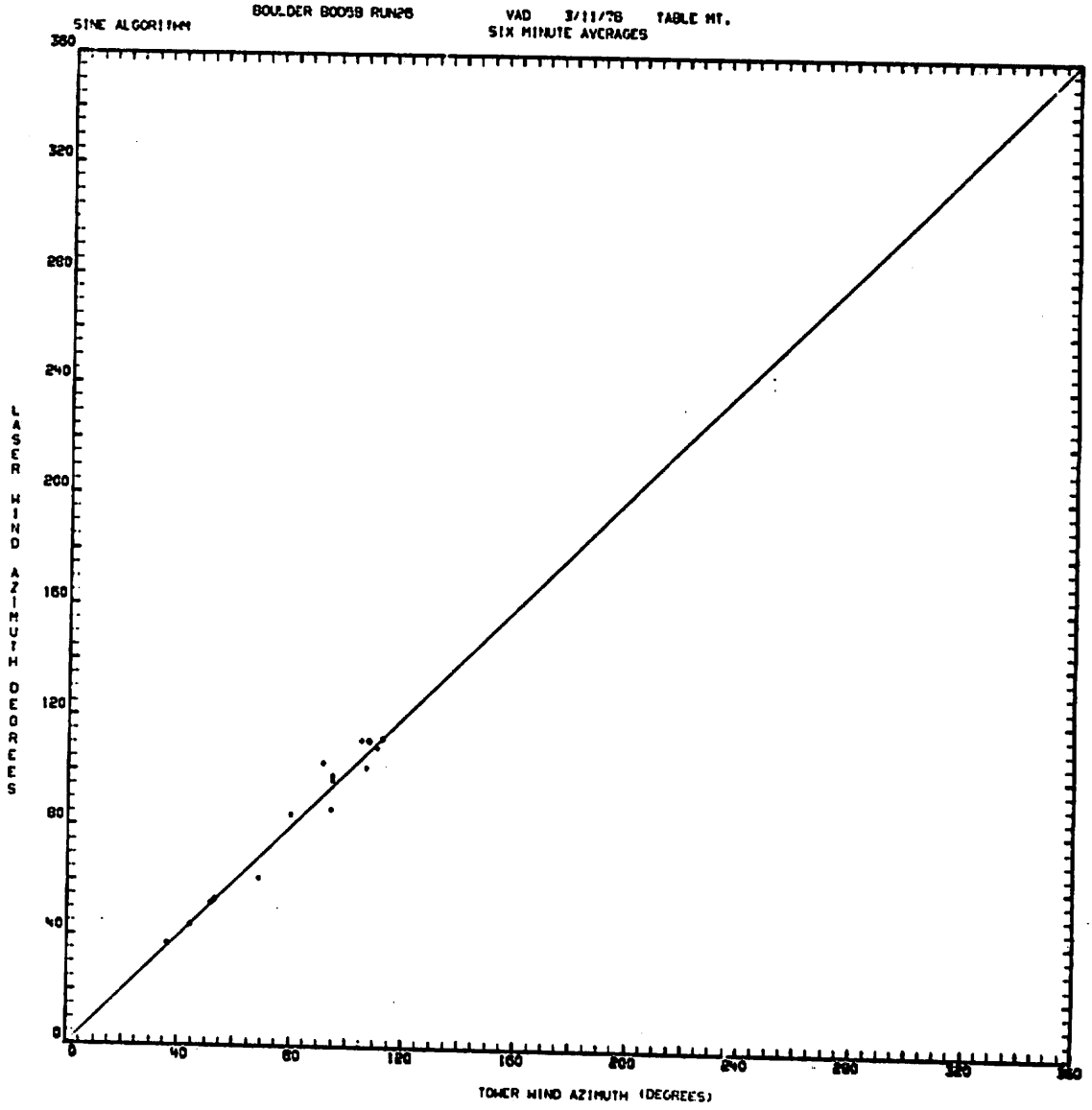

FIGURE B-1 (Continued).

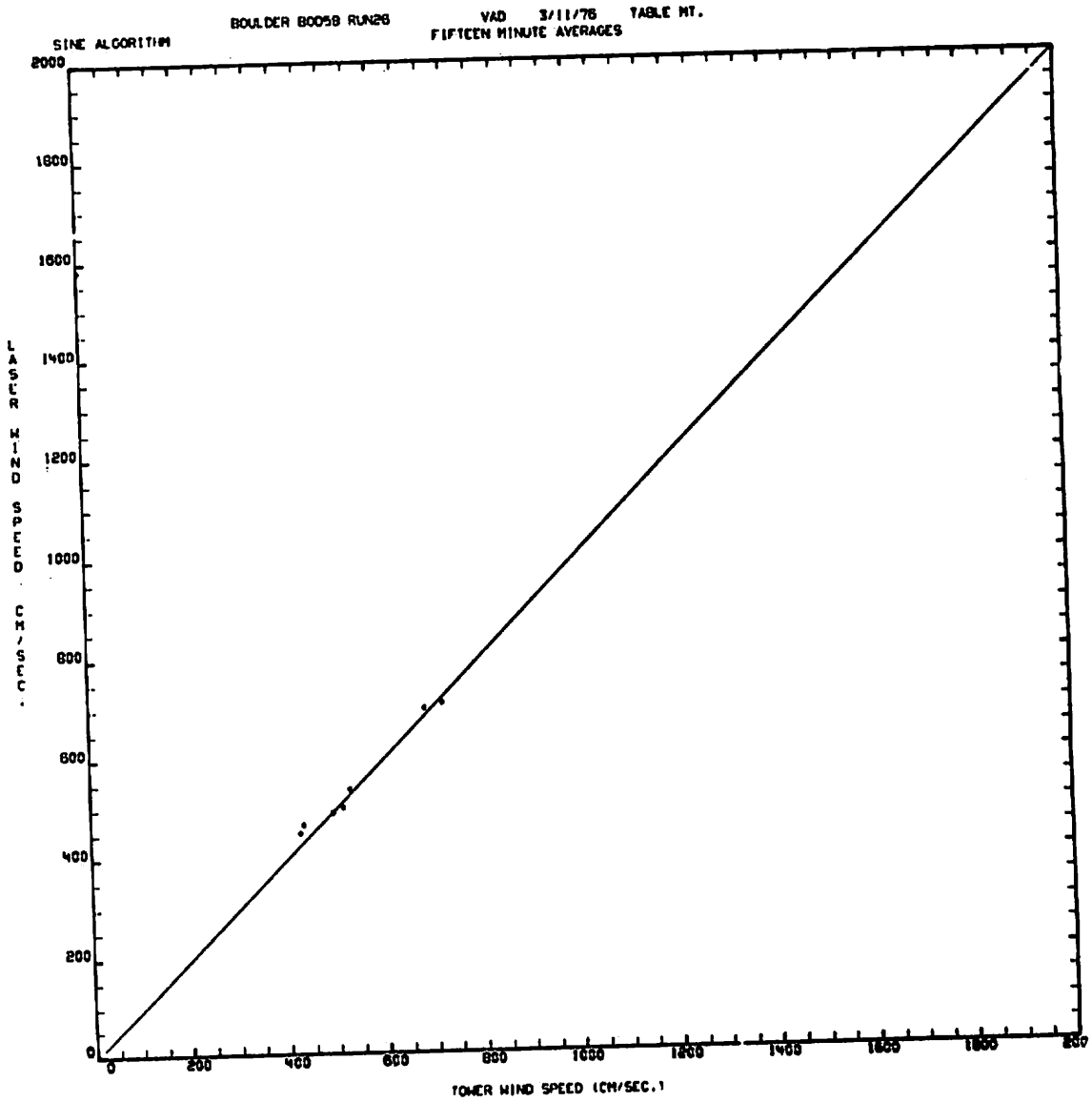

FIGURE B-1 (Continued).

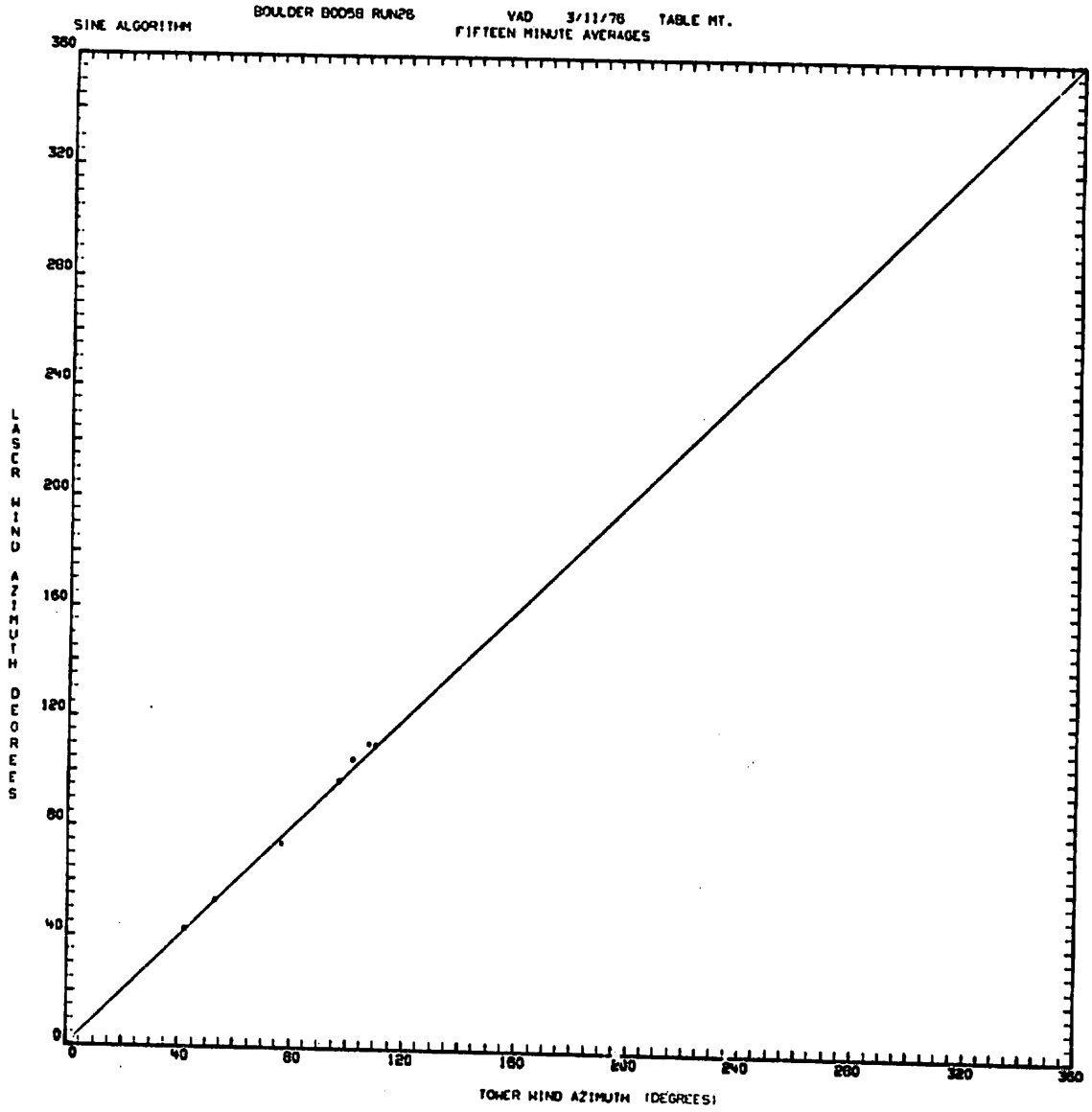

FIGURE B-1 (Continued)

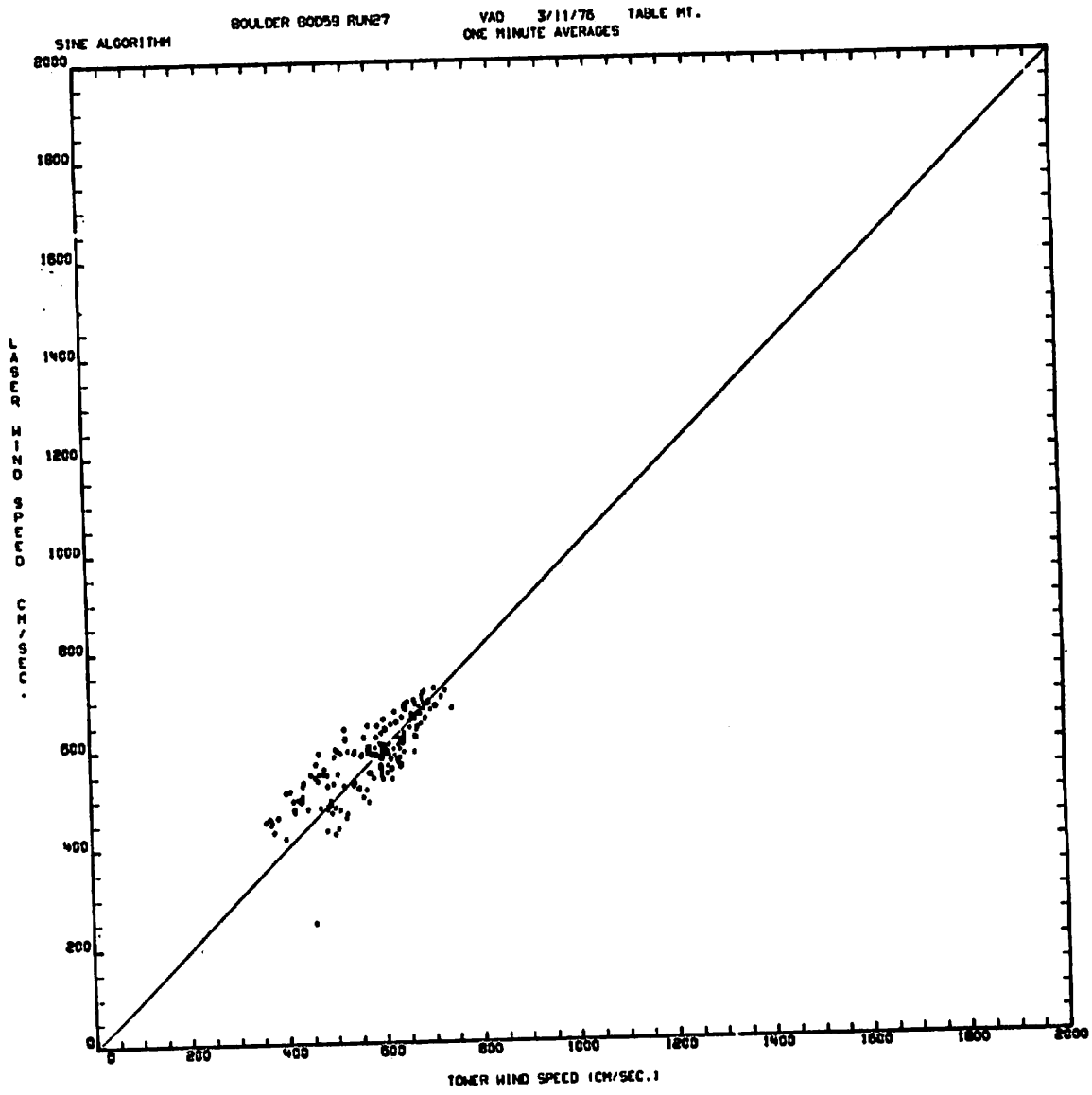

FIGURE B-1 (Continued).

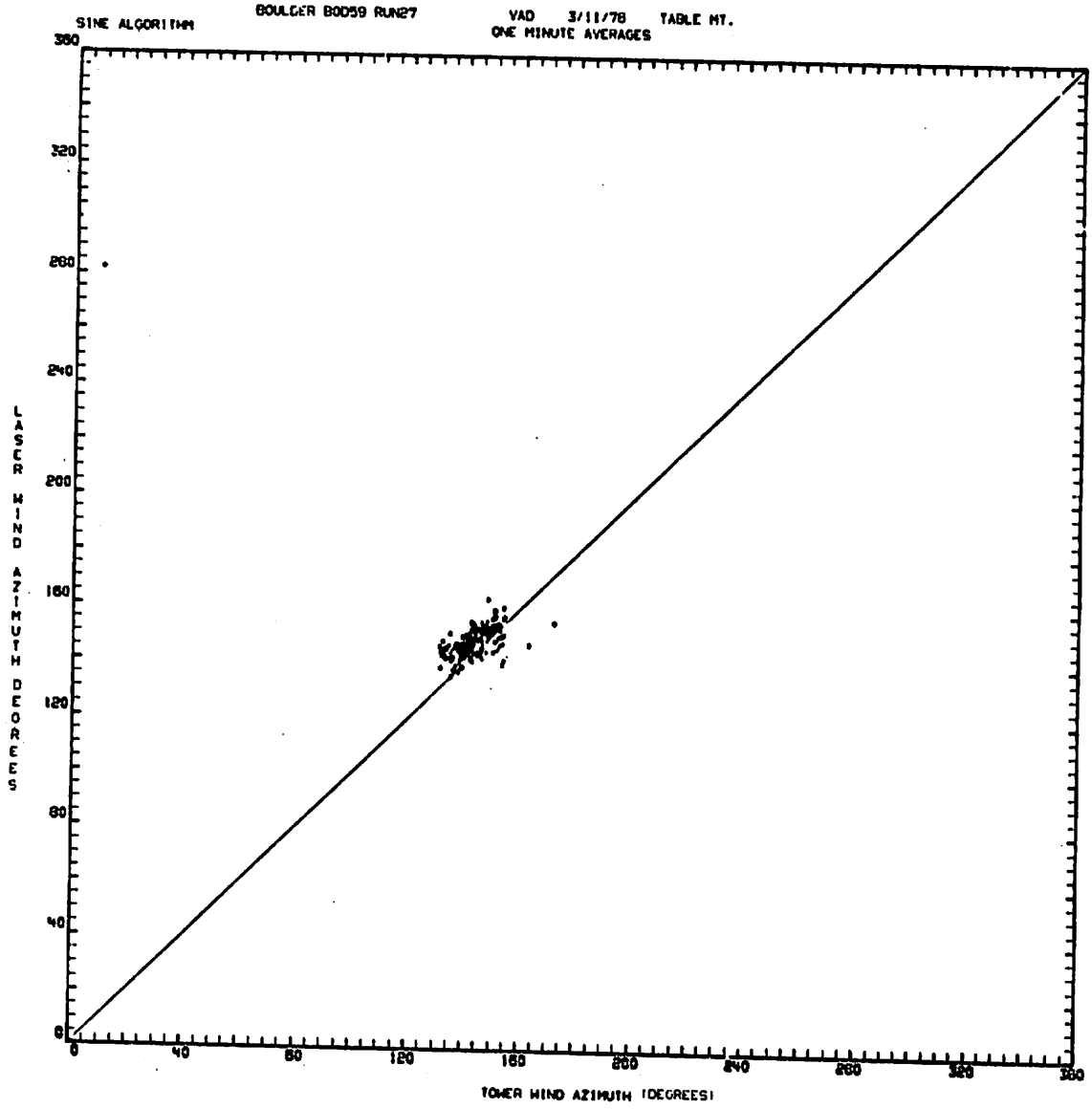

FIGURE B-1 (Continued).

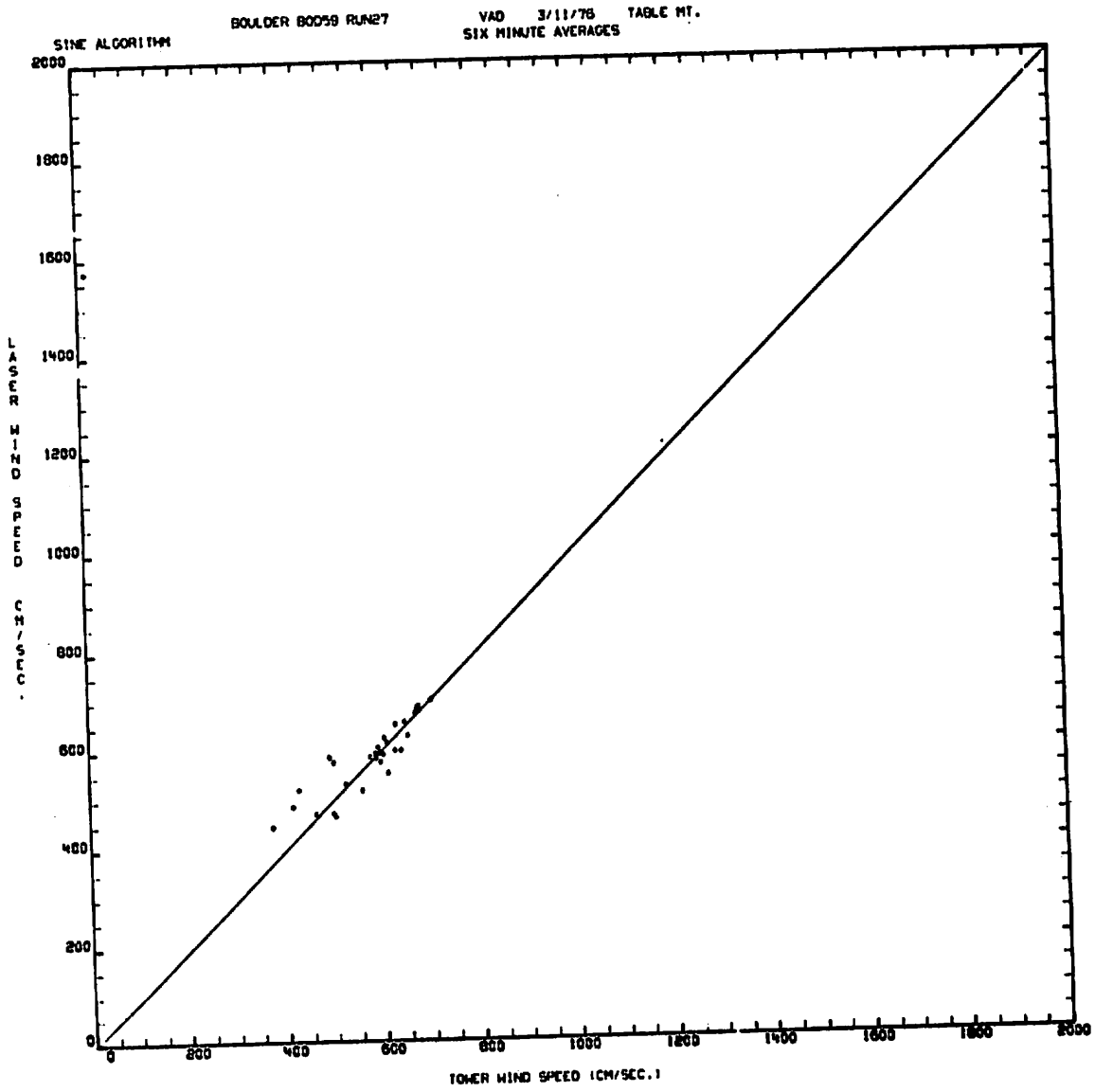

FIGURE B-1 (Continued).

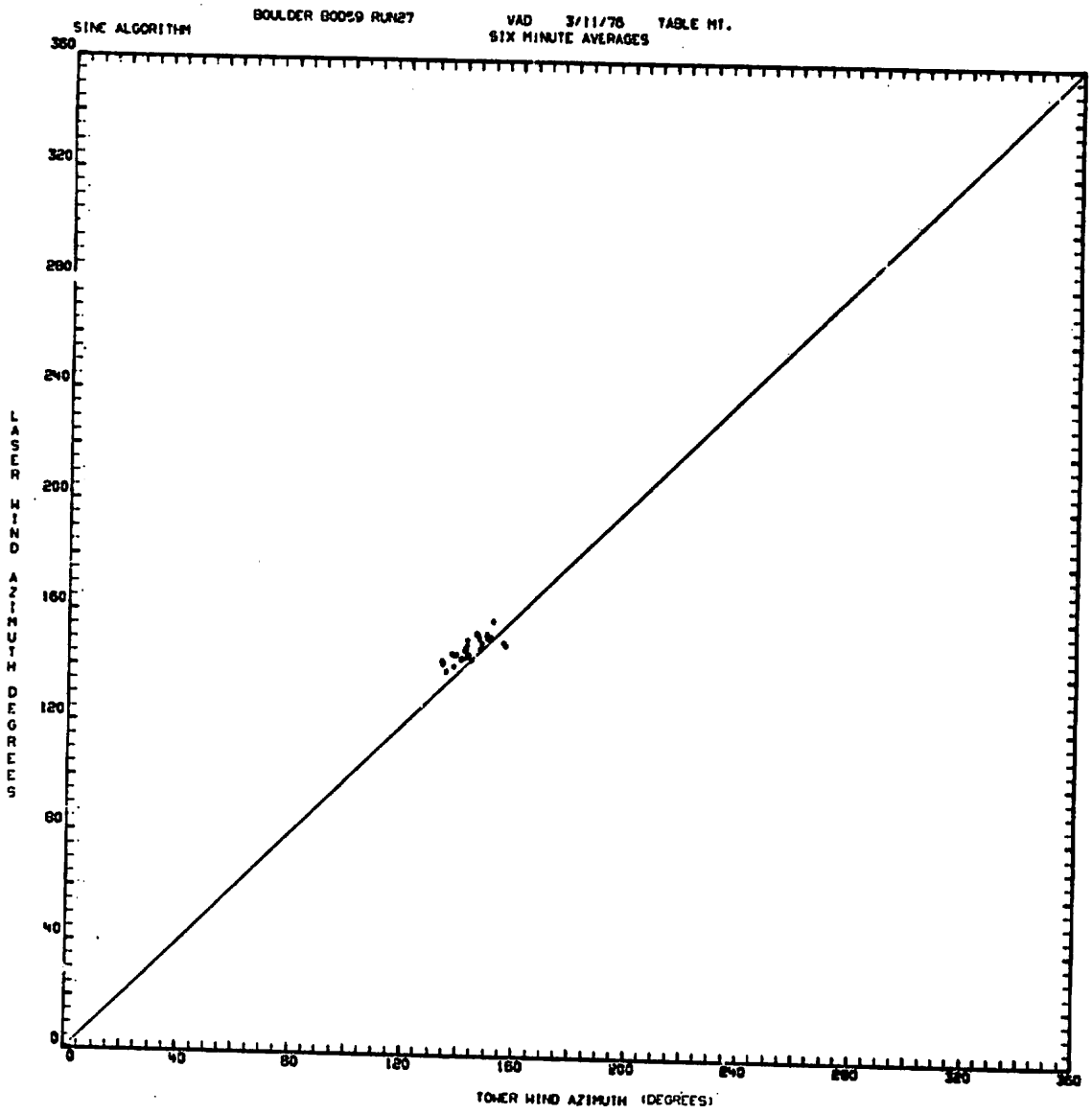

FIGURE B-1 (Continued).

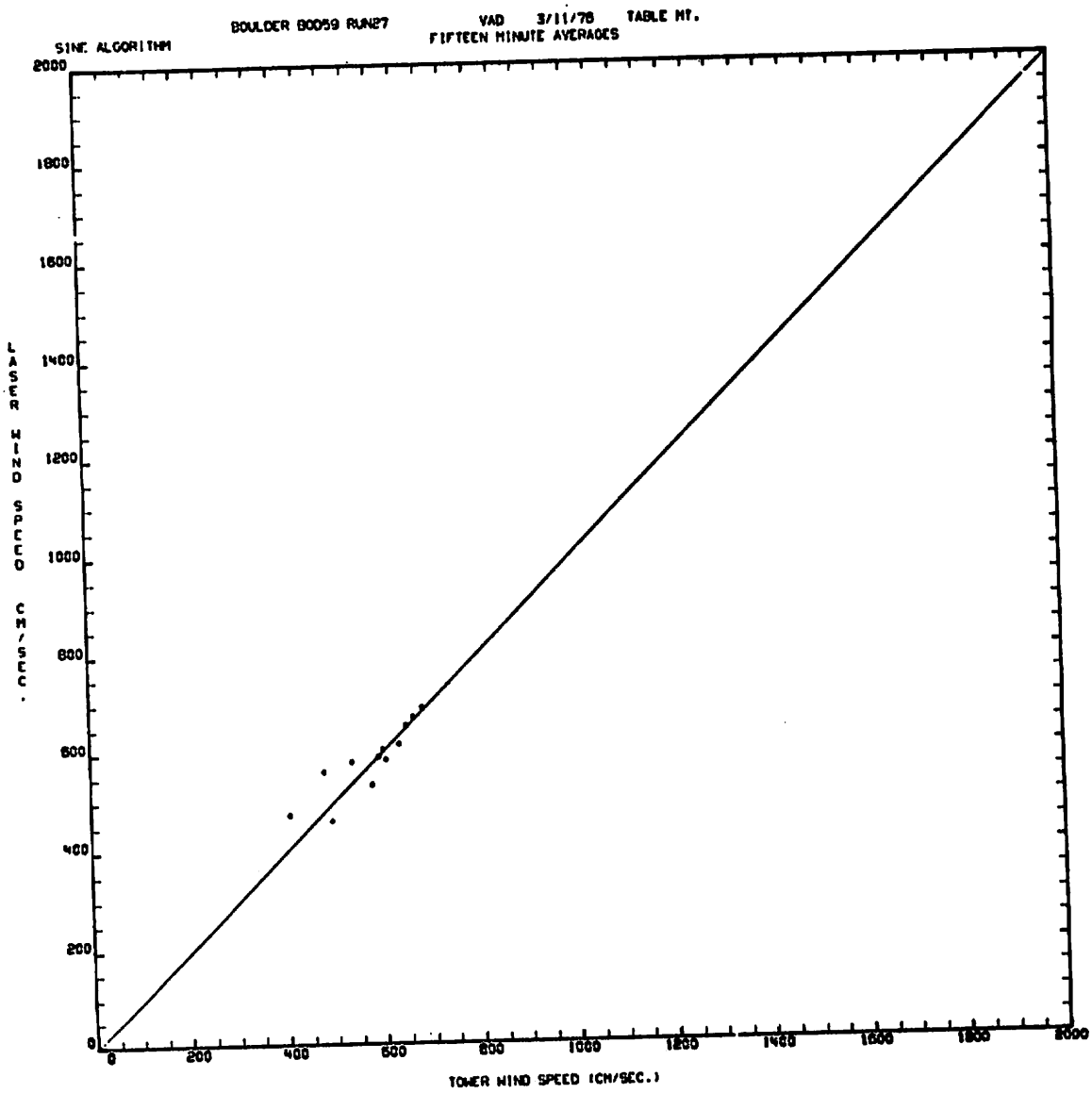

FIGURE B-1 (Continued).

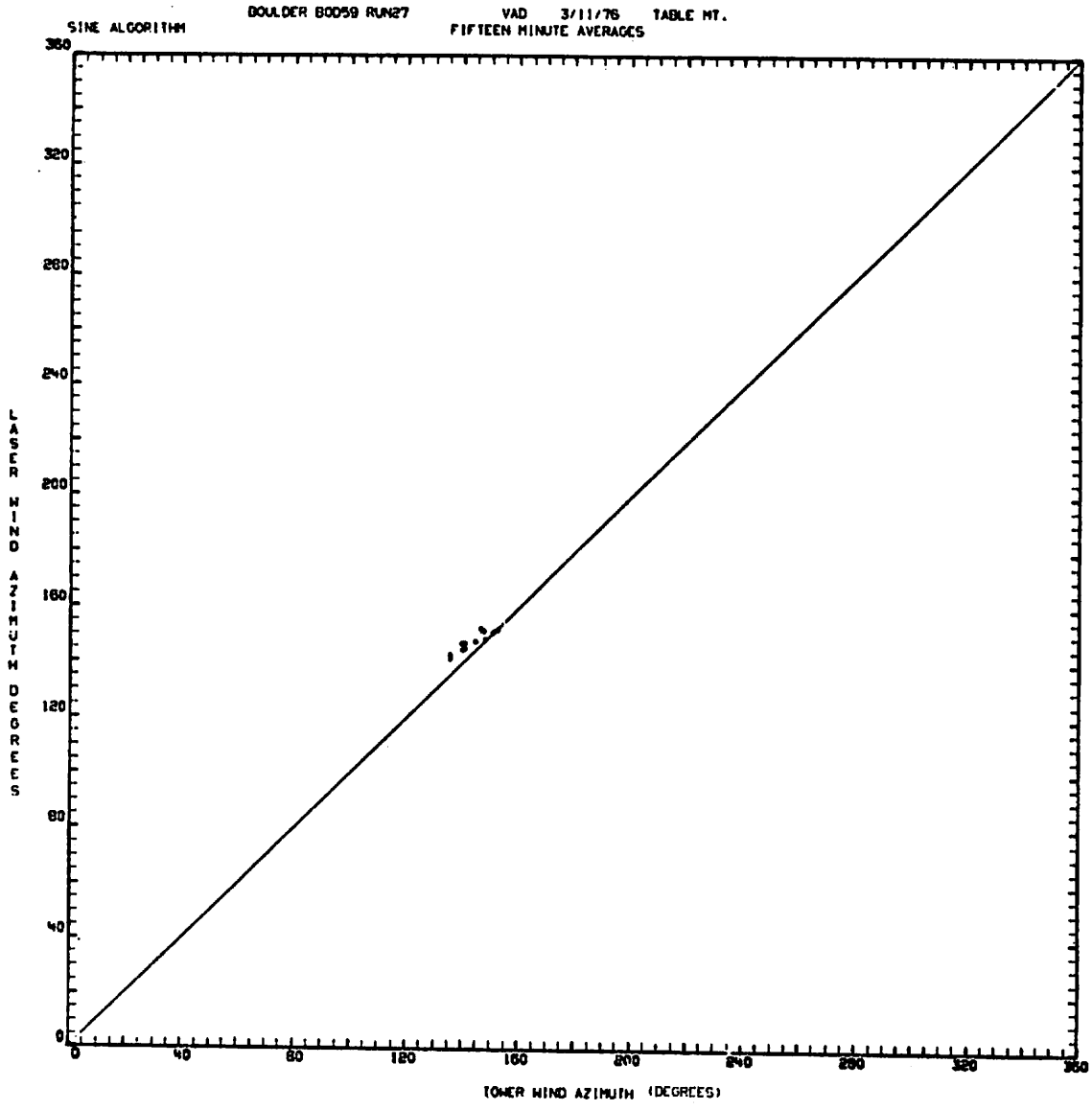

FIGURE B-1 (Continued).

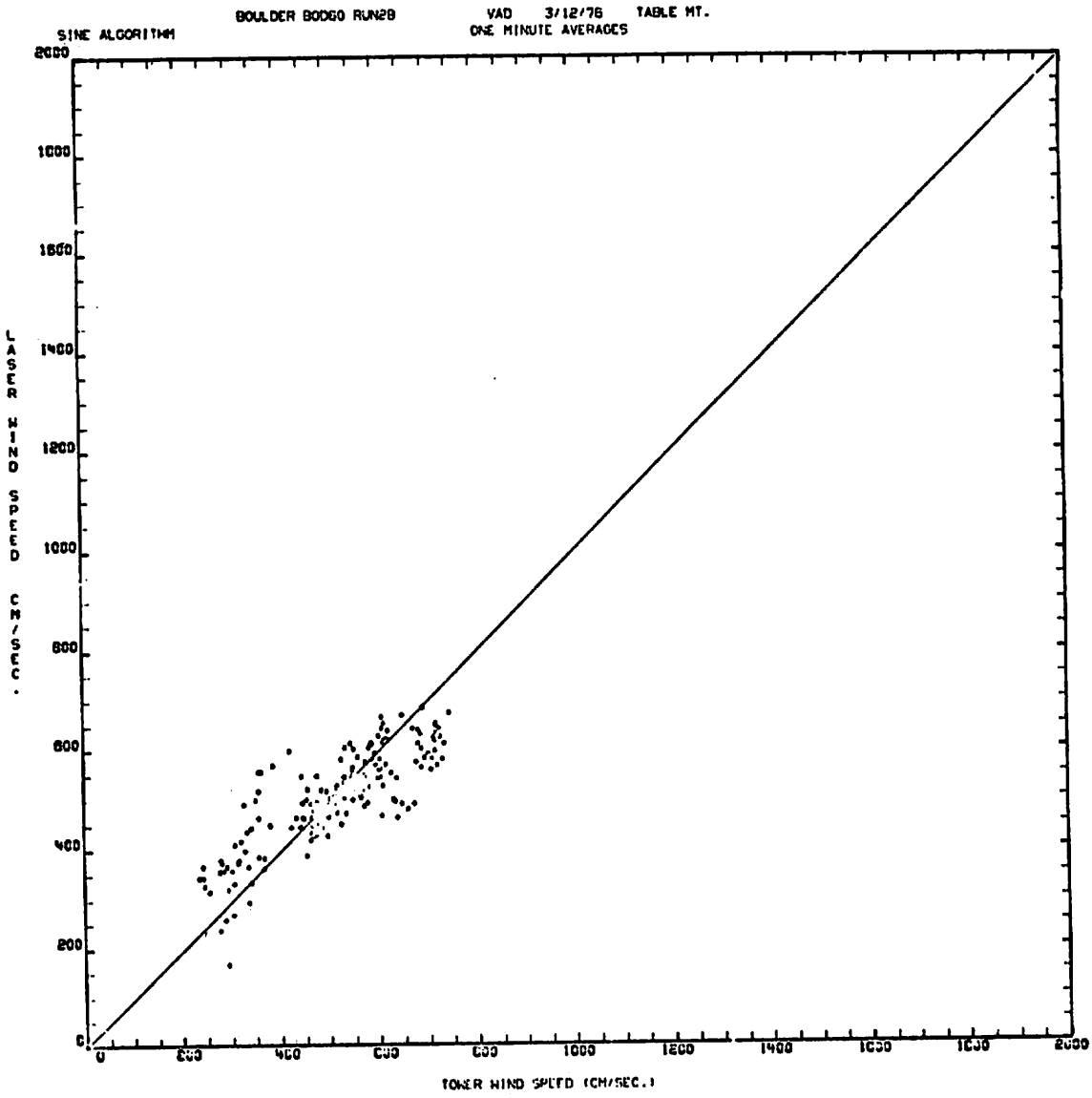

FIGURE B-1 (Continued).

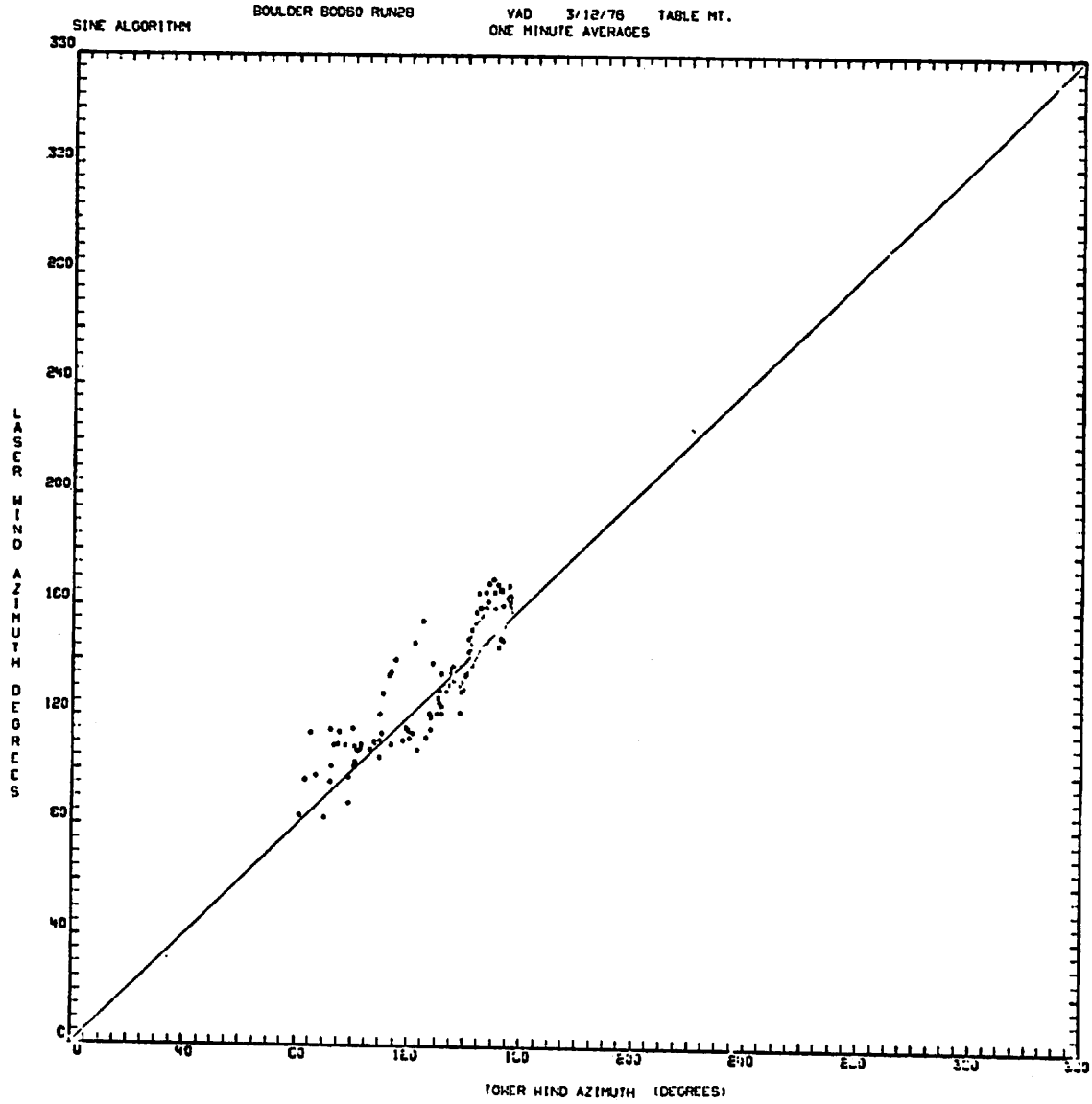

FIGURE B-1 (Continued).

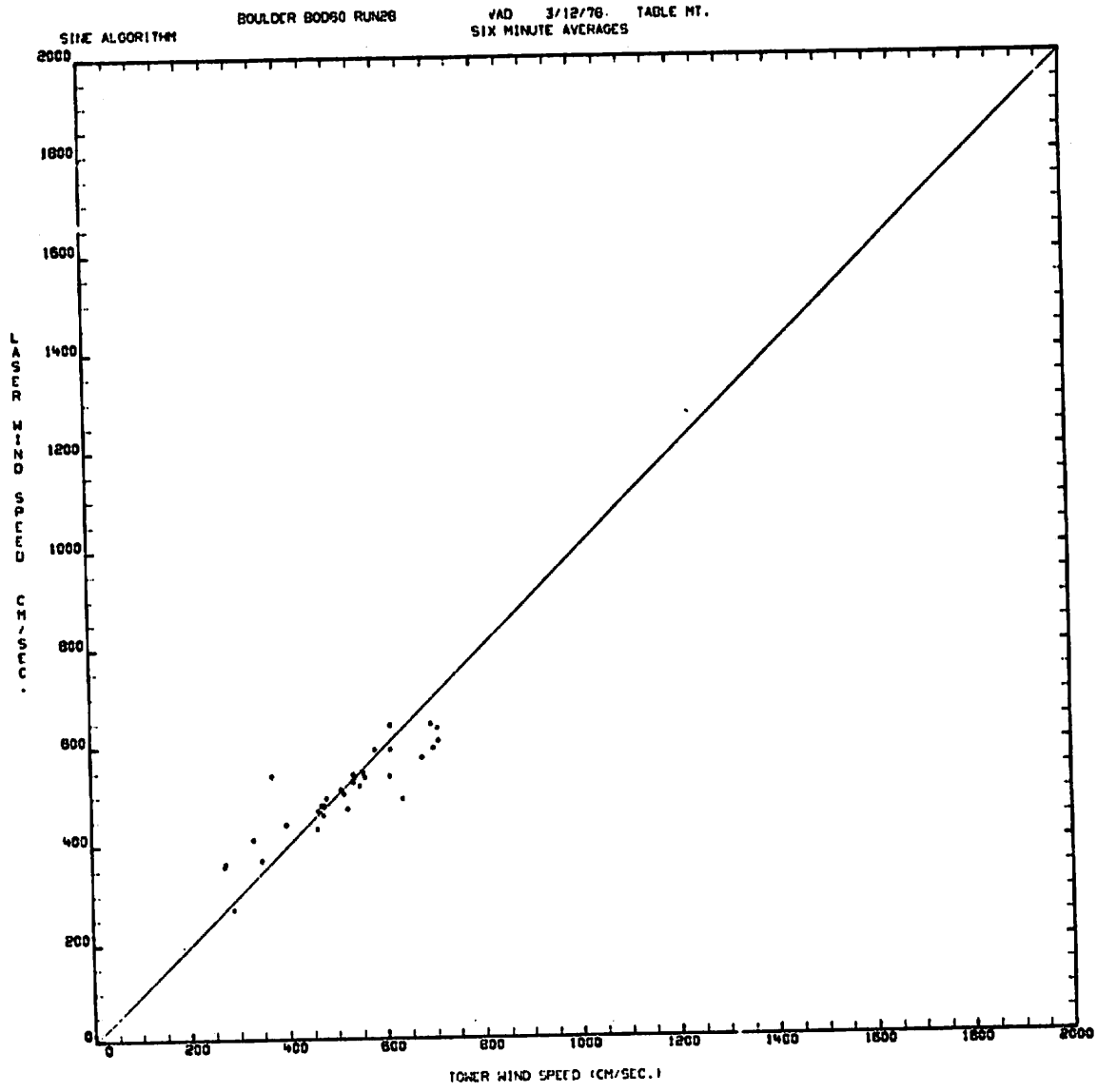

FIGURE B-1 (Continued).

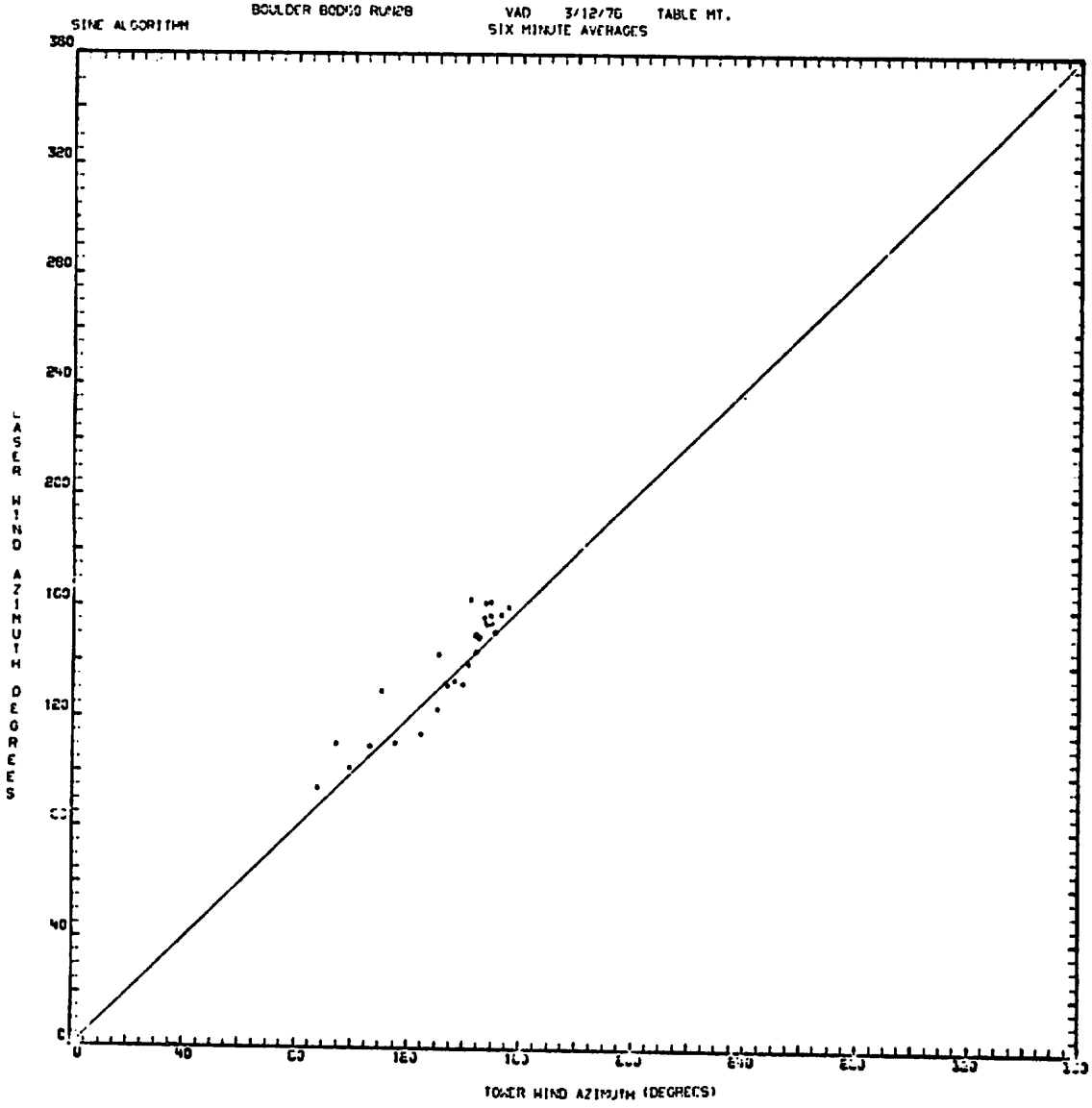

FIGURE B-1 (Continued).

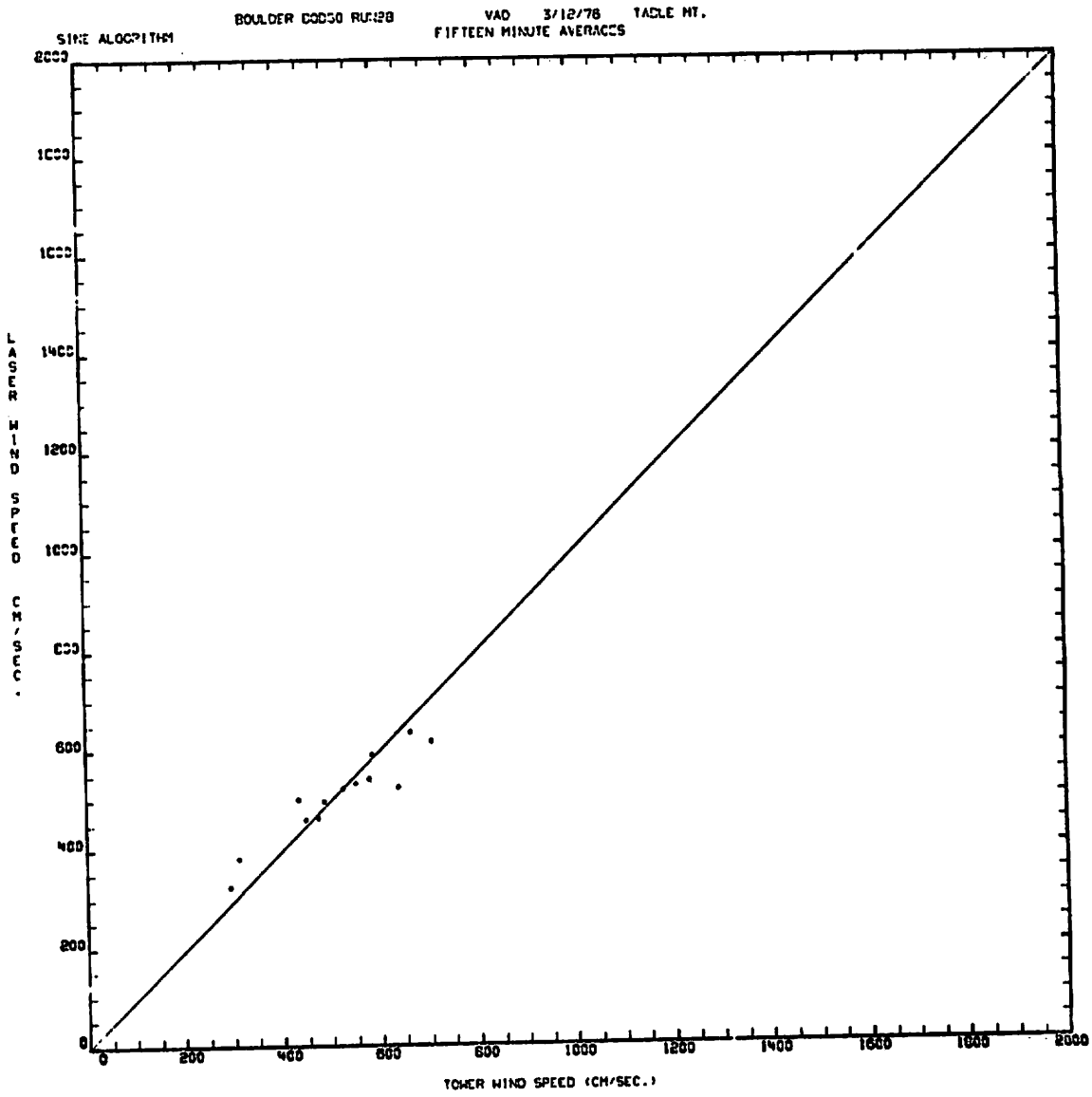

FIGURE B-1 (Continued).

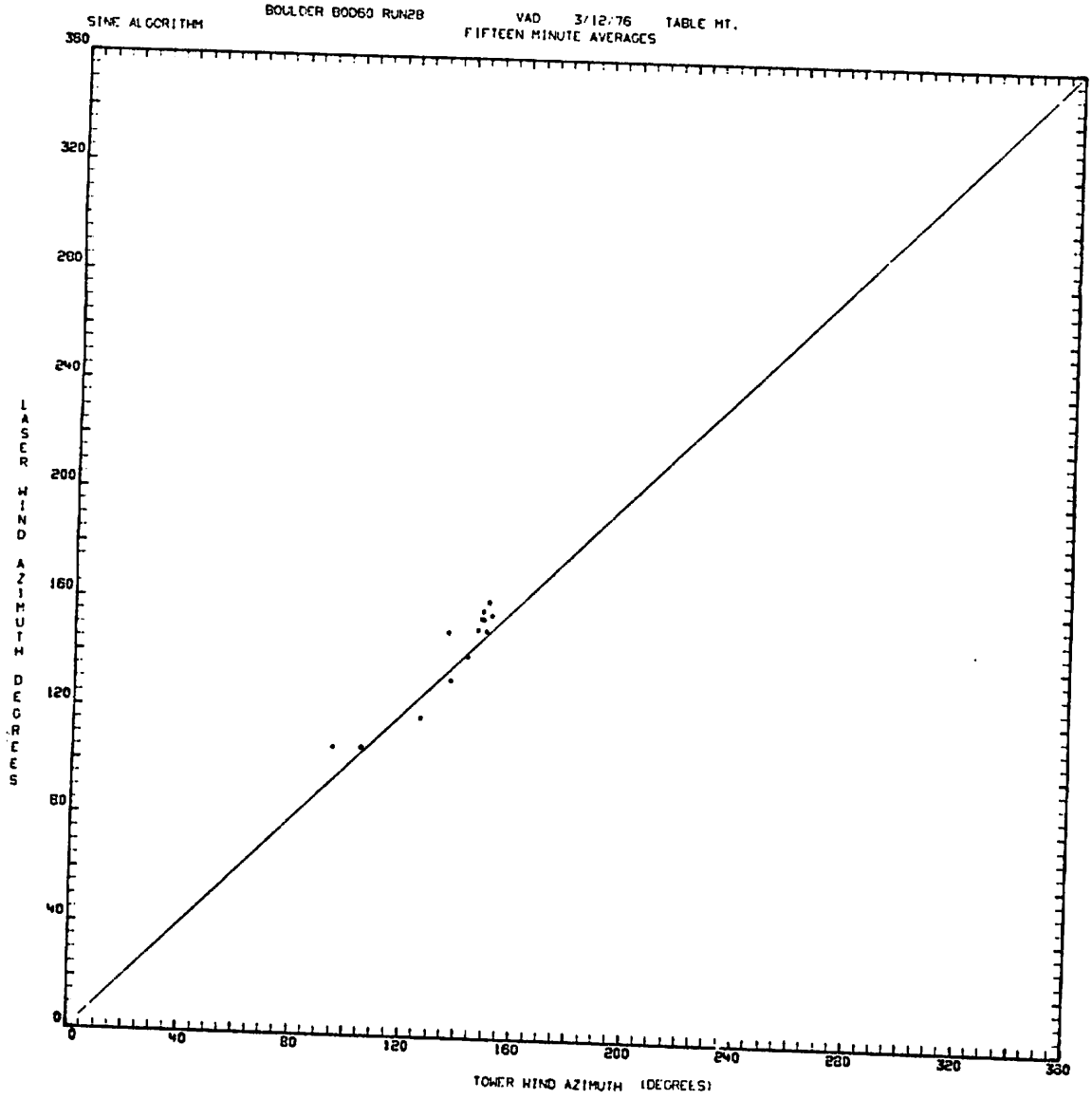

FIGURE B-1 (Concluded).

Appendix C
REPORT OF INVENTIONS

The purpose of the work performed under this contract and reported herein was the verification of the capability of an existing remote-sensing device to measure atmospheric winds accurately. The methods for accomplishing wind measurement had previously been established, but had not been verified for laser Doppler velocimetry.

Because the purpose of the test was the use of established techniques on an existing device, no innovations, discovery, improvement, or invention was made.

220copies

☆ U. S. GOVERNMENT PRINTING OFFICE: 1977--701-767--202